Universitat de Lleida

Targeted carotenoid metabolite profiling in transgenic cereals and correlations with carotenoid gene expression

Sol Maiam Rivera Vélez

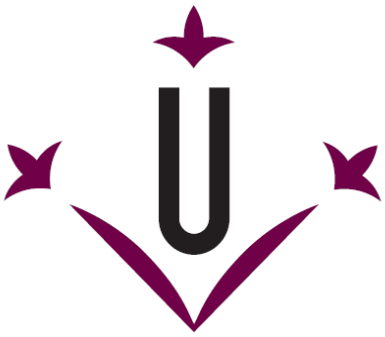

Universitat de Lleida
Escola Tècnica Superior d'Enginyeria Agrària

Targeted carotenoid metabolite profiling in transgenic cereals and correlations with carotenoid gene expression

Sol Maiam Rivera Vélez

Lleida, October 2012

Targeted carotenoid metabolite profiling in transgenic cereals and correlations with carotenoid gene expression

Presented by

Sol Maiam Rivera Vélez

Submitted to fulfill the requirements for a

PhD degree

At the department of Chemistry

School of Agriculture and Forestry Engineering
University of Lleida

This research work was undertaken with the guidance and support of thesis directors:

Dr. Ramón Canela i Garayoa
Department of Chemistry
School of Agriculture and Forestry Engineering
University of Lleida

Dr. Paul Christou
Department of Plant Production and Forest Science
School of Agriculture and Forestry Engineering
University of Lleida

ACKNOWLEDGEMENTS/ AGRADECIMIENTOS

First of all I would like to show my gratitude to my supervisors Ramón Canela and Paul Christou for their guidance on my PhD thesis. It has been a challenging opportunity and a pleasure to work in your group. This thesis document would not have been possible without your enthusiasm and professionalism. Thank you for your support, encouragement and for all the knowledge you gave me.

I gratefully acknowledge the Agència de Gestió d'Ajuts Universitaris i de Recerca (AGAUR) and the Comissionat per a Universitats i Recerca del DIUE de la Generalitat de Catalunya (Barcelona, Spain) and to the European Social Fund (ESF) for providing me with the PhD fellowship.

To Teresa Capell and Nuria Gabernet for their assistance in organizing the official paper work to run smoothly.

I would like to thank Dr. Changfu Zhu for helping me to understand about metabolic engineering of carotenoids and his kind advice.

I am also grateful to Francisca Vilaró for her guidance and assistance in the managing of the liquid chromatograph and her cooperation and valuable feedback.

I would like to thank Chao Bai and Gemma Farré who carried out the analysis of gene expression. Thanks for your contributions to my research.

To Remei Viladrich, Ferran Gatius, Montserrat Lloveras and Albert Tomàs who were always willing to help me in different issues.

To members of Chemistry and Applied Plant Biotechnology laboratories: Jordi Eras, Carmen Solarte, Edinson Yara, Sandrine Mongin, Antoni del Pino, Olalla Novo, Anna Canela, Silvia López, Mireia Oromí, Gemma Villorbina, Mercè Balcells, Marc Escribà, Eva Avilla, Evangelia Vamvaka, Raviraj Banakar, Uxue Zorrilla, Judit Berman, Maite Sabalza, Georgina Sanahuja, Bruna Miralpeix, Dawei Yuan, Eduard Perez, Gemma Masip, Svetlana Dashevskaya, Ariadna Peremarti, Koreen Ramessar, Shaista Naqvi, Sonia Gómez and Ludovic Bassie. I really enjoyed my days in the lab with all of you. Thanks for contributing to my happiness through their support and confidence.

To Prof. Gerhard Sandmann (Goethe University Frankfurt, Germany) for teaching me about carotenoid analysis during the time I was in his laboratory.

To Prof. Peter Bramley for allowing me to undertake a stay with his research group and Prof. Paul Fraser for his extreme kindness and help during the time I was at the Royal Holloway, University of London.

To my friends, Rogelio Sanchez, Liu Bing, Rebeca Muñoz, Emilia Martín, María Lidón, Roger Ros, Valentina Atanackovic and Paola Echavarría with whom I shared a lovely and fun time and special thanks to Elizabeth Breeze for her lovely and excellent friendship.

A John Jairo Méndez y Carlos Rivera que de alguna manera u otra contribuyeron a que mi sueño de realizar un doctorado fuera posible.

A mis padres Hipólito Rivera y Leonara Vélez. Gracias por inculcarme el amor al conocimiento y formar a la persona que soy hoy en día.

A mi hermana, Toa Sumak y a mi tía Myriam Facchini por su amor y soporte.

A Harry Barragán por su paciencia, soporte, comprensión y amor.

SUMMARY

My research program focused on the development and optimization of qualitative and quantitative analytical methodology for carotenoid determination in cereal crops. Initially, I improved the protocol to extract carotenoids from maize and rice tissues. I compared different combinations of solvents in order to identify the most suitable mixture that allowed me to extract, in spite of its different polarities, all the carotenoids present in the samples. I also improved and developed two chromatographic methods by high performance liquid chromatography (HPLC) and ultra high performance liquid chromatography (UHPLC) to separate these pigments. Various stationary and mobile phases were evaluated in order to obtain the most optimal resolution among the different pigments found in the samples. The identification of these molecules was carried out using photo diode array (PDA) and mass (MS) detectors. I investigated the effect of ionizing carotenoids using electrospray ionization (ESI), atmospheric pressure chemical ionization (APCI) and atmospheric pressure photoionization (APPI) techniques. The use of several dopants in APPI was also investigated. Thus, I was able to demonstrate that APCI was the most appropriate ionization technique for these molecules. To assess the reliability of the analytical method I determined basic validation parameters such as relative recovery, limit of detection (LOD), limit of quantification (LOQ) and matrix effects.

Although my main research focus was on the analytical determination of carotenoids, I also was involved in exploring relationships between gene expression and the accumulation of selected metabolites in the different transgenic lines in an effort to identify rate-limiting steps in the carotenoid pathway in cereals. To achieve this goal, the group of Applied Plant Biotechnology at the University of Lleida introduced different carotenogenic genes into rice and maize deficient for carotenoid synthesis. They recovered a diverse population of transgenic maize lines and rice callus and plants expressing different carotenogenic gene combinations and exhibiting distinct metabolic phenotypes. I analyzed these lines and in collaboration with other colleagues (who carried out the analysis for gene expression) we worked towards the elucidation of the biosynthetic step(s) that control carotenoid accumulation in the target tissues. Three different experiments were carried out in order to analyze the carotenoid pathway: (1) analysis of carotenoid accumulation at different developmental stages of transgenic maize seeds (from 15 to 60 days after pollination –DAP-); (2) analysis of ketocarotenoid accumulation in maize seed; and (3) analysis of carotenoids in rice callus. These experiments allowed us to identify rate-limiting steps in the pathway. A number of different lines contained extraordinary levels of *β*-carotene and other carotenoids, including complex mixtures of hydroxycarotenoids and ketocarotenoids. I also performed preliminary tests to identify new carotenoids found in the transgenic maize lines and rice callus.

RESUMEN

Mi trabajo de investigación consistió en la mejora, desarrollo y aplicación de técnicas analíticas para el análisis cualitativo y cuantitativo de carotenoides en cereales, principalmente en maíz y arroz. Inicialmente trabajé en la optimización del método de extracción de estos pigmentos. Diferentes combinaciones de solventes fueron comparadas para determinar el mejor solvente de extracción, que permitiera liberar de la semilla de maíz, todos los carotenoides a pesar de sus distintas polaridades. Adicionalmente, mejoré y desarrollé dos métodos cromatográficos por HPLC y UHPLC para conseguir realizar la separación de estos pigmentos. Varias fases estacionarias y móviles fueron comparadas con el fin de encontrar el mejor sistema que permitiera la separación de la mayoría de estos compuestos. La identificación de los analitos se realizó mediante el uso detectores de fotodiodos en serie y de masas. Técnicas de ionización tales como ESI, APCI y APPI fueron comparadas para ionizar los pigmentos. Además, también se investigó el uso de dopantes en la ionización por APPI. Los resultados demostraron que la mejor técnica para ionizar los carotenoides es APCI.

Para demostrar la fiabilidad del método analítico, se realizó la validación del mismo mediante la determinación de los siguientes parámetros: recuperación relativa, límites de detección y cuantificación, precisión, exactitud y efecto matriz.

Aunque mi trabajo de investigación se enfocó principalmente en la determinación analítica de carotenoides, también estuve involucrada en correlacionar la expresión del gen con la acumulación de estos pigmentos en los cereales. Para lograr este objetivo, trabajé junto al grupo de Biotecnología Vegetal Aplicada de la Universidad de Lleida, quienes transfirieron varios genes relacionados con la síntesis de estos compuestos a plantas de maíz y arroz. De tal manera, se obtuvieron plantas de maíz y callos de arroz transgénicas que expresaban diferentes combinaciones de estos genes y mostraban distintos fenotipos. Yo analicé estas líneas transgénicas y en colaboración con otros colegas (quienes realizaron el análisis de la expresión del gen) trabajamos en la elucidación de los pasos biosintéticos que controlan la síntesis de carotenoides en estos tejidos. Se llevaron a cabo tres experimentos para obtener información sobre la ruta metabólica de los carotenoides: el primero consistió en analizar el contenido de carotenoides en diferentes etapas del desarrollo de la semilla de maíz (desde los 15 hasta los 60 DAP), el segundo experimento consistió en el análisis químico de una gran variedad de oxocarotenoides encontrados en plantas de maíz transgénico, y el último experimento consistió en analizar el contenido de carotenoides en callos de arroz transgénico expresando distintas combinaciones de genes involucrados en la ruta metabólica de los carotenoides así como también en su almacenamiento. Finalmente, realicé pruebas preliminares para tratar de elucidar las estructuras de los nuevos pigmentos sintetizados en el maíz y en los callos de arroz transgénico.

RESUM

El meu treball de recerca va consistir en la millora, desenvolupament i aplicació de tècniques analítiques per a l'anàlisi qualitatiu i quantitatiu de carotenoides en cereals, principalment en blat de moro i arròs. Inicialment vaig treballar en l'optimització del mètode d'extracció d'aquests pigments. Es compararen diferents combinacions de solvents per determinar el millor solvent extractant que permetés alliberar tots els carotenoides de la llavor de blat de moro, malgrat les seves diferents polaritats. Addicionalment, vaig millorar i desenvolupar dos mètodes cromatogràfics per HPLC i UHPLC per realitzar la separació d'aquests pigments. Es compararen diverses fases estacionàries i mòbils amb la finalitat de trobar el millor sistema que permetés la separació de la majoria d'aquests compostos. La identificació dels analits es va realitzar mitjançant l'ús detectors de fotodíodes en sèrie i de masses. Es compararen tècniques d'ionització com ara ESI, APCI i APPI per ionitzar aquests pigments. A més a més, també s'investigar l'ús de dopants en la ionització per APPI,. Els resultats van demostrar que la millor tècnica per ionitzar els carotenoides és l'APCI.

Per demostrar la fiabilitat del mètode analític, es va realitzar la validació del mateix mitjançant la determinació dels següents paràmetres: recuperació relativa, límits de detecció i quantificació, precisió, exactitud i efecte matriu.

Encara que el meu treball de recerca es va enfocar principalment en la determinació analítica de carotenoides, també vaig estar involucrada en relacionar l'expressió del gen amb la síntesi d'aquests pigments. Per aconseguir aquest objectiu, vaig col·laborar amb el grup de Biotecnologia Vegetal Aplicada de la Universitat de Lleida. Aquest grup va transferir diversos gens relacionats amb la síntesi d'aquests compostos a plantes de blat de moro i arròs. El resultat van ser diferents plantes de blat de moro i calls d'arròs transgèniques, que expressaven diferents combinacions d'aquests gens i mostraven diferents fenotips. Vaig analitzar aquestes línies transgèniques i en col · laboració amb altres companys (que van realitzar l'anàlisi de la expressió del gen) vam treballar en l'elucidació dels passos biosintètics que controlen la síntesi de carotenoides en aquests teixits. Es van realitzar tres experiments per obtenir informació sobre la ruta metabòlica d'aquests pigments: el primer va consistir a analitzar el contingut de carotenoides en diferents etapes del desenvolupament de la llavor de blat de moro (des dels 15 fins als 60 DAP), el segon experiment va consistir en l'anàlisi química d'una gran varietat de oxocarotenoides trobats en plantes de blat de moro transgènic, i l'últim experiment va consistir en l'anàlisi química de calls d'arròs transgènic expressant diferents combinacions de gens involucrats en la ruta metabòlica dels carotenoides, així com també en l'emmagatzematge. Finalment, vaig realitzar proves preliminars per intentar elucidar les estructures de nous pigments sintetitzats en el blat de moro i arròs transgènic.

ABBREVIATIONS

ABA: abscisic acid

ACN: acetonitrile

ANOVA: analysis of variance

APCI: atmospheric pressure chemical ionization

API: atmospheric pressure ionization

API-MS/MS: atmospheric pressure ionization-tandem mass spectrometry

BCH: β-carotene hydroxylase

BEH: ethylene bridged hybrid

BHT: 2,6-bis(1,1-dimethylethyl)-4-methylphenol (butylhydroxytoluene)

BKT: β-carotene ketolase

CRTB: bacterial phytoene synthase

CRTE: bacterial geranylgeranyl diphosphate synthase

CRTI: bacterial phytoene desaturase/isomerase

CRTISO: carotenoid isomerase

CRTO: β-carotene ketolase

CRTW: β-carotene ketolase

CRTY: bacterial lycopene cyclase

CRTZ: bacterial β-carotene hydroxylase

CYP97C: carotene ε-ring hydroxylase

DA-APPI: dopant assisted-atmospheric pressure photoionization

DAP: days after pollination

DMAPP: dimethylallyl diphosphate

DRI: dietary reference intake for vitamin A

DW: dry weight

%Er: relative error

ESI: electrospray ionization

GC: gas chromatography

GGPP: geranylgeranyl diphosphate

GGPPS: GGPP synthase

GR: golden rice

H: height equivalent to a theoretical plate

HIV: human immunodeficiency virus

HPLC: high performance liquid chromatography

HSS: High strength silica

HYDB: β-carotene hydroxylase

IEs: ionization energies

IPP: isopentenyl diphosphate

IPPI: isopentenyl diphosphate isomerase

LC: liquid chromatographic or liquid chromatography

LC-MS: liquid chromatography-mass spectrometry

LC–MS/MS: liquid chromatography-tandem mass spectrometry

LOD: limit of detection

LOQ: limit of quantification

LYCB: lycopene *β*-cyclase

LYCE: lycopene *ε*-cyclase

MeOH: methanol

MS: mass or mass spectrometry

MTBE: *tert*-butyl methyl ether

NMR: nuclear magnetic resonance

PDA: photo diode array

PDS: phytoene desaturase

PSY: Phytoene synthase

Q1: quantifier

Q2: qualifier

R^2: Correlation coefficient

Rs: resolution parameter

%RSD: relative standard deviation

RT: retention time(s)

RAE: retinol activity equivalent

SD: standard deviation

TC: transgenic rice callus

TIC: total ion current

TM: transgenic maize line

THF: tetrahydrofuran

UHPLC: ultra high-performance liquid chromatography

UV-vis: ultraviolet-visible

VAD: vitamin A deficiency

VDE: violaxanthin de-epoxidase

Z-ISO: *ζ*-carotene isomerase

ZDS: *ζ*-carotene desaturase

ZEP: zeaxanthin epoxidase

λmax: wavelength of maximum absorption

%III/II: fine structure

TABLE OF CONTENTS

INDEX OF FIGURES

INDEX OF TABLES

GENERAL INTRODUCTION

GENERAL INTRODUCTION

a) Overview of carotenoid distribution and function

Carotenoids are natural pigments, which are synthesized by phototrophic organisms, but also by many non-phototrophic species (except animals). They are synthesized by an enormous range of organisms within the archaeae and eubacteria (including cyanobacteria) as well as within eukaryotes (algae, fungi and plants) serving a multitude of functions [1].

Carotenoids exhibit yellow, orange and red colors but when they are bound to proteins acquire green, purple or blue colors [2]. They are found in a large number of fruits and vegetables (oranges, tomates, carrots, spinach, sweet potatoes, pumpkins), in spices (papikra), some animal products (eggs, butter, milk) and seafoods (salmon, shrimp, trout, mollusc, etc.) [3].

In plants, carotenoids are required for the correct assembly of photosystems [4]. They absorb light across a broader range of the spectral region in which the sun irradiates maximally and transfer the energy to chlorophyll, initiating the photochemical events of photosynthesis [5]. Plants are able to balance between absorbing sufficient light for photosynthetic processes while avoiding photo oxidative damage to membranes and proteins caused by excessive light. To meet this balance carotenoids (a) quench triplet chlorophyll, (b) scavenge ROS like singlet oxygen which damage membranes and proteins, thereby behaving as antioxidants (along with ascorbate and tocopherols) and (c) dissipate excess energy via xanthophyll-mediated non-photochemical quenching (NPQ) [6].

In addition, carotenoids serve as precursors for the hormones abscisic acid (ABA) and strigolactones [7] as well as other signalling molecules (e.g. blumenin and mycorradicin) (Fig. 1) [6]. They also serve as attractants for animals, such as pollinating insects and seed-disbursing herbivores [8].

In animals, carotenoids also exhibit a number of functions. For example, they boost the immune system and promote general health [6]. These pigments are critical in determining sexual behaviour, reproduction and avoiding predation as well as parasitism. Animals typically place different priorities on fitness-enhancing activities (e.g. gametic investment in females, sexual attraction in males) and carotenoid allocation appears to track such investment patterns in the two sexes [6]. For example, environmental and physiological factors influence colour expression in house finches (Fig. 1) and the type of dietary carotenoids is one determinant of their ability to become bright red through orange to drab yellow. Male house finches with redder plumage have been shown to be more sexually attractive and have higher fitness [9].

Carotenoids also play important roles in animals to avoid predation and reduce parasitism. For example, aphids (e.g. *Acyrthosiphon pisum*) are the first known animal to have acquired the carotenoid biosynthetic machinery to produce carotenoids such as torulene and dehydro- γ, Ψ-carotene, which provide a reddish coloration distinguishing them from their green forms, which accumulate γ-carotene, β-carotene and α-carotene [10]. The colour polymorphism is maintained by

frequency-dependent selection imposed by natural predators that preferentially prey upon the red morphs (Fig. 1) and higher rates of parasitism in the green forms [6].

In humans, one of the most important physiological functions of carotenoids is their role as vitamin A precursors [11]. These pigments are also known to contribute to prevention and protection against serious health disorders such as cancer, heart disease and macular degeneration [2, 12].

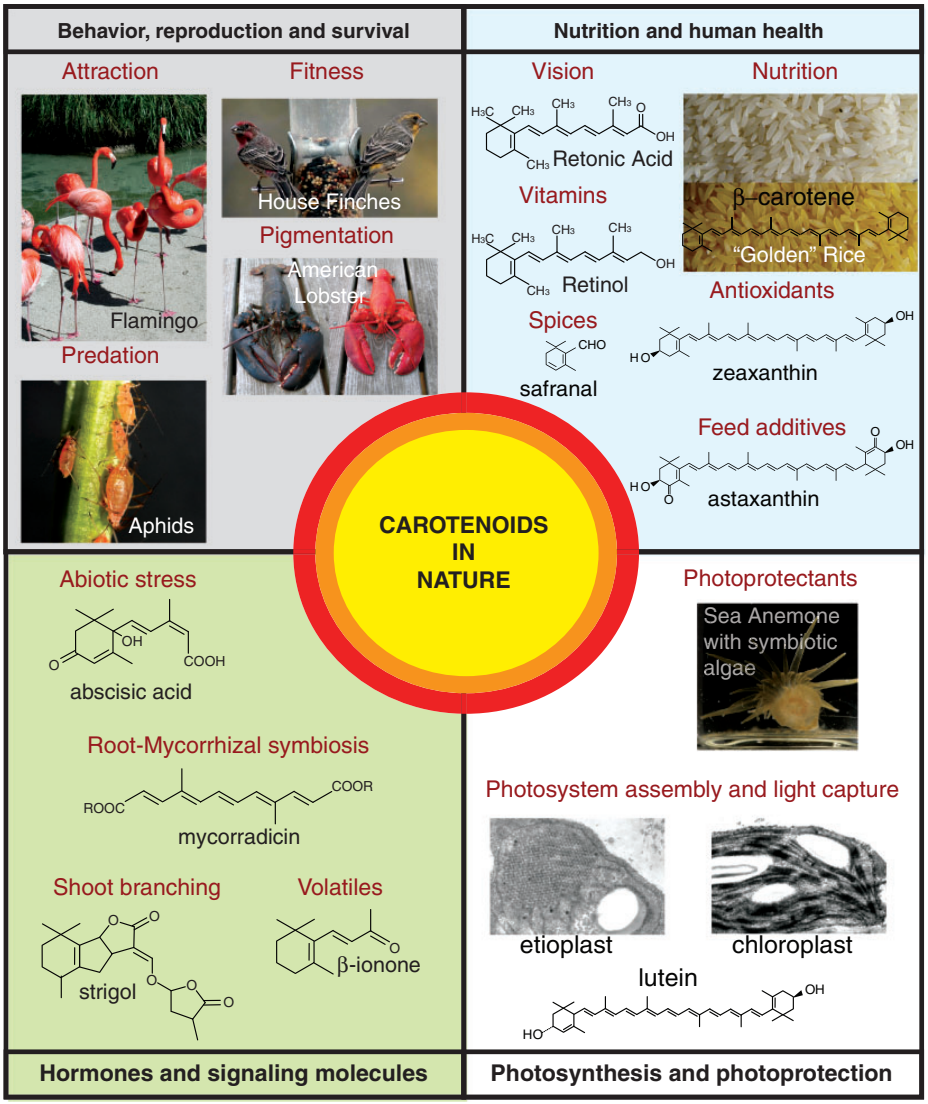

Figure 1. The many essential functions for carotenoids in nature. Carotenoids play important roles in: (a) promoting animal behaviour, reproduction and survival; (b) improving nutrition and human health; (c) assembly of photosystems, light capture and photoprotection; and (d) providing substrates for the biosynthesis of plant hormones and signalling molecules [6].

In industry, carotenoids are used: (a) in nutrient supplementation, (b) for pharmaceutical purposes, (c) in animal feed, (d) as food colorants (such as bixin and crocetin, found in annatto seeds and saffron respectively) and (e) fragrances (such as ionones, damascones, and damascenones) [2, 7].

b) Nutritionally important carotenoids and ketocarotenoids

Humans are not able to synthesize carotenoids de novo, therefore, they need to acquire them through their diet. Although more than 700 carotenoids have been described in nature, not all natural sources are present in our normal diet. It is estimated that we only have access to about 40 carotenoids that can be absorbed, metabolized, and/or used in our bodies [13]. However, of these 40 about 20 carotenoids have been identified in the human blood and tissues [14]. Close to 90% of the carotenoids in the diet and human body is represented by α- and β-carotene, lycopene, β-cryptoxanthin, zeaxanthin and lutein, which are regularly present in the food [14]. Biological functions and benefits to health of these carotenoids are illustrated in Table 1.

Table 1. Biological functions and benefits to health of the main carotenoids found in the human body.

Carotenoid	Functions and benefits to health	Sources	Ref.
β-carotene	Provitamin A function	Carrots, sweet potato, pumpkin, tomato, orange colored fruits such as apricot, grapefruit, mango, papaya, persimmon, pink guava and watermelon and green leafy vegetables	[11, 12, 14, 19, 20]
	In colorectal cancer		
	In the prevention of acute and chronic coronary syndromes		
	Photoprotection of skin against UV light		
α-Carotene	Provitamin A function	Carrot, tomato, apricot, banana, pineapple, pepper, corn, beans and pumpkin	[12, 19, 20]
Lycopene	Prevention in prostatic hyperplasia and prostate cancer	Papaya, pink grapefruit, pink guava, persimmon, watermelon, tomato and related tomato products	[11, 12, 19, 21-23]
	Prevention of atherosclerosis and acute and chronic coronary syndromes		
	Photoprotection of skin against UV light		
Zeaxanthin	Active against liver neoplasms	Yellow corn, orange pepper, orange, honeydew, mango, lettuce, spinach, papaya, peach and chicken egg yolk	[11, 12, 19, 24]
	In the prevention of acute and chronic coronary syndromes		
	Helps to maintain a normal visual function		
	In the prevention of cataracts		
	To prevent macular degeneration associated with age		
Lutein	In the prevention of acute and chronic coronary syndromes and stroke	Green bean, broad bean, broccoli, pea, spinach, lettuce, kale, pepper, sweet corn, carrot, apricot, parsley and brussel sprout	[11, 12, 14, 25]
	Helps to maintain a normal visual function		
	In the prevention of cataracts		
	To prevent macular degeneration associated with age		
	In the prevention of retinitis		
	To avoid gastric infection by *H. Pylori*		
β-Cryptoxanthin	Provitamin A function	Papaya, persimmon, starfruit, orange, peach, chili, maize, pepper and tomato	[14, 16, 19, 20]
	Reduction in the risk of lung cancer		

Consumption of ketocarotenoids, most notably astaxanthin, is also increasingly associated with a range of health benefits. Some evidence suggests astaxanthin is a potential therapeutic agent for the treatment of oxidative stress, inflammation and cardiovascular diseases in humans and animals [11, 15-17]. Ketocarotenoids are currently being used as a feed additive for the aquaculture and poultry industries [8]. Thus, these pigments are responsible for the attractive pink and red color of the feathers and skin of many birds (e.g., flamingo, scarlet ibis, and roseate spoonbill) and the shells of lobster, shrimp, krill, crabs, and other crustaceans [15]. Ketocarotenoids are synthesized by certain bacteria, several fungi, some green algae, and a few species of the flowering plant genus *Adonis* [8, 17, 18]. The majority of the demand for astaxanthin is met by chemical synthesis [15, 17], but natural sources are becoming more important [15, 17].

c) Chemistry of carotenoids

Carotenoids are extremely hydrophobic molecules with little or no solubility in water. They are thus expected to be restricted to hydrophobic areas in the cell, such as the inner core of membranes, except when association with protein allows them access to an aqueous environment [26]. These pigments are isoprenoid compounds, biosynthesized by tail-to-tail linkage of two C_{20} geranylgeranyl diphosphate molecules. This produces the parent C_{40} carbon skeleton from which all the individual variations are derived [26].

In Fig. 2.A, this basic structure is illustrated by lycopene and *β*, *β*-carotene; the carotenoid numbering scheme is also shown. This skeleton can be modified: (a) by cyclization at one or both ends of the molecule to give the seven different end groups (illustrated in Fig. 2.B) [27]; (b) by changes in the degree of saturation; and (c) by addition of oxygen-containing functional groups. Carotenoids that contain one or more oxygen functions are known as xanthophylls, the parent hydrocarbons are carotenes [26]. Examples of xanthophylls are violaxanthin (epoxy), canthaxanthin (oxo), zeaxanthin (hydroxy), spirilloxanthin (methoxy) and torularhodin (carboxylic acid) (illustrated in Fig. 2.C) [2].

The most striking and characteristic feature of the carotenoid structure is the long system of alternating double and single bonds that forms the central part of the molecule. This structure constitutes a system in which the π-electrons are delocalized along the entire polyene chain. It is this feature that confers carotenoids their unique molecular shape, chemical reactivity, and light-absorbing properties [26].

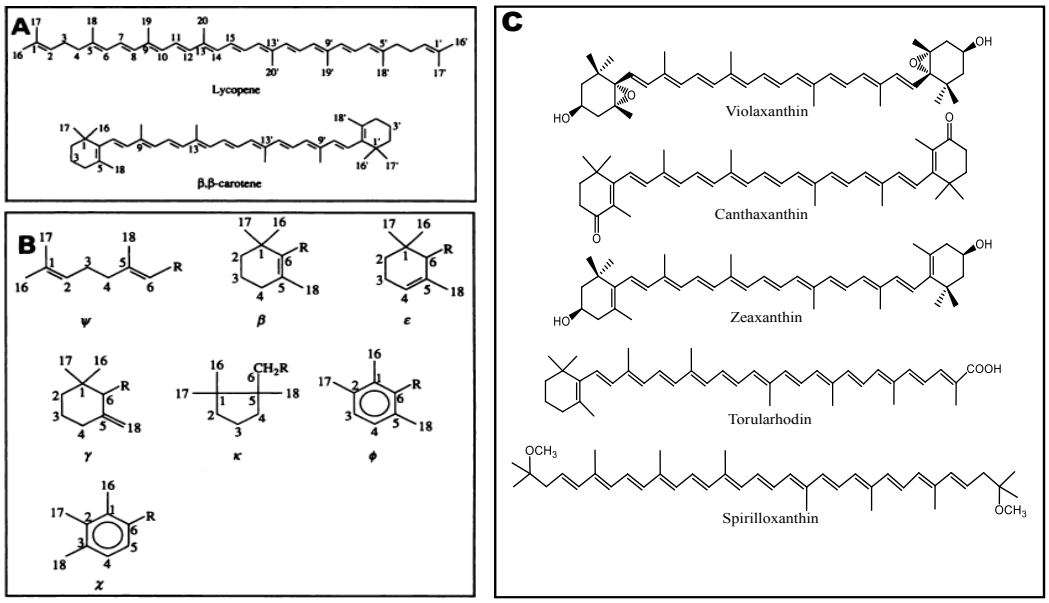

Figure 2. A) Basic structure and numbering scheme of an acyclic carotenoid (lycopene) and a dicyclic carotenoid (*β*, *β*-carotene). B) The seven different end groups found in natural carotenoids. C) Examples of xanthophylls: violaxanthin, canthaxanthin, zeaxanthin, torularhodin and spirilloxanthin. Figs. 2.A and 2.B [26]; Fig. 2.C [2].

d) Analytical methods for carotenoids

Based on chemical and physical properties of carotenoids, high performance liquid chromatography (HPLC) using various absorbance detectors [2] has become the most common analytical method for determining carotenoid profiles both qualitatively and quantitatively. Detection techniques such as nuclear magnetic resonance (NMR) spectroscopy and mass spectrometry (MS) [28] have also been used to identify these pigments.

Analysis of carotenoids by HPLC

Normal- and reversed-phase systems, in isocratic or gradient elution modes, have been used to analyze carotenoids. However, most separations of these compounds reported in the literature involve reversed-phase HPLC using C18 and C30 columns [2]. Various mixtures of solvents have been used with these reversed-phases, including water, methanol (MeOH), acetonitrile (ACN), 2-propanol, acetone, ethyl acetate, tetrahydrofuran (THF), *tert*-butyl methyl ether (MTBE), dichloromethane and chloroform [3, 29]. In general, polymeric C30 phases provide better separations of carotenoid geometric isomers than C18 ones. This finding is attributed to be the enhanced shape selectivity of the former [2]. However, C18 stationary phases have also been reported to yield relatively good separations of these isomers; for example, polymeric C18 phases have provided acceptable selectivity for the separation of the geometric isomers of *β*-carotene, lutein and zeaxanthin [2]. C30 phases also provide a satisfactory resolution for carotenoids with similar polarity [2].

Analysis of carotenoids by ultra high performance liquid chromatography (UHPLC)

UHPLC is a promising tool for carotenoid analysis. High strength silica (HSS) C18 and T3 and ethylene bridged hybrid (BEH) C18 stationary phases have been successfully used to separate several

carotenoids [2]. One of the main differences between HPLC and UHPLC columns is the particle size of the stationary phase. While in HPLC particles are over 2 μm, they are smaller in UHPLC. When run at the optimal flow rate, the pressure produced by smaller particles will exceed the pressure limitations of conventional HPLC systems. Therefore, UHPLC columns are used in a liquid chromatography (LC) instrument designated to operate at the optimal linear velocity (and resulting pressure) for these particles while minimizing the dispersion of the flow path such that theoretical performance of the separation column could be achieved. The key to UHPLC separations is the combination of the instrument and column performance that allows researchers to fully realize and harness the power of sub-2 μm particle columns. This is achieved by minimizing band spreading within (intra-column) and outside (extra-column) of the column and being able to operate at the optimal linear velocities (and pressures) of these small particles columns [30].

MS for carotenoid identification

In HPLC, UV–vis instruments are the most common detectors used to identify carotenoids. However, given that the UV–vis spectra of many carotenoids are similar (e.g., α-cryptoxanthin and zeinoxanthin) and a number of structurally related molecules coelute, many researchers have complemented the identification of carotenoids using mass spectrometers equipped with atmospheric pressure ionization (API) sources: electrospray ionization (ESI) or atmospheric pressure chemical ionization (APCI) [31]. Mass detectors have shown great advantages for the analysis of these substances, including the elucidation of their structure on the basis of the molecular mass and their fragmentation pattern. These properties facilitate the quantification of individual carotenoids that coelute. APCI has become the most widely used ionization technique for carotenoids and shows high sensitivity for their analysis [31, 32]. APCI has been used to successfully ionize not only xanthophylls and carotenes but also carotenoid esters [2], thereby demonstrating the suitability of this approach to ionize carotenoids with different polarities.

e) Carotenoid biosynthesis

Carotenoids are localized in subcellular organelles (plastids), *i.e.* chloroplasts and chromoplasts. In chloroplasts, the carotenoids are primarily associated with proteins and serve as accessory pigments in photosynthesis, whereas in chromoplasts they are deposited in crystalline form or as oily droplets [4, 19]. In plants, the synthesis of carotenoids is initiated by the enzyme phytoene synthase (PSY), which mediates the condensation of two molecules of geranylgeranyl diphosphate, leading to the colorless carotene phytoene [34]. Then, 15-*cis*-phytoene undergoes four desaturation steps catalyzed by phytoene desaturase (PDS), ζ-carotene isomerase (Z-ISO) and ζ-carotene desaturase (ZDS) to generate the first colored carotene, prolycopene, which is converted to all-*trans*-lycopene by carotene isomerase (CRTISO) in non-green tissue, but by light in green tissue [7, 35]. Lycopene is the substrate for lycopene β- and ε-cyclases (LCYB and LCYE), which catalyze the formation of β- and α-carotene [36].

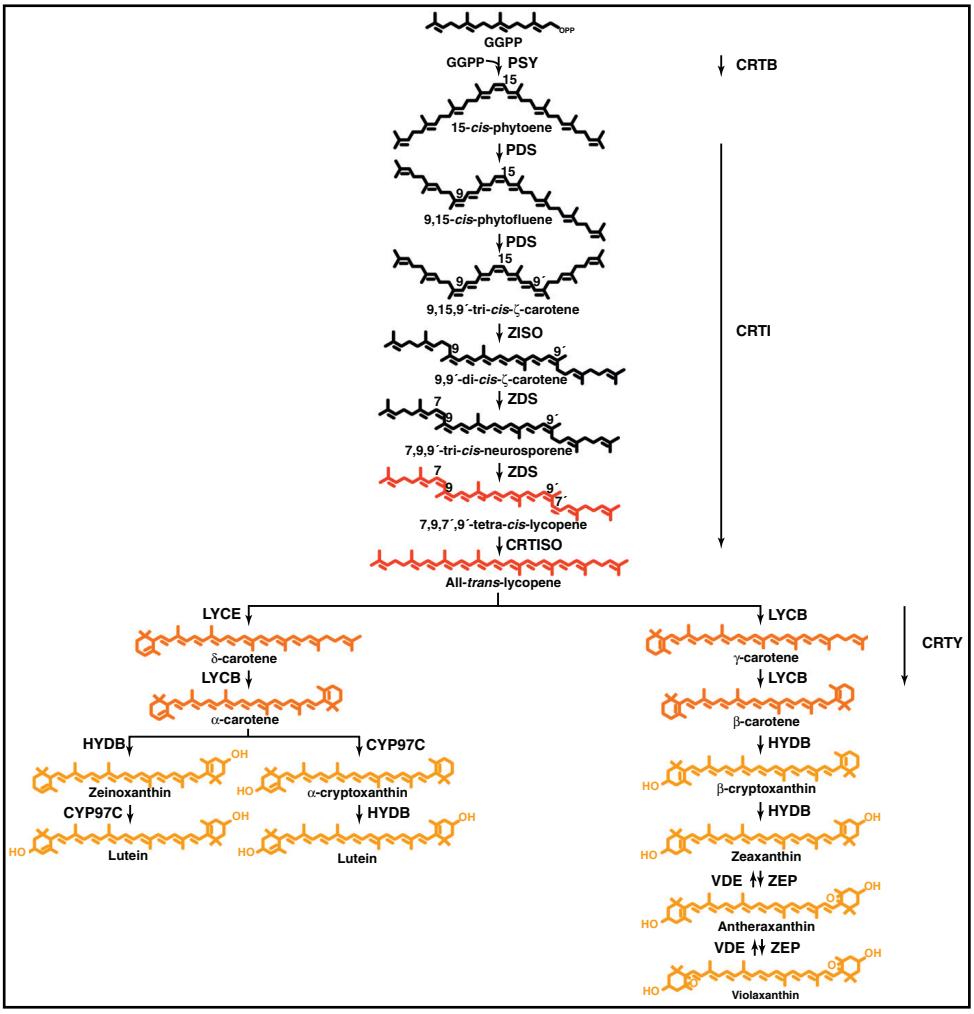

Figure 3. Carotenoid biosynthesis pathway in plants and equivalent steps in bacteria. Bacterial enzymes are on the right side of the pathway [33].

The latter is converted into zeinoxanthin by the di-iron non-heme *β*-carotene hydroxylase (BCH) and/or the P450-type *β*-carotene hydroxylases (CYP97A and CYP97B), and then into the yellow pigment lutein by the P450-type *ε*-hydroxylase, CYP97C [36] while subsequent oxygenation of *β*-carotene results in the formation of *β*-cryptoxanthin and then zeaxanthin by BCH and/or CYP97A and CYP97B [37]. Zeaxanthin is a constituent of the xanthophyll cycle and can be reversibly converted into violaxanthin via antheraxanthin. These reactions are mediated by the enzymes zeaxanthin epoxidase (ZEP) and violaxanthin de-epoxidase (VDE) [7]. In contrast to plants, some nonphotosynthetic bacteria, such as *Erwinia*, utilize only three enzymes (i.e. phytoene synthase *crtB*, phytoene desaturase/isomerase *crtI*, and lycopene cyclase *crtY*) to perform the synthesis of *β*-carotene from geranylgeranyl diphosphate [33]. Fig. 3 shows the carotenoid biosynthesis pathway in plants and equivalent steps in bacteria.

f) Metabolic pathway engineering in plants using combinatorial transformation

Metabolic engineering is the modification of endogenous metabolic pathways to increase flux towards particular desirable molecules or divert flux towards the synthesis of new molecules. Metabolic

engineering in plants has been carried out to enhance the production of industrial or pharmaceutical metabolites, and to improve agronomic or nutritional characteristics, in the hope of addressing food security [38].

Studying and manipulating secondary metabolism in plants can be compromised by the sheer complexity of the pathways, which may have multiple branches, multifunctional enzymes, cell-type-specific and compartmentalized enzymes, and complex feedback mechanisms [39]. One approach to overcome this challenge is to clone genes encoding pathway enzymes and modify their expression, but manipulating single enzymes is often unhelpful because pathways are regulated at multiple points. It is becoming increasingly apparent that multi-step engineering, where partial or complete pathways are reconstructed or extended by the expression of two or more enzymes simultaneously, is the most desirable way to study and modulate complex pathways such as carotenoid biosynthesis [40, 41].

However, a significant hurdle to the application of multi-gene engineering in complex pathway analysis is the diminishing rate of returns when generating multiplex-transgenic plants [42]. As the number of individual transgenes increases, the proportion of plants showing stable expression of all input genes across generations decreases, so larger populations need to be generated. This challenge has been addressed by a combinatorial nuclear transformation technique, which is a novel method for the rapid production of multiplex-transgenic plants [42].

This approach provides a unique and surprisingly straightforward strategy for metabolic pathway analysis and multi-gene metabolic engineering in plants. It involves the introduction and coordinated expression of multiple transgenes followed by the selection of stable lines expressing the specific combination of transgenes required for particular metabolic outputs. Individual lines, producing specific metabolites, can be goals in themselves if the aim is to engineer particular molecules. However, by examining the entire diverse population of plants, it becomes possible to dissect the pathway and subsequently reconstruct it either in its original form or with modifications, thus providing a basis for understanding and subsequently engineering the synthesis of novel metabolites [42]. The broad significance of this approach is that it considerably simplifies the process of metabolic engineering by making it analogous to screening a library of metabolic variants for the correct functional combination [42]

g) Genetic engineering of carotenoids in plants

Vitamin A deficiency (VAD) affects 127 million people in developing countries, including 25% of pre-school children, causing more than half a million cases of permanent blindness in children and 2.2 million deaths per year [43]. In addition, VAD impairs the immune system, increasing the severity of diseases such as measles, diarrhea, and maternal transmission of human immunodeficiency virus (HIV) [44]. The dietary reference intake (DRI) for vitamin A is best expressed as the retinol activity equivalent (RAE), which takes bioavailability into account. The recommended DRI for males is 900 RAE, for females it is normally 700 RAE (770 RAE during pregnancy, and 1200–1300 RAE when

lactating) and for children it is 400–500 RAE. One RAE is equivalent to 1 µg of retinol or 2 μg of β-carotene (which has 100% pro-vitamin A activity) supplement dissolved in oil. A DRI of 900 RAE for males is therefore equivalent to 900 µg (3,000 IU) of retinol or 1,800 µg of β-carotene supplement [36].

Addressing VAD in the developing world requires a robust strategy to increase access to foods rich in (pro)-vitamin A, and several approaches can be considered. Dietary supplements (vitamin tablets and suspensions) and fortification (artificially increasing vitamin levels by adding vitamins to processed food) campaigns have been highly successful in the developed world and have significantly reduced the incidence of deficiency diseases. Many processed foods, including bread, packaged cereals, milk, and soft drinks, are fortified with vitamins and minerals so that the average diet contains micronutrients well in excess of requirements. In developing countries, the less-robust and less-reliable food distribution infrastructure, poor governance, and the lack of funding renders such programs inefficient and unsustainable, especially when trying to reach remote areas [36]. Vitamin A supplementation campaigns have enjoyed limited success, but most programs have failed to address VAD, especially at the local level when dealing with small and remote villages [45]. An alternative approach to adding vitamin A directly to the diet is to enhance the accumulation of pro-vitamin A carotenoids in crops [36]. Currently, many researchers are attempting to enhance β-carotene levels (and other carotenoids with beneficial properties for health) in staple crops by introducing the corresponding metabolic pathway. The first significant advance in increasing the levels of β-carotene in cereals was ‘‘Golden Rice 1’’, where the entire β-carotene biosynthetic pathway was reconstructed in the endosperm by expressing daffodil (*Narcissus pseudonarcissus*) phytoene synthase and lycopene β-cyclase, and a bacterial (*Erwinia uredovora*) phytoene desaturase; the resulting grains contained up to 1.6 μg/g of carotenoids by dry weight [43]. Later, the daffodil phytoene synthase gene was substituted with the equivalent gene from maize, resulting in ‘‘Golden Rice 2’’, in which the total carotenoid content of the endosperm increased to 37 μg/g dry weight [43]. Both Golden Rice lines were donated to the Golden Rice Humanitarian Board, and up to six events of Golden Rice 2 were developed in the background of the American Kaybonnet rice variety, with one event selected for regulatory approval and commercialization. This line provides enough β-carotene in a 100-g portion of milled rice to achieve the recommended daily intake (RDI) of vitamin A for a child under five and could therefore prevent vitamin A deficiency (VAD) if consumed on a regular basis [43].

Using combinatorial nuclear transformation in maize and rice, the group of **Applied Plant Biotechnology at the University of Lleida** has generate a combinatorial metabolic library for the investigation of carotenoid biosynthesis and the synthesis of specific combinations of carotenoids. They have created elite inbred South African transgenic maize plants, in which the levels of carotenoids were increased specifically in the endosperm. The transgenic kernels contained 169-fold the normal amount of β-carotene [42]. In addition, the same transgenic kernels also had increased levels of lycopene, zeaxanthin, lutein and astaxanthin, all nutritionally and industrially important

carotenoids. Thus, this approach opens up perspectives for the nutritional improvement of staple crops in the context of food security in the developing world.

REFERENCES

[1] Walter MH, Strack D (2011) Carotenoids and their cleavage products: Biosynthesis and functions. Natural Product Reports.28:663-92.

[2] Rivera SM, Canela-Garayoa R (2012) Analytical tools for the analysis of carotenoids in diverse materials. Journal of Chromatography A.1224:1-10.

[3] Lesellier E, Tchapla A, Marty C, Lebert A (1993) Analysis of carotenoids by high-performance liquid chromatography and supercritical fluid chromatography. Journal of Chromatography A.633:9-23.

[4] Matthews PD, Luo R, Wurtzel ET (2003) Maize phytoene desaturase and ζ-carotene desaturase catalyse a poly-Z desaturation pathway: Implications for genetic engineering of carotenoid content among cereal crops. Journal of Experimental Botany.54:2215-30.

[5] Polívka T, Frank HA (2010) Molecular factors controlling photosynthetic light harvesting by carotenoids. Accounts of Chemical Research.43:1125-34.

[6] Cazzonelli CI (2011) Carotenoids in nature: Insights from plants and beyond. Functional Plant Biology.38:833-47.

[7] Zhu C, Bai C, Sanahuja G, Yuan D, Farré G, Naqvi S, Shi L, Capell T, Christou P (2010) The regulation of carotenoid pigmentation in flowers. Archives of Biochemistry and Biophysics.504:132-41.

[8] Zhu C, Naqvi S, Capell T, Christou P (2009) Metabolic engineering of ketocarotenoid biosynthesis in higher plants. Archives of Biochemistry and Biophysics.483:182-90.

[9] Landrum JT (2009) Carotenoids: physical, chemical, and biological functions and properties: CRC Press. p. 488.

[10] Moran NA, Jarvik T (2010) Lateral transfer of genes from fungi underlies carotenoid production in aphids. Science.328:624-7.

[11] Vílchez C, Forján E, Cuaresma M, Bédmar F, Garbayo I, Vega JM (2011) Marine carotenoids: Biological functions and commercial applications. Marine Drugs.9:319-33.

[12] Fraser PD, Bramley PM (2004) The biosynthesis and nutritional uses of carotenoids. Progress in lipid research.43:228-65.

[13] Paiva SAR, Russell RM (1999) β-carotene and other carotenoids as antioxidants. Journal of the American College of Nutrition.18:426-33.

[14] Rao A, Rao L (2007) Carotenoids and human health. Pharmacological Research.55:207-16.

[15] Cunningham Jr FX, Gantt E (2011) Elucidation of the pathway to astaxanthin in the flowers of Adonis aestivalis. Plant Cell.23:3055-69.

[16] Shindo K, Hasunuma T, Asagi E, Sano A, Hotta E, Minemura N, Miyake C, Maoka T, Misawa N (2008) 4-Ketoantheraxanthin, a novel carotenoid produced by the combination of the bacterial enzyme β-carotene ketolase CrtW and endogenous carotenoid biosynthetic enzymes in higher plants. Tetrahedron Letters.49:3294-6.

[17] Gerjets T, Sandmann G (2006) Ketocarotenoid formation in transgenic potato. Journal of Experimental Botany.57:3639-45.

[18] Zhong YJ, Huang JC, Liu J, Li Y, Jiang Y, Xu ZF, Sandmann G, Chen F (2011) Functional characterization of various algal carotenoid ketolases reveals that ketolating zeaxanthin efficiently is essential for high production of astaxanthin in transgenic Arabidopsis. Journal of Experimental Botany.62:3659-69.

[19] Khoo HE, Prasad KN, Kong KW, Jiang Y, Ismail A (2011) Carotenoids and their isomers: Color pigments in fruits and vegetables. Molecules.16:1710-38.

[20] Fernández-García E, Carvajal-Lérida I, Jarén-Galán M, Garrido-Fernández J, Pérez-Gálvez A, Hornero-Méndez D (2012) Carotenoids bioavailability from foods: From plant pigments to efficient biological activities. Food Research International.46:438-50.

[21] Montesano D, Fallarino F, Cossignani L, Bosi A, Simonetti MS, Puccetti P, Damiani P (2008) Innovative extraction procedure for obtaining high pure lycopene from tomato. European Food Research and Technology.226:327-35.

[22] Ermakov IV, Sharifzadeh M, Ermakova M, Gellermann W (2005) Resonance Raman detection of carotenoid antioxidants in living human tissue. Journal of Biomedical Optics.10:1-35.

[23] Bramley PM (2000) Is lycopene beneficial to human health? Phytochemistry.54:233-6.

[24] Sajilata MG, Singhal RS, Kamat MY (2008) The carotenoid pigment zeaxanthin - A review. Comprehensive Reviews in Food Science and Food Safety.7:29-49.

[25] Aman R, Biehl J, Carle R, Conrad J, Beifuss U, Schieber A (2005) Application of HPLC coupled with DAD, APCI-MS and NMR to the analysis of lutein and zeaxanthin stereoisomers in thermally processed vegetables. Food Chemistry.92:753-63.

[26] Britton G (1995) Structure and properties of carotenoids in relation to function. The FASEB Journal.9:1551-8.

[27] Britton G, Liaaen-Jensen S, Pfander H (2004) Carotenoids handbook: 1st ed; Birkhäuser: Basel, Switzerland. p. 15.

[28] Su Q, Rowley KG, Balazs NDH (2002) Carotenoids: Separation methods applicable to biological samples. Journal of Chromatography B: Analytical Technologies in the Biomedical and Life Sciences.781:393-418.

[29] Feltl L, Pacakova V, Stulik K, Volka K (2005) Reliability of carotenoid analyses: a review. Current Analytical Chemistry.1:93-102.

[30] Grumbach E, Arsenault J, McCabe D (2009) Beginners Guide to UPLC. Waters Corporation: Milford, MA.

[31] Rivera S, Vilaró F, Canela R (2011) Determination of carotenoids by liquid chromatography/mass spectrometry: Effect of several dopants. Analytical and Bioanalytical Chemistry.400:1339-46.

[32] Hao Z, Parker B, Knapp M, Yu L (2005) Simultaneous quantification of α-tocopherol and four major carotenoids in botanical materials by normal phase liquid chromatography- atmospheric pressure chemical ionization-tandem mass spectrometry. Journal of Chromatography A.1094:83-90.

[33] Farré G, Bai C, Twyman RM, Capell T, Christou P, Zhu C (2011) Nutritious crops producing multiple carotenoids - a metabolic balancing act. Trends in Plant Science.16:532-40.

[34] Misawa N, Yamano S, Linden H, De Felipe MR, Lucas M, Ikenaga H, Sandmann G (1993) Functional expression of the Erwinia uredovora carotenoid biosynthesis gene crtl in transgenic plants showing an increase of β-carotene biosynthesis activity and resistance to the bleaching herbicide norflurazon. Plant Journal.4:833-40.

[35] Chen Y, Li F, Wurtzel ET (2010) Isolation and characterization of the Z-ISO gene encoding a missing component of carotenoid biosynthesis in plants. Plant Physiology.153:66-79.

[36] Bai C, Twyman RM, Farré G, Sanahuja G, Christou P, Capell T, Zhu C (2011) A golden era-pro-vitamin A enhancement in diverse crops. In Vitro Cellular and Developmental Biology - Plant.47:205-21.

[37] Kim M, Kim SC, Song KJ, Kim HB, Kim IJ, Song EY, Chun SJ (2010) Transformation of carotenoid biosynthetic genes using a micro-cross section method in kiwifruit (Actinidia deliciosa cv. Hayward). Plant Cell Reports.29:1339-49.

[38] Christou P, Twyman RM (2004) The potential of genetically enhanced plants to address food insecurity. Nutrition Research Reviews.17:23-42.

[39] Verpoorte R, Van der Heijden R, Memelink J (2000) Engineering the plant cell factory for secondary metabolite production. Transgenic research.9:323-43.

[40] Capell T, Christou P (2004) Progress in plant metabolic engineering. Current Opinion in Biotechnology.15:148-54.

[41] Sandmann G, Römer S, Fraser PD (2006) Understanding carotenoid metabolism as a necessity for genetic engineering of crop plants. Metabolic Engineering.8:291-302.

[42] Zhu C, Naqvi S, Breitenbach J, Sandmann G, Christou P, Capell T (2008) Combinatorial genetic transformation generates a library of metabolic phenotypes for the carotenoid pathway in maize. Proceedings of the National Academy of Sciences of the United States of America.105:18232-7.

[43] Yuan D, Bassie L, Sabalza M, Miralpeix B, Dashevskaya S, Farre G, Rivera S, Banakar R, Bai C, Sanahuja G, Arjó G, Avilla E, Zorrilla-López U, Ugidos-Damboriena N, López A, Almacellas D, Zhu C, Capell T, Hahne G, Twyman RM, Christou P (2011) The potential impact of plant biotechnology on the Millennium Development Goals. Plant Cell Reports.30:249-65.

[44] Semba RD, Miotti PG, Chiphangwi JD, Saah AJ, Canner JK, Dallabetta GA, Hoover DR (1994) Maternal vitamin A deficiency and mother-to-child transmission of HIV-1. Lancet.343:1593-7.

[45] Underwood BA (2003) Scientific research: essential, but is it enough to combat world food insecurities? The Journal of nutrition.133:1434S.

Objectives

GENERAL OBJECTIVES

The main objective of my research was to develop and improve analytical methods for qualitative and quantitative determination of carotenoids in maize and rice tissues. A second objective was to contribute to elucidating biosynthetic steps, which are believed to control carotenoid accumulation in cereals by correlating gene expression patterns to carotenoid accumulation.

SPECIFIC OBJECTIVES

1. To improve the extraction method of carotenoids from maize endosperm.
2. To develop and improve analytical methods for qualitative and quantitative determination of carotenoids by HPLC and UHPLC using a PDA detector.
3. To develop and improve MS techniques based on API interfaces (ESI, APCI and APPI) for qualitative and quantitative determination of carotenoids by using UHPLC.
4. To describe the carotenoid profile of four transgenic maize lines which expressed different enzyme combinations at different developmental stages.
5. To use the carotenoid metabolic profile of maize and rice tissues to investigate the specific contribution(s) of carotenogenic genes and correlate this to mRNA expression levels of the corresponding transgenes.
6. To carry out preliminary analysis in order to identify new pigments detected in the transgenic lines.

Chapter 1

Development and optimization of analytical methods to analyze carotenoids in cereals

1.1 ABSTRACT

This chapter deals with the development and optimization of analytical methods for the determination of carotenoids in maize endosperm and rice callus tissues. In the first instance I improved the protocol to extract these pigments. I compared different combinations of solvents in order to identify the most suitable solvent system to permit extraction of all carotenoids, with different polarities, present in the samples. I also improved and developed two chromatographic methods to separate these pigments using high performance liquid chromatography (HPLC) and ultra high performance liquid chromatography (UHPLC). Different types of stationary and mobile phases were assessed in order to obtain the most optimal resolution for the different carotenoids in the samples. The identification of these molecules was carried out using a photo diode array (PDA) detector. Lastly, I analyzed carotenoid standards and different samples containing various carotenoids in order to gather information about chromatographic and spectral characteristics of these pigments, including retention time, the wavelength of maximum absorption (λmax) and fine structure.

1.2 INTRODUCTION

1.2.1 Extraction of carotenoids

The choice of extraction method for carotenoid analysis of foods matrices is crucial because errors associated with the extraction process are potentially significant [1]. Given the wide variety of food products containing these compounds and the great range of carotenoids found in these samples, there is no universally accepted or standard method for carotenoid extraction. However, the most widely accepted procedures involve extraction with organic solvents, including pentane, hexane, dichloromethane, chloroform, tetrahydrofuran (THF), methanol (MeOH), ethanol, acetone, ethyl acetate, *n*-butanol, and petroleum ether [2-6]. Many procedures propose the use of freeze-dried material [7], a saponification step to hydrolyze carotenol esters, and removal of lipids and chlorophylls, which may interfere with the chromatographic detection of carotenoids [4, 5, 8]. Mixtures of MeOH and THF are commonly used as first extracting solvents to extract these pigments from maize seeds. Afterwards, the pigments are transferred into a more apolar solvent (hexane, petroleum ether, ethyl ether, methylene chloride, etc.) [9-13]

Although THF and ethyl ether are widely used because of their high capacity to solubilize carotenoids, such solvents can form peroxides, which can rapidly degrade carotenoids and may contribute to secondary products[1]. Therefore, it has been recommended that antioxidants such as 2,6-bis(1,1-dimethylethyl)-4-methylphenol (BHT) be added to the solvent [5]. In addition, the extraction of carotenoids must be carried out rapidly, avoiding exposure to light, oxygen, high temperatures and to prooxidant metals, such as iron or copper, in order to minimize autooxidation and *cis–trans* isomerization [5].

1.2.2 High-performance chromatographic analysis

1.2.2.1 Separation

Among the high performance chromatographic methods available, gas chromatography (GC) is unsuitable for the analysis of carotenoids because of the inherent instability and low volatility of these molecules. Therefore, high performance liquid chromatography (HPLC) using absorption and mass detection techniques is currently the most common chromatographic method used for their analysis [14]. Improvements in chromatographic performance using ultra high performance liquid chromatography (UHPLC) have recently been reported [15-19]. This technique uses narrow-bore columns packed with very small particles (below 2 μm) and mobile phase delivery systems operating at high back-pressures. While in conventional HPLC the maximum back-pressure is in the region of 35–40 MPa depending on the instrument, back-pressures in UHPLC can reach up to 103.5 MPa [20].

[1] Most of the methods used to eliminate peroxides require highly reactive reagents, are time consuming and require extreme caution throughout the process of eliminating peroxides.

Thus, UHPLC offers several advantages over conventional HPLC, such as faster analyses (shorter retention times), narrower peaks (giving increased signal-to-noise ratio) and greater sensitivity [21].

1.2.2.2 Analysis of carotenoids by HPLC

Normal- and reversed-phase systems, in isocratic or gradient elution modes, have been used to analyze carotenoids. However, most separations of these compounds reported in the literature involve reversed-phase HPLC using C18 and C30 columns [14]. The performance of the columns is dependent on several parameters including alkyl phase length, silanol activity, bonding density, substrate pore diameter, etc. The combination of these properties must be considered when separating analytes. Various mixtures of solvents have been used with these reversed-phases, including water, MeOH, acetonitrile (ACN), 2-propanol, acetone, ethyl acetate, THF, *tert*-butyl methyl ether (MTBE), dichloromethane and chloroform [22, 23]. In general, polymeric C30 phases provide better separations of carotenoid geometric isomers than C18 ones. This finding is attributed to be the enhanced shape selectivity of the former [14]. The term "shape selectivity" is commonly used to denote a chromatographic quality exhibited by certain stationary phases for which enhanced separations of geometric isomers result based on their molecular structure, rather than other physical or chemical differences of the solutes [24]. However, C18 stationary phases have also been reported to yield relatively good separations of these isomers; for example, polymeric C18 phases have provided acceptable selectivity for the separation of the geometric isomers of β-carotene, lutein and zeaxanthin [14]. C30 phases also provide a satisfactory resolution for carotenoids with similar polarity [14].

1.2.2.3 Analysis of carotenoids by UHPLC

UHPLC is a promising tool for carotenoid analysis. High strength silica (HSS) C18 and T3 and ethylene bridged hybrid (BEH) C18 stationary phases have been successfully used to separate several carotenoids [14]. One of the main differences between HPLC and UHPLC columns is the particle size of the stationary phase. While in HPLC particles are over 2 μm, they are smaller in UHPLC. Smaller particles tend to reduce the H value (height equivalent to a theoretical plate), and this means that the column is more efficient as it provides more theoretical plates per unit length. Moreover, small particles tend to allow solutes to transfer into and out of the particle more quickly because their diffusion path lengths are shorter. Thus, the solute is eluted as a narrow peak because it spends less time in the stationary and stagnant mobile phases where band broadening occurs. The increase in efficiency boosts the resolution parameter (Rs). Consequently, a higher resolution between analytes is expected.

When run at the optimal flow rate, the pressure produced by smaller particles will exceed the pressure limitations of conventional HPLC systems. Therefore, UHPLC columns are used in a liquid chromatography (LC) instrument designated to operate at the optimal linear velocity (and resulting

pressure) for these particles while minimizing the dispersion of the flow path such that theoretical performance of the separation column could be achieved. For example, in these instruments the distance between the injector and column inlet have been minimized in order to reduce band spreading [25]. The key to UHPLC separations is the combination of the instrument and column performance that allows scientists to fully realize and harness the power of sub-2 μm particle columns. This is achieved by minimizing band spreading within (intra-column) and outside (extra-column) the column and being able to operate at the optimal linear velocities (and pressures) of these small particles columns.

Because I used BEH C18 stationary phase to separate carotenoids, I will only describe this type of column in more detail. The BEH particles are hybrids of inorganic and organic components that are homogeneously blended throughout the particle synthesis process. As shown in Fig. 1, BEH Technology^{TM} particles are prepared from two high purity monomers: tetraethoxysilane [TEOS] and bis(triethoxysilyl)ethane [BTEE, which incorporates the preformed ethylene bridge]. The use of hybrid technology allows for the best properties of both silica (inorganic component) and polymeric (organic component) particles. The silica combined with the organic bridging group provides the mechanical strength needed for UHPLC. The bridged ethylene group provides the high pH stability that allows the use of pH 12 mobile phase [26].

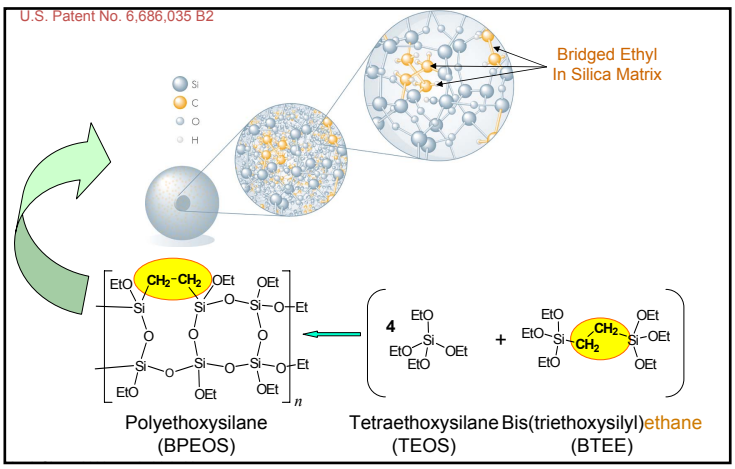

Figure 1-1. Bridged ethyl hybrid particles [26].

With BEH C18 column as well as with HPLC C18 columns, xanthophylls are eluted before carotenes. The order of elution of the xanthophylls depends on the number and type of functional groups present. Thus, carotenoids containing hydroxyl groups elute earlier than those with keto groups (comparing xanthophylls with the same backbone structure) [14].

1.2.3 Spectral characteristics of carotenoids

1.2.3.1 Light absorption

Because of their long conjugated double-bond system, carotenoids absorb light strongly and exhibit intense main absorption bands in the visible or, in some case, ultraviolet (UV) region. Most carotenoids exhibit three absorption maxima between 400-500 nm resulting in three-peak spectra (Fig. 2) [4]. The greater the number of conjugated double bonds, the higher the wavelength of maximum absorption (λmax). Nevertheless, cyclization of the molecule results in: a hypsochromic shift (displacement of λmax to shorter wavelength), a hypochromic effect (decrease in absorbance), and a loss of fine structure (spectrum with less defined peaks). Lycopene, an unsaturated acyclic carotenoid, is red and has λmax at 444, 470, 502 nm; bicyclic β-carotene, although possessing the same number of conjugated double bonds as lycopene, is yellow orange and has a λmax at 450 and 477 nm and a mere inflection (shoulder) at 425 nm. Monocyclic γ-carotene is red orange and exhibits a λmax and spectrum, intermediate between those of lycopene and β-carotene [4, 27]. Other carotenoids instead of having a three peak spectra, have a spectrum that consists of a rounded almost symmetrical single maximum peak. This is the case for ketocarotenoids, such as astaxanthin and canthaxanthin [28].

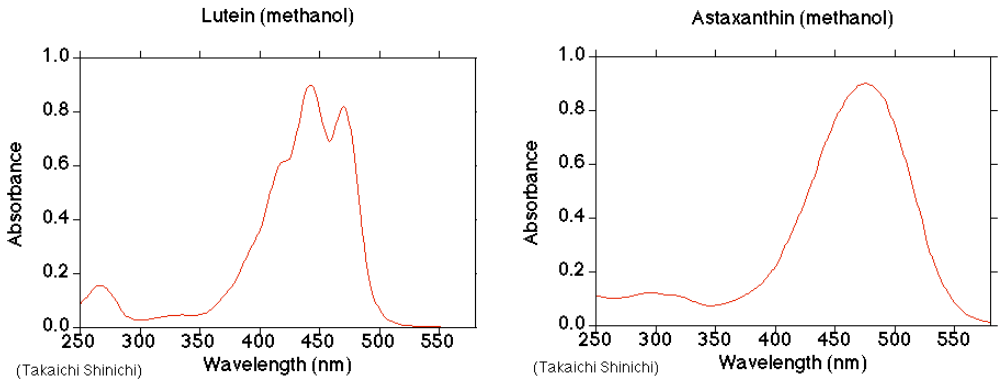

Figure 1-2. Absorption spectra of lutein and astaxanthin. Lutein absorbs maximally at three wavelengths between 400-500 nm resulting in three-peak spectra whereas the ketocarotenoid astaxanthin has a spectrum that consists of a rounded almost symmetrical single maximum peak [29].

The majority of natural carotenoids have double bonds in the all-*trans* configuration; however, some exhibit a *cis–trans* configuration [30, 31]. *cis*-Isomerization of the double-bonded system gives the compound a slightly lighter color and brings about both a hypsochromic shift (normally between 2 and 6 nm at shorter wavelengths) and a hypochromic effect (decrease in absorbance due to the appearance of a "*cis*" peak approximately 142 nm below the λmax of its *trans*-isomer) (Fig. 3) [32].

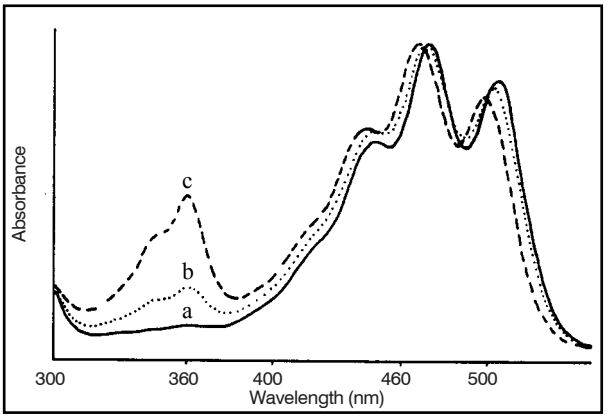

Figure 1-3. Ultraviolet-visible (UV-vis) spectra of all-*trans*-lycopene (a), 13-*cis*-lycopene (b) and 15-*cis*-lycopene (c). Mobile phase: ACN:ethyl acetate:MeOH (8.5:1:5, v/v) [33].

Carotenoids in solution obey the Beer-Lambert law (their absorbance is directly proportional to concentration in a large concentration range). Thus, carotenoids can be quantified spectrophotometrically. The absorption coefficient $A_{1\,cm}^{1\%}$ of a carotenoid (absorbance at a given wavelength of a 1% solution in 1 cm light-path spectrophotometer cuvette) is used in the calculation of its concentration [28].

1.2.3.2 Fine structure

Although the main absorption bands for most carotenoids fall within the 400-500 nm wavelength region, there is considerable variation in the shape of the spectrum for different carotenoids. The fine structure (Fig. 4) can also be indicated numerically as "%III/II". This indicates the relationship between the peak heights of the longest-wavelength absorption band, designated III, and that of the middle absorption band, designated II, taking the minimum between the two peaks as baseline, multiplied by 100 [33].

The λmax and the shape of the spectrum (spectral fine structure) are characteristic of the chromophore of the molecule and provide valuable information for identifying carotenoids.

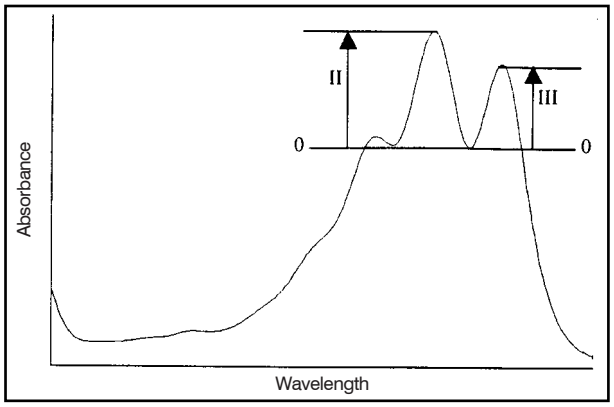

Figure 1-4. Calculation of %III/II as indication of spectral fine structure (%III/II = III/II × 100) [33].

1.3 OBJECTIVES

- To improve the extraction method of carotenoids from maize endosperm.
- To develop and improve analytical methods for qualitative and quantitative determination of carotenoids by HPLC and UHPLC using a photo diode array (PDA) detector.
- To analyze carotenoid standards and different matrices containing diverse carotenoids in order to gather information about the chromatographic and spectral characteristics of these pigments.

1.4 MATERIALS AND METHODS

1.4.1 Chemicals

β-Carotene, lycopene, lutein, *β*-cryptoxanthin, astaxanthin, *β*-apo-8′-carotenal were purchased from Sigma-Aldrich Fine Chemicals (St. Louis, MO, USA). Canthaxanthin and zeaxanthin were acquired from Fluka (Buchs SG, Switzerland). Phytoene, violaxanthin, neoxanthin, and antheraxanthin were purchased from Carotenature (Lupsingen, Switzerland). Ethanol, 2-propanol, MeOH, ethyl acetate, hexane, ethyl eter, TBME, THF, ACN and acetone (HPLC grade purity) were acquired from J.T. Baker (Deventer, The Netherlands). Water was prepared using a Milli-Q reagent water system.

1.4.2 Plant material

The transgenic maize seeds and rice callus were generated by combinatorial nuclear transformation as reported in Zhu et al. [34]. A transgenic maize line (TM) 1, expressing *Zea mays* phytoene synthase 1 (*Zmpsy1)*, *Pantoea ananatis* phytoene desaturase (*PacrtI*), *Gentiana lutea* lycopene *β*-cyclase (*Gllycb*) and *Paracoccus β*-carotene ketolase (*ParacrtW*), was selected to optimize the extraction process.

The following plant material was used in order to develop and optimize the chromatographic systems and determine the chromatographic and spectral characteristics of the carotenoids:

TM: TM1; TM2, expressing *Zmpsy*1 and *PacrtI*; TM3, expressing *Zmpsy*1*,* biochemically synthesized *sCrBkt* from *Chlamydomonas reinhardtii* and biochemically synthesized *sBrcrtZ* from *Brevundimonas sp. Strain SD212*; TM4, which corresponded to the cross of TM2 with TM3, therefore, expressing *Zmpsy*1, *PacrtI, sCrBkt* and *sBrcrtZ*; and TM5, which corresponded to the cross of TM3 with a wild type maize plant NSL76, therefore, expressing *Zmpsy*1, *sCrBkt,* and *sBrcrtZ*.

Transgenic rice callus (TC): TC1, expressing *Zmpsy*1 and *Pacrtl*; TC2, expressing *Zmpsy*1, *Pacrtl* and 1-deoxy-D-xylulosa 5-phosphate synthase from *Arabidopsis thaliana* (*Atdxs*); TC3, expressing *Zmpsy*1, *Pacrtl* and *β*-carotene ketolase from *Brevundimonas* sp. Strain SD212 chemically synthesized (s*BrcrtW*) and TC4, expressing *Zmpsy*1, *Pacrtl* and *sCrBkt*.

1.4.3 Extraction of carotenoids from maize endosperm

To protect carotenoids from degradation and oxidation, the extraction was conducted under limited light.

1.4.3.1 Reference method

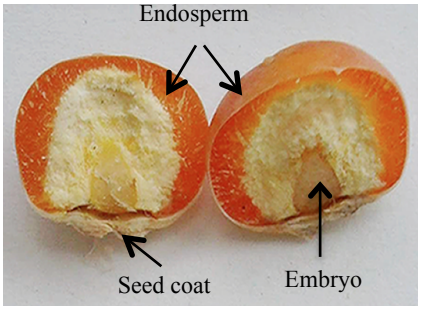

Figure 1-5. Components of maize seed.

The procedure described by Naqvi 2009 [13] was used as a reference method. Maize endosperm was excised by removing the seed coat and embryo (Fig. 5). Only the maize endosperm was used for extraction because carotenoids were designed to accumulate only in this tissue by virtue of the genetic construct used to create the transgenic maize plants (endosperm specific expression) [37]. Samples were freeze-dried and ground into a fine powder using a mortar and pestle. 50 or 100[2] mg of sample was extracted with 15 mL of MeOH: THF (1:1, v/v) at 60 °C for 20 min and this mixture was continuously shaken. It was then put on ice until it reached room temperature and the liquid phase was filtered into a separatory funnel (if the residue exhibited color after extraction, then it was re-extracted with 5 mL of MeOH: THF (1:1, v/v) at 60 °C for 5 min and the second extract was combined with the first one). 15 mL of hexane: diethyl ether (9:1, v/v) was added to the organic extract and the mixture was shaken vigorously. Then, 20 mL of saturated sodium chloride solution was added and the mixture was shaken again. The aqueous phase was removed and the organic phase was washed with water once again. The organic phase was dried under N_2 at 37 ºC until the volume was adjusted to 5 mL. 1 mL of blank solution was transferred to a cuvette and this was used to set the baseline absorbance of the spectrophotometer at 450 nm. The absorbance of 1 mL of the organic phase was determined. This organic phase was returned back into the tube and left under N_2 for further drying. When the sample was completely dry, Ar was flushed into the vial and carotenoids were stored at -80 ºC until LC analysis. Fig. 6 shows the carotenoid extraction process in a schematic form.

No saponification step was included because carotenoids are generally not present in the ester forms in maize [7]. This step also has the inherent disadvantage of causing carotenoid losses [12]. When carotenoids are the only pigments present in the samples, extraction is facilitated as the process can be

[2] The amount depends on the color intensity of the samples. For pale color maize samples, extract 100 mg of sample. For darker color maize samples, it is sufficient to extract 50 mg of sample.

monitored. Consequently, loss of color was used as an indication of complete or satisfactory carotenoid extraction from the matrix.

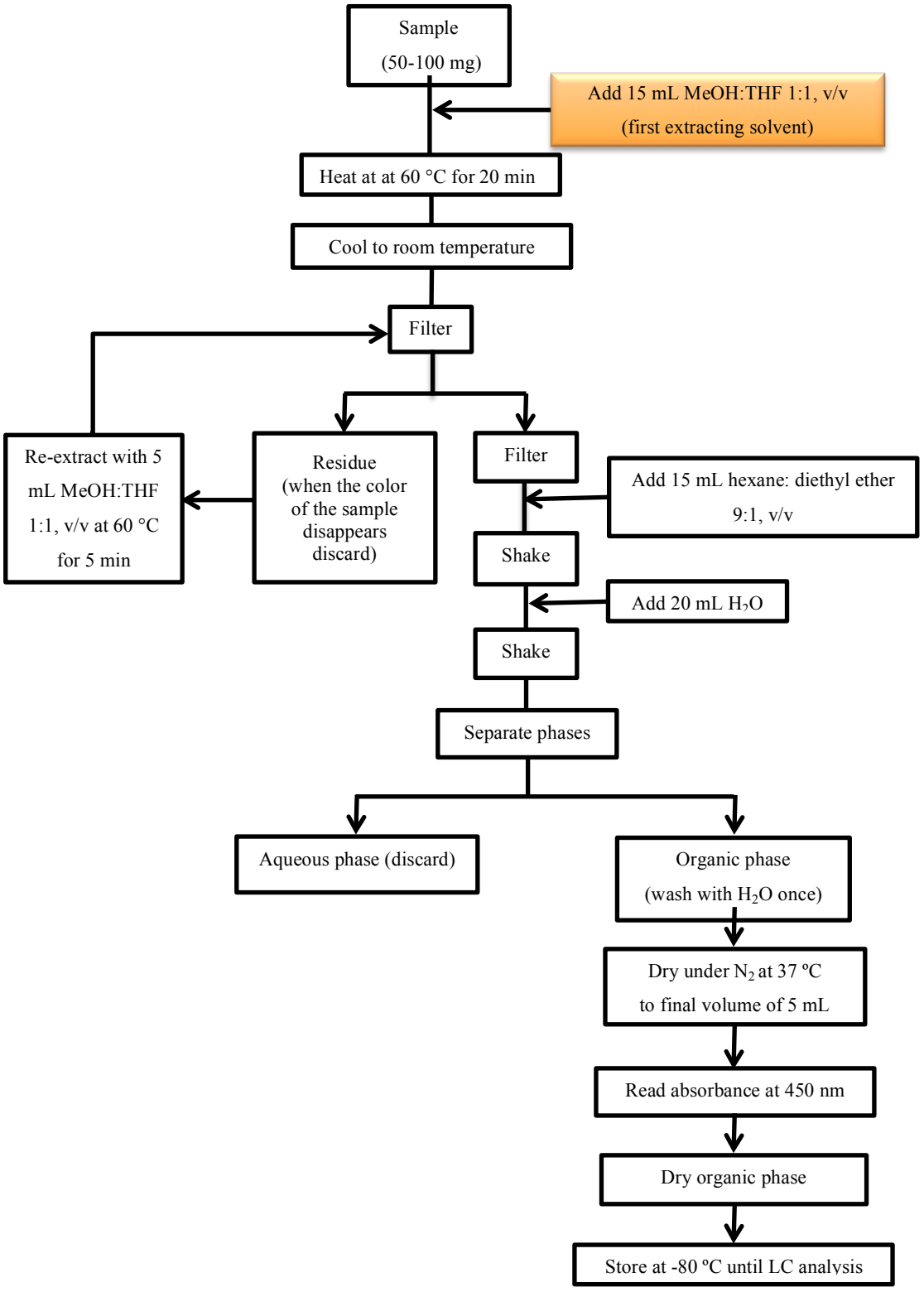

Figure 1-6. Schematic diagram of carotenoid extraction process [13].

1.4.3.2 Blank solution

A blank solution was prepared by carrying out the same extraction process described in section 1.4.3.1, without sample.

1.4.3.3 Modified Optimization

In order to compare solvents or combinations of the same in the first step of the carotenoid extraction to replace THF, we evaluated five modifications of the solvent system used to extract total carotenoids from maize seeds under otherwise identical conditions.

Modification 1: ethanol (100%); *modification 2*: acetone (100%); *modification 3*: acetone (100%) but after weighing, the sample was covered with water (about 400 μL) and the mixture allowed to stand at room temperature for 1 h before commencing extraction with this solvent; *modification 4*: acetone: ethanol: hexane (1:1:2, v/v); and *modification 5*: MeOH: ethyl acetate (6:4, v/v).

1.4.3.4 Extraction using BHT

BHT at a concentration of 0.1% was added to the extraction solvents used in *modification 5*: MeOH: ethyl acetate 6:4, v/v and hexane: diethyl ether 9:1, v/v. Each extraction was carried out in triplicate.

1.4.4 Preparation of carotenoid standards

Standard solutions of antheraxanthin, violaxanthin, neoxanthin, astaxanthin, canthaxanthin, zeaxanthin, lutein, β-apo-8′-carotenal, β-cryptoxanthin, lycopene, β-carotene, and phytoene were prepared in the injection solvent [ACN: MeOH 7:3, v/v]: acetone 6.7:3.3, v/v at concentrations of 1.10, 0.51, 0.61, 0.64, 0.71, 0.54, 0.54, 0.70, 1.17, 2.00, 1.55 and 1.00 μg/mL, respectively.

1.4.5 Chromatographic analysis

1.4.5.1 UHPLC-PDA analysis

UHPLC analysis was carried out using an ACQUITY Ultra Performance LC™ system linked to a PDA 2996 detector (Waters, Milford, MA, USA). MassLynx™ software version 4.1 (Waters, Milford, MA, USA) was used to control the instruments, and also for data acquisition and processing.

UHPLC chromatographic separations were performed on reversed-phase columns ACQUITY UPLC® C18 BEH 130Å, 1.7 μm, 2.1×100 mm and 300Å, 1.7 μm, 2.1×150 mm (Waters, Milford, MA). Final mobile phase consisted of solvent A: ACN: MeOH 7:3, v/v and solvent B: water 100%. The gradient program used is shown in Table 1. The column and sample temperatures were set at 32°C and 25 °C respectively. Injection volume was 5 μL.

Each sample extract for LC analysis was dissolved in 300 μL and 1000 μL (for light and dark color extract respectively) of the injection solvent [ACN: MeOH 7:3, v/v]: acetone 6.7:3.3, v/v. Before use, all solutions were filtered through Millex 0.2 μm nylon membrane syringe filters (Millipore, Bedford,

MA, USA).

Table 1-1. Gradient profile used in the separation of carotenoids by UHPLC. Linear gradient.

Time[a] (min)	Flow rate (mL/min)	A (%, v/v)	B (%, v/v)
Initial	0.4	80	20
2.0	0.4	80	20
3.0	0.4	100	0
7.0	0.4	100	0
8.0	0.6	100	0
11.6	0.6	100	0
12.6	0.4	80	20

[a] After this time, the system was left 2 min more to reach its re-equilibration before injecting a new sample.

1.4.5.2 HPLC-PDA analysis

HPLC analysis separations was carried out using a Waters Alliance 2695 separation module linked to a PDA 2998 detector (Waters, Milford, MA, USA). Empower software version 2 (Waters, Milford, MA, USA) was used to control the instruments, and also for data acquisition and processing.

HPLC chromatographic separations were performed on X-Bridge HPLC C18 BEH 100Å, 5 μm, 2.1×150 mm and 300Å, 3.5 μm, 2.1×250 mm columns and a YMC C30 carotenoid 3 μm, 2.0×100 mm column (Waters, Milford, MA). The mobile phase used with the X-Bridge HPLC BEH C18 columns was ACN: MeOH: 2-propanol 8.5:1:0.5, v/v/v with isocratic separation and flow rate at 0.2 mL/min. The column and sample temperatures were set at 32 °C and 25 °C respectively. Injection volume was 10 μL. The mobile phase used with the YMC C30 column consisted of solvent A: MeOH: water 8:2, v/v and solvent B: TBME 100%. The gradient program used is shown in Table 2. Both, the column and the sample temperatures were set at 25 °C. Injection volume was 10 μL.

Table 1-2. Gradient profile used in the separation of carotenoids by HPLC. Linear gradient.

Time[a] (min)	Flow rate (mL/min)	A (%, v/v)	B (%, v/v)
Initial	0.25	97	3
6.0	0.25	97	3
7.0	0.25	62	38
15.0	0.25	62	38
16.0	0.25	32	68
18.0	0.25	32	68
19.0	0.25	0	100
25.0	0.25	0	100
26.0	0.25	32	68
27.0	0.25	50	50
28.0	0.25	70	30
29.0	0.25	97	3

[a] After this time, the system was left 6 min more to reach its re-equilibration before injecting a new sample.

1.4.6 UV-vis spectroscopy

Absorption spectra and absorbance were recorded using a UV/VIS Spectrometer UV2 ATI UNICAM, Cambridge, UK.

1.4.7 Statistical analysis

The Student's *t*-test was used to determine differences in the mean values of carotenoid content obtained by the extraction methods. Microsoft Excel version 2010 (Microsoft Corp.) was used for data analysis.

1.5 RESULTS AND DISCUSSION

1.5.1 Improvements in the extraction process

Initially, the method described by Naqvi [13] was used to extract carotenoids from maize endosperm. However, as this approach involves THF in the first step of the carotenoid extraction procedure (section 1.4.3.1), I replaced it to prevent the formation of peroxides, which are known to catalyze carotenoid decomposition. Thus, I evaluated five modifications of the solvent system used to extract carotenoids from maize seeds. *Modification 1,* used ethanol 100%; *modification 2*, acetone 100%; *modification 3*, acetone 100% but after weighing, the sample was covered with water (about 400 μL) and the mixture was allowed to stand at room temperature for 1 h before starting the extraction with this solvent; *modification 4,* acetone: ethanol: hexane (1:1:2, v/v); and *modification 5*, MeOH: ethyl acetate (6:4, v/v). Table 3 shows the various methods studied for carotenoid extraction.

Table 1-3. Total carotenoids extracted with different solvent systems.

Modified method	Solvents	Replicates	Output Factor[c] (μg/g DW)	% Non- extracted carotenoids	Ref.
1	Ethanol	2	111.8±7.10	21.3	[38, 39]
2	Acetone	3	106.5±2.61	25.0	[40, 41]
3	Acetone[a]	3	126.3±2.50	11.10	[42]
4	Acetone:ethanol:hexane (1:1:2, v/v)	2	120.9±3.64	14.9	[43]
5	MeOH:ethyl acetate (6:4, v/v)[b]	3	141.6±2.12	0	-
Reference	MeOH:THF (1:1, v/v)	3	142.1±1.94	0	[13, 44, 45]

[a] Samples were hydrated
[b] This mixture of solvents was developed in our laboratory
[c] Results are presented as means ± standard deviation (SD) from the same sample batch

Each extraction was replicated 2 or 3 times and the mean value of the total carotenoid content was used as the Output Factor. Higher values indicate better extraction capacity. The total carotenoid content was calculated spectrophotometrically using the following equation [46]:

$$C = \frac{Abs \times 10^4 \times V}{A_{1cm}^{1\%} \times w}$$

Where,

$A_{1\,cm}^{1\%}$ = absorption coefficient, which is defined as the theoretical absorbance of a solution of 1% (w/v) concentration (*i.e.* g in 100 mL) in a cuvette of 1 cm path length. Lutein and zeaxanthin are the major carotenoids in maize. Therefore, an average value for $A_{1\,cm}^{1\%}$ equal to 2332 was used [46].

C = total carotenoid content (μg/g) in a given sample on dry weight basis

Abs = absorbance measured at 450 nm

V = volume (mL)

W = weight of sample (g)

10^4 = conversion factor to obtain the concentration in units of μg/g

The total carotenoid content obtained with the six methods ranged from 106.5 to 142.1 μg/g DW. The percentage of un-extracted carotenoids was calculated by assigning a value of 100% to the method that resulted in the highest total carotenoids extracted (Table 3).

The solvents tested to replace the THF were selected taking into account the following reasons: MeOH and ethanol were tested because they can affect cell wall permeability. This feature is relevant because carotenoids are confined within plant cells and the walls of these cells are complex in terms of chemical composition. We tested mixtures of MeOH, ethanol, acetone (polar solvents), ethyl acetate (medium-polar solvent) and hexane, a non-polar solvent, searching for the co-solubilization of carotenoids with different polarities present in the samples. Non-polar carotenoids (e.g. lycopene and β-carotene) are more soluble in hexane and ethyl acetate [35, 36] while more polar carotenoids (e.g. lutein or epoxy carotenoids) show greater solubility in ethanol and acetone [6, 37]. Because several researchers have reported the use of acetone alone for carotenoid extraction [5], it was also evaluated as the first extraction solvent to replace the THF.

1.5.1.1 Comparison of the extraction methods

The reference method and *modification 5* (using THF: MeOH 1:1, v/v and MeOH: ethyl acetate 6:4, v/v as solvents, respectively) were the most effective in extracting carotenoids from maize endosperm. Indeed, only with these methods was a complete loss of color observed in the samples (from yellow to white), thereby indicating a suitable extraction capacity. The total extracted carotenoids for the reference method and *modification 5* were: 142.1 and 141.6 μg/g DW, respectively. A Student's *t*-test determined that there was no statistically significant difference between the total carotenoid content obtained with the two methods (*t* calculated value: 0.27 < *t* critical value: 2.78 for 4 degrees of freedom at the α = 0.05 level). *Modification 3* resulted in a higher

total content of extracted carotenoid than *modification 4*, followed by *modifications 1* and *2*. The total carotenoids extracted with these methods were 126.3, 120.9, 111.8 and 106.5 μg/g DW, respectively.

The Student's *t*-test showed a statistically significant difference (*t* calculated value: 12.38 > *t* critical value: 2.78 for 4 degrees of freedom at the α = 0.05 level) between the total carotenoid content obtained in *modifications 2* and *3*. Consequently, it could be concluded that the degree of hydration of the samples accounts for the differences observed in the amount of carotenoids extracted with acetone. *Modification 3* was shown to perform better for extracting carotenoids from maize endosperm. Higher carotenoid content obtained using this method might be attributable to the fact that water helped acetone to penetrate the endosperm more efficiently, thus increasing the extractability of the carotenoids [42]. The presence of water in the sample has an effect on the extractability of carotenoids. Hence, the level of hydration of the sample influences the choice of solvents used to extract carotenoids efficiently and reproducibly [6, 33].

Howe et al. [7] compared several procedures to extract maize kernels. Among those examined, that described by Kurilich and Juvik [47] was found to be the most reliable method to determine the content of carotenoids in maize. The method requires the saponification of the sample with 80% potassium hydroxide w/v at 85 ºC before extraction of carotenoids with hexane. Although carotenoids in maize are generally not present in the ester form [7], saponification was performed to remove saponifiable lipids, which could interfere with the chromatographic analysis. Contrary to Howe et al. [7], our procedures did not require a saponification step since the embryo was removed to eliminate the presence of lipids. These results demonstrate the relevance of initial sample preparation prior to extraction. *Modification 5* was chosen to carry out the carotenoid extraction in the further analyses, since the reference method included THF.

1.5.1.2 Effect of adding BHT to the extraction solvents

In order to establish whether the addition of BHT to the extraction solvents used in *modification 5* favored the carotenoid stability during analysis, transgenic maize TM2 was extracted with and without BHT. Samples were injected into a chromatograph 48 h after extraction. There was no statistically significant difference between the individual and total carotenoid content in samples in spite of using an antioxidant (Table 4). Indeed, the *t* calculated value was always lower than the *t* critical value for all the cases (Table 4). These results demonstrate that the addition of BHT to the extraction solvents can be omitted provided that carotenoids are analyzed within 48 h of storage at -80 ºC.

Table 1-4. Comparison of the individual and total carotenoid content of samples extracted with and without BHT.

Carotenoid	With BHT (µg/g DW)	Without BHT (µg/g DW)	*t* Calculated[a]	*t* Critical
Astaxanthin	8.18±0.06	8.22±0.06	0.76	2.78
Adonixanthin	2.46±0.03	2.51±0.11	0.80	2.78
Zeax+lut	2.25±0.11	2.37±0.36	0.56	2.78
Adonirubin	1.52±0.02	1.52±0.01	0.36	2.78
Canthaxanthin	0.98±0.00	0.96±0.05	0.47	2.78
Total carotenoid	15.39±0.16	15.84±0.58	1.29	2.78

[a] $\alpha = 0.05$; degree of freedom: 4
Abbreviations: Zeax+lut, sum of the concentrations of zeaxanthin and lutein; Total carotenoids, total carotenoid content.

As no difference was observed in the concentration of carotenoids when these were quantified with or without BHT, no antioxidant was added to the extraction solvents in the further analysis.

Although initially the optimization of the carotenoid extraction method was carried out to extract carotenoids from maize endosperm, *modification 5* was also found to be effective for the extraction of carotenoids from rice callus. In this case, the same criterion of loss of color was employed as an indication of complete or satisfactory extraction. For pale color callus samples, 20 mg were extracted and for darker color callus samples, 10 mg were extracted. The volumes of the solvents used in the extraction process were the same as those used for extracting carotenoids from maize endosperm.

1.5.2 Performance of the LC systems

As most separations of carotenoids reported in the literature employ C18 and C30 stationary phases [14], I also used these stationary phases to separate the carotenoids presents in the maize endosperm and rice callus.

1.5.2.1 Comparison of the performance of C18 stationary phases on carotenoid separation

Initially, I compared the effect of the particle and pore size of four C18 stationary phases in the separation of carotenoids. The particle substrate and bonded phase chemistry of the four columns were identical. The different combinations of particle and pore size of the stationary phases allowed me to develop four different chromatographic systems: two for HPLC (systems I and II) and two for UHPLC (systems III and IV). Table 5 shows the properties of these C18 stationary phases.

Table 1-5. Properties of the C18 stationary phases.

System[a]	LC	Pore size (Å)	Particle size (µm)	Column dimensions (mm)	Flow rate (mL/min)[b]	Stationary phase
I	HPLC	100	5	2.1 × 150	0.2	X-Bridge HPLC BEH C18
II	HPLC	300	3.5	2.1 × 250	0.2	X-Bridge HPLC BEH C18
III	UHPLC	130	1.7	2.1 × 100	0.4	ACQUITY UPLC BEH C18
IV	UHPLC	300	1.7	2.1 × 150	0.4	ACQUITY UPLC BEH C18

[a] For all the systems, the column and sample temperatures were 32°C and 25°C respectively and injection volume was 10 μL.
[b] Isocratic separation: ACN: MeOH: 2-propanol 8.5:1:0.5, v/v/v.

The four chromatographic systems were evaluated using the transgenic maize TM1 to ascertain the effect of all parameters on diverse carotenoids. Identical conditions were used in the four chromatographic systems with the exception of flow rate.

Fig. 7 shows that retention times (RT) for all carotenoids were shorter in the UHPLC compared to the HPLC systems. Total time for carotenoid elution was 8.0 and 6.0 min for UHPLC systems III and IV, respectively, while total carotenoid RT in HPLC systems II and I was 24.0 and 22.0 min, respectively. This latter result is in accordance with results reported by different authors [7, 48-50] who reported total analysis times of up to 15 min and 25 min for xanthophylls and carotenes, respectively, using HPLC systems.

Chromatographic peak resolution was usually higher in the UHPLC systems compared with that obtained in HPLC. Fig. 7 shows how two carotenoids that coelute (peak 4) in HPLC systems II and I were better resolved (peaks 4a and 4b) using UHPLC systems III and IV. Similarly, the resolution of the peaks labeled 1 and 2 in UHPLC systems III and IV was improved compared with that obtained in HPLC systems I and II.

These results demonstrated that the smaller particle size of the stationary phases in the UHPLC columns improved resolution of peaks that were poorly resolved or unresolved with the columns used in HPLC. Smaller particles tend to reduce the H value (height equivalent to a theoretical plate), increasing the column efficiency as it provides more theoretical plates per unit length. Moreover, small particles tend to allow solutes to transfer into and out of the particle more quickly because their diffusion path lengths are shorter. Thus, the solute is eluted as a narrow peak because it spends less time in the stationary and stagnant mobile phase where band broadening occurs. The increase in efficiency boosts the resolution parameter (Rs). Consequently, a higher resolution between analytes is expected.

An effect of the pore size on carotenoid RT was observed with the UHPLC C18 stationary phases tested. Both UHPLC columns had the same particle size but different pore size and column dimensions. UHPLC column used in system IV had a bigger pore size and a longer length than the corresponding column used in system III (300 Å, 150 mm and 130 Å, 100 mm, respectively). Because of the length of these columns, it was expected that system IV would result in the longest total analysis time; however, this did not occur. Most likely, the shorter analysis time with system IV was due to the fact that carotenoids had a less effective interaction with the stationary phase as a result of the bigger pore size of this phase. It is known that small pores provide greater surface area [51], thus enabling higher interaction between analytes and the stationary phase. Therefore, the difference in pore size of these stationary phases rather than the difference in column length appeared to influence the RT of the carotenoids more. Conversely, no effect of the pore size of the stationary phase on carotenoid RT was observed with the HPLC columns. However, it should be noted that the HPLC columns had more differences in their properties (dimensions, particle and pore size) than UHPLC

columns, consequently making it more difficult to observe clearly an effect of the pore size of the stationary phase.

Because UHPLC system III (as well as system IV) resulted in the shortest analysis time and exhibited a much better resolution for carotenoids, I selected this system to separate these molecules.

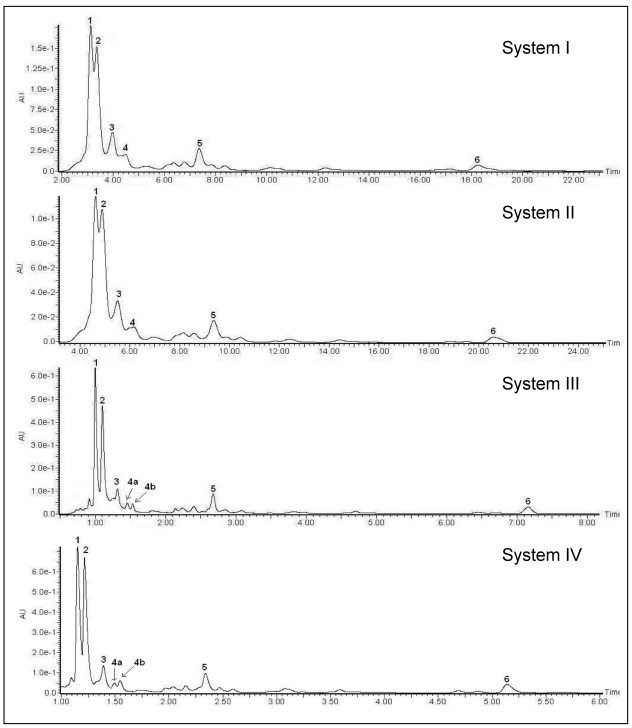

Figure 1-7. Comparison of the carotenoid separation employing HPLC and UHPLC systems. Chromatographic conditions are given in section 1.4.5. System I and II using HPLC; system III and IV using UHPLC. Peak identification: (1) Adonixanthin, (2) zeaxanthin coeluting with lutein, (3), (4a) and (4b) *cis*-isomers of zeaxanthin and lutein (5) *α*-cryptoxanthin and (6) *β*-carotene. Samples were dissolved in ACN: MeOH: 2-propanol 8.5:1:0.5, v/v/v.

1.5.2.2 Appropriateness of the UHPLC system III for the profiling of carotenoids in maize seeds and rice callus

Further improvements to the chromatographic system to separate carotenoids are described here.

Mobile phase:

Originally, a mobile phase consisting of ACN: MeOH: 2-propanol 8.5:1:0.5, v/v/v, which has been used in the separation of carotenoids employing C18 columns [34, 52], was tested. However, when samples were solubilized in 100% acetone [34] and separated using this mobile phase, it was not possible to obtain a good separation for these molecules. As it is advisable to prepare the sample in the operating mobile phase for the best peak shape and sensitivity [53], I dissolved the samples in the mobile phase. I also evaluated a second mobile phase comprising ACN: MeOH 7:3, v/v in order to determine the most optimal conditions to separate the carotenoids. Fig. 8 shows the comparison of the separation of carotenoids of transgenic maize TM2 employing both mobile phases and various injection solvents.

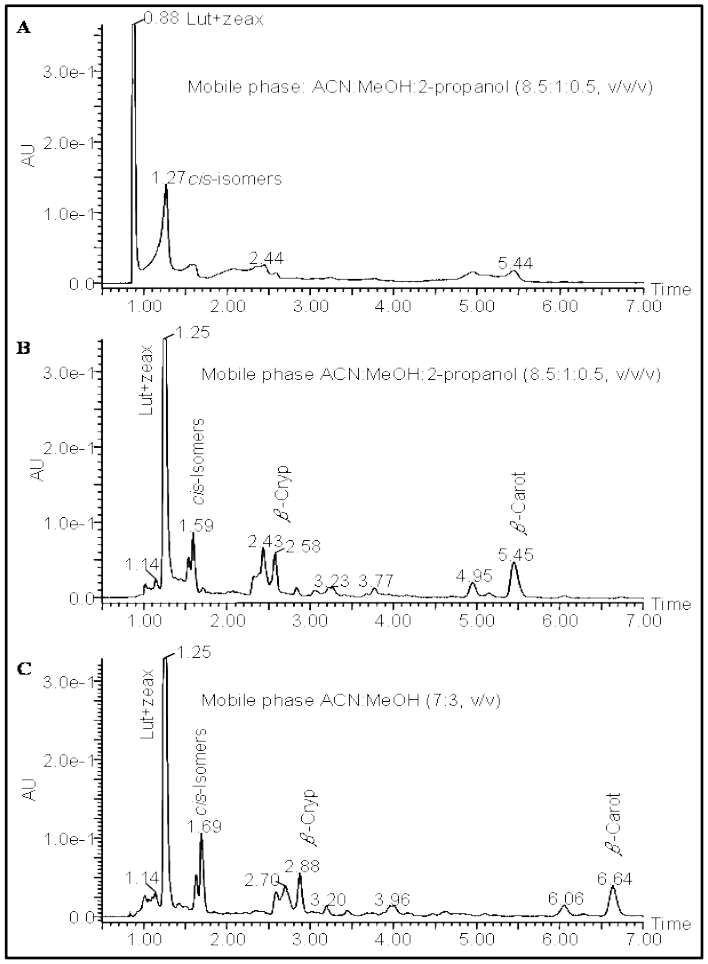

Figure 1-8. Comparison of the separation of carotenoids of transgenic maize TM2 employing different mobile phases and injection solvents. A) Sample dissolved in 100% acetone; B) and C) samples dissolved in ACN: MeOH: 2-propanol 8.5:1:0.5, v/v/v. Column, BEH 130Å C18, 1.7 μm, 2.1×100 mm; isocratic separation; flow rate, 0.4 mL/min; detection at 450 nm; injection volume, 10 μL.

A chromatographic peak distortion was observed when carotenoids were dissolved in acetone, the mobile phase was a mixture of ACN: MeOH: 2-propanol 8.5:1:0.5, v/v/v and isocratic conditions were used (Fig. 8.A). On the other hand, better peak shape was achieved when samples were dissolved in a solvent equal or similar to the mobile phase (Fig. 8.B and 8.C).

Mobile phase consisting of ACN: MeOH 7:3, v/v appeared to result in better resolution than ACN: MeOH: 2-propanol 8.5:1:0.5, v/v/v (Figs. 8.B and 8.C). Consequently, it was selected to continue the process of improvement of the chromatographic system. After various studies, a gradient mobile phase containing water (as described in section 1.4.5.1) was chosen as the final chromatographic mobile phase, which was able to resolve most of the carotenoids present in maize endosperm and rice callus. The chromatographic conditions for each test are given in the figure legends.

Injection solvent:

Most carotenoids are insoluble in water and soluble in organic solvents, such as acetone, alcohol, THF, ethyl ether, chloroform and ethyl acetate [33]. Nevertheless, their solubility changes depending on the presence of different functional groups. To ensure the complete solubilization of these pigments and to avoid incompatibility of the injection solvent with the mobile phase, various combinations of solvents were tested to dissolve the samples before injection into the chromatograph. Because of the solubility range of carotenoids in a sample, combinations of the mobile phase (only solvent A, which was ACN: MeOH 7:3, v/v) with acetone and 2-propanol were tested. These solvents were selected because they are miscible with solvent A and more non-polar than ACN and MeOH. It was therefore considered that these solvents could contribute to increasing the miscibility of carotenes. Various aliquots of the same maize sample (TM1) were obtained. Each one was dissolved in the same amount of injection solvent and the injection volume was equal in all cases. This approach facilitated comparison between the corresponding chromatographic peaks and hence the effect of the various injection solvents.

Fig. 9 shows the different combinations of injection solvents used to dissolve the carotenoids present in transgenic maize TM1. No variations in RT were observed when samples were dissolved in the different injection solvents (Fig. 9) and contrary to what was observed in Fig. 8.A, when carotenoids were solubilized in 100% acetone and separated using a gradient mobile phase containing water, no peak distortion was observed (Fig. 9.A). The difference in the peak shape observed in Figs. 8.A and 9.A can be attributed to some extent to the addition of water to the mobile phase, which might have helped to improve the resolution of the carotenoids, specially the early eluting pigments (xanthophylls). In addition, smaller injection volumes were used in the chromatographic system employing the gradient mobile phase containing water, and this might have helped to narrow the peak width and, therefore, yield a much better resolution.

The highest concentrations of pigments were obtained using a mixture of solvent A: acetone 6.7:3.3, v/v rather than solvent A alone as the injection solvent, which exhibited the most similar chemical composition to the mobile phase (Figs. 9.B and 9.C). For example, with the mixture of solvent A: acetone 6.7:3.3, v/v, the content obtained for zeaxanthin and lutein was 4.49 μg/g while with the solvent A alone, the sample content was 3.89 μg/g. A reduced percentage of acetone (sample dissolved in solvent A: acetone 7.5:2.5, v/v) led to a decrease in the entire content of all the carotenoids (Table 6). With this injection solvent, a concentration of 4.20 μg/g was obtained for zeaxanthin and lutein. The sample dissolved in ACN: MeOH: 2-propanol 8.5:1:0.5, v/v/v (Fig. 9.E) did not show any increase in the carotenoid contents (3.05 μg/g was obtained for zeaxanthin and lutein). Nevertheless, the lowest content of carotenoids were obtained dissolving the sample in 100% acetone (Table 6). Acetone produced 2.20 μg/g of zeaxanthin and lutein content. Therefore, these

results indicated that combinations of solvents were more advantageous to improve sample solubility than a single solvent such as acetone.

Because of the polarity of carotenoids present in TM1 (antheraxanthin, adonixanthin, lutein, zeaxanthin and α-cryptoxanthin), acetone was required to increase the solubility of these pigments under the specific chromatographic conditions used. Thus, the mixture of solvent A: acetone 6.7:3.3, v/v was chosen as the injection solvent.

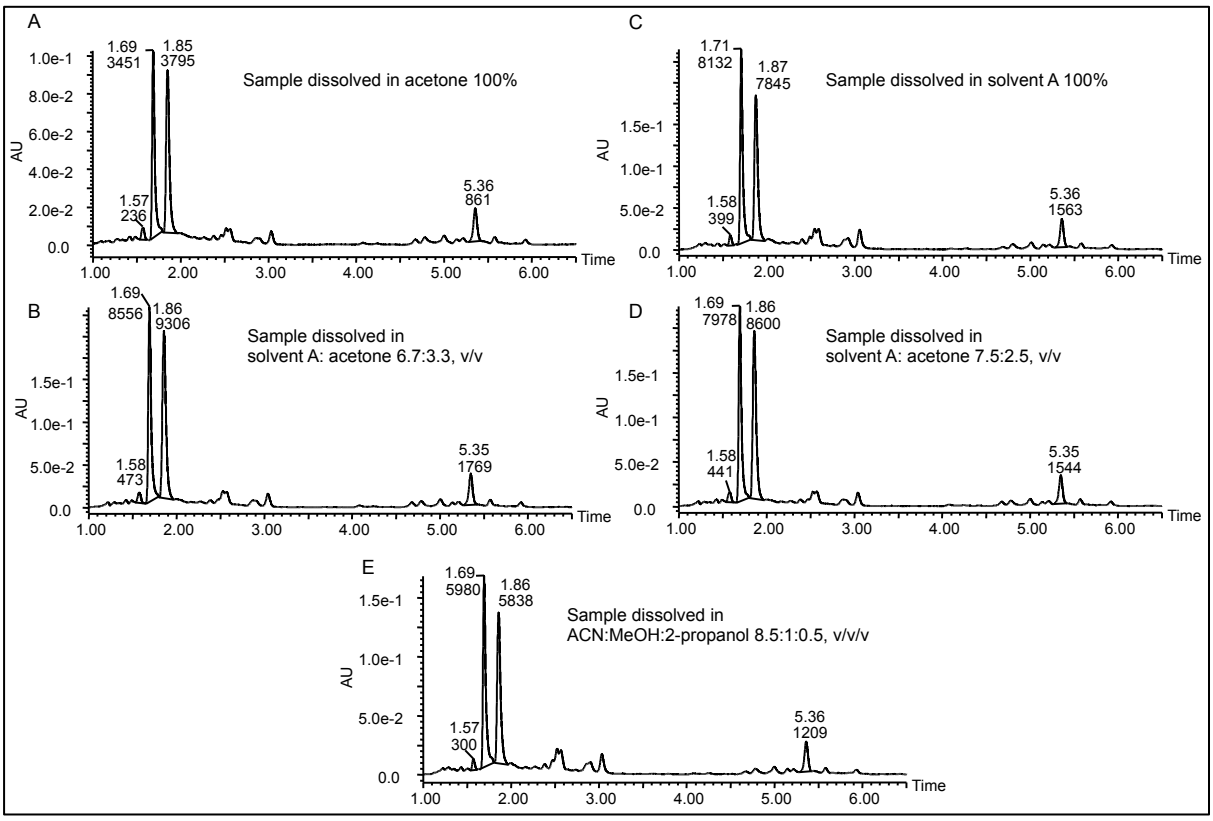

Figure 1-9. Comparison of carotenoid peak areas when carotenoids were dissolved in different injection solvents. The peaks correspond to antheraxanthin (1.58 min), adonixanthin (1.69 min), zeaxanthin coeluting with lutein (1.86 min) and α-cryptoxanthin (5.35 min). Column, BEH 130Å C18, 1.7 µm, 2.1×100 mm; mobile phase, solvent A: ACN: MeOH 7:3, v/v and solvent B: water 100%, initial conditions 95% solvent A and 5% solvent B for 2 min; change with linear gradient to 100% solvent A in 1 min, hold for 7 min; then return to initial conditions in 0.1 min, followed by equilibration for 2 min; flow rate, 0.35 mL/min; detection at 450 nm; injection volume, 5 μL.

Table 1-6. Effect of the injection solvent on the determination of the final carotenoid contents in transgenic maize TM1.

Injection solvent	Antheraxanthin μg/g DW	Adonixanthin μg/g DW	Lutein+zeax μg/g DW	α-Cryptoxanthin μg/g DW
Acetone 100%	0.12	1.93	2.20	0.98
Solvent A[a]:acetone 6.7:3.3, v/v	0.24	4.71	4.49	1.36
Solvent A[a] 100%	0.20	4.48	3.89	1.27
Solvent A[a]:acetone 7.5:2.5, v/v	0.22	4.39	4.20	1.26
ACN:MeOH:2-propanol 8.5:1:0.5, v/v/v	0.15	3.31	3.05	1.12

[a] Solvent A, ACN: MeOH 7:3, v/v.

Injection volume:

In order to determine an appropriate injection volume that would permit a suitable UV-vis spectrum without affecting resolution negatively, I evaluated injection volumes of 5, 10 and 15 μL under the same chromatographic conditions. The effect of loading is shown in Fig. 10. The results demonstrated how overloading of injection volume can severely decrease the resolution of carotenoids during analysis by LC. Therefore, 5 μL was selected as the standard injection volume for the analysis of samples by UHPLC.

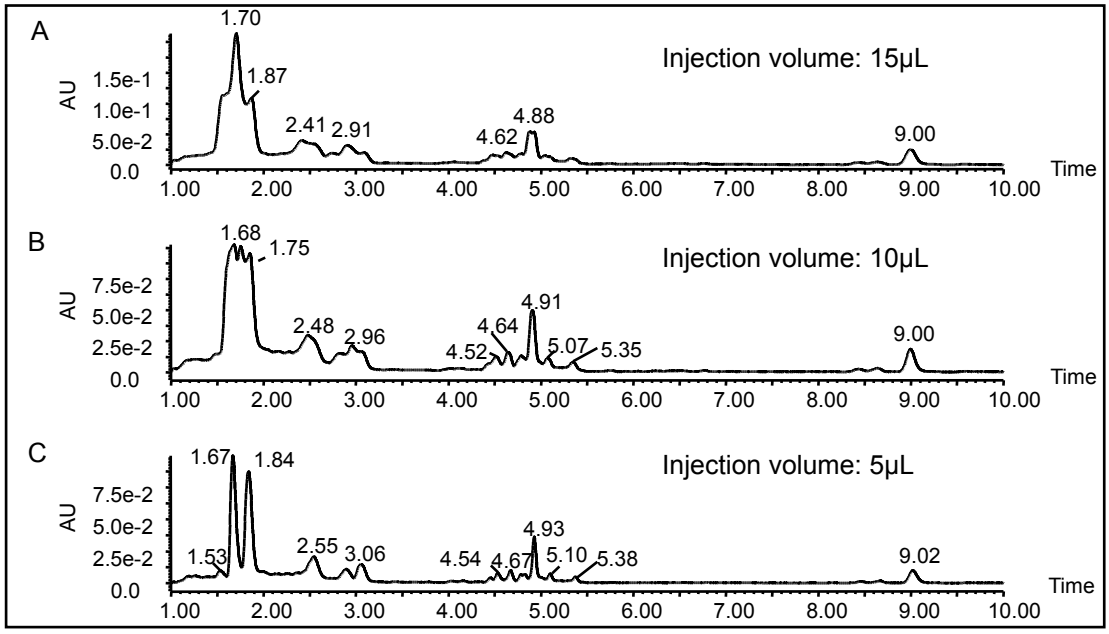

Figure 1-10. Comparison of the separation of carotenoids in TM1 by using different injection volumes. Column, BEH 130Å C18, 1.7 μm, 2.1×100 mm; mobile phase, solvent A: ACN: MeOH 7:3, v/v and solvent B: water 100%, initial conditions 95% solvent A and 5% solvent B for 2 min; change with linear gradient to 100% solvent A in 1 min, hold for 7 min; then return to initial conditions in 0.1 min, followed by equilibration for 2 min; flow rate, 0.35 mL/min; detection at 450 nm; samples dissolved in [ACN: MeOH 7:3, v/v]: acetone 6.7:3.3, v/v.

In addition to injection volume and solvent, other parameters need to be evaluated for improving the chromatographic system further. For example, attention should be paid to the carotenoid concentration in the samples and standard solutions, because if the carotenoid solution is nearly saturated it could cause peak tailing and broad bands. Furthermore, sample temperature plays an important role in sample solubility. Thus, to ensure a complete solubilization of the carotenoids, a sample temperature of 25 ºC was used in the chromatographic systems.

The UHPLC system was improved continuously because each time more complex mixtures of carotenoids were analyzed. The description of the final UHPLC system, which was able to resolve most of the carotenoids present in maize endosperm and rice callus, can be found in section 1.4.5.1. Separation of carotenoids (Fig. 11) with the final UHPLC system is shown below.

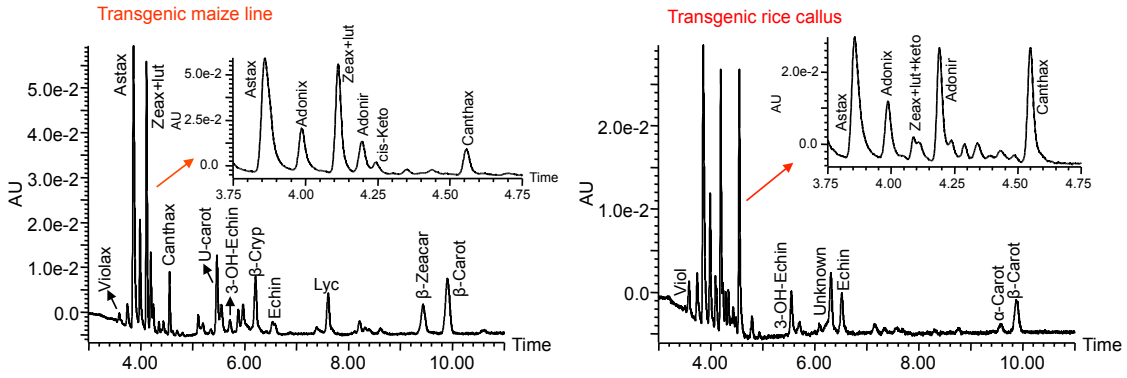

Figure 1-11. Separation of carotenoids present in TM4 and TC4 using an ACQUITY UPLC® BEH C18 column. Chromatographic conditions are given in section 1.4.5.1. Abbreviations: Violax, violaxanthin; Ast, astaxanthin; Adonix, adonixanthin; Zeax+lut, zeaxanthin coeluting with lutein; Zeax+lut+keto, zeaxanthin coeluting with lutein and an unknown ketocarotenoid1; Adonir, adonirubin; cis-Keto, cis-unknown ketocarotenoid 2; Canthax, canthaxanthin; U-carot, unknown carotenoid 1; 3-OH-Echin, 3-hydroxyechinenone; *β*-Cryp, *β*-cryptoxanthin; Unknown, unknown carotenoid 2, Echin, echinenone; Lyc, lycopene, *β*-Zeacar, *β*-zeacarotene; *α*-Carot, *α*-carotene; *β*-Carot, *β*-carotene.

1.5.2.3 Separation of lutein and zeaxanthin

In spite of the several modifications made to the UHPLC system in order to separate lutein and zeaxanthin, it was not possible to get its separation using an ACQUITY UPLC® C18 BEH 130Å, 1.7 *μ*m, 2.1×100 mm column. As these pigments are major carotenoids in maize seeds, it was important to separate them. Therefore, I used a second chromatographic system for this purpose. It comprised an YMC C30 column and a mobile phase consisting of solvent A: MeOH: water 8:2, v/v and solvent B: TBME 100% with gradient elution (details of this HPLC system can be found in section 1.4.5.2). With this chromatographic system, lutein and zeaxanthin were distinctly separated. Fig. 12 shows the separation of zeaxanthin and lutein as well as other carotenoid standards.

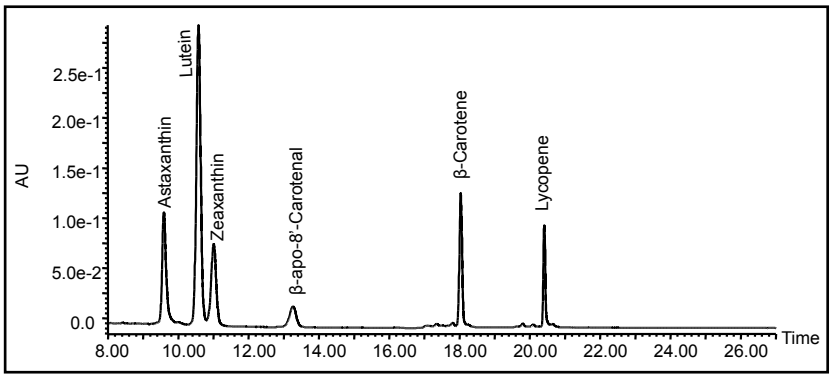

Figure 1-12. Separation of a mixture of carotenoid standards using an YMC C30 column. Chromatographic conditions are given in section 1.4.5.2.

1.5.3 Chromatographic and spectral characteristics of carotenoids

Several carotenoid standards and matrices containing carotenoids were analyzed in order to gather information about the chromatographic and spectral characteristics of these pigments under the chromatographic system used (for plant material see section 1.4.2).

Table 1-7. Chromatographic and spectral characteristics of carotenoids.

No.	RT[a] (min)	Carotenoid	λmax (nm)[b]	λmax (nm) reported[c]	%III/II[b]	%III/II reported[c]
1	3.40	cis-Neoxanthin	413,437,466	413,437,466, ethanol	85	80
2	3.58	Violaxanthin	417,440,470	419,440,470, ethanol	91	95
3	3.85	Antheraxanthin	446,475	444,472, ethanol	61	60
4	3.85	Astaxanthin	476	478, ethanol	-	-
5	3.98	Adonixanthin	465	465, ethanol	-	-
6	4.11	Zeaxanthin[d]	453,479	452,479, acetone	25	25
7	4.11	Lutein[d]	446,474	445,474, ethanol	59	60
8	4.19	Adonirubin	475	474, acetone	-	-
9	4.53	Canthaxanthin	472	474, ethanol	-	-
10	4.77	*β*-apo-8'-Carotenal	459	456, ethanol	-	-
11	5.68	3-Hydroxyechinenone	464	466, ethanol	-	-
12	5.96	*α*-Cryptoxanthin	447,475	446,473, ethanol	64	60
13	6.19	*β*-Cryptoxanthin	453,479	450,478, ethanol	23	25
14	6.45	Echinenone	461	461, ethanol	-	-
15	7.58	Lycopene[d]	446,472[e]	446,472,504, ethanol	-	65
16	9.39	*β*-zeacarotene	428,454	428,454, ethanol	40	52
17	9.46	*α*-Carotene	447,475	448,476, acetone	50	55
18	9.74	*β*-Carotene	453,478	452,478, acetone	13	15
19	9.90	Phytofluene	332,344,367	331,347,367, hexane	86	85
20	10.98	cis-Phytoene	286	286, hexane	-	-
21	11.31	*trans*-Phytoene	286,298	285,297, hexane	-	-

[a] Retention time
[b] Data obtained with the mobile phase, gradient elution of ACN: MeOH (7:3, v/v) and water.
[c] Data reported in the literature.
[d] *cis*-Isomers of this carotenoid were also detected.
[e] The PDA detector used here only read wavelengths up to 500 nm, as a result, the third maximum absorption of lycopene was not provided.

Table 7 summarizes the chromatographic and spectral characteristics of carotenoids obtained using the UHPLC system, which was the separation method that allowed most effective resolution. In addition, the *λ*max and %III/II obtained are compared with those reported in the literature [28, 29].

In general, three wavelengths were used to detect carotenoids: at 286 nm (for phytoene), 344 nm (for phytofluene) and 450 nm (for the rest of the carotenoids). However, for some carotenoids absorbing in the visible region, their *λ*max were observed below (e.g. *β*-zeacarotene) or above (e.g. ketocarotenoids) 450 nm. The UV-vis spectra of these carotenoids can be seen in the supplementary data. Most of the carotenoids identified were in the all-*trans* form. *cis*-Isomers were also observed but in small amounts, except for *cis*-phytoene which was observed as a major component. Coelution between antheraxanthin and astaxanthin, and zeaxanthin and lutein was observed with the UHPLC system.

1.6 CONCLUSIONS

I concluded that the most optimal extraction methods for carotenoids from maize endosperm were the reference method and *modification 5*. As the reference method incorporates THF, I elected to use *modification 5* for all subsequent experiments discussed in the thesis. This allows me to easily avoid the possible presence of peroxides in the extracting solvents. The modified extraction *method 5* is relatively fast for the determination of carotenoid pigments in maize endosperm and rice callus and allows the simultaneous determination of various carotenoids present in the samples. Several factors such as the polarity of particular carotenoids present in the sample, sample preparation before extraction and the chemical form of carotenoids in a given sample matrix (free form or bound to other compounds) need to be considered in order to develop the most optimal extraction method in different matrices.

The ACQUITY UPLC® BEH C18 column proved to be an optimal stationary phase to separate several carotenoids simultaneously. The UHPLC system developed allowed for a reduction of the time of the analysis compared to conventional HPLC systems. The polarity range of carotenoids and their concentrations in the samples make it necessary for chromatographic systems to be adapted to suit the particular carotenoid profile being analyzed. My experiments demonstrated the importance of injection volume, injection solvent and composition of the mobile phase for optimal resolution. These parameters can be optimized further to increase sensitivity, better selectivity and more reliable quantitation.

1.7 REFERENCE

[1] Kimura M, Rodriguez-Amaya DB (1999) Sources of errors in the quantitative analysis of food carotenoids by HPLC. Archivos Latinoamericanos de Nutricion.49:58S-66S.

[2] Meléndez-Martínez AJ, Vicario IM, Heredia FJ (2007) Review: Analysis of carotenoids in orange juice. Journal of Food Composition and Analysis.20:638-49.

[3] Oliver J, Palou A (2000) Chromatographic determination of carotenoids in foods. Journal of Chromatography A.881:543-55.

[4] Rodriguez-Amaya DB, Kimura M (2004) HarvestPlus handbook for carotenoid analysis. Washington: International Food Policy Research Institute. http://www.ifpri.org/sites/default/files/publications/hptech02.pdf, acceded online 05/03/12.

[5] Rodríguez-Bernaldo de Quirós A, Costa HS (2006) Analysis of carotenoids in vegetable and plasma samples: A review. Journal of Food Composition and Analysis.19:97-111.

[6] Su Q, Rowley KG, Balazs NDH (2002) Carotenoids: Separation methods applicable to biological samples. Journal of Chromatography B: Analytical Technologies in the Biomedical and Life Sciences.781:393-418.

[7] Howe JA, Tanumihardjo SA (2006) Evaluation of analytical methods for carotenoid extraction from biofortified maize (Zea mays sp.). Journal of Agricultural and Food Chemistry.54:7992-7.

[8] Azevedo-Meleiro CH, Rodriguez-Amaya DB (2004) Confirmation of the identity of the carotenoids of tropical fruits by HPLC-DAD and HPLC-MS. Journal of Food Composition and Analysis.17:385-96.

[9] Berardo N, Brenna OV, Amato A, Valoti P, Pisacane V, Motto M (2004) Carotenoids concentration among maize genotypes measured by near infrared reflectance spectroscopy (NIRS). Innovative Food Science and Emerging Technologies.5:393-8.

[10] Scott CE, Eldridge AL (2005) Comparison of carotenoid content in fresh, frozen and canned corn. Journal of Food Composition and Analysis.18:551-9.

[11] Menkir A, Liu W, White WS, Maziya-Dixon B, Rocheford T (2008) Carotenoid diversity in tropical-adapted yellow maize inbred lines. Food Chemistry.109:521-9.

[12] Muzhingi T, Yeum KJ, Russell RM, Johnson EJ, Qin J, Tang G (2008) Determination of carotenoids in Yellow Maize, the effects of saponification and food preparations. International Journal for Vitamin and Nutrition Research.78:112-20.

[13] Naqvi S (2009) Metabolic engineering of complex pathways in plants by combinatorial genetic trasnormation. Doctoral thesis, University of Lleida, Lleida, Spain.

[14] Rivera SM, Canela-Garayoa R (2012) Analytical tools for the analysis of carotenoids in diverse materials. Journal of Chromatography A.1224:1-10.

[15] Swartz ME (2005) UPLC™: an introduction and review. Journal of Liquid Chromatography & Related Technologies.28:1253-63.

[16] Swartz ME (2005) Ultra performance liquid chromatography (UPLC): An introduction. Separation Science Redefined (Special Issues of LC–GC NAm).

[17] Wren SAC, Tchelitcheff P (2006) UPLC/MS for the identification of β-blockers. Journal of Pharmaceutical and Biomedical Analysis.40:571-80.

[18] Chen S, Kord A (2009) Theoretical and experimental comparison of mobile phase consumption between ultra-high-performance liquid chromatography and high performance liquid chromatography. Journal of Chromatography A.1216:6204-9.

[19] Nováková L, Vlčková H (2009) A review of current trends and advances in modern bio-analytical methods: Chromatography and sample preparation. Analytica Chimica Acta.656:8-35.

[20] Nováková L, Solichová D, Solich P (2006) Advantages of ultra performance liquid chromatography over high-performance liquid chromatography: Comparison of different analytical approaches during analysis of diclofenac gel. Journal of Separation Science.29:2433-43.

[21] Gruz J, Novák O, Strnad M (2008) Rapid analysis of phenolic acids in beverages by UPLC-MS/MS. Food Chemistry.111:789-94.

[22] Feltl L, Pacakova V, Stulik K, Volka K (2005) Reliability of carotenoid analyses: a review. Current Analytical Chemistry.1:93-102.

[23] Lesellier E, Tchapla C (1993) Analysis of carotenoids by high-performance liquid chromatography and supercritical fluid chromatography. Journal of Chromatography A.633:9-23.
[24] Sander LC, Pursch M, Wise SA (1999) Shape selectivity for constrained solutes in reversed-phase liquid chromatography. Analytical Chemistry.71:4821-30.

[25] Grumbach E, Arsenault J, McCabe D (2009) Beginners Guide to UPLC. Waters Corporation: Milford, MA.

[26] Wyndham KD, Walter TH, Iraneta PC, Neue UD, McDonald PD, Morrison D, Baynham M (2007) A Review of Waters Hybrid Particle Technology. Part 2. Ethylene-Bridged [BEH Technology™] Hybrids and Their Use in Liquid Chromatography. Waters Corporation.

[27] Meléndez-Martínez AJ, Britton G, Vicario IM, Heredia FJ (2006) Relationship between the colour and the chemical structure of carotenoid pigments. Food Chemistry.101:1145-50.

[28] Britton G, Liaaen-Jensen S, Pfander H (2004) Carotenoids handbook. 1st ed; Birkhäuser: Basel, Switzerland. pp. 3-404.

[29] JCBL (2007) LipidBank. http://lipidbank.jp/cgi-bin/main.cgi?id=VCA, accesed online 01/02/12.

[30] Britton G (1995) Structure and properties of carotenoids in relation to function. The FASEB Journal.9:1551-8.

[31] Khoo HE, Prasad KN, Kong KW, Jiang Y, Ismail A (2011) Carotenoids and their isomers: Color pigments in fruits and vegetables. Molecules.16:1710-38.

[32] Taylor KL, Brackenridge AE, Vivier MA, Oberholster A (2006) High-performance liquid chromatography profiling of the major carotenoids in Arabidopsis thaliana leaf tissue. Journal of Chromatography A.1121:83-91.

[33] Rodriguez-Amaya DB (1999) A guide to carotenoid analysis in foods: International Life Sciences Inst ILSI. *pdf.usaid.gov/pdf_docs/PNACQ929.pdf,* acceded online 09/07/12.

[34] Zhu C, Naqvi S, Breitenbach J, Sandmann G, Christou P, Capell T (2008) Combinatorial genetic transformation generates a library of metabolic phenotypes for the carotenoid pathway in maize. Proceedings of the National Academy of Sciences of the United States of America.105:18232-7.

[35] FAO (2009) Lycopene extract from tomate. http://www.fao.org/fileadmin/templates/agns/pdf/jecfa/cta/71/lycopene_extract_from_tomato.pdf, acceded online 29/02/12.

[36] Lucini L, Pellizzoni M, Baffi C, Molinari GP (2011) Rapid determination of lycopene and β-carotene in tomato by liquid chromatography/electrospray tandem mass spectrometry. Journal of the Science of Food and Agriculture.

[37] Strati IF, Oreopoulou V (2011) Process optimisation for recovery of carotenoids from tomato waste. Food Chemistry.129:747-52.

[38] Moros EE, Darnoko D, Cheryan M, Perkins EG, Jerrell J (2002) Analysis of xanthophylls in corn by HPLC. Journal of Agricultural and Food Chemistry.50:5787-90.

[39] Howard LA, Wong AD, Perry AK, Klein BP (1999) β-Carotene and ascorbic acid retention in fresh and processed vegetables. Journal of Food Science.64:929-36.

[40] Matthews PD, Luo R, Wurtzel ET (2003) Maize phytoene desaturase and ζ-carotene desaturase catalyse a poly-Z desaturation pathway: Implications for genetic engineering of carotenoid content among cereal crops. Journal of Experimental Botany.54:2215-30.

[41] Rodrigues P, Morais H, Mota T, Olivera S, Forgács E, Cserháti T (1998) Use of HPLC and multivariate methods for the evaluation of the stability of colour pigments of paprika (Capsicum annuum) powder. Analytica Chimica Acta.372:411-6.

[42] Kimura M, Kobori CN, Rodriguez-Amaya DB, Nestel P (2007) Screening and HPLC methods for carotenoids in sweetpotato, cassava and maize for plant breeding trials. Food Chemistry.100:1734-46.

[43] Sérino S, Gomez L, Costagliola GUY, Gautier H (2009) HPLC assay of tomato carotenoids: Validation of a rapid microextraction technique. Journal of Agricultural and Food Chemistry.57:8753-60.

[44] Burkhard S, Böhm V (2007) Development of a new method for the complete extraction of carotenoids from cereals with special reference to durum wheat (Triticum durum Desf.). Journal of Agricultural and Food Chemistry.55:8295-301.

[45] Aluru M, Xu Y, Guo R, Wang Z, Li S, White W, Wang K, Rodermel S (2008) Generation of transgenic maize with enhanced provitamin A content. Journal of Experimental Botany.59:3551-62.

[46] Mishra P, Singh N (2010) Spectrophotometric and TLC based characterization of kernel carotenoids in short duration maize. Maydica.55:95-100.

[47] Kurilich AC, Juvik JA (1999) Quantification of carotenoid and tocopherol antioxidants in Zea mays. Journal of Agricultural and Food Chemistry.47:1948-55.

[48] Marinova D, Ribarova F (2007) HPLC determination of carotenoids in Bulgarian berries. Journal of Food Composition and Analysis.20:370-4.

[49] Burt AJ, Grainger CM, Young JC, Shelp BJ, Lee EA (2010) Impact of postharvest handling on carotenoid concentration and composition in High-carotenoid maize (Zea mays L.) kernels. Journal of Agricultural and Food Chemistry.58:8286-92.

[50] Lozano-Alejo N, Carrillo GV, Pixley K, Palacios-Rojas N (2007) Physical properties and carotenoid content of maize kernels and its nixtamalized snacks. Innovative Food Science and Emerging Technologies.8:385-9.

[51] Rimmer CA, Sander LC, Wise SA (2005) Selectivity of long chain stationary phases in reversed phase liquid chromatography. Analytical and Bioanalytical Chemistry.382:698-707.

[52] Breitenbach J, Visser H, Verdoes JC, van Ooyen AJJ, Sandmann G (2011) Engineering of geranylgeranyl pyrophosphate synthase levels and physiological conditions for enhanced carotenoid and astaxanthin synthesis in Xanthophyllomyces dendrorhous. Biotechnology Letters.33:755-61.

[53] Waters Corporation (2006) Acquity UPLC BEH Column Care and Use Instructions. http://www.waters.com/webassets/cms/support/docs/715001371.pdf, accessed online 14/03/12.

Chapter 2

Factors influencing carotenoid analysis

2.1 ABSTRACT

Carotenoid analysis is inherently difficult and error prone. Analysts must be well informed about the nature and properties of carotenoids and the challenges associated with their identification and quantification. Knowledge of the possible sources of error in each step of the procedure for carotenoid analysis will assist in appraising the performances of the methods. Thus, in this chapter, some of the factors influencing carotenoid analysis are evaluated in order to seek the appropriate information that permits us to handle, treat and analyze these pigments correctly to guarantee reliability of results. Firstly, I investigated which API technique (ESI, APCI and APPI) could be suitable for ionizing these pigments and determined characteristic transitions for their unequivocal identification using each ionization technique. I also assessed the reliability of the analytical method by determining basic validation parameters including relative recovery, accuracy, precision, LOD, LOQ and matrix effects. Finally, I assessed the stability of the carotenoids in maize seeds during storage. Thus, the amount of carotenoids was monitored for 6 months, using UHPLC-PDA.

2.2 INTRODUCTION

2.2.1 MS for carotenoid identification

In HPLC, UV–vis instruments are the most common detectors used to identify carotenoids. However, given that the UV–vis spectra of many carotenoids are similar (e.g., *α*-cryptoxanthin and zeinoxanthin) and a number of structurally related molecules coelute, many researchers have complemented the identification of carotenoids using mass spectrometers equipped with atmospheric pressure ionization (API) sources: electrospray ionization (ESI) or atmospheric pressure chemical ionization (APCI) [1]. Mass detectors have shown great advantages for the analysis of these substances, including the elucidation of their structure on the basis of the molecular mass and their fragmentation pattern. These properties facilitate the quantification of individual carotenoids that coelute. APCI has become the most widely used ionization technique for carotenoids and shows high sensitivity for their analysis [1, 2]. APCI has been used to successfully ionize not only xanthophylls and carotenes but also carotenoid esters [3], thereby demonstrating the suitability of this approach to ionize carotenoids with different polarities. A highly promising technique to ionize non-polar compounds [4-6], such as carotenoids, is *atmospheric pressure photoionization (*APPI). This method has recently been introduced as a new ionization method for liquid chromatography-mass spectrometry (LC–MS) and can be considered complementary to the other two API techniques, namely ESI and APCI. Most mass spectra of carotenoids have been acquired using positive ion mode; however, negative ion mode has also been reported [7-9].

In APCI, the liquid sample is first evaporated, after which a charged plasma is formed by using a corona discharge and the ionization of analytes takes place by gas-phase reactions. In ESI, gas-phase ions of the analytes are formed by using a high electric field. The best ionization is achieved when the analytes are already charged in solution, and therefore ESI is best suited for the analysis of polar and ionic compounds. In APPI, the liquid sample is vaporized in a heated nebulizer identical to the one in an APCI source, after which the gaseous analytes are ionized through photoionization and gas-phase reactions. The ionization in APPI is initiated by 10 eV photons emitted by a krypton discharge lamp. The photons can ionize molecules that possess ionization energies (IEs) below 10 eV. This includes most analytes, but excludes solvents generally used in LC, such as MeOH, ACN, and water, as well as the gases used in the nebulization or that are otherwise present in the atmospheric pressure ion source [10]. Signals in APPI-MS can be increased substantially by adding dopants. The 10 eV vacuum-UV photons have a short penetration depth in a dense, atmospheric pressure mixture of gases and vapors and, by using a large amount of an easily ionizable compound (a dopant) that can further ionize the analyte, the sensitivity of the ionization of the analyte can be greatly enhanced [11]. There is no universal dopant for APPI, and the effect of a dopant depends on the IEs and proton affinities of the analytes, the dopants, and the eluents [12].

2.2.2 Validation of analytical procedures

Method validation is the process used to confirm that the analytical procedure employed for a specific test is suitable for its intended use. Results from method validation can be used to judge the quality, reliability and consistency of analytical results; it is an integral part of any good analytical practice. Typical validation parameters which should be considered are: (1) recovery, (2) limit of detection (LOD), (3) limit of quantification (LOQ), (4) matrix effect, (5) linearity, (6) accuracy and (7) precision.

Recovery: the recovery of an analyte in an assay is the detector response obtained from an amount of the analyte added to and extracted from the biological matrix, compared to the detector response obtained for the true concentration of the pure authentic standard. Recovery of the analyte need not be 100%, but the extent of recovery of an analyte and of the internal standard should be consistent, precise, and reproducible. Recovery experiments should be performed by comparing the analytical results for extracted samples at some given concentrations with unextracted standards that represent 100% recovery [13].

LOD: is the lowest amount of analyte in a sample which can be detected but not necessary quantified as an exact value [13].

LOQ: is the lowest amount of analyte in a sample which can be quantitatively determined with suitable precision and accuracy [13].

Matrix effect: validation of LC-MS or LC–MS/MS assays includes an assessment of matrix effects, which is the direct or indirect alteration or interference in response due to the presence of unintended analytes (for analysis) or other interfering substances in the sample [13].

Linearity: the linearity of an analytical procedure is its ability (within a given range) to obtain test results which are directly proportional to the concentration (amount) of analyte in the sample [14].

Accuracy: it expresses the closeness of agreement between the value, which is accepted either as a conventional true value or accepted reference value and the value found. This is sometimes termed trueness [13].

Precision: it expresses the closeness of agreement (degree of scatter) between a series of measurements obtained from multiple sampling of the same homogenous sample under the prescribed conditions [13].

2.2.3 Stability of carotenoids

The fact that carotenoids are made up of a system of conjugated double bonds make them susceptible to degradation. The structures break down following attack by free radicals, such as single molecular oxygen and other reactive species. Carotenoids *per se* have different susceptibilities to degradation [15]. The common degradation pathways are isomerization, oxidation and fragmentation of the molecules (Fig.1).

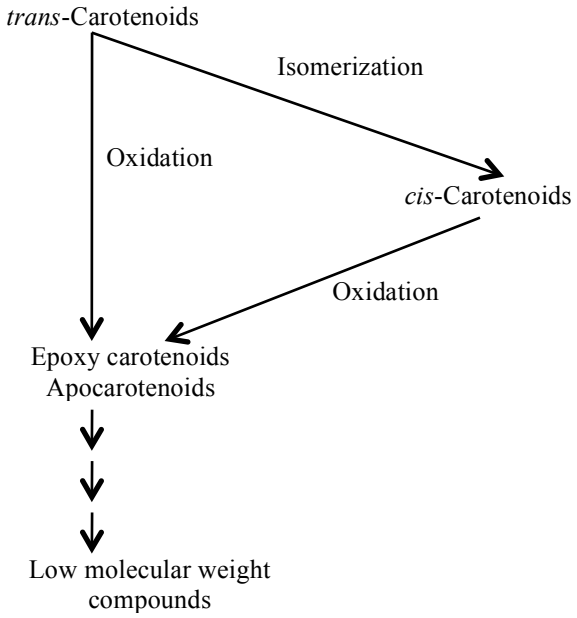

Figure 2-1. Possible scheme for carotenoid degradation [17].

Heat, light and acids promote isomerization of the *trans*- to the *cis*-form. Light, enzymes, pro-oxidant metals and co-oxidation with unsaturated lipids, induce oxidation. Pyrolysis occurs under intense heat with removal of low molecular weight molecules. Many of the degradation products occur only in small quantities with similar polarities and high reactivity, and hence are difficult to analyze [16].

Whatever the analytical method chosen, precautionary measures to avoid artifacts and quantitative losses should be taken. These include [17]: completion of the analysis within the shortest possible time, exclusion of oxygen, protection from light, avoiding high temperatures, avoiding contact with acid, use of high purity solvents and free from harmful impurities, antioxidants (e.g., BHT, pyrogallol) may also be used, especially when the analysis is prolonged. In this case, the extracted carotenoids should be stored in the dark at -20 ºC or lower in the complete absence of oxygen, either in vacuum or in an inert atmosphere (Ar or N_2).

2.3 OBJECTIVES

- To investigate which API technique (ESI, APCI and APPI) is more appropriate for ionizing carotenoids.
- To provide information concerning the different molecular ions and transitions obtained for each carotenoid in each ionization technique.
- To find fragment ions that may be related with functional groups present in the carotenoid structures.
- To study the effect of four dopants on the ionization of carotenoids by APPI.
- To develop a fast analytical method to determine carotenoid content in the transgenic seed maize and rice callus.
- To assess the reliability of the analytical method by determining basic validation parameters including relative recovery, accuracy, precision, LOD, LOQ and matrix effects.
- To study the stability of the carotenoids in maize seeds over a period of 6 months of storage.

2.4 MATERIALS AND METHODS

2.4.1 Chemicals

β-Carotene, lycopene, lutein, *β*-cryptoxanthin, astaxanthin, *β*-apo-8′-carotenal were purchased from Sigma-Aldrich Fine Chemicals (St. Louis, MO, USA). Canthaxanthin and zeaxanthin were acquired from Fluka (Buchs SG, Switzerland). Phytoene, violaxanthin, neoxanthin, and antheraxanthin were purchased from Carotenature (Lupsingen, Switzerland). MeOH, ethyl acetate, ethyl eter, TBME, ACN and acetone (HPLC grade purity) were acquired from J.T. Baker (Deventer, The Netherlands). Water was prepared using a Milli-Q reagent water system.

2.4.2 Plant material

The transgenic maize seeds and rice callus were generated by combinatorial nuclear transformation as reported in Zhu et al. [18]. A transgenic maize line TM1, expressing *Zea mays* phytoene synthase 1 (*Zmpsy1)*, *Pantoea ananatis* phytoene desaturase (*PacrtI*), *Gentiana lutea* lycopene *β*-cyclase (*Gllycb*) and *Paracoccus β*-carotene ketolase (*ParacrtW*) was selected to carry to out the study of the stability of carotenoids.

The plant material used to carry out the tests with the mass spectrometer was the same employed in Chapter 1, section 1.4.2.

TM: TM1; TM2, expressing *Zmpsy*1 and *PacrtI*; TM3 expressing *Zmpsy*1, biochemically synthesized *sCrBkt* from *Chlamydomonas reinhardtii* and biochemically synthesized *sBrcrtZ* from *Brevundimonas sp. Strain SD212*; TM4, which corresponded to the cross of TM2 with TM3, therefore, expressing *Zmpsy*1, *PacrtI, sCrBkt* and *sBrcrtZ*; and TM5, which corresponded to the cross of TM3 with a wild type maize plant NSL76, therefore, expressing *Zmpsy*1, *sCrBkt,* and *sBrcrtZ*.

TC: TC1, expressing *Zmpsy*1 and *Pacrtl*; TC2, expressing *Zmpsy*1, *Pacrtl* and 1-deoxy-D-xylulosa 5-phosphate synthase from *Arabidopsis thaliana* (*Atdxs*); TC3, expressing *Zmpsy*1, *Pacrtl* and *β*-carotene ketolase from *Brevundimonas* sp. Strain SD212 chemically synthesized (s*BrcrtW*) and TC4, expressing *Zmpsy*1, *Pacrtl* and *sCrBkt*.

2.4.3 Preservation of TM1 seeds

Seeds of TM1 were lyophilized and subsequently mixed and ground. Then, the material was divided into 6 lots. The samples of maize were then placed in polyethylene bags and vacuum sealed. Subsequently, all samples were frozen at -80 °C in the dark.

2.4.4 Extraction of carotenoids

To protect carotenoids from degradation and oxidation, the extraction was conducted under limited light. Samples (transgenic maize endosperm and rice callus) were freeze-dried and ground into a fine powder using a mortar and pestle. 10 or 100[3] mg of sample was extracted with 15 mL of MeOH: ethyl acetate (6:4, v/v) at 60 °C for 20 min and this mixture was continuously shaken. It was then put on ice until it reached room temperature and the liquid phase was filtered into a separatory funnel (if the residue exhibited color after extraction, then it was re-extracted with 5 mL of MeOH: ethyl acetate (6:4, v/v) at 60 °C for 5 min and the second extract was combined with the first one). 15 mL of hexane: diethyl ether (9:1, v/v) was added to the organic extract and the mixture was shaken vigorously. Then, 20 mL of saturated sodium chloride solution was added and the mixture was shaken again. The aqueous phase was removed and the organic phase was washed with water once again. The organic phase was dried under N_2 at 37 ºC. When the sample was completely dry, Ar was flushed into the vial and carotenoids were stored at -80 ºC until LC analysis.

2.4.5 Preparation of carotenoid standards

Stock carotenoid solutions of antheraxanthin, violaxanthin, neoxanthin, astaxanthin, canthaxanthin, zeaxanthin, lutein, *β*-cryptoxanthin, lycopene, *β*-carotene, and phytoene were prepared in the injection solvent [ACN: MeOH 7:3, v/v]: acetone 6.7:3.3, v/v at concentrations of 17.53, 16.26, 19.64, 5.12, 5.70, 32.31, 21.57, 35.00, 8.26, 24.85, and 16.16 μg/mL, respectively. Then, a set of standard solutions was prepared from stock solutions by sampling an aliquot and diluting it with injection solvent and their concentrations assessed by UHPLC analysis. For those carotenoids dissolved in hexane (canthaxanthin, *β*-cryptoxanthin, *β*-carotene, lycopene and phytoene), standard solutions were prepared from stock solutions by evaporating an aliquot under nitrogen and diluting it with injection solvent. All solutions were stored at -80 ºC before LC analysis.

[3] For pale color rice callus and maize samples, extract 20 and 100 mg of sample, respectively. For darker color rice callus and maize samples, it is sufficient to extract 10 and 50 mg of sample, respectively.

2.4.6 Chromatographic analysis

2.4.6.1 UHPLC-PDA-MS analysis

UHPLC analysis was carried out using an ACQUITY Ultra Performance LC™ system linked to a PDA 2996 detector (Waters, Milford, MA, USA). Mass detection was carried out using an Acquity™ TQD tandem-quadrupole MS equipped with a Z-spray electrospray interface (Manchester, UK). MassLynx™ software version 4.1 (Waters, Milford, MA, USA) was used to control the instruments, and also for data acquisition and processing.

UHPLC chromatographic separations were performed on reversed-phase column ACQUITY UPLC® C18 BEH 130Å, 1.7 μm, 2.1×100 mm (Waters, Milford, MA). Mobile phase consisted of solvent A: ACN: MeOH 7:3, v/v and solvent B: water 100%. The gradient program used is shown in Table 1. The column and sample temperatures were set at 32 °C and 25 °C respectively. Injection volume was 5 μL.

Table 2-1. Gradient profile used in the separation of carotenoids by UHPLC. Linear gradient.

Time[a] (min)	Flow rate (mL/min)	A (%, v/v)	B (%, v/v)
Initial	0.4	80	20
2.0	0.4	80	20
3.0	0.4	100	0
7.0	0.4	100	0
8.0	0.6	100	0
11.6	0.6	100	0
12.6	0.4	80	20

[a] After this time, the system was left 2 min more to reach its re-equilibration before injecting a new sample.

Each sample extract for LC analysis was dissolved in 300 μL and 1000 μL (for light and dark color extract respectively) of the injection solvent [ACN: MeOH 7:3, v/v]: acetone 6.7:3.3, v/v. Before use, all solutions were filtered through Millex 0.2 μm nylon membrane syringe filters (Millipore, Bedford, MA, USA).

2.4.6.2 MS optimization

The most abundant API-tandem mass spectrometry (MS/MS) transition for each compound was monitored in the multiple-reaction monitoring mode to obtain the highest quantitative sensitivity. Cone voltages, energy collisions and other instrument parameters were individually investigated for each compound to obtain the most intense signal for the fragmentation products chosen. These studies were carried out in the combining flow state mode through direct infusion of standard solutions. Optimized MS conditions are listed in Table 2.

Table 2-2. MS conditions.

MS conditions	ESI	APCI	APPI
Polarity	Positive	Positive	Positive
Capillary (kV)	3.5	–	–
Repeller (kV)	–	–	1.5
Corona (kV)	–	4.0	–
Cone (V)	40	30	40
Extractor (V)	2	3	3
RF (V)	0.5	0.1	0.1
Source Temperature (°C)	150	150	150
Probe Temperature (°C)	450	450	450
Cone Gas Flow (L/h)	10	10	10
Desolvation Gas Flow (L/h)	500	150	150
Collision Gas Flow (mL/min)	0.15	0.15	0.15

2.4.6.3 HPLC-PDA analysis

HPLC analysis separations was carried out using a Waters Alliance 2695 separation module linked to a PDA 2998 detector (Waters, Milford, MA, USA). Empower software version 2 (Waters, Milford, MA, USA) was used to control the instruments, and also for data acquisition and processing.

HPLC chromatographic separations were performed on a YMC C30 carotenoid 3 μm, 2.0×100 mm column (Waters, Milford, MA). Mobile phase consisted of solvent A: MeOH: water 8:2, v/v and solvent B: TBME 100%. The gradient program used is shown in Table 3. Both, the column and the sample temperatures were set at 25 °C. Injection volume was 10 μL.

Table 2-3. Gradient profile used in the separation of carotenoids by HPLC. Linear gradient.

Time[a] (min)	Flow rate (mL/min)	A (%, v/v)	B (%, v/v)
Initial	0.25	97	3
6.0	0.25	97	3
7.0	0.25	62	38
15.0	0.25	62	38
16.0	0.25	32	68
18.0	0.25	32	68
19.0	0.25	0	100
25.0	0.25	0	100
26.0	0.25	32	68
27.0	0.25	50	50
28.0	0.25	70	30
29.0	0.25	97	3

[a] After this time, the system was left 6 min more to reach its re-equilibration before injecting a new sample.

2.4.7 UV-vis spectroscopy

Absorption spectra and absorbance were recorded using a UV/VIS Spectrometer UV2 ATI UNICAM, Cambridge, UK.

2.4.8 Statistical analysis

Results are expressed as means ± standard deviations (SD). An analysis of variance (ANOVA) of the factor time at a significance level of 5% was used to determine significant differences in carotenoid concentration between months. Microsoft Excel version 2010 (Microsoft Corp.) was used for data analysis.

2.5 RESULTS AND DISCUSSION

2.5.1 Effect of the ESI, APCI, and APPI systems on carotenoid ionization

Fig. 2 shows the structures of the xanthophylls: antheraxanthin, violaxanthin, neoxanthin, astaxanthin, adonixanthin, zeaxanthin, lutein, *β*-apo-8′-carotenal, 3-hydroxyechinenone, *α*-cryptoxanthin, *β*-cryptoxanthin, echinenone and carotenes: lycopene, *β*-carotene, phytofluene and phytoene, ionized by ESI, APCI, and APPI. For all of the carotenoids tested, it was possible to obtain characteristic transitions for their identification in each of the three ionization techniques employed. The most sensitive transition was used to generate a quantifier (Q1) and the second most sensitive transition to generate a qualifier (Q2). The transitions obtained for each carotenoid using the three different API techniques are shown in Tables 4 and 5.

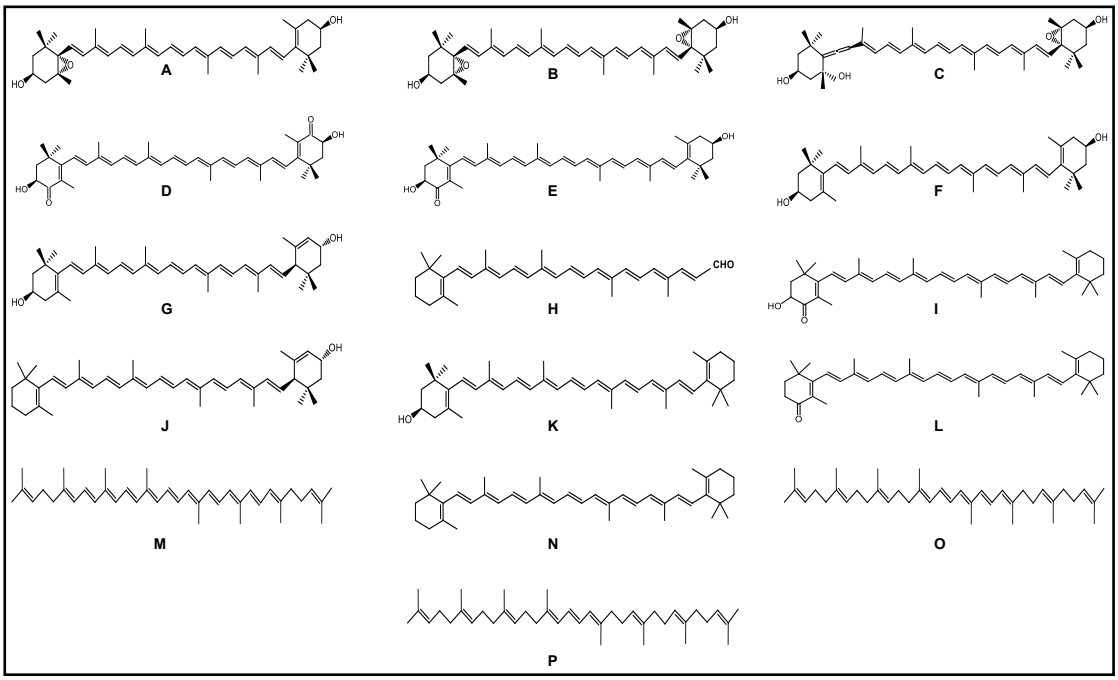

Figure 2-2. Carotenoid structures used in this study: xanthophylls, (**A**) antheraxanthin, (**B**) violaxanthin, (**C**) neoxanthin, (**D**) astaxanthin, (**E**) adonixanthin, (**F**) zeaxanthin, (**G**) lutein, (**H**) *β*-apo-8′-carotenal, (**I**) 3-hydroxyechinenone, (**J**) *α*-cryptoxanthin, (**K**) *β*-cryptoxanthin, (**L**) echinenone and carotenes, (**M**) lycopene, (**N**) *β*-carotene, (**O**) phytofluene and (**P**) phytoene.

All of the carotenoids ionized by APCI showed the protonated molecular ion $[M+H]^+$: 585.3 for antheraxanthin, 601.3 for violaxanthin, 601.4 for neoxanthin, 597.6 for astaxanthin, 583.4 for adonixanthin, 569.4 for lutein and zeaxanthin, 417.5 for *β*-apo-8′-carotenal, 567.3 for 3-hydroxyechinenone, 553.6 for *β*-and *α*-cryptoxanthin, 551.6 for echinenone, 537.7 for lycopene and

β-carotene, 543.5 for phytofluene and 545.5 for phytoene. In the other two API techniques, the molecular ions observed could be either the protonated molecular ion $[M+H]^+$, the molecular ion $[M]^+$, or both. For ESI, the protonated molecular ions obtained were: 585.3 for antheraxanthin, 601.3 for violaxanthin, 601.4 for neoxanthin, 597.6 for astaxanthin, 583.4 for adonixanthin, 417.5 for *β*-apo-8′-carotenal, 553.6 for *β*- and *α*-cryptoxanthin and 551.6 for echinenone. The molecular ions obtained were: 568.7 for lutein and zeaxanthin, 566.3 for 3-hydroxyechinenone, 536.7 for lycopene and *β*-carotene, 542.5 for phytofluene and 544.5 for phytoene. For APPI, the protonated molecular ions obtained were: 585.3 for antheraxanthin, 601.3 for violaxanthin, 601.4 for neoxanthin, 597.6 for astaxanthin, 583.4 for adonixanthin, 569.4 for zeaxanthin and lutein, 417.5 for *β*-apo-8′-carotenal and 567.3 for 3-hydroxyechinenone. Finally, the molecular ions obtained were: 568.7 for lutein, 552.6 for *β*- and *α*-cryptoxanthin, 550.6 for echinenone, 536.7 for lycopene and *β*-carotene, 542.5 for phytofluene and 544.5 for phytoene. The molecular ion and most of the carotenoid fragments obtained in each of the API techniques are in agreement with the results reported by several authors [2, 19-24].

Table 2-4. Characteristic carotenoid transitions.

Antheraxanthin		
API	Transition (*m*/*z*)	Collision Energy (V)
ESI	585.3 > 93.1 (Q_1)	40
ESI	585.3 > 105.2 (Q_2)	50
APCI	585.3 > 93.1 (Q_1)	55
APCI	585.3 > 105.2 (Q_2)	45
APPI	585.3 > 119.1 (Q_1)	45
APPI	585.3 > 145.2 (Q_2)	40

Violaxanthin		
API	Transition (*m*/*z*)	Collision Energy (V)
ESI	601.3 > 93.1 (Q_2)	45
ESI	601.3 > 221.3 (Q_1)	25
APCI	601.3 > 93.1 (Q_1)	45
APCI	601.3 > 133.3 (Q_2)	40
APPI	601.3 > 93.1 (Q_2)	55
APPI	601.3 > 221.3 (Q_1)	25

Neoxanthin		
API	Transition (*m*/*z*)	Collision Energy (V)
ESI	601.4 > 167.3 (Q_1)	20
ESI	601.4 > 105.3 (Q_2)	60
APCI	601.4 > 583.4 (Q_1)	10
APCI	601.4 > 167.3 (Q_2)	20
APPI	601.4 > 167.3 (Q_1)	20
APPI	601.4 > 105.3 (Q_2)	60

Astaxanthin		
API	Transition (*m*/*z*)	Collision Energy (V)
ESI	597.6 > 505.4 (Q_2)	10
ESI	597.6 > 147.1 (Q_1)	20
APCI	597.6 > 579.4 (Q_2)	20
APCI	597.6 > 147.1 (Q_1)	20
APPI	597.6 > 579.6 (Q_2)	10
APPI	597.6 > 147.1 (Q_1)	40

Adonixanthin		
API	Transition (*m*/*z*)	Collision Energy (V)
ESI	583.4 > 565.4 (Q_2)	15
ESI	583.4 > 147.4 (Q_1)	40
APCI	583.4 > 565.4 (Q_2)	15
APCI	583.4 > 147.4 (Q_1)	40
APPI	583.4 > 565.4 (Q_2)	15
APPI	583.4 > 147.4 (Q_1)	40

Zeaxanthin		
API	Transition (*m*/*z*)	Collision Energy (V)
ESI	568.7 > 476.6 (Q_1)	15
ESI	568.7 > 283.2 (Q_2)	15
APCI	569.4 > 551.5 (Q_2)	10
APCI	569.4 > 135.0 (Q_1)	30
APPI	569.4 > 477.6 (Q_2)	15
APPI	569.4 > 135.0 (Q_1)	50

Table 2-5. Characteristic carotenoid transitions.

Lutein		
API	Transition (*m/z*)	Collision Energy (V)
ESI	568.7 > 476.6 (Q_1)	15
ESI	568.7 > 283.2 (Q_2)	15
APCI	569.4 > 551.5 (Q_2)	10
APCI	569.4 > 135.0 (Q_1)	30
APPI	569.4 > 135.0 (Q_2)	15
APPI	568.7 > 338.5 (Q_1)	15

β-apo-8‘-Carotenal		
API	Transition (*m/z*)	Collision Energy (V)
ESI	417.5 > 325.3 (Q_2)	10
ESI	417.5 >121.0 (Q_1)	15
APCI	417.5 > 325.3 (Q_2)	10
APCI	417.5 > 94.9 (Q_1)	25
APPI	417.5 > 145.2 (Q_2)	20
APPI	417.5 > 119.0 (Q_1)	40

3-Hydroxyechinenone		
API	Transition (*m/z*)	Collision Energy (V)
ESI	566.3 > 93.0 (Q_1)	45
ESI	566.3 > 69.0 (Q_2)	50
APCI	567.3 > 93.0 (Q_1)	50
APCI	567.3 > 69.0 (Q_2)	50
APPI	567.3 > 93.0 (Q_2)	50
APPI	567.3 > 69.0 (Q_1)	50

α-Cryptoxanthin		
API	Transition (*m/z*)	Collision Energy (V)
ESI	553.6 > 461.6 (Q_1)	15
ESI	553.6 > 119.0 (Q_2)	35
APCI	553.6 > 461.6 (Q_1)	15
APCI	553.6 > 119.0 (Q_2)	35
APPI	552.6 > 460.6 (Q_1)	15
APPI	552.6 > 119.0 (Q_2)	35

β-Cryptoxanthin		
API	Transition (*m/z*)	Collision Energy (V)
ESI	553.6 > 461.6 (Q_1)	15
ESI	553.6 > 119.0 (Q_2)	35
APCI	553.6 > 461.6 (Q_1)	15
APCI	553.6 > 119.0 (Q_2)	35
APPI	552.6 > 460.6 (Q_1)	15
APPI	552.6 > 119.0 (Q_2)	35

Echinenone		
API	Transition (*m/z*)	Collision Energy (V)
ESI	551.6 > 93.0 (Q_2)	35
ESI	551.6 > 69.0 (Q_1)	45
APCI	551.6 > 93.0 (Q_2)	35
APCI	551.6 > 69.0 (Q_1)	45
APPI	550.6 > 93.0 (Q_2)	35
APPI	550.6 > 69.0 (Q_1)	45

β-carotene		
API	Transition (*m/z*)	Collision Energy (V)
ESI	536.7 > 444.7 (Q_1)	15
ESI	536.7 > 69.0 (Q_2)	40
APCI	537.7 > 445.7 (Q_1)	15
APCI	537.7 > 119.0 (Q_2)	40
APPI	536.7 > 444.7 (Q_1)	15
APPI	536.7 > 119.0 (Q_2)	40

Lycopene		
API	Transition (*m/z*)	Collision Energy (V)
ESI	536.7 > 444.7(Q_2)	10
ESI	536.7 > 69.0 (Q_1)	40
APCI	537.7 > 93.0 (Q_2)	50
APCI	537.7 > 69.0 (Q_1)	40
APPI	536.7 > 93.0 (Q_2)	50
APPI	536.7 > 69.0 (Q_1)	40

Phytofluene		
API	Transition (*m/z*)	Collision Energy (V)
ESI	542.5 > 93.0 (Q_2)	45
ESI	542.5 > 69.0 (Q_1)	45
APCI	543.5 > 93.0 (Q_2)	45
APCI	543.5 > 69.0 (Q_1)	45
APPI	542.5 > 93.0 (Q_2)	45
APPI	542.5 > 69.0 (Q_1)	45

Phytoene		
API	Transition (*m/z*)	Collision Energy (V)
ESI	544.5 > 81.0 (Q_1)	45
ESI	544.5 > 69.0 (Q_2)	45
APCI	545.5 > 81.0 (Q_1)	35
APCI	545.5 > 69.0 (Q_2)	35
APPI	544.5 > 81.0 (Q_1)	45
APPI	544.5 > 69.0 (Q_2)	45

APCI was seen to be a more powerful technique to ionize carotenoids than ESI or APPI. Table 6 compares the total ion current (TIC) of the carotenoids obtained by ESI, APCI, and APPI (without dopant). For antheraxanthin, neoxanthin, astaxanthin, adonixanthin, zeaxanthin, β-apo-8′-carotenal, 3-hydroxyechinenone, β- and α-cryptoxanthin, echinenone, phytofluene, and phytoene the strongest signal was observed by APCI. For violaxanthin and lutein, the strongest signal was observed by ESI. For lycopene and β-carotene, the strongest signal was observed by APPI.

Under the chromatographic conditions used in the UHPLC analysis it was observed that antheraxanthin coeluted with astaxanthin and lutein with zeaxanthin (Table 6). However, these carotenoids should be distinguishable and quantified using transitions that are specific for each of them according to the data shown in Tables 4 and 5. To corroborate this hypothesis the transitions obtained by APCI for antheraxanthin (585.3>93.1 and 585.3>105.2) were tested with astaxanthin and the transitions obtained by APCI for astaxanthin (597.6>147.1 and 597.6>579.4) were tested with antheraxanthin. Neither antheraxanthin nor astaxanthin showed signals when the transitions of its counterpart species were monitored (see supplementary data). Consequently, the transitions obtained by APCI for antheraxanthin and astaxanthin make it possible to distinguish these carotenoids and therefore they can be quantified, although they show the same chromatographic RT.

Table 2-6. Comparison of the TIC obtained by ESI, APCI and APPI for each carotenoid.

Carotenoid	RT[a] (min)	Concentration (μg/mL)	Area ESI^+	Area $APCI^+$	Area $APPI^+$
cis-Neoxanthin	3.40	5.0	2011	26842	2641
Violaxanthin	3.58	5.0	15908	15661	5569
Antheraxanthin	3.85	5.0	3481	15372	2069
Astaxanthin	3.85	1.9	13112	238521	17215
Adonixanthin	3.98	4.1	4326	77328	1789
Lutein	4.11	5.0	1837	1259	586
Zeaxanthin	4.11	5.0	77	3701	296
β-apo-8′-Carotenal	4.77	1.8	994	129069	9924
3-Hydroxyechinenone	5.68	0.4	679	9215	356
α-Cryptoxanthin	5.96	1.8	1789	4595	916
β-Cryptoxanthin	6.19	0.9	1147	3297	1071
Echinenone	6.45	0.3	109	1636	131
Lycopene	7.58	0.7	35544	35131	68040
β-Carotene	9.74	1.0	16089	21319	70020
Phytofluene	9.90	2.6	1774	24549	342
cis-Phytoene	10.98	9.0	146	102938	165

[a] Retention time

Lutein and zeaxanthin are usually very difficult to separate because they differ only in the position of a double bond in one of the terminal rings (Fig. 2). However, they could be distinguished and quantified if they are ionized by APPI. It was observed that the transition 568.7>338.5 was specific for lutein when the APPI technique was used to ionize it.

The use of the transition 568.7>338.5 was tested with a sample of transgenic maize TM1 (for plant

material see section 2.4.2) that contained zeaxanthin and lutein. This sample was analyzed by HPLC (chromatographic conditions are given in section 2.4.6.3). This LC system allows the separation of lutein from zeaxanthin chromatographically. The HPLC system made it possible to compare the response given by the PDA and mass detectors. Fig. 3 shows that the ratio lutein:zeaxanthin given by the PDA detector was similar to the ratio obtained by the mass detector using the transition 569.4>135.0, which is characteristic for both carotenoids: lutein and zeaxanthin. The transition 568.7>338.5 was only given by lutein. The research work presented in this section has been published [1].

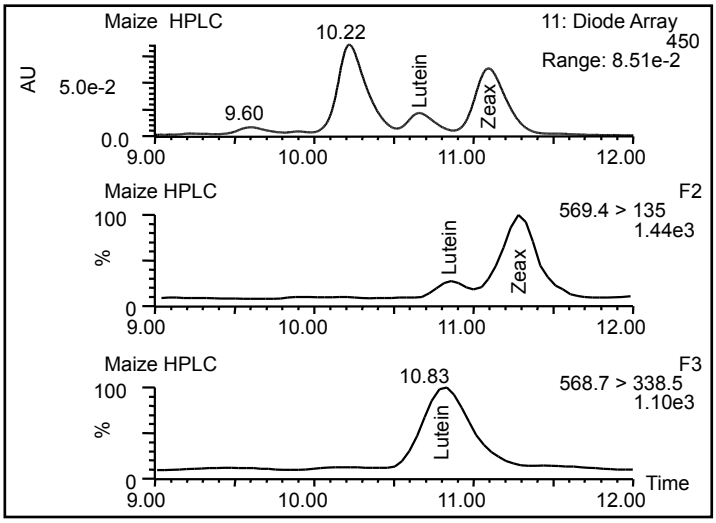

Figure 2-3. Comparison of response given by PDA and mass detectors to identify lutein and zeaxanthin in TM1. Abbreviations: Zeax, zeaxanthin.

2.5.2 Improvements in the detection of carotenoids using mass detector

2.5.2.1 APCI-MS/MS

Since MS/MS can provide high sensitivity and selectivity for the identification and quantitative analysis of carotenoids in biological samples, I tried finding characteristic fragment ions that may be related with functional groups present in the carotenoid structures. In order to achieve this goal, I conducted a search in the literature of characteristic carotenoid ions [3, 7, 19, 20, 24-27] and tested those theoretical ions with the extracted carotenoids from transgenic maize seeds and rice callus and carotenoid standards under UHPLC-APCI-MS/MS conditions (chromatographic conditions are given in section 2.4.6).

Using protonated molecules as precursor ions and the theoretical ions reported in the literature as daughter ions in positive ion mode, transitions were identified that may be used to distinguish between carotenoids. In addition, characteristic fragment ions were identified that might be helpful for structural characterization.

Based on my previous work (section 2.5.1), where I had investigated characteristic carotenoid ions through direct infusion of standard solutions, and the results obtained from testing several

characteristic carotenoid ions reported in the literature, I selected the most sensitive transitions to identify carotenoids. These final transitions are summarized in Table 7. All the structures of the carotenoids registered in Table 7 can be seen in the supplementary data.

Table 7 shows that there are common carotenoid daughter ions among pigments bearing the same functional group. Thus, for example, for ketocarotenoids containing in the same *β*-ring a hydroxyl group in carbon 3, (3') and a keto group in carbon 4, (4'), the ion at *m/z* 147 was observed. In addition, the transition obtained with this ion gave rise to the strongest ketocarotenoid signal strength. Van Breemen et al. [24] suggested that the fragment at *m/z* 147 corresponded to a dehydrated terminal ring with cleavage of the 7,8 carbon–carbon bond (fragmentation of the molecules can be seen in the supplementary data). The carotenoid daughter ion at *m/z* 203.1 was characteristic of carotenoids containing a keto group conjugated to the polyene chain. Van Breemen et al. [24] proposed that this ion is produced due to fragmentation at the 10,11 carbon–carbon bond with the charge remaining on the ketone moiety (see supplementary data). The ion at *m/z* 135.1 was characteristic of hydroxylated xanthophylls such as adonixanthin, lutein, zeaxanthin and *β*-cryptoxanthin. These xanthophylls have in common the presence of a hydroxyl group as the only substituent on the *β*-ring. Therefore, this ion was assigned to carotenoids with this characteristic in its structures and corresponded to the dehydrated terminal ring with cleavage at the 7,8 carbon–carbon bond [24] (see supplementary data).

Other characteristic carotenoid fragments reported in the literature were used to make transitions. For example, the ion $[M-92]^+$ was detected for *α*-cryptoxanthin and *β*-zeacarotene, which corresponded to loss of a neutral molecule of toluene and indicate the presence of extensive conjugation within the molecule [3]. The removal of a molecule of water $[M+H-18]^+$ was evidenced for carotenoids such as neoxanthin and astaxanthin, which is characteristic of hydroxylated xanthophylls (Table 7) [3].

Table 2-7. The most sensitive carotenoid transitions

Funtional group	Carotenoid	Precursor ion (*m/z*)	Daughter ion (*m/z*)	Collision Energy (V)
Epoxycarotenoids	Neoxanthin	601.4	167.2(Q2)	20
	Neoxanthin	601.4	583.4[a](Q1)	10
	Violaxanthin	601.4	93(Q1)	45
	Violaxanthin	601.4	133.3(Q2)	40
	Antheraxanthin	585.3	93.1(Q1)	55
	Antheraxanthin	585.3	105.2(Q2)	45
Ketocarotenoids	Astaxanthin	597.6	**147**(Q1)	40
	Astaxanthin	597.6	579.6[a](Q2)	15
	Adonixanthin	583.4	**135.1**(Q2)	40
	Adonixanthin	583.4	**147**(Q1)	40
	Adonirubin	581.5	**147**(Q1)	40
	Adonirubin	581.5	**203.1**(Q2)	40
	Canthaxanthin	565.9	69(Q2)	40
	Canthaxanthin	565.9	**203.1**(Q1)	40
	3-Hydroxyechinenone	567.3	93(Q2)	50
	3-Hydroxyechinenone	567.3	**147**(Q1)	40
	Echinenone	551.6	69(Q1)	45
	Echinenone	551.6	93(Q2)	35
	Echinenone	551.6	**203.1**(Q3)	40
Hydroxycarotenoids	Lutein	569.4	69(Q1)	40
	Lutein	569.4	**135.1**(Q2)	30
	Zeaxanthin	569.4	93(Q2)	40
	Zeaxanthin	569.4	**135.1**(Q1)	30
	α-Cryptoxanthin	553.6	119(Q2)	35
	α-Cryptoxanthin	553.6	461.6[b](Q1)	15
	β-Cryptoxanthin	553.6	119(Q1)	35
	β-Cryptoxanthin	553.6	**135.1**(Q2)	30
Carotenes	Lycopene	537.7	69(Q1)	40
	Lycopene	537.7	93(Q2)	50
	β-Zeacarotene	539.6	69.3(Q1)	35
	β-Zeacarotene	539.6	447[b](Q2)	10
	α-Carotene	537.6	95.1(Q2)	35
	α-Carotene	537.6	**123.1(Q1)**	40
	β-Carotene	537.6	68,9(Q2)	40
	β-Carotene	537.6	95.1(Q1)	35
	phytofluene	543.5	69(Q1)	45
	phytofluene	543.5	93(Q2)	45
	Phytoene	545.5	69(Q2)	35
	Phytoene	545.5	81(Q1)	35

2.5.2.2 Distinguishing carotenoids through comparison of the intensities of their fragments

Carotenoids with a very similar structure can be differentiated through comparison of the intensities of their fragments. Lutein and zeaxanthin have the same chemical formula ($C_{40}H_{56}O_2$) but are distinguishable by the position of the hydroxyl group. In the lutein, this functional group is located in the allylic position of the *ε*-ring while in zeaxanthin it is located in the *β*-ring and thus not in an allylic position (Fig. 2). In lutein mass spectrum (Fig. 4), the fragment at *m/z* 551 $[M+H-18]^+$ was a much more abundant ion than the protonated molecular ion (*m/z* 569), while zeaxanthin exhibited the opposite behavior (Fig. 4). The loss of water due to the presence of the hydroxyl group in an allylic position (a hydroxyl group located in *ε*-ring) produces the $[M+H-18]^+$ ion, which is stabilized by mesomeric effects (see supplementary data). Consequently, this ion is more stable than the ion formed by the loss of water due to the presence of the hydroxyl group, which is not in an allylic position (a hydroxyl group located in *β*-ring). This mass spectrometric behavior was used to confirm the identity of carotenoids such as lutein epoxide and antheraxanthin [28].

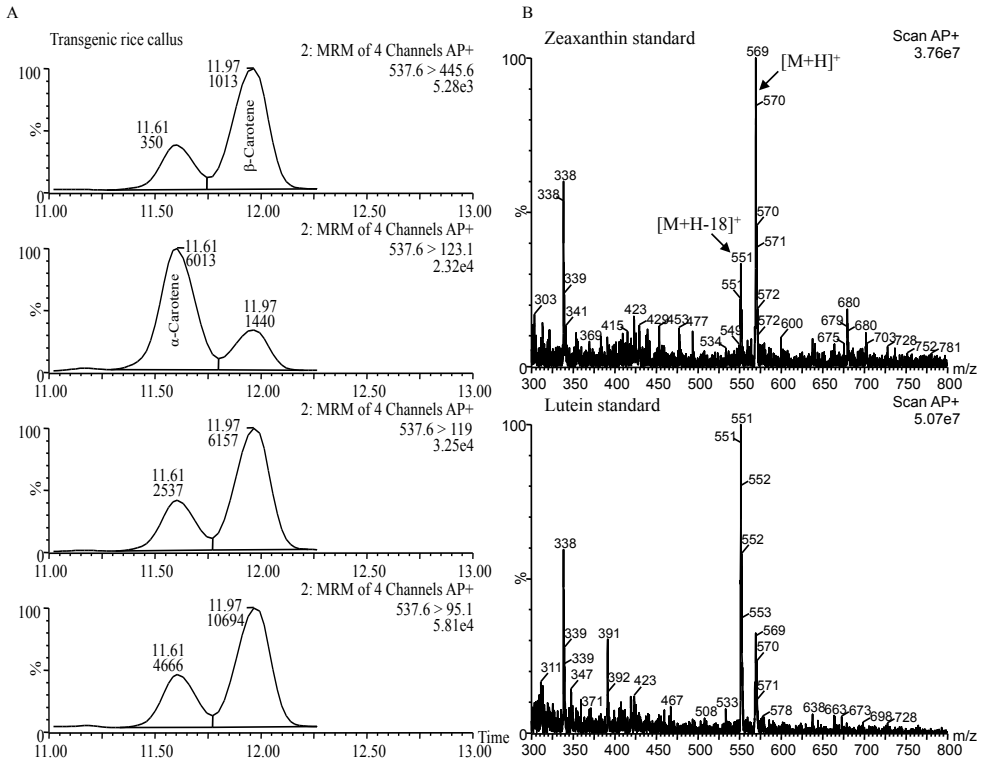

Figure 2-4. A) Comparison of the intensities of the transitions between *β*-carotene and *α*-carotene and B) positive ion APCI mass spectra of zeaxanthin and lutein standards.

Similarly, differences in the intensities of the transitions between *β*-carotene and *α*-carotene were observed. *α*-Carotene differs from *β*-carotene only by the position of a double bond in one of the terminal rings, an *α*-ionone moiety (see supplementary data). All the transitions given by the *α*-carotene (Fig. 4) were the same as those for *β*-carotene (e.g., 537.6>445.6, 537.6>123.1, 537.6>119 and 537.6>95.1). However, the most intense transition for *α*-carotene in the positive ion mode

corresponded to the transition 537.6>123.1, which was observed as well for *β*-carotene but in lower intensity. Formation of the ion at *m/z* 123.1 was facilitated by the position of the double bond in the terminal ring, which helped stabilize the resulting carbocation [24] (see supplementary data). Thus, by comparison of the intensities of this ion or the transition formed with this ion, it may be used to identify carotenoids with *ε*-ring in their structures.

Although some carotenoids show the same or a very similar fragmentation pattern (meaning that their structures are similar and therefore they might coelute), differences between the intensities of their fragments can be used to distinguish the molecules. Moreover, these differences can provide an insight into the predominant carotenoid when coelution occurs.

2.5.2.3 Dopant effect

Four dopants—acetone, toluene, anisole, and chlorobenzene— were tested to improve the ionization and enhance the carotenoid signal in APPI. These compounds have been extensively used in APPI as dopants [29-32]. Fig. 5 shows the effect of adding a post-column dopant in APPI. The dopant was introduced at a flow rate of 15 *μ*L/min to the eluent before entering the APPI probe.

The results can be analyzed by grouping the compounds depending on whether they belong to either the xanthophyll or the carotene groups. The signal strength of most of the xanthophylls analyzed was improved when a dopant was used (Fig. 5). Chlorobenzene enhanced 3.4-, 1.3-, 1.6-, 2.8-, and 3.2-fold the signal strength of neoxanthin, astaxanthin, *β*-apo-8′-carotenal, *α*-cryptoxanthin and *β*-cryptoxanthin, respectively. Toluene was the best dopant for violaxanthin, antheraxanthin, adonixanthin, 3-hydroxyechinenone and echinenone. It enhanced the signal strength of these compounds 2.3-, 3.5-, 3.5-, 2.5-, and 3.3-fold, respectively. Anisole was the dopant that best enhanced the signal strength of lutein: 1.8-fold. It also produced the same enhancement of signal strength for antheraxanthin and echinenone as toluene. Finally, acetone only improved the signal strength of zeaxanthin by 2.4-fold.

The signal strength of the tested carotenes was usually improved when a dopant was used (Fig. 5). Chlorobenzene was the dopant that most enhanced the signal strength of lycopene and *β*-carotene, 4.9- and 3.5-fold respectively. Anisole was the dopant that most enhanced the signal strength of phytofluene and phytoene, 16- and 178-fold respectively.

Only in a few cases was the signal strength of the compounds studied similar or lower using a dopant than the value obtained without a dopant. Thus, astaxanthin and *β*-apo-8′-carotenal did not show any improvement in their signals when acetone, toluene and anisole were used as the dopant. Astaxanthin and *β*-apo-8′-carotenal signal strengths obtained with these dopants were similar to the values obtained without a dopant. Lutein showed a slightly weaker signal strength with acetone and a similar signal strength using toluene and chlorobenzene. Phytoene showed a slightly weaker signal strength with acetone and a similar signal strength with toluene. Finally, chlorobenzene did not affect the signal strength of zeaxanthin.

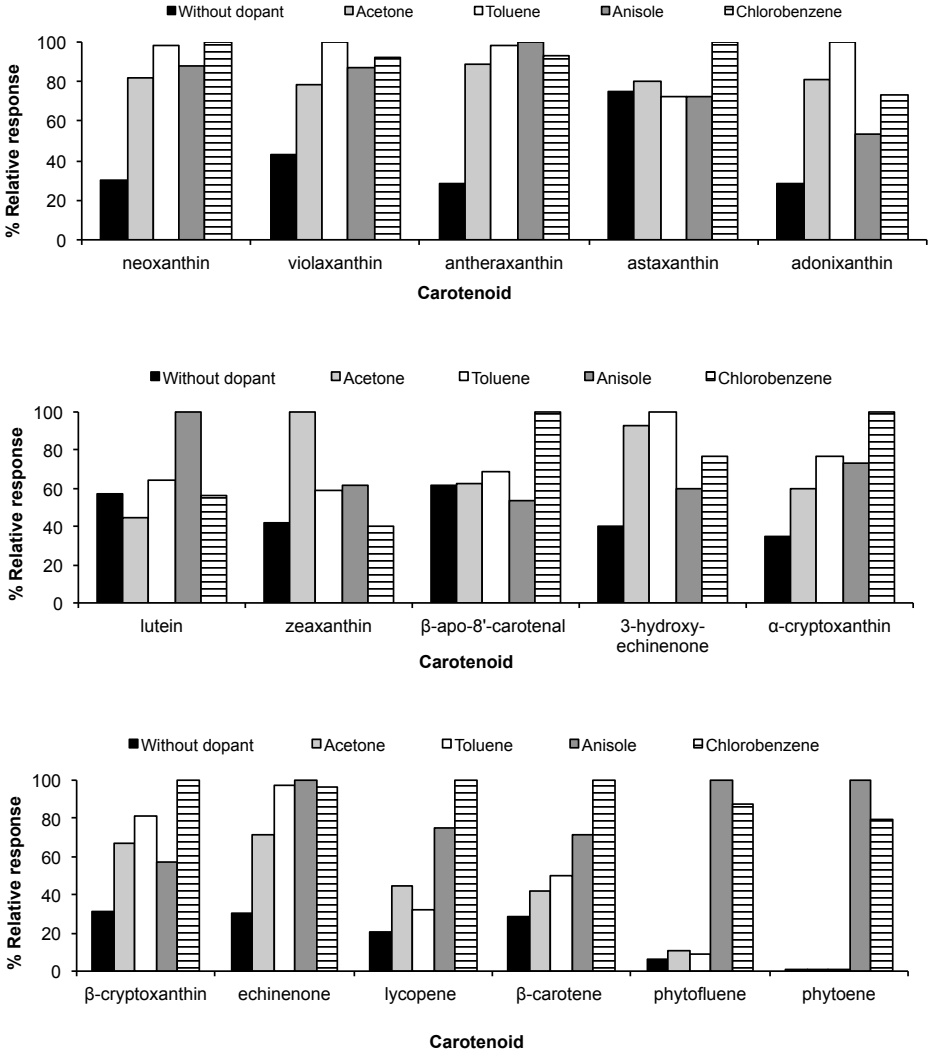

Figure 2-5. Effect of dopants on the signal strength of different carotenoids ionized by APPI. Xanthophylls: antheraxanthin, violaxanthin, neoxanthin, astaxanthin, adonixanthin, zeaxanthin, lutein, *β*-apo-8′-carotenal, 3-hydroxyechinenone, *α*-cryptoxanthin, *β*-cryptoxanthin, echinenone and carotenes: lycopene, *β*-carotene, phytofluene and phytoene.

Although the signal strength of the xanthophylls tested was improved with the different dopants used, the highest enhancement of the signal strength was observed with carotenes (Fig. 5). These results could be because of the difference of polarities among the carotenoids studied. Although all carotenoids are considered nonpolar compounds, the xanthophylls are more polar compounds than carotenes. Consequently, the effect of the tested dopants on the signal strength will be higher for the less polar carotenoids. Several authors have already noted that dopant assisted (DA)-APPI gives the best results when less polar compounds were used.

2.5.3 Validation method

As most of the carotenoids analyzed are quantified with the UHPLC-PDA technique, the validation test was carried using this analytical method. Thus, calibration curves estimation, LOD, LOQ, precision and relative recovery were investigated to evaluate the integrity of this analytical method. In

addition, matrix effects in maize samples was investigated since astaxanthin and antheraxanthin coelute and, therefore, they are quantified with mass detector.

2.5.3.1 Calibration curves

The choice of the solvent used to dissolve the carotenoids was based on either the previously reported carotenoid solubility or the availability of its absorption coefficient [19].

Stock carotenoid solutions were prepared in ethanol, acetone and hexane [19]. Carotenoid concentrations were determined spectrophotometrically. Table 8 shows the solvent and the value of $A^{1\%}_{1\,cm}$ used to quantify each pigment. Standard solutions were prepared from stock solutions by sampling an aliquot and diluting it with injection solvent and their concentrations assessed by UHPLC analysis. For those carotenoids dissolved in hexane (canthaxanthin, *β*-cryptoxanthin, *β*-carotene, lycopene and phytoene), standard solutions were prepared from stock solutions by drying an aliquot under nitrogen and diluting it with injection solvent. Calibration curves were obtained by injecting known concentrations of mixtures of standards and recording the resulting area. Between 10 and 5 standard solutions were prepared to determine the calibration curve and three replicate measurements were made for each standard solution. Figs. 6 and 7 show the calibration curve obtained for each carotenoid standard.

Solubilization problems were encountered for carotenes (when lycopene and *β*-carotene were dissolved in hexane) and for ketocarotenoids (when astaxanthin and canthaxanthin were dissolved in ethanol and hexane respectively). Chloroform, dichloromethane, hexane, ethyl acetate and tetrahydrofuran [33-36] are known to dissolve lycopene and *β*-carotene. Thus, I chose hexane to solubilize these compounds. Initially, I attempted to prepare 100 *μ*g/mL stock solutions of lycopene and *β*-carotene in hexane, but a precipitate was observed in the bottom of the vessels. Consequently, to ensure that carotenes were completely dissolved, stock solutions of carotenes were prepared again in hexane but in lower concentrations (Table 8). Thus, stock solutions of 24.85 *μ*g/mL for *β*-carotene and 8.26 *μ*g/mL for lycopene were prepared. We did not encounter solubilization problems with these concentrations. In addition, the calibration curves of these pigments (Fig. 6) indicated that the chromatographic peak areas of carotenes gave a linear plot throughout the concentration range studied.

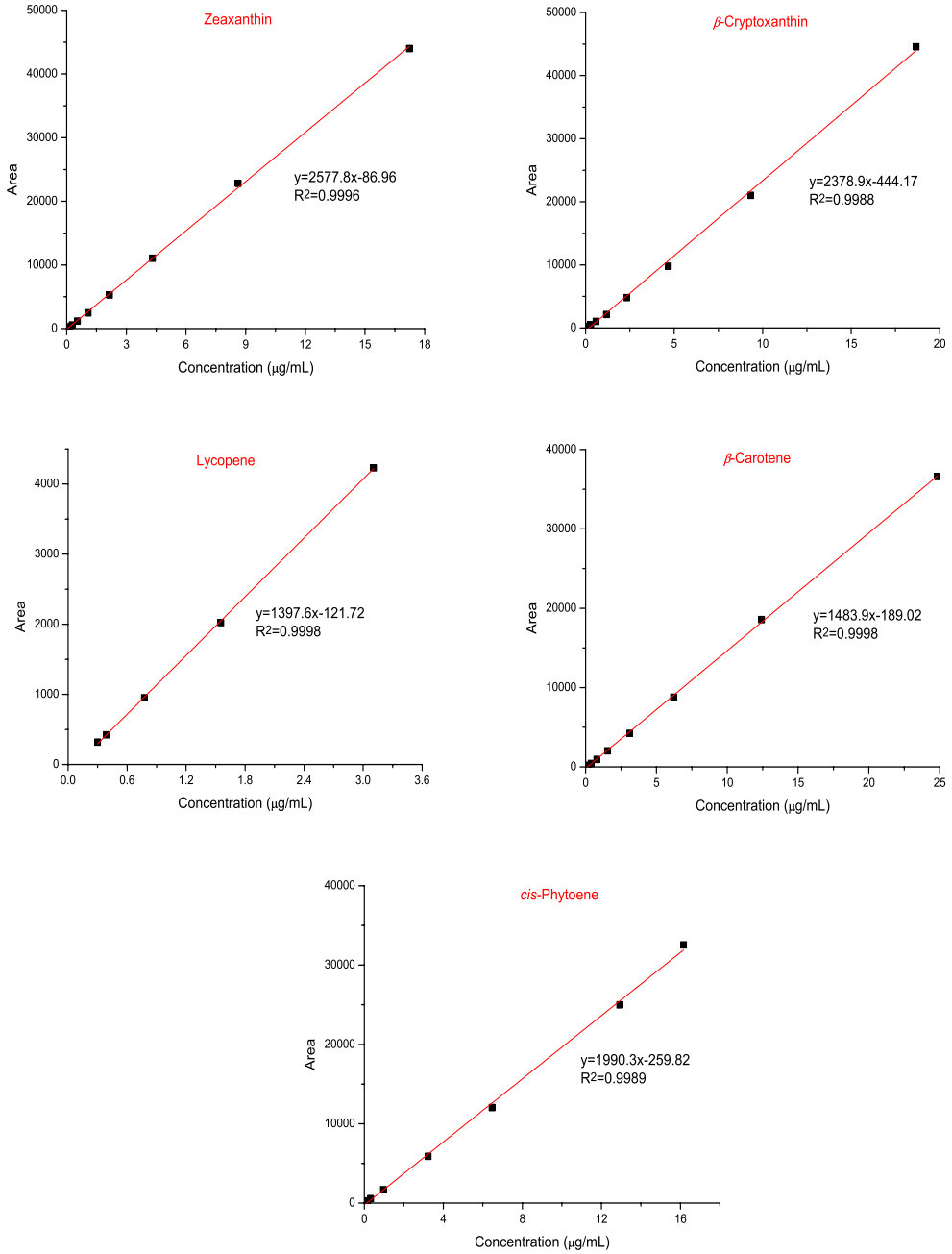

Figure 2-6. Calibration curves of carotenoid standards. The zeaxanthin curve was built from stock solutions prepared in acetone. The *β*-cryptoxanthin, *β*-carotene, lycopene and *cis*-phytoene curves were built from stock solutions prepared in hexane.

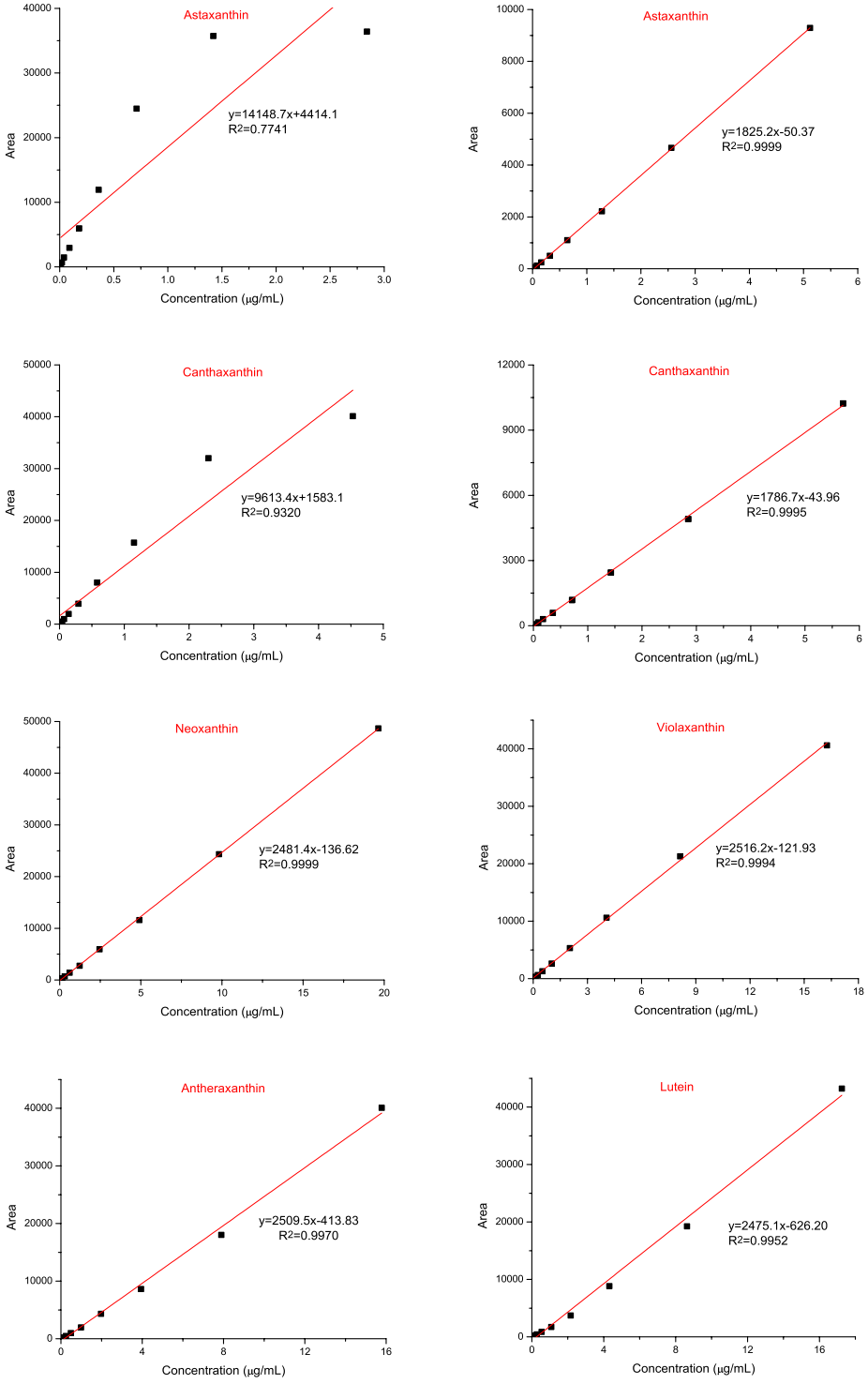

Figure 2-7. Calibration curves of carotenoid standards. The canthaxanthin and astaxanthin curves on the left were built from stock solutions prepared in hexane and ethanol respectively while those on the right were built from stock solutions prepared in the injection solvent. The violaxanthin, antheraxanthin, neoxanthin and lutein curves were built from stock solutions prepared in ethanol.

Similarly, canthaxanthin and astaxanthin were not properly dissolved in hexane and ethanol respectively. Because of the problems of solubilization observed with these compounds, I determined and compared their concentrations using two different methods: dividing the mass of the carotenoid by the total volume of solution (theoretical concentration) and spectrophotometrically (experimental concentration). The theoretical and experimental concentration obtained for canthaxanthin was 4.53 and 0.27 μg/mL, respectively whereas for astaxanthin it was 4.96 and 1.55 μg/mL, respectively. The lower concentrations of ketocarotenoids obtained experimentally indicated that hexane and ethanol were not appropriate solvents for canthaxanthin and astaxanthin, respectively. In addition, Fig. 7 shows that the calibration curves of these two pigments were characterized by a poor r-squared ($R^2 <$ 0.93). Therefore, I prepared stock ketocarotenoid solutions in the injection solvent of 5.12 μg/mL for astaxanthin and 5.70 μg/mL for canthaxanthin (Table 8). In this case, the concentration was determined only by dividing the mass of the carotenoid by the total volume of solution. Fig. 7 shows that the calibration curves of these pigments dissolved in the injection solvent gave a linear plot throughout the concentration range studied. I did not encounter any solubilization problems with the concentration range used for: a) violaxanthin, antheraxanthin, neoxanthin and lutein, dissolved in ethanol; or b) zeaxathin, dissolved in acetone and c) β-cryptoxanthin, dissolved in hexane. As reported previously [37-40], xanthophylls showed satisfactory solubility in methanol, ethanol and acetone.

Table 2-8. Concentrations of carotenoid stock solutions used to build calibration curves.

Carotenoid	Solvent	$A^{1\%}_{1\,cm}$	Stock carotenoid concentration (μg/mL)	Standard solutions range (μg/mL)
Neoxanthin	Ethanol	2380	19.64[a]	0.04-19.64
Violaxanthin	Ethanol	2550	16.26[a]	0.03-16.26
Antheraxanthin	Ethanol	2350	17.53[a]	0.03-15.78
Astaxanthin	Ethanol	2100	1.55[a] and 4.96[b]	0.01-2.84
Astaxanthin	Injection solvent	-	5.12[b]	0.04-5.12
Zeaxanthin	Acetone	2340	32.31[a]	0.03-17.23
Lutein	Ethanol	2550	21.57[a]	0.02-17.25
Canthaxanthin	Hexane	2200	0.27[a] and 4.53[b]	0.01-4.53
Canthaxanthin	Injection solvent	-	5.70[b]	0.02-5.70
β-Cryptoxanthin	Hexane	2400	35.00[a]	0.04-18.67
β-Carotene	Hexane	2590	24.85[a]	0.1-24.85
Lycopene	Hexane	3450	8.26[a]	0.3-3.11
Phytoene	Hexane	915	16.16[a]	0.08-16.16

[a] Concentration was determined spectrophotometrically.
[b] Concentration was determined by dividing the mass of the carotenoid by the total volume of solution.

Konings et al. [39] prepared stock solutions of lutein, zeaxanthin, β-carotene and lycopene with the same solvents used in this study. However, they used a mixture of MeOH: THF (7.5:2.5, v/v) as injection solvent. Under the chromatographic conditions applied, they observed a higher linear range

for lutein, zeaxanthin and β-carotene than for lycopene. The smaller linearity range of lycopene (from 0 to 3.5 μg/mL) was explained by the lower solubility of this compound in the injection solvent. Nevertheless, the choice of the injection solvent was a compromise between satisfactory solubility of carotenoids, compatibility with mobile phase and the absence of peak distortions.

In general, the carotenoid calibration curves showed a satisfactory linearity under the concentration range studied. Correlation coefficients (R^2) obtained ranged from 0.9952 to 0.9999 (Table 9). Given the concentrations of carotenoids expected in maize samples, I did not prepare standard concentrations above 40 μg/mL. However, in my experience, higher concentrations of oxygen-functionalized carotenoids can be prepared with the injection solvent used here when needed. For example, concentrations of 100 μg/mL can be prepared for violaxanthin and neoxanthin.

When carotenoid standard solutions are used several times and stored under N_2 or Ar, their concentrations should be evaluated since the inert gas introduced several times into the vial evaporates the solvent, thereby changing the original carotenoid concentration. Thus, it is advisable to either divide the volume of carotenoid standard solutions into vials, putting only the volume required for each analysis into single vials, or to dry the standard solutions and redissolve these in each analysis. In addition, attention should be paid when many carotenoid standards at high concentrations are solubilized in the same solvent as some might precipitate. Thus, it is preferable to prepare various mixtures of carotenoids to ensure the complete solubilization of all analytes.

Carotenoids in samples were quantified mainly with the PDA detector through the external standard method. For those carotenoids for which there was no standard, they were assessed using the standard curves of the most similar carotenoids considering their structures and properties. Thus, the concentrations of adonixanthin and adonirubin were determined using the calibration curve of astaxanthin, 3-hydroxyechinenone and echinenone using the calibration curve of canthaxanthin, α-cryptoxanthin using the calibration curve of lutein and β-zeacarotene and α-carotene using the calibration curve of β-carotene.

2.5.3.2 LOD and LOQ

The LOD and LOQ were calculated using the equations:

$$LOD = 3.3 \cdot Sb/a$$

$$LOQ = 10 \cdot Sb/a$$

Where,

a is the curve slope and Sb is the SD of the intercept [41].

The LODs and LOQs reported in the Table 9 correspond to values obtained with the UHPLC-PDA technique. However, as astaxanthin coelutes with antheraxanthin and lutein with zeaxanthin, the LOD and LOQ for these pigments were also obtained using the UHPLC-APCI-MS/MS technique for

astaxanthin and antheraxanhtin and the HPLC-PDA technique for zeaxanthin and lutein. The LOD for carotenoids ranged from 0.01 to 0.11 μg/mL and LOQ from 0.02 to 0.35 μg/mL.

Table 2-9. Linear regression data, LOD and LOQ obtained by UHPLC-PDA.

Carotenoid	Linear range (μg/mL)	Slope	Intercept	LOD (μg/mL)	LOQ (μg/mL)	R^2
cis-Neoxanthin	0.04-19.64	2481±7.57	-136.62±16.28	0.02	0.07	0.9999
Violaxanthin	0.03-16.26	2516±5.59	-121.93±12.97	0.02	0.05	0.9994
Antheraxanthin	0.03-15.78	2509±22.13	-413.83±4.13	0.01	0.02	0.9970
Antheraxanthin[a]	0.03-15.78	3342±427	97.20±116.40	0.11	0.35	0.9994
Astaxanthin	0.04-5.12	1825±6.43	-50.37±10.51	0.02	0.06	0.9999
Astaxanthin[a]	0.05-5.79	2549.9±42.85	311.45±54	0.07	0.21	0.9999
Lutein	0.02-17.25	2475±81.74	-626.20±35.78	0.05	0.14	0.9952
Lutein[b]	0.02-17.25	257617±1144	18306±1646	0.02	0.06	0.9999
Zeaxanthin	0.03-17.23	2578±38.04	-86.96±25.8	0.03	0.10	0.9996
Zeaxanthin[b]	0.03-17.23	273243±2001	9099±786	0.01	0.03	0.9999
Canthaxanthin	0.02-5.70	1787±4.24	-43.96±16.13	0.03	0.09	0.9995
β-Cryptoxanthin	0.04-18.67	2379±0.35	-444.17±31.46	0.04	0.13	0.9988
Lycopene	0.3-3.11	1398±104.40	-121.72±24.88	0.06	0.18	0.9998
β-Carotene	0.1-24.85	1484±27.22	-189.02±29.80	0.07	0.20	0.9998
cis-Phytoene	0.08-16.16	1990±285.46	-259.82±37.32	0.06	0.19	0.9989

[a] Linear regression data and LOD and LOQ obtained by UHPLC-MS/MS.
[b] Linear regression data and LOD and LOQ obtained by HPLC-PDA.

2.5.3.3 Relative recovery, precision and accuracy

The **relative recovery** of seven standards was determined at two concentration levels (Table 10) by spiking the "blank" samples with the appropriate concentration and extracting according to the method (see section 2.4.4). In addition, "blank" unspiked samples were extracted concurrently. The "blank" sample was the South African elite white maize variety M37W, which has very few carotenoids and in low concentration. After reconstituting in solvent, the samples were analyzed. The relative recovery was determined by comparing the response ratios of samples from spiked maize to the response ratios of concentration of fortification.

$$\text{Relative recovery} = (C1-C2)/C3*100\%$$

Where,

C1 = concentration determined in spiked maize

C2 = concentration determined in unfortified sample

C3 = concentration of fortification

Relative recoveries of *β*-carotene, zeaxanthin, lutein, astaxanthin, antheraxanthin and *β*-cryptoxanthin ranged from 82% to 108% (Table 10) at the level tested. However, the relative recovery for lycopene ranged from 58 to 62%. Its low recovery may be attributed to the fact that lycopene seems to be an unstable compound comparing with other carotenoids [35, 42] and/or it may have a lower solubility in the solvents used during the extraction process or chromatographic analysis. With the exception of lycopene, satisfactory recoveries were obtained for the other tested analytes within the mentioned validation interval, suggesting that the analytical method is reliable.

The **accuracy** was expressed as relative error (%Er) and determined as follows [43]:

$$\%Er = [(\text{Mean of measured conc.} - \text{Theoretical conc.})/\text{Theoretical conc.}]*100$$

Where,

Mean of measured conc. = mean of measured concentration

Theoretical conc. = theoretical concentration

The %Er obtained from the lowest concentration of *β*-carotene, zeaxanthin, lutein, astaxanthin, antheraxanthin and *β*-cryptoxanthin was below 7.7% (Table 10) while from the highest concentration of *β*-carotene, zeaxanthin, lutein, astaxanthin, antheraxanthin and *β*-cryptoxanthin, it was below 18% (Table 10). For acceptance, %Er values should be below 15% [13, 44]. Thus, a satisfactory level of accuracy was observed for most of the carotenoids with the concentration level studied. In the case of lycopene, as commented above, it exhibited a poor recovery, therefore, its %Er were outside of the range of acceptance, up to 42% (Table 10).

The **precision** was estimated by the evaluation of the intra-day precision (repeatability). The intra-day precision was determined by calculating the relative standard deviation (%RSD) as follows:

$$\%RSD = (SD/\bar{x})*100\%$$

Where, SD= sample standard deviation, $\bar{x}$ = mean value of the sample data set.

The %RSD for all analytes studies was below 13.15% and 10.55% for low and high concentration levels, respectively (Table 10). For acceptance, %RSD values should be below 15% [13, 44]. Therefore, a satisfactory level of precision was observed with the concentration level tested. Therefore, the quantification of lycopene in samples was corrected based on its recovery.

Table 2-10. Method accuracy and carotenoid relative recoveries in maize samples.

β-Carotene							Relative recovery (%)		
Level	Theoretical conc.[a] *μ*g/mL	N	Measured conc.[b] *μ*g/mL	SD	%RSD	%Er	Mean	SD	%RSD
Low	0.48	6	0.46	0.03	6.13	3.7	96	7.67	7.96
High	5.52	6	4.54	0.20	4.40	18	82	4.34	5.27
Zeaxanthin							Relative recovery (%)		
Level	Theoretical conc.[a] *μ*g/mL	N	Measured conc.[b] *μ*g/mL	SD	%RSD	%Er	Mean	SD	%RSD
Low	0.35	5	0.36	0.02	5.52	3.9	104	8.15	7.83
High	3.93	5	3.66	0.19	5.19	6.8	93	4.98	5.34
Astaxanthin							Relative recovery (%)		
Level	Theoretical conc.[a] *μ*g/mL	N	Measured conc.[b] *μ*g/mL	SD	%RSD	%Er	Mean	SD	%RSD
Low	0.14	5	0.14	0.01	9.88	2.1	102	10.40	10.17
High	5.66	5	5.55	0.29	5.18	2.0	98	3.62	3.69
Lycopene							Relative recovery (%)		
Level	Theoretical conc.[a] *μ*g/mL	N	Measured conc.[b] *μ*g/mL	SD	%RSD	%Er	Mean	SD	%RSD
Low	0.69	5	0.43	0.06	13.15	38	62	7.03	11.35
High	1.79	5	1.03	0.11	10.55	42	58	4.97	8.56
Antheraxanthin							Relative recovery (%)		
Level	Theoretical conc.[a] *μ*g/mL	N	Measured conc.[b] *μ*g/mL	SD	%RSD	%Er	Mean	SD	%RSD
Low	0.62	6	0.57	0.06	9.71	7.42	93	8.36	9.02
High	3.88	6	3.52	0.24	6.83	9.23	90	7.01	7.75
Lutein							Relative recovery (%)		
Level	Theoretical conc.[a] *μ*g/mL	N	Measured conc.[b] *μ*g/mL	SD	%RSD	%Er	Mean	SD	%RSD
Low	0.55	6	0.54	0.03	5.29	2.0	98	7.29	7.43
High	5.57	6	5.41	0.18	3.34	2.8	97	4.81	4.94
β-cryptoxanthin							Total recovery (%)		
Level	Theoretical conc.[a] *μ*g/mL	N	Measured conc.[b] *μ*g/mL	SD	%RSD	%Er	Mean	SD[a]	%RSD
Low	0.30	5	0.33	0.02	6.65	7.7	108	7.37	6.84
High	3.20	5	3.34	0.10	2.91	4.3	104	5.77	5.53

[a] Theoretical concentration
[b] Mean of measured concentration

2.5.3.4 Matrix effect

Carotenoids were analyzed by UHPLC-APCI-MS/MS, as reported in section 2.4.6. Between 4 and 6 standard solutions were employed to build a linear regression plot of carotenoid area in solvent vs. carotenoid area in matrix (Fig. 8). The matrix effect was evaluated through multiplying the value of the slope of the line by 100. In this context, a value > 100% indicates ionization enhancement, whereas a value < 100% indicates ionization suppression. The matrix effects were determined for antheraxanthin, astaxanthin, violaxanthin, *β*-cryptoxanthin, zeaxanthin, *β*-carotene and phytoene (Table 11).

The results showed slight ionization suppression for violaxanthin (97%) and *β*-carotene (97%) whereas antheraxanthin (120%), zeaxanthin (103%) and phytoene (107%) showed ionization enhancement. Since these values ranged from 97 to 120% with %RSD lower than 10.8% (Table 11) and there is already an error inherent to the method [13, 44], it was considered that the matrix slightly influences the quantification of these compounds. Therefore, APCI allows the analysis of these pigments. On the contrary, *β*-cryptoxanthin showed a more severe enhancement matrix effect (slope 130%), hence, this compound demonstrated matrix effect problems with APCI (Table 11).

Table 2-11. Matrix effect evaluation in maize seeds using APCI technique.

Carotenoid	Concentration range (µg/mL)	Slope	Intercept	R^2	Matrix effect (%)	%RSD
Antheraxanthin	0.12-7.89	1.1987±0.02	160.39±7.06	0.9994	120	1.36
Astaxanthin	0.05-5.79	1.0001±0.03	337.96±32.17	0.9977	100	3.00
Violaxanthin	0.51-16.26	0.9741±0.11	950.56±168.01	0.9933	97	10.79
β-Cryptoxanthin	0.15-9.33	1.3045±0.00	291.07±14.05	0.9987	130	0.16
Zeaxanthn	1.08-17.23	1.026±0.04	259.49±35.93	0.9976	103	3.90
β-Carotene	0.78-24.85	0.9681±0.01	1126±195.49	0.9981	97	1.14
Phytoene	0.22-1.70	1.0666±0.01	96.989±61.50	0.9984	107	1.12

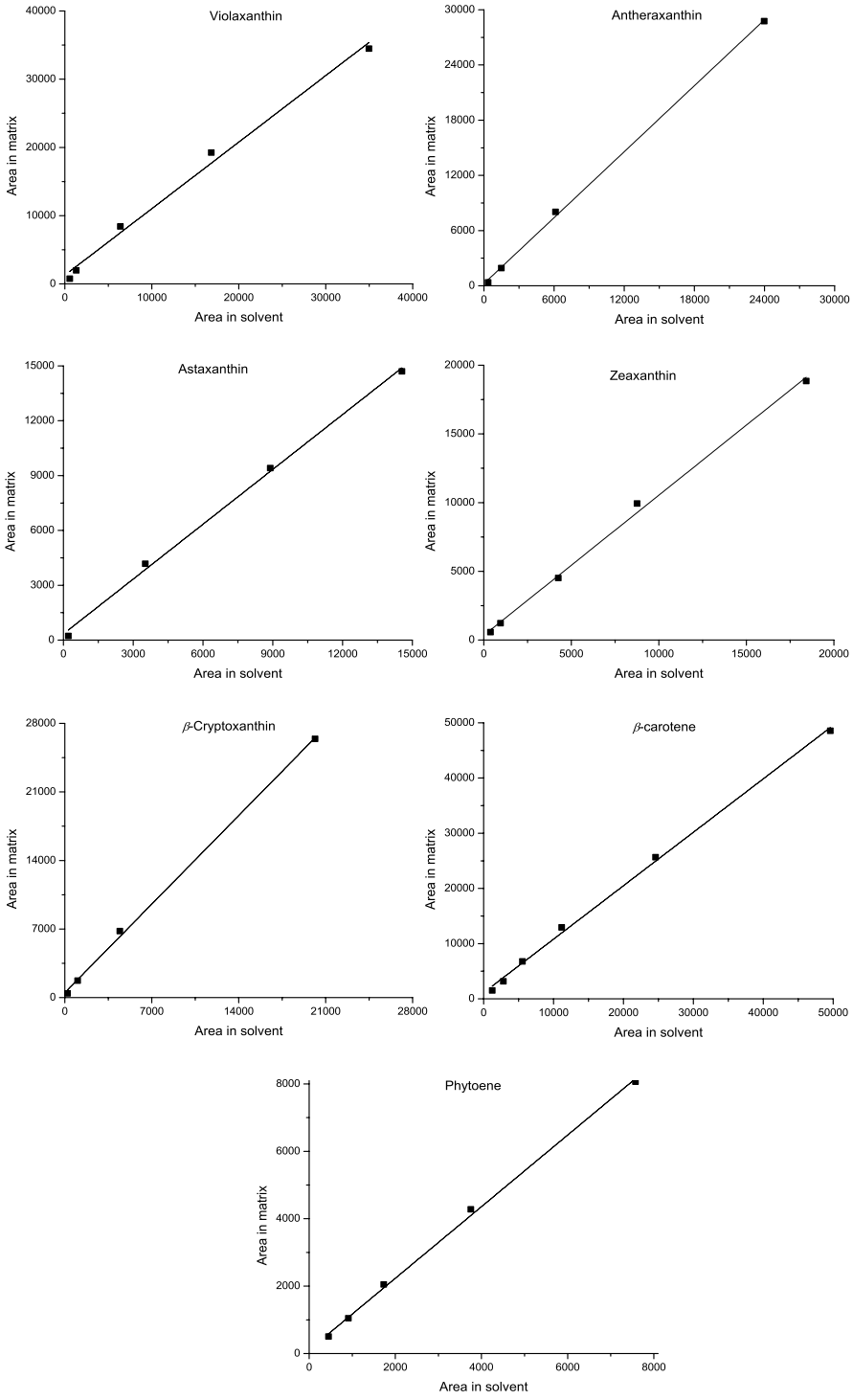

Figure 2-8. The regression plots of carotenoid area in solvent vs. carotenoid area in matrix, used to determine the matrix effects for antheraxanthin, astaxanthin, violaxanthin, β-cryptoxanthin, zeaxanthin, β-carotene and phytoene.

2.5.4 Determination of the stability of the carotenoids in maize seeds during storage

Line TM1 was used to assess the stability of carotenoids in maize seeds under storage. Each month, a bag of one of the six TM1 lots prepared as described in Section 2.4.3 was analyzed in triplicate and concentrations of the pigments in the seeds were determined.

Fig. 9 shows the evolution over six months of the individual and total carotenoid concentrations in TM1. The ANOVA test at a significance level of 5% was used to estimate significant differences in carotenoid concentration between months. The results demonstrated that the total carotenoid concentration in line TM1 remained stable during the whole of the storage period. There were no changes in the concentrations of astaxanthin, adonixanthin, zeaxanthin, lutein, phytoene, *α*-cryptoxanthin, *β*-cryptoxanhtin, lycopene, and 3-hydroxyechinenone during the six months of storage at -80 ºC in the darkness.

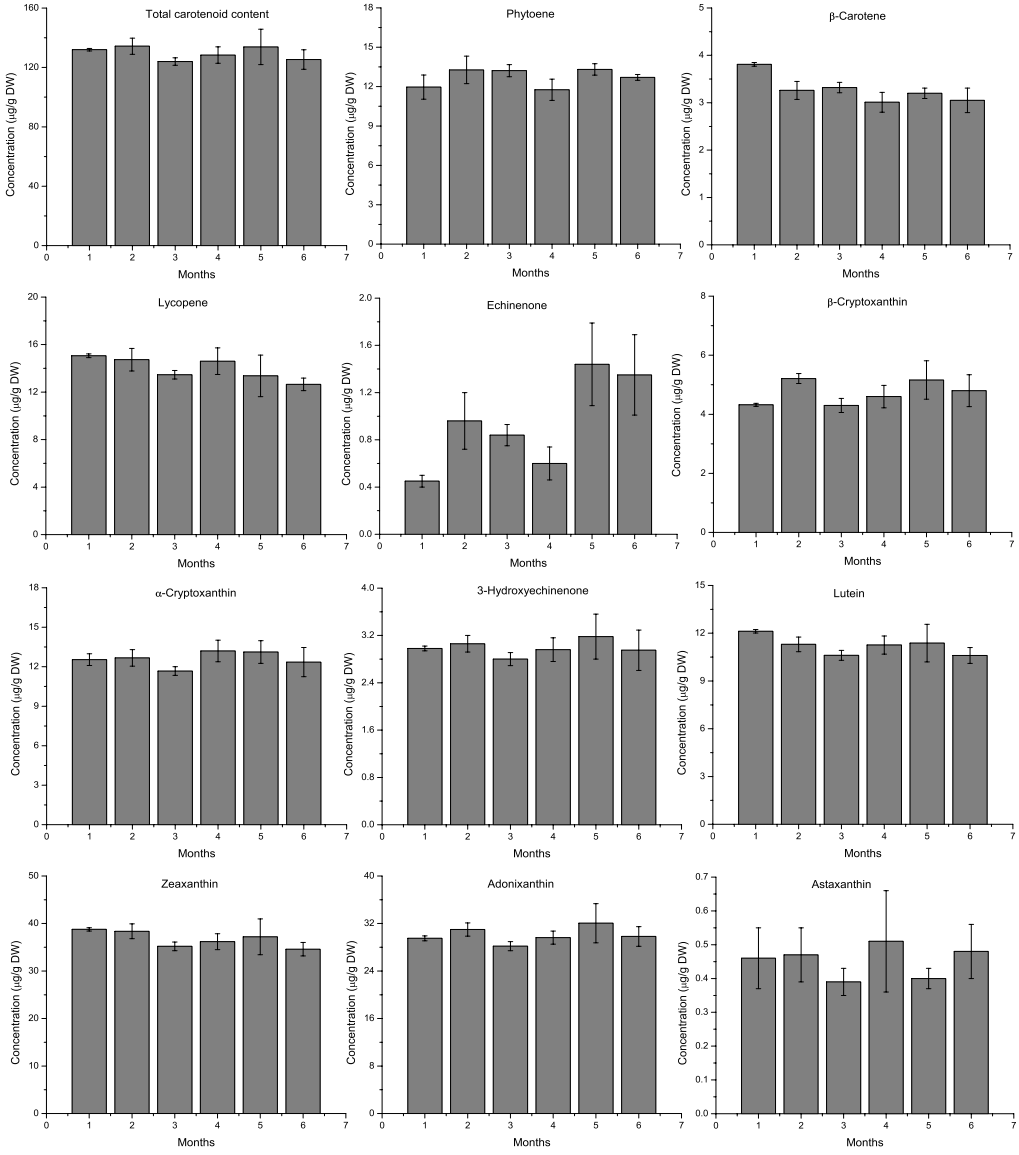

Figure 2-9. Behavior of the individual and total carotenoid content in TM1 between 0 and 6 months of storage at -80 º C in the dark.

For all the cases, *F* calculated value was lower than the *F* critical value (Table 11). However, there were significant differences in the concentrations of *β*-carotene and echinenone between months. The amount of *β*-carotene decreased during month 1 (around 14%), but was generally stable during the next five months (Fig. 9). In contrast, the amount of echinenone showed a tendency of increasing with the pass of the time (Fig. 9).

Since most of the carotenoids under study did not show changes in their concentrations after six months of storage, it can be considered that carotenoids are stable for six months under the following conditions: vacuum packaged, stored at -80 º C and protected from light.

Table 2-12. *F*-Test values for the comparison of carotenoid concentration between months.

Carotenoid	*F* calculated value	*F* critical value
Phytoene	2.55	3.11
Lycopene	2.89	3.11
β-Carotene	8.77	3.11
Echinenone	8.76	3.11
β-Cryptoxanhtin	3.01	3.11
α-Cryptoxanthin	1.69	3.11
3-Hydroxyechinenone	0.88	3.11
Lutein	2.52	3.11
Zeaxanthin	2.29	3.11
Adonixanthin	1.90	3.11
Astaxanthin	0.90	3.11
Total conc.[a]	1.58	3.11

[a] Total carotenoid concentration.

2.6 CONCLUSIONS

The similar chemical configurations of many carotenoids make it difficult to identify and distinguish properly among some carotenoids in different matrices. Therefore, carotenoid detection using mass spectrometer could provide helpful information for distinguishing between some carotenoids, which coelute, and for structural characterization. In the present study, I have demonstrated that APCI is a more suitable technique to ionize carotenoids than ESI or APPI. In addition, I determined transitions and characteristic fragment ions that could be related with functional groups present in the carotenoid structures in order to provide further support for its identification.

Using APPI in positive ion mode, the signal strength of the carotenoids was improved using acetone, toluene, anisole and chlorobenzene as dopants. However, the highest enhancement of the signal strength was observed with carotenes.

The UHPLC–PDA technique has been validated and has been shown to be accurate (%Er below 18%) and to have a satisfactory intra-day precision (%RSD below 13.15%). For most of the carotenoids studied, it showed excellent relative recoveries (ranging from 82 to 108%) and the calibration curves exhibited satisfactory linearity (R^2>0.9952). Thus, a reliable method for qualitative and quantitative

analysis of carotenoids in maize endosperm was developed.

In general, carotenoids present in TM1 were stable for six months under the following conditions: vacuum packaged, stored at -80 º C and protected from light.

2.7 REFERENCE

[1] Rivera S, Vilaró F, Canela R (2011) Determination of carotenoids by liquid chromatography/mass spectrometry: Effect of several dopants. Analytical and Bioanalytical Chemistry.400:1339-46.

[2] Hao Z, Parker B, Knapp M, Yu L (2005) Simultaneous quantification of α-tocopherol and four major carotenoids in botanical materials by normal phase liquid chromatography- atmospheric pressure chemical ionization-tandem mass spectrometry. Journal of Chromatography A.1094:83-90.

[3] Rivera SM, Canela-Garayoa R (2012) Analytical tools for the analysis of carotenoids in diverse materials. Journal of Chromatography A.1224:1-10.

[4] Itoh N, Aoyagi Y, Yarita T (2006) Optimization of the dopant for the trace determination of polycyclic aromatic hydrocarbons by liquid chromatography/dopant-assisted atmospheric-pressure photoionization/mass spectrometry. Journal of Chromatography A.1131:285-8.

[5] Marchi I, Rudaz S, Veuthey JL (2009) Atmospheric pressure photoionization for coupling liquid-chromatography to mass spectrometry: A review. Talanta.78:1-18.

[6] Robb DB, Blades MW (2005) Effects of solvent flow, dopant flow, and lamp current on dopant-assisted atmospheric pressure photoionization (DA-APPI) for LC-MS. Ionization via proton transfer. Journal of the American Society for Mass Spectrometry.16:1275-90.

[7] van Breemen RB, Huang CR (1996) Tan Y, Sander LC, Schilling AB. Liquid chromatography/mass spectrometry of carotenoids using atmospheric pressure chemical ionization. Journal of Mass Spectrometry.31:975-81.

[8] Tian Q, Duncan CJG, Schwartz SJ (2003) Atmospheric pressure chemical ionization mass spectrometry and in-source fragmentation of lutein esters. Journal of Mass Spectrometry.38:990-5.

[9] van Breemen RB (2001) Current Protocols in Food Analytical Chemistry, John Wiley & Sons Inc. p. F2.4.

[10] Kauppila T (2004) Atmospheric pressure photoionization-mass spectrometry. http://ethesis.helsinki.fi/julkaisut/far/farma/vk/kauppila/atmosphe.pdf, accessed online 04/03/12.

[11] Kauppila TJ, Kostiainen R, Bruins AP (2004) Anisole, a new dopant for atmospheric pressure photoionization mass spectrometry of low proton affinity, low ionization energy compounds. Rapid Communications in Mass Spectrometry.18:808-15.

[12] Raffaelli A, Saba A (2003) Atmospheric pressure photoionization mass spectrometry. Mass spectrometry reviews.22:318-31.

[13] US FDA (2001) Guidance for industry: bioanalytical method validation. http://www.fda.gov/downloads/Drugs/GuidanceComplianceRegulatoryInformation/Guidances/UCM070107.pdf, acceded online 04/03/12

[14] ICHHT Guideline (2005) Validation of analytical procedures: text and methodology Q2 (R1). http://c11bw1rt.securesites.net/ich/q/q2r2_97_10_28e.pdf, acceded online 04/03/12.

[15] Dutta D, Chaudhuri UR, Chakraborty R (2005) Structure, health benefits, antioxidant property and processing and storage of carotenoids. African Journal of Biotechnology.4:1510-20.

[16] Bonnie T, Choo Y (1999) Oxidation and thermal degradation of carotenoids. Journal of Oil Palm Research.11:62-78.

[17] Rodriguez-Amaya DB, Kimura M (2004) HarvestPlus handbook for carotenoid analysis. Washington: International Food Policy Research Institute. http://www.ifpri.org/sites/default/files/publications/hptech02.pdf, acceded online 05/03/12.

[18] Zhu C, Naqvi S, Breitenbach J, Sandmann G, Christou P, Capell T (2008) Combinatorial genetic transformation generates a library of metabolic phenotypes for the carotenoid pathway in maize. Proceedings of the National Academy of Sciences of the United States of America.105:18232-7.

[19] Britton G, Liaaen-Jensen S, Pfander H (2004) Carotenoids handbook: 1st ed; Birkhäuser: Basel, Switzerland. pp. 3-404.

[20] Lacker T, Strohschein S, Albert K (1999) Separation and identification of various carotenoids by C30 reversed-phase high-performance liquid chromatography coupled to UV and atmospheric pressure chemical ionization mass spectrometric detection. Journal of Chromatography A.854:37-44.

[21] Nishida Y, Adachi K, Kasai H, Shizuri Y, Shindo K, Sawabe A, Komemushi S, Miki W, Misawa N (2005) Elucidation of a Carotenoid Biosynthesis Gene Cluster Encoding a Novel Enzyme, 2, 2'-{beta}-Hydroxylase, from Brevundimonas sp. Strain SD212 and Combinatorial Biosynthesis of New or Rare Xanthophylls. Applied and Environmental Microbiology.71:4286.

[22] Clarke PA, Barnes KA, Startin JR, Ibe FI, Shepherd MJ (1996) High performance liquid chromatography/atmospheric pressure chemical ionization-mass spectrometry for the determination of carotenoids. Rapid Communications in Mass Spectrometry.10:1781-5.

[23] Tonhosolo R, D'Alexandri FL, de Rosso VV, Gazarin ML, Matsumura MY, Peres VJ, Merino EF, Carlton JM, Wunderlich G, Mercadante AZ, Kimura EA, Katzin AM (2009) Carotenoid biosynthesis in intraerythrocytic stages of Plasmodium falciparum. Journal of Biological Chemistry.284:9974-85.

[24] Van Breemen RB, Dong L, Pajkovic ND (2012) Atmospheric pressure chemical ionization tandem mass spectrometry of carotenoids. International Journal of Mass Spectrometry.312:163-72.

[25] De Rosso VV, Mercadante AZ (2007) Identification and quantification of carotenoids, by HPLC-PDA-MS/MS, from Amazonian fruits. Journal of Agricultural and Food Chemistry.55:5062-72.

[26] De Rosso VV, Mercadante AZ (2007) HPLC-PDA-MS/MS of anthocyanins and carotenoids from dovyalis and tamarillo fruits. Journal of Agricultural and Food Chemistry.55:9135-41.

[27] Řezanka T, Olšovská J, Sobotka M, Sigler K (2009) The use of APCI-MS with HPLC and other separation techniques for identification of carotenoids and related compounds. Current Analytical Chemistry.5:1-25.

[28] Meléndez-Martínez AJ, Britton G, Vicario IM, Heredia FJ (2005) Identification of isolutein (lutein epoxide) as cis-antheraxanthin in orange juice. Journal of Agricultural and Food Chemistry.53:9369-73.

[29] Robb DB, Blades MW (2008) State-of-the-art in atmospheric pressure photoionization for LC/MS. Mass Spectrometry.627:34-49.

[30] Cai SS, Hanold KA, Syage JA (2007) Comparison of atmospheric pressure photoionization and atmospheric pressure chemical ionization for normal-phase LC/MS chiral analysis of pharmaceuticals. Analytical Chemistry.79:2491-8.

[31] Tubaro M, Marotta E, Seraglia R, Traldi P (2003) Atmospheric pressure photoionization mechanisms. 2. The case of benzene and toluene. Rapid Communications in Mass Spectrometry.17:2423-9.

[32] Hanold KA, Fischer SM, Cormia PH, Miller CE, Syage JA (2004) Atmospheric pressure photoionization. 1. General properties for LC/MS. Analytical Chemistry.76:2842-51.

[33] Su Q, Rowley KG, Balazs NDH (2002) Carotenoids: Separation methods applicable to biological samples. Journal of Chromatography B: Analytical Technologies in the Biomedical and Life Sciences.781:393-418.

[34] Craft NE, Scares Jr JH (1992) Relative solubility, stability, and absorptivity of lutein and β-carotene in organic solvents. Journal of Agricultural and Food Chemistry.40:431-4.

[35] Shi J, Le Maguer M (2000) Lycopene in tomatoes: Chemical and physical properties affected by food processing. Critical Reviews in Biotechnology.20:293-334.

[36] FAO (2009) Lycopene extract from tomate. http://www.fao.org/fileadmin/templates/agns/pdf/jecfa/cta/71/lycopene_extract_from_tomato.pdf, acceded online 29/02/12.

[37] Rodriguez-Amaya DB (1999) A guide to carotenoid analysis in foods: International Life Sciences Inst ILSI. *pdf.usaid.gov/pdf_docs/PNACQ929.pdf,* acceded online 09/07/12.

[38] Fratianni A, Cinquanta L, Panfili G (2010) Degradation of carotenoids in orange juice during microwave heating. LWT - Food Science and Technology.43:867-71.

[39] Konings EJM, Roomans HHS (1997) Evaluation and validation of an LC method for the analysis of carotenoids in vegetables and fruit. Food Chemistry.59:599-603.

[40] Strati IF, Oreopoulou V (2011) Process optimisation for recovery of carotenoids from tomato waste. Food Chemistry.129:747-52.

[41] Vilaró F, Pérez-Hedo M, Eras J, Canela R, Eizaguirre M (2012) UHPLC-MS analysis of juvenile hormone II in Mediterranean corn borer (Sesamia nonagrioides) hemolymph using various ionization techniques. Journal of Agricultural and Food Chemistry.60:3020-5.

[42] Oliver J, Palou A (2000) Chromatographic determination of carotenoids in foods. Journal of Chromatography A.881:543-55.

[43] Vilaró F, Canela-Xandri A, Canela R (2006) Quantification of abscisic acid in grapevine leaf (Vitis vinifera) by isotope-dilution liquid chromatography–mass spectrometry. Analytical and Bioanalytical Chemistry.386:306-12.

[44] Bansal S, DeStefano A (2007) Key elements of bioanalytical method validation for small molecules. AAPS Journal.9.

Chapter 3

Understanding complex metabolic pathways in plants: reconstruction and extension of the carotenoid pathway in corn

3.1 ABSTRACT

Vitamin A deficiency (VAD) affects 127 million people in developing countries, including 25% of pre-school children, causing more than half a million cases of permanent blindness in children and 2.2 million deaths per year [1]. Therefore, biofortification of major staple crops with carotenoids can contribute to alleviating nutritional global challenges. To enhance levels of carotenoids and facilitate predictive metabolic engineering in food crops, the elucidation of biosynthetic step(s) that control carotenoid accumulation in tissues is necessary. Combinatorial nuclear transformation was used by the group of Applied Plant Biotechnology of UdL to dissect and modify carotenoid metabolic pathway in maize. They transferred several carotenogenic genes controlled by different endosperm-specific promoters into a white maize variety deficient for endosperm carotenoid synthesis. They recovered a diverse population of transgenic maize lines expressing different enzyme combinations and showing distinct metabolic phenotypes. I analyzed these lines and described the carotenoid accumulation in the target tissue. I was also involved in exploring relationships between gene expression and the accumulation of metabolites in the different transgenic lines in an effort to identify rate-limiting steps in the carotenoid pathway in maize endosperm.

3.2 INTRODUCTION

In plants, the synthesis of carotenoids is initiated by the enzyme phytoene synthase (PSY), which mediates the condensation of two molecules of geranylgeranyl diphosphate, leading to the carotene 15-*cis*-phytoene [2]. Then, 15-*cis*-phytoene undergoes four desaturation steps catalyzed by phytoene desaturase (PDS), ζ-carotene isomerase (Z-ISO) and ζ-carotene desaturase (ZDS) to generate the first colored carotene, prolycopene, which is converted to all-*trans*-lycopene by carotene isomerase (CRTISO) in non-green tissue, but by light in green tissue [3, 4]. In bacteria, a single enzyme encoded by the *crt*I gene accomplishes all the above steps and produces all-*trans*-lycopene from 15-*cis*-phytoene directly (Fig. 1). Lycopene is an important branch point in the carotenoid pathway because it acts as the substrate for two competing enzymes, lycopene *β*-cyclase (LYCB) and lycopene *ε*-cyclase (LYCE) [5]. Both enzymes cyclize the linear backbone to generate terminal ionone rings, but the structures of these rings are distinct. In one branch, the addition of one *ε*-ring to lycopene by lycopene *ε*-cyclase (LYCE) generates *δ*-carotene. This is a poor substrate for LYCE so it is unusual for the second *ε*-cyclization to take place, but it is a good substrate for lycopene *β*-cyclase (LYCB), which adds a *β*-ring to the free end generating the orange pigment *α*-carotene. In turn, *α*-carotene is converted into zeinoxanthin by the di-iron non-heme *β*-carotene hydroxylase (BCH) and/or the P450-type *β*-carotene hydroxylases (CYP97A and CYP97B), and then into the yellow pigment lutein by the P450-type *ε*-hydroxylase, CYP97C [5]. In another branch, lycopene is cyclized to produce provitamin A carotenoids of *γ*-carotene and *β*-carotene which results from the addition of two *β*-rings to both ends of the linear lycopene molecule by LYCB. Subsequent oxygenation of *β*-carotene results in the formation of *β*-cryptoxanthin and then the zeaxanthin by BCH and/or CYP97A and CYP97B (Fig. 1) [6].

In both prokaryotes and eukaryotes, *β*-carotene can be converted into astaxanthin catalyzed by *β*-carotene ketolase and *β*-carotene hydroxylase (HYDB), respectively (Fig. 2). There are two main distinct pathways for the synthesis of astaxanthin. In one pathway, *β*-carotene can be catalyzed by *β*-carotene hydroxylase to form zeaxanthin, and then catalyzed by *β*-carotene ketolase to form astaxanthin. In another way, *β*-carotene first catalyzed by *β*-carotene ketolase to form canthaxanthin and then further catalyzed by *β*-carotene hydroxylase to form astaxanthin.

Extensive studies have implicated PSY, the first committed step in the carotenoid pathway, as a rate-limiting step in carotenoid endosperm accumulation [7-11]. For instance, the endosperm specific expression of *psy1* in corn resulted in overcoming the bottleneck and increasing the total carotene content 52-fold, and leading to the predominant accumulation of lutein and zeaxanthin [11]. The enzymatic activity of two lycopene cyclases (LYCE and LYCB) producing *ε*- and *β*-carotenoids has an important role in the modulation of the ratio of the most abundant carotenoid such as lutein and *β*-carotene, which it is another limiting step in the pathway. The overexpression of *lycb* shifts the balance from *α* to the *β*-branch, and should therefore theoretically enhance *β*-carotenoids levels at the expense of *α*-carotene and lutein [12, 13]. In transgenic canola, seeds expressing *crt*B, *crt*I and *crt*Y

genes resulted not only in higher carotenoid content also the β- to α-carotene ratio increased from 2:1 to 3:1 showing that the additional lycopene β-cyclase activity provided by the bacterial *crt*Y gene skewed the competition for the common precursor lycopene and increased flux specifically towards β-carotene [14]. Similar results were observed in transgenic maize seeds expressing *psy1*, *crt*I and *lycb* resulting in an increase from 1.21 to 3.51 in the β:α-carotene ratio, showing that the additional LYCB activity skewed the competition for the common precursor lycopene and increased flux towards β-carotene [11]. Nevertheless, there was also enhanced flux through the α-branch of the pathway, producing nearly 25-fold the normal levels of lutein (up to 13.12 μg/g dry weight –DW-). These examples show that even when shifting the metabolic flux towards β-carotene, there is still enough flux through the ε-branch of the pathway to produce more than enough lutein for human nutrition [15]. Finally, carotenoid content can be reduced by downstream degradative pathway through the conversion of zeaxanthin to violaxanthin.

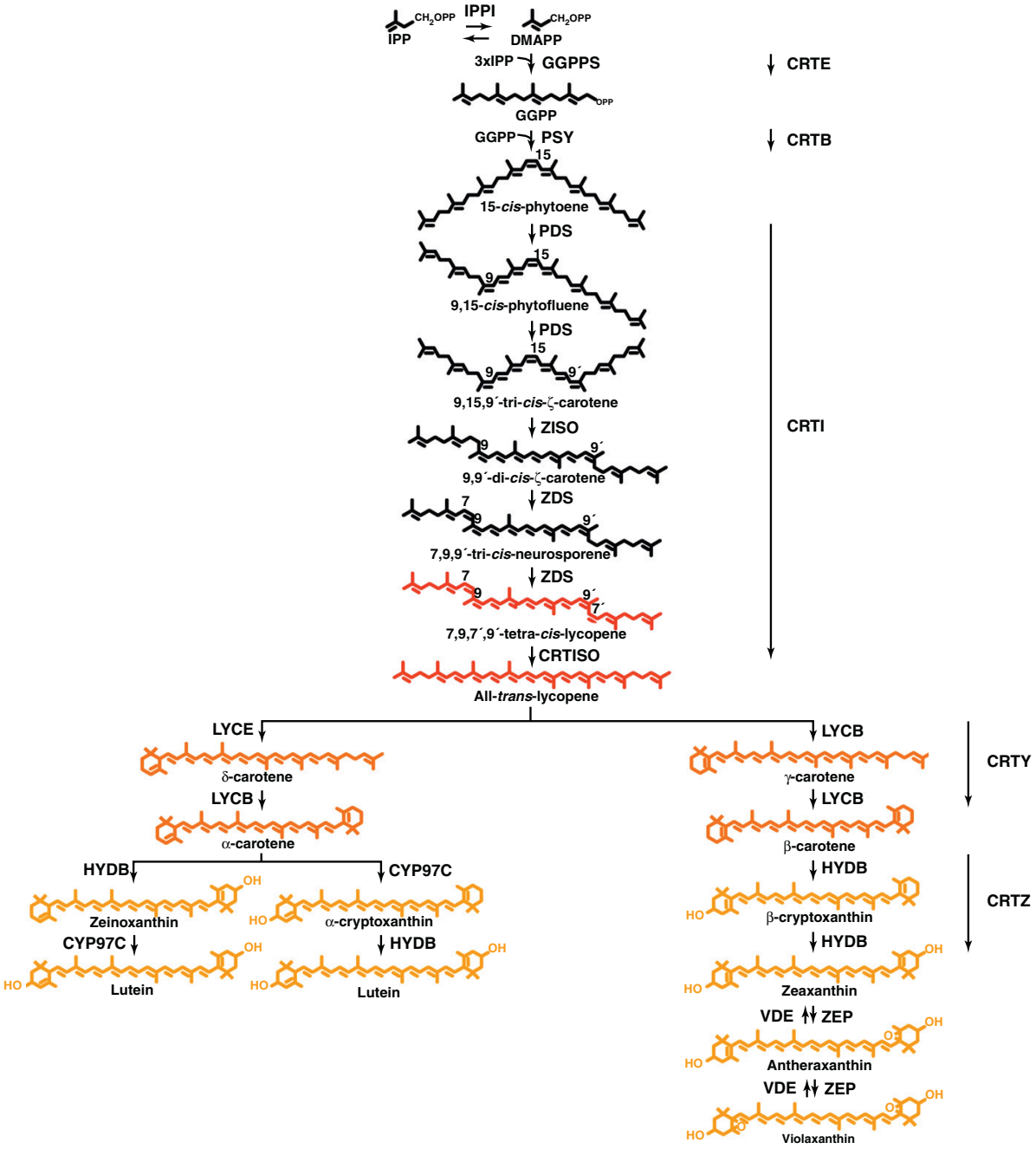

Figure 3-1. The carotenoid biosynthesis pathway in plants and equivalent steps in bacteria. CRTB, bacterial phytoene synthase; CRTE, bacterial geranylgeranyl diphosphate synthase; CRTI, bacterial phytoene desaturase/isomerase; CRTISO, carotenoid isomerase; CRTY, bacterial lycopene cyclase; CRTZ, bacterial *β*-carotene hydroxylase; CYP97C, carotene *ε*-ring hydroxylase; DMAPP, dimethylallyl diphosphate; GGPP, geranylgeranyl diphosphate; GGPPS, GGPP synthase; HYDB, *β*-carotene hydroxylase [non-heme di-iron hydroxylases, *β*-carotene hydroxylase (BCH) and heme-containing cytochrome P450 *β*-ring hydroxylases, CYP97A and CYP97B]; IPP, isopentenyl diphosphate; IPPI, isopentenyl diphosphate isomerase; LYCB, lycopene *β*-cyclase; LYCE, lycopene *ε*-cyclase; PDS, phytoene desaturase; PSY, phytoene synthase; VDE, violaxanthin de-epoxidase; ZDS, *ζ*-carotene desaturase; ZEP, zeaxanthin epoxidase; Z-ISO, *ζ*-carotene isomerase [16].

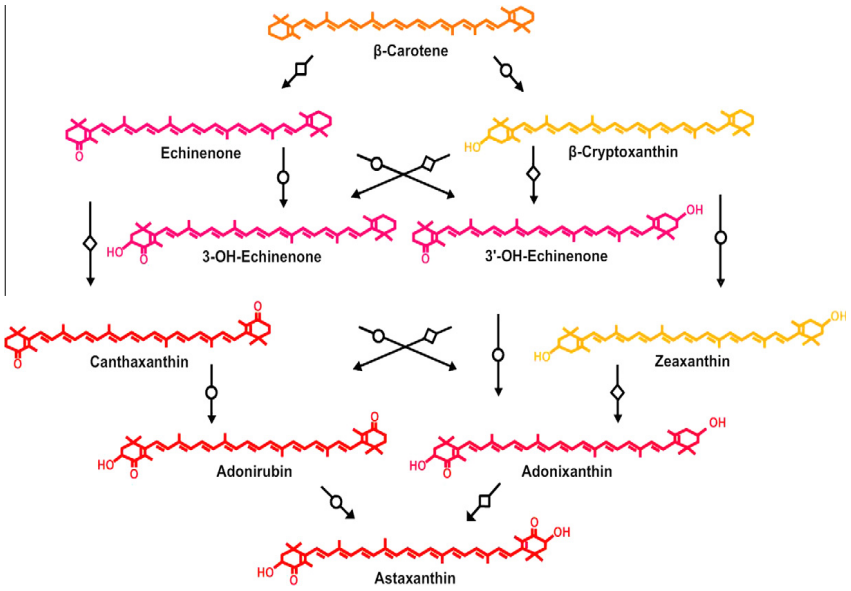

Figure 3-2. Astaxanthin biosynthesis pathway from *β*-carotene. Arrow with inset square represents *β*-carotene ketolase – BKT, CRTW or CRTO. Arrow with inset circle represents *β*-carotene hydroxylase (HYDB) – BCH, CYP97A, CYP97B or CRTZ [4].

3.3 OBJECTIVES

- To describe the carotenoid profile of four transgenic maize lines expressing different enzyme combinations at different developmental stages (from 15 to 60 days after pollination -DAP).
- To use the metabolite profile of carotenoids to investigate the specific contribution(s) of carotenogenic genes in the carotenoid pathway considering the mRNA levels.

3.4 MATERIALS AND METHODS

3.4.1 Chemicals

β-Carotene, lycopene, lutein, *β*-cryptoxanthin, astaxanthin, were purchased from Sigma-Aldrich Fine Chemicals (St. Louis, MO, USA). Canthaxanthin and zeaxanthin were acquired from Fluka (Buchs SG, Switzerland). Phytoene, violaxanthin, and antheraxanthin were purchased from Carotenature (Lupsingen, Switzerland). MeOH, ethyl acetate, ethyl eter, TBME, ACN and acetone (HPLC grade purity) were acquired from J.T. Baker (Deventer, The Netherlands). Water was prepared using a Milli-Q reagent water system.

3.4.2 Plant material

The transgenic maize was generated by combinatorial nuclear transformation as reported in Zhu et al. [11]. The transgenic maize lines used to measure the levels of carotenoids at DAP were: TM1, expressing *Zea mays* phytoene synthase 1 (*Zmpsy1)* and *Pantoea ananatis* phytoene desaturase (*PacrtI*), TM2, expressing *Zmpsy*1, *PacrtI* and *Gentiana lutea* lycopene *β*-cyclase (*Gllycb*); TM3, expressing *Zmpsy1*, *PacrtI*, *Gllycb* and *Paracoccus β*-carotene ketolase (*ParacrtW*) and TM4,

expressing *Zmpsy1*, *PacrtI*, *Gllycb, ParacrtW* and *Gentiana lutea β*-carotene hydroxylase (*Glbch*). Table 1 summarizes the genes expressed in the different TM.

Table 3-1. Genes expressed in the TM recovered.

Line	Expressed genes
TM1	*Zmpsy1*, *Pacrt*I
TM2	*Zmpsy1, Pacrt*I, *Gllycb*
TM3	*Zmpsy1, Pacrt*I, *Gllycb*, *Pacrt*W
TM4	*Zmpsy1, Pacrt*I, *Gllycb*, *Pacrt*W, *Glbch*

3.4.3 Extraction of carotenoids

To protect carotenoids from degradation and oxidation, the extraction was conducted under limited light. Samples were freeze-dried and ground into a fine powder using a mortar and pestle. 50 or 100[4] mg of sample was extracted with 15 mL of MeOH: ethyl acetate (6:4, v/v) at 60 °C for 20 min and this mixture was continuously shaken. It was then put on ice until it reached room temperature and the liquid phase was filtered into a separatory funnel (if the residue exhibited color after extraction, then it was re-extracted with 5 mL of MeOH: ethyl acetate (6:4, v/v) at 60 °C for 5 min and the second extract was combined with the first one). 15 mL of hexane: diethyl ether (9:1, v/v) was added to the organic extract and the mixture was shaken vigorously. Then, 20 mL of saturated sodium chloride solution was added and again the mixture was shaken. The aqueous phase was removed and the organic phase was washed with water once again. The organic phase was dried under N_2 at 37 ºC. When the sample was completely dry, Ar was flushed into the vial and carotenoids were stored at -80 ºC until LC analysis. Each extraction was carried out in triplicate.

3.4.4 Chromatographic analysis

Chromatographic systems used to analyze the transgenic lines were the same employed in Chapter 2, section 2.4.6.

3.4.4.1 UHPLC-PDA-MS analysis

UHPLC analysis was carried out using an ACQUITY Ultra Performance LC™ system linked to a PDA 2996 detector (Waters, Milford, MA, USA). Mass detection was carried out using an Acquity™ TQD tandem-quadrupole MS equipped with a Z-spray electrospray interface (Manchester, UK). MassLynx™ software version 4.1 (Waters, Milford, MA, USA) was used to control the instruments, and also for data acquisition and processing.

UHPLC chromatographic separations were performed on reversed-phase column ACQUITY UPLC® C18 BEH 130Å, 1.7 μm, 2.1×100 mm (Waters, Milford, MA). Mobile phase consisted of solvent A: ACN: MeOH 7:3, v/v and solvent B: water 100%. The gradient program used is shown in Table 2.

[4] For pale color maize samples, extract 100 mg of sample. For darker color maize samples, it is sufficient to extract 50 mg of sample.

The column and sample temperatures were set at 32 °C and 25 °C respectively. Injection volume was 5 μL.

Each sample extract for LC analysis was dissolved in 300 μL and 600 μL (for light and dark color extracts respectively) of the injection solvent [ACN: MeOH 7:3, v/v]: acetone 6.7:3.3, v/v. Before use, all solutions were filtered through Millex 0.2 μm nylon membrane syringe filters (Millipore, Bedford, MA, USA).

Table 3-2. Gradient profile used in the separation of carotenoids by UHPLC. Linear gradient.

Time[a] (min)	Flow rate (mL/min)	A (%, v/v)	B (%, v/v)
Initial	0.4	80	20
2.0	0.4	80	20
3.0	0.4	100	0
7.0	0.4	100	0
8.0	0.6	100	0
11.6	0.6	100	0
12.6	0.4	80	20

[a] After this time, the system was left 2 min more to reach its re-equilibration before injecting a new sample.

3.4.4.2 MS conditions

Optimized MS conditions are listed in Table 3.

Table 3-3. MS conditions.

MS conditions	APCI
Polarity	Positive
Corona (kV)	4.0
Cone (V)	30
Extractor (V)	3
RF (V)	0.1
Source Temperature (°C)	150
Probe Temperature (°C)	450
Cone Gas Flow (L/h)	10
Desolvation Gas Flow (L/h)	150
Collision Gas Flow (mL/min)	0.15

3.4.4.3 HPLC-PDA analysis

HPLC analysis separations was carried out using a Waters Alliance 2695 separation module linked to a PDA 2998 detector (Waters, Milford, MA, USA). Empower software version 2 (Waters, Milford, MA, USA) was used to control the instruments, and also for data acquisition and processing.

HPLC chromatographic separations were performed on a YMC C30 carotenoid 3 μm, 2.0×100 mm column (Waters, Milford, MA). Mobile phase consisted of solvent A: MeOH: water 8:2, v/v and solvent B: TBME 100%. The gradient program used is shown in Table 4. Both, the column and the sample temperatures were set at 25 °C. Injection volume was 10 μL.

Table 3-4. Gradient profile used in the separation of carotenoids by HPLC. Linear gradient.

Time[a] (min)	Flow rate (mL/min)	A (%, v/v)	B (%, v/v)
Initial	0.25	97	3
6.0	0.25	97	3
7.0	0.25	62	38
15.0	0.25	62	38
16.0	0.25	32	68
18.0	0.25	32	68
19.0	0.25	0	100
25.0	0.25	0	100
26.0	0.25	32	68
27.0	0.25	50	50
28.0	0.25	70	30
29.0	0.25	97	3

[a] After this time, the system was left 6 min more to reach its re-equilibration before injecting a new sample.

3.4.4.4 Carotenoid identification and quantification

Identification of carotenoids was carried out by analysis and comparison of the following parameters: chromatographic retention time, UV-vis spectra, %III/II [17] and *m/z* fragments according literature data [18] and that of the authentic standards. Those standards were also used for quantitation.

3. 5 RESULTS AND DISCUSSION

3.5.1 Carotenoid accumulation during endosperm development

The group of Applied Plant Biotechnology of UdL used as a model system the South African elite white maize variety M37W, which lacks carotenoids in the endosperm because of the absence of the enzyme PSY1 [11]. After transforming white maize embryos with 5 carotenogenic transgenes (Fig. 3), they recovered several transgenic lines carrying all combinations of the input genes. This combinatorial population was mined for phenotypes corresponding to the production of specific carotenoids. I determined the metabolic profile of those lines and my colleague Gemma Farré performed the analysis of gene expression [19].

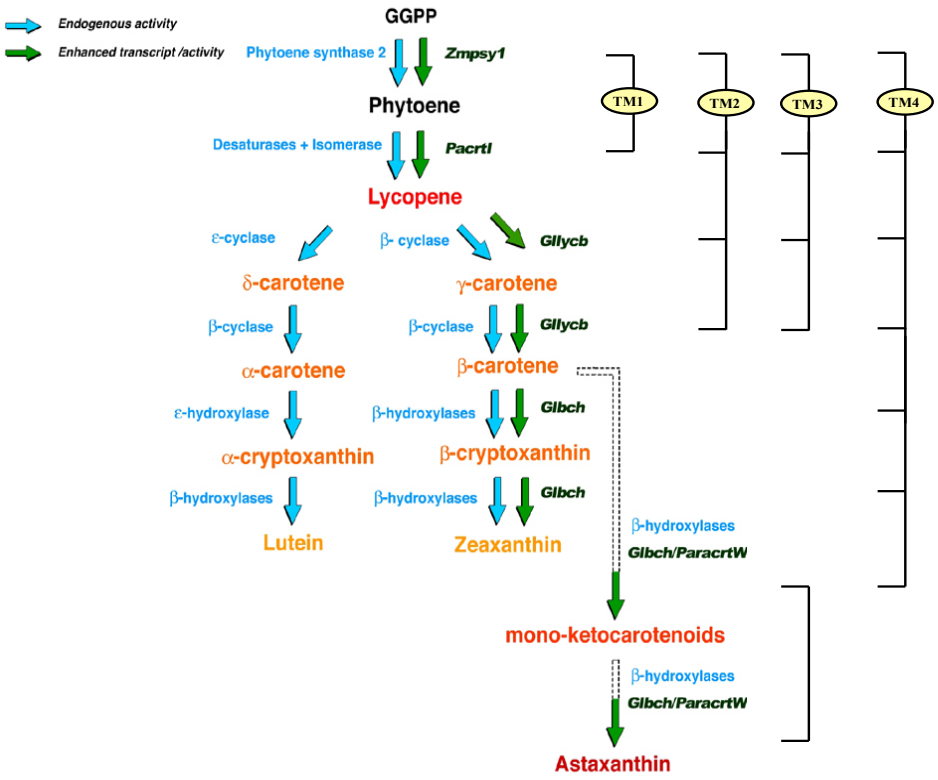

Figure 3-3. Reconstruction and extension of the carotenoid biosynthetic pathway in white maize endosperm. On the right, four distinct transgenic lines are indicated on the basis of gene expression to dissect the endogenous maize carotenoid biosynthetic pathway and extend it to produce ketocarotenoids. The bars in the drop-off lines indicate the enzyme activities present in the different transgenic lines.

3.5.1.1 Carotenoid measurement

Carotenoid levels were measured from 15 to 50 DAP (days after pollination) in TM1 and from 15 to 60 DAP in TM2, TM3 and TM4. It was found that most carotenoids are synthesized continuously in corn endosperm from 15 DAP onwards. However, the concentration of most carotenoids peaked during development (Table 5) and then declined as the seeds matured.

Table 3-5. DAP in which each TM reached its maximum of total and individual carotenoid accumulation.

Carotenoid	DAP TM1	DAP TM2	DAP TM3	DAP TM4
Phytoene	50	40-50	50	40
Lycopene	50	-	40-50	-
β-Zeacarotene	50	40	25-60	50
β-Carotene	30-50	40	50	30-40
α-Carotene	-	-	50	30-50
β-Cryptoxanthin	25-30	40	40-60	25-60
α-Cryptoxanthin	25-40	40	40-60	50
Lutein	30-40	30-40	30-40	50
Zeaxanthin	25-30	25	25-30	30-50
Antheraxanthin	20-25	25	20	25
Echinenone	-	-	40-50	30-60
3-Hydroxyechinenone	-	-	30-50	20
Adonixanthin	-	-	40	25
Astaxanthin	-	-	25	-
Total conc.	30-50	40	30-40	30-40

Abbreviations: Total conc., total carotenoid concentration.

The levels of some carotenoids declined marginally after peaking (e.g. lutein) whereas others declined significantly (e.g. antheraxanthin). This may reflect degradation caused by light or heat, or the consumption of carotenoids in other metabolic pathways (such as carotenoid epoxides acting as precursors for ABA synthesis). The individual carotenoid content and profile of each transgenic line was distinct and different to that of the wild-type M37W variety (Fig. 4).

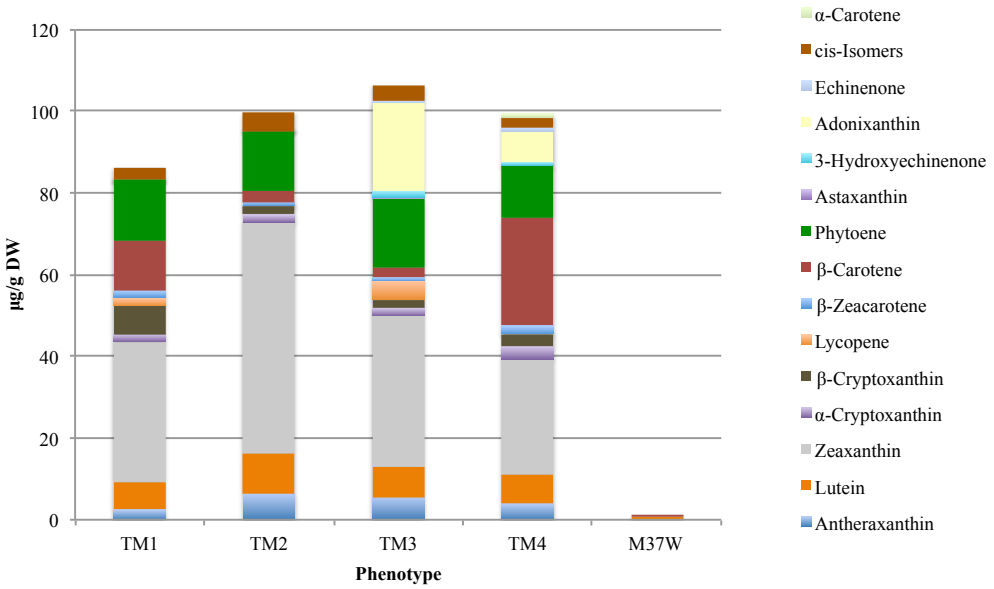

Figure 3-4. Carotenoid composition in the four transgenic lines and wild type M37W at 30 DAP.

3.5.1.2 Total carotenoid accumulation though endosperm development

Although individually the carotenoid concentration peaked at different DAP, the maximum of total carotenoid concentration was observed for all transgenic lines mainly at day 30 and 40 (Fig. 5.A). Initially, the total carotenoid accumulation of the TM1, TM2 and TM4 was similar at day 15 while TM3 exhibited a higher concentration. The period from 15 to 25 DAP showed the most significant increase of total carotenoid concentration for the TM1, TM2 and TM3 while for TM4 it was at day 15 to 30. Then, it increased slightly in TM1, TM3 and TM4 until reached its maximum. However, TM2 during the period of 25 to 30 DAP underwent a slight decrease in its total carotenoid concentration but then it started increasing. The maximum of total carotenoid content in TM1 was observed at day 30-50 (86.34±0.65 μg/g DW), TM2 at 40 DAP (104,4 ±3.08 μg/g DW) and TM3 and TM4 at 30-40 (110.21±0.72 μg/g DW and 99.42±0.27 μg/g DW, respectively). In TM2, TM3 and TM4 evidenced a loss of concentration after reaching its maximum of concentration. TM3, which expressed *Zmpsy1+PacrtI+Gllycb+PacrtW*, showed the highest total carotenoid concentration (Fig. 5.A). The total carotenoid content in wild-type M37W variety was 1.10 μg/g DW (Fig. 4). Thus, carotenoid content was increased in TM1, TM2, TM3 and TM4, 78.5, 94.9, 100.2 and 90.4-fold, respectively.

3.5.1.3 Individual carotenoid accumulation through endosperm development

All the individual carotenoid graphs use the same scale, which was established based on the carotenoid that showed the highest concentration in the samples (zeaxanthin).

Phytoene was already present at day 15 in TM3 and after this day in the case of TM1, TM2 and TM4 (Fig. 5.B). Then, it increased through the period studied until it reached its maximum of accumulation. However, TM4 showed a slight increase from day 30 until it reached its maximum of concentration. Its maximum of concentration was observed at day 50, 40-50, 50 and 40 for the TM1, TM2, TM3 and TM4, respectively. The highest concentration of phytoene was observed in TM3, followed by TM2, TM1 and TM4 (22.08±2.44, 21.21±2.30, 19.38±1.04 and 12.94±0.32 μg/g DW, respectively).

Lycopene was only detected in TM1 and TM3, the lines which were expressing the transgenes *Zmpsy1+PacrtI* and *Zmpsy1+PacrtI+Gllycb+PacrtW*, respectively (Fig. 5.C). Lycopene accumulation started after 15-20 DAP for both lines. The most significant increase of lycopene was observed from 20 to 25 DAP in TM3. Then, it increased slightly until reached its maximum at day 40-50 and a loss of concentration was observed at day 60. However, TM1 showed a different behavior. Lycopene increased from day 15 to 20 but its concentration remained unchanged from day 20 to 25. Then, from day 25 to 30, an important increase was again observed but from day 30 to 40 just a slight increase was evidenced. From day 40 to 50, lycopene showed an important increase and reached its maximum of concentration at day 50. The highest concentration of lycopene was obtained in TM3, followed by TM1 (6.25±0.22 μg/g DW and 3.72±0.41 μg/g DW, respectively).

TM4 showed the highest concentration of ***β*-carotene** compared with all lines, followed by TM1, TM2 and TM3 (26.33±0.15, 13.62±0.45, 5.36±0.14 and 5.34±0.33 μg/g DW, respectively) (Fig. 5.D). β-Carotene accumulation started at day 15 in the TM1, after day 15 in the TM3 and TM4 and after day 20 in TM2. Then, β-carotene concentration increased through the days until reached its maximum at days 30-50, 40, 50 and 30-40 for the TM1, TM2, TM3 and TM4, respectively. In all the lines, except in TM1, β-carotene accumulation decreased after reaching its maximum of concentration.

α-Carotene was only detected in TM4 and in a low amount (0.91±0.03 μg/g DW). In addition, the α-carotene accumulation started later compared with other carotenoids.

***β*-Zeacarotene** showed a similar behavior of carotenoid accumulation in the TM2 and TM3 and in the TM1 and TM4. The highest level of β-zeacarotene accumulation was observed for TM4, followed by TM1, TM2 and TM3 (2.37±0.22, 2.33±0.46, 1.26±0.10 and 1.03±0.20 μg/g DW, respectively) (Fig. 5.E). It commenced its accumulation after day 15 in the TM1 and after day 20 in the TM2, TM3 and TM4 and then, its concentration increased through the days until it reached its maximum of concentration at day 50, 40, 25-60 and 50 for the TM1, TM2, TM3 and TM4, respectively. Only TM1 and TM3 did not show a decrease in β-zeacarotene accumulation after reaching its maximum of concentration.

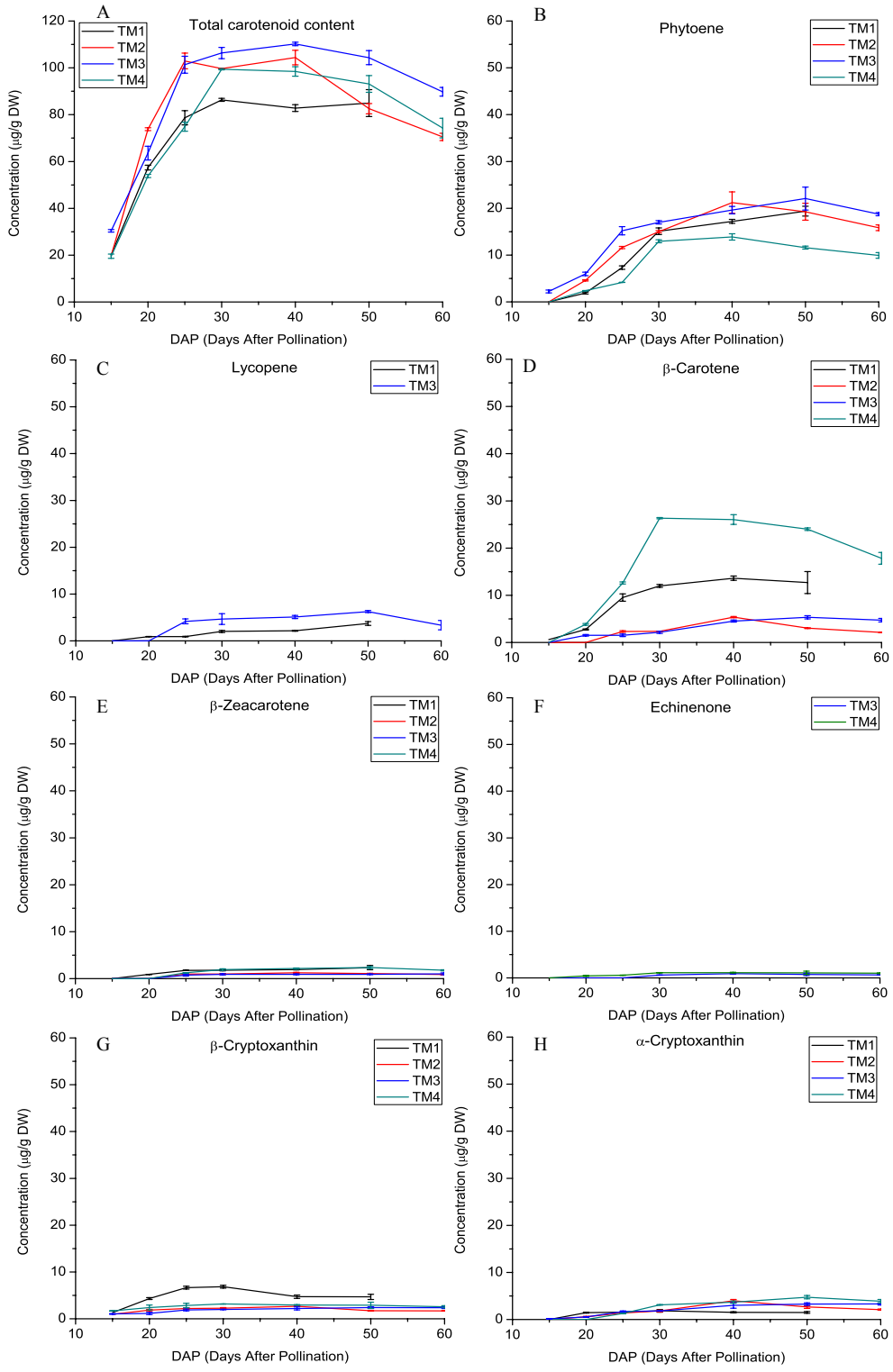

Figure 3-5. Behavior of the total and individual carotenoid concentration along different DAP. Carotenoid content is given in μg/g DW; (A) Total carotenoid content, (B) phytoene, (C) lycopene, (D) β-carotene, (E) β-zeacarotene, (F) echinenone, (G) β-cryptoxanthin, (H) α-cryptoxanthin. Abbreviations: DW, dry weight.

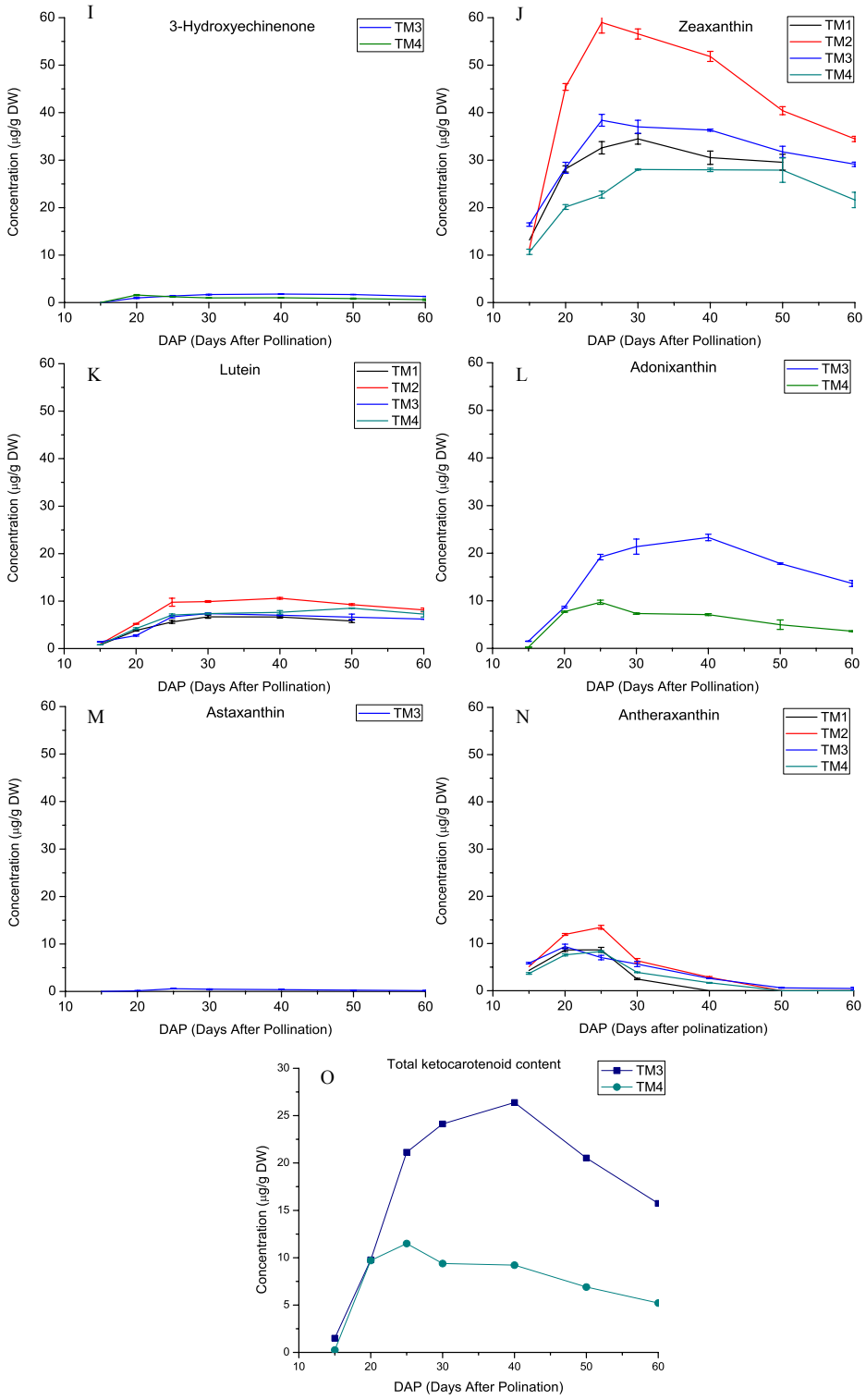

Figure 3-6. Behavior of the total ketocarotenoid and individual carotenoid concentration along different DAP. Carotenoid content is given in μg/g DW; carotenoids detected in the samples: (I) 3-hydroxyechinenone, (J) zeaxanthin, (K) lutein, (L) adonixanhtin, (M) astaxanthin, (N) antheraxanthin, (O) total ketocarotenoid content. Abbreviations: DW, dry weight.

Antheraxanthin showed a similar behavior for all the lines (Fig. 6.N). The highest level of antheraxanthin accumulation was observed for TM2, followed by TM3, TM1 and TM4 (13.44±0.39, 9.37±0.48, 8.66±0.52 and 8.32±0.16 μg/g DW, respectively). Antheraxanthin accumulation started at day 15, increased through day 20 and peaked at day 20-25 (depending on the line). At later developmental stages it decreased dramatically to below detection levels. It is noteworthy that antheraxanthin underwent a dramatic loss of concentration after reaching its maximum of concentration. One possible hypothesis to explain this behavior may be the fact that antheraxanthin was more reactive than other carotenoids present in the same mixture of carotenoids since antheraxanthin bears an epoxy group, which is known to be more reactive than other functional groups.

Lutein showed a similar behavior in all the lines (Fig. 6.K). It increased through the days and peaked at days 30-40 (TM1, TM2 and TM3) and at day 50 (TM4). After reaching its maximum of concentration, it decreased slightly in all the lines. The highest level of lutein was observed in TM2, followed by TM4, TM3 and TM1 (10.59±0.17, 8.51±0.02, 7.35±0.17 and 6.70±0.33 μg/g DW, respectively).

Zeaxanthin was the major carotenoid found in all the four lines. The highest accumulation of zeaxanthin was obtained in TM2, followed by TM3, TM1 and TM4 (58.98±2.23, 38.39±1.24, 34.47±1.10 and 28.02±0.12 μg/g DW, respectively corresponding to the percentages of 49.65, 32.95, 39.92 and 28.18% of the total carotenoid content, respectively) (Fig. 6.J). In all the lines, its accumulation started at day 15 and increased through the days until it peaked. The maximum of accumulation of zeaxanthin was observed at different DAP depending on the expressor line. Thus, in TM1 and TM3, it was reached at day 25-30, in TM2, at day 25 and in TM4, at days 30-50.

***β*-Cryptoxanthin** showed a similar behavior of carotenoid accumulation in the TM2, TM3 and TM4. TM1 showed the highest levels of β-cryptoxanthin along all the different DAP and its maximum accumulation was obtained at days 25-30 (6.85±0.30 μg/g DW) (Fig. 5.G). Only TM1 and TM2 showed a decrease in β-cryptoxanthin accumulation after reaching its maximum of concentration.

The maximum of concentration of ***α*-cryptoxanthin** was observed at days 25-40 (1.85±0.29 μg/g DW), 40 (3.97±0.28 μg/g DW), 40-60 (3.29±0.27 μg/g DW) and 50 (4.74±0.35 μg/g DW) for the TM1, TM2, TM3 and TM4, respectively (Fig. 5.H). Only TM3 did not show a decrease in α-cryptoxanthin accumulation after reaching its maximum of concentration.

Ketocarotenoids were only detected in TM3 and TM4 as a result of the expression of a bacterial ketolase gene, *Paracrt*W, in addition to *Zmpsy1+PacrtI+Gllycb* (TM3) or *Zmpsy1+PacrtI+Gllycb+Glbch* (TM4).

Adonixanthin showed the highest accumulation among the different ketocarotenoids detected in both lines (Fig. 6.L). The period from 15 to 25 DAP represented the most significant increase of adonixanthin in TM3. Then, it increased more moderately until reached its maximum of concentration at day 40. In TM4, the most significant increase of adonixanthin was from 15 to 20 DAP and it

continued increasing until it reached its maximum of concentration at day 25. After reaching its maximum, adonixanthin decreased its concentration in both lines. TM3 exhibited the highest levels of adonixanthin along all the time frame. The highest accumulation of adonixanthin was obtained at day 40 in TM3 and at day 25 in TM4 (23.29±0.67 and 9.69±0.44 μg/g DW respectively).

Echinenone and 3-hydroxyechinenone were also detected in TM3 and TM4 (Figs. 5.F and 6.I repectively). However, their concentrations were far lower than adonixanthin.

Echinenone accumulation started after day 15 in the TM4 and after day 25 in the TM3. Then, echinenone concentration increased through the days until it reached its maximum of concentration at day 40-50 and 30-60 for the TM3 and TM4, respectively (Fig. 5.F). The maximum of concentration amount was similar for both lines. Only in TM3 was a loss evidenced in echinenone concentration at day 60.

In TM3, **3-hydroxyechinenone** concentration increased through the days until it peaked at day 30-50 while TM4 peaked at an earlier stage-day 20. In both lines a loss was evidenced in its concentration after it peaked. The highest levels of 3-hydroxyechinenone were observed in TM3 (Fig. 6.I).

Astaxanthin was only detected in TM3 and in low concentration (Fig. 6.M). Its accumulation started after day 15 and the period of 20 to 25 DAP represented the most significant increase of astaxanthin; it later decreased.

TM3 showed the highest **total ketocarotenoid** accumulation up to 26 μg/g DW started at day 15 (Fig. 6.O). The period from 15 to 25 and 15 to 20 DAP represented the most significant increase in total ketocarotenoid accumulation in TM3 and TM4, respectively. Then, it increased more moderately until it peaked at day 40 and 25 for TM3 and TM4, respectively. In both lines a loss was evidenced in ketocarotenoid concentration after it reached its maximum of concentration.

The accumulation profiles of individual carotenoids indicate that although carotenoid synthesis begins at the earliest stages of endosperm development, their accumulation depends on feedback regulations. For example, accumulation of zeaxanthin is already observed at 15 DAP in all four transgenic lines whereas the accumulation of β-carotene (its precursor) is detected at 15 DAP in TM1, after 15 DAP in TM3 and 4 and after 20 DAP in TM2. The accumulation of β-carotene could not be detected earlier than zeaxanthin because it was consumed to make the end product. Another example can be illustrated with antheraxanthin, one of the carotenoids appearing at the end of the carotenoid pathway, (Fig. 1). Its accumulation is already observed at 15 DAP in all four transgenic lines and peaked at 20-25 DAP whereas phytoene (the first carotenoid of the metabolic pathway) is present at day 15 in TM3 and after this day in the case of TM1, TM2 and TM4 and peaked at the last DAP (40-50).

3.5.2 Correlation of carotenoid content with gene expression

Carotenoids accumulate in all types of plastids of fruits, flowers, roots and seeds. Their biosynthesis occurs on membranes of chloroplast, chromoplasts and amyloplasts [20]. In starchy corn kernels, carotenoids are present in substantial levels in amyloplasts, and play important roles in ABA

production and seed dormancy and being antioxidants they also limit free radical-induced membrane deterioration [21]. In corn kernels, carotenoids mainly occur in endosperm tissue of the grain.

Important advances have been made in characterizing the function of carotenogenic genes in several different plant species. The regulation of the carotenoid biosynthesis is complex and restricted to specific tissues. In order to understand fully carotenogenesis in plants a comprehensive understanding of gene regulation, biochemical interactions of the enzymatic complexes catalyzing carotenoid biosynthesis and interconversion of different metabolites is necessary.

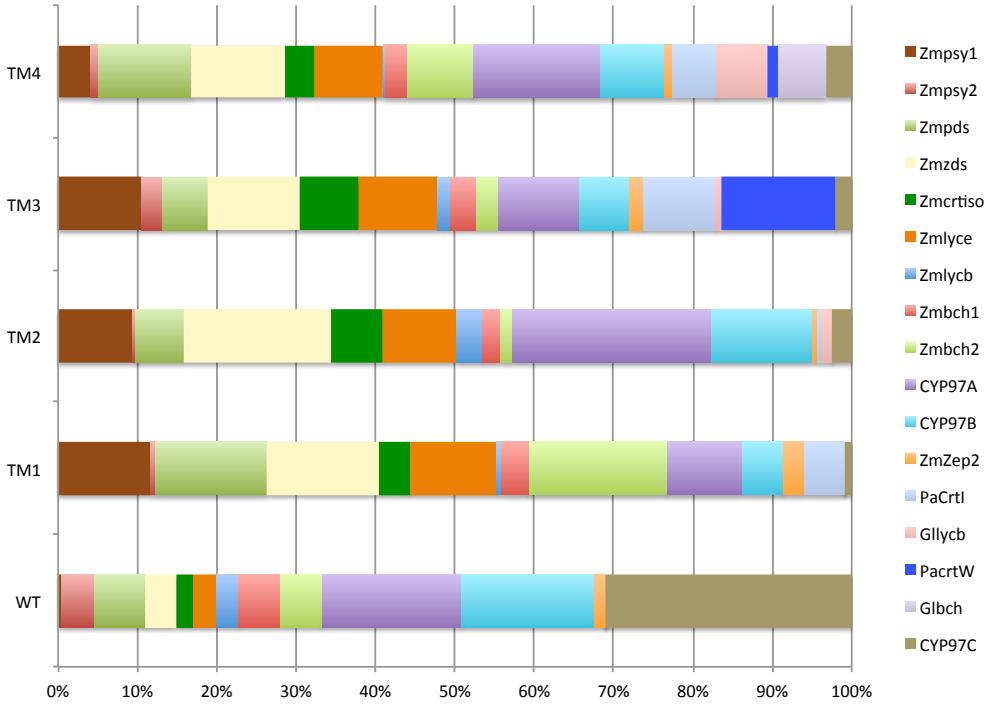

Figure 3-7. Real-time RT-PCR analysis showing relative mRNA levels for transgenes and endogenous carotenogenic genes in immature corn endosperm in the wild-type (WT) and four transgenic lines (TM1, TM2, TM3 and TM4) at 30 DAP. Abbreviations: Zm, *Zea mays*; Pa, *Pantoea annatis*; Gl, *Gentanua lutea*; Para, *Paracoccus*; PSY1/2, phytoene synthase 1/2; PDS, phytoene desaturase; ZDS, ζ-carotene desaturase; CRTISO, carotene isomerase; LYCB, lycopene *β*-cyclase; LYCE, lycopene *ε*-cyclase; BCH1/2, *β*-carotene hydroxylase 1/2. *β*-carotene hydroxylase; CYP97A, carotene *ε*-hydroxylase; CYP97C; ZEP2, zeaxanthin epoxidase 2.

The data presented in the study constitute a direct comparison of the expression of particular transgenes in the four TM at 30 DAP (Fig. 7). The determination of gene expression was carried out by Gemma Farré, therefore, more information about this analysis as well as a more detailed description of transcriptional-metabolic networks in corn plants can be found in her doctoral thesis [19].

Relative quantification through real time PCR revealed which transgenes (*Zmpsy1, Pacrt*I, *Gllycb, Pacrt*W *and Gllycb*) were expressed in the transgenic lines (Fig. 7). In addition, eleven endogenous carotenogenic genes were analyzed in the four transgenic lines and wild-type M37W, namely *Zmpsy2, Zmpds, Zmzds, Zmcrtiso, Zmlyce, Zmlycb, Zmbch1, Zmbch2, ZmCYP97A, ZmCYP97B* and *ZmCYP97C* (Fig. 7).

All the four transgenic lines showed the presence of phytoene (TM1: 15.08±0.71, TM2: 14.99±0.24, TM3: 17.00±0.37 and TM4: 12.94±0.32 μg/g DW at 30 DAP) (Fig. 5.B) whereas in the white endosperm M37W, it was not detected. Moreover, the behavior of phytoene was similar in the four transgenic lines during all the time period studied. Quantitative real-time RT-PCR analysis revealed the absence of *Zmpsy1* transcript in white M37W corn endosperm (confirming previous results obtained in the same maize [11]) while all transgenic lines showed high expression levels. Phytoene synthase (PSY) is the first committed enzyme in carotenoid biosynthesis and it has been extensively studied in corn because it is rate-limiting for endosperm carotenoids [7, 8]. Corn, along with other members of the *Poaceae* family appears to have three *psy* transcripts. In corn endosperm, only *psy1* transcript abundance is correlated with carotenoid content [22]. The three paralogous *psy* genes vary in tissue specificity in terms of expression in responses to abiotic stress [8]. Corn *psy3* transcripts were found predominately in root and embryo [23]. These tissue-specific transcript patterns suggested that the corn *psy* genes might be sub-functionalized and not merely constitute redundant copies [24].

Quantitative real-time RT-PCR showed that *Zmpsy2* was expressed at low levels in all four lines and slightly greater in wild-type plants. Although *Zmpsy2* transcripts were detected in M37W endosperm, the total carotenoid content was low (Fig. 4), suggesting that the residual carotenoid content in M37W endosperm is due perhaps to the activity of PSY2 and confirming that PSY1, and not PSY2, plays a crucial role in the accumulation of carotenoids in the endosperm.

Phytoene undergoes four desaturation and subsequent isomerization steps (catalyzed by both endogenous desaturases/isomerases and by *Pacrt*I in addition to endogenous desaturases and isomerase in the transgenic lines) to produce all-*trans*-lycopene (Fig. 1), a pigment that was only detected in TM1 and TM3 (Fig. 5.C). In transgenic lines, the transcript levels of ζ-carotene desaturase (*zds*) and carotene isomerase (*crtiso*) were higher than in the wild-type M37W (Fig. 7). The highest *Zmpds* transcript levels were observed in TM1 and TM4, followed by wild-type M37W, TM2 and TM3. The *Pacrt*I and *Zmcrtiso* mRNAs were most abundant in TM3, which is consistent with the higher accumulation of lycopene in this line. However, phytoene could still be detected in all lines. Therefore, these results suggest that the conversion of phytoene to lycopene is a rate-limiting step for carotenoid biosynthesis in the transgenic lines.

All the four transgenic lines showed the presence of β-carotene (TM1: 11.98±0.30, TM2: 2.36±0.02, TM3: 2.15±0.23 and TM4: 26.33±0.15 μg/g DW at 30 DAP) (Fig. 5.D) whereas α-carotene was only detected in trace amounts in TM4 (Fig. 4). Nevertheless, the content of β-carotene in TM4 was clearly higher than in the other lines. Both pigments are the product of the cyclization of all-*trans*-lycopene, which is an important branch point in carotenoid biosynthesis (Fig. 1). Symmetrical cyclization catalyzed by LYCB produces β-carotene, whereas LYCE adds one ε-ring and a second cyclization by LYCB produces α-carotene [25]. We found the highest *Gllycb* transcript levels in TM4, which is consistent with the higher accumulation of β-carotene in this line. However, accumulation of lycopene

in TM1 and TM3, despite the expression of *Gllycb* in TM3, indicated that LYCB is also a rate-limiting enzyme.

The ratio of *β*- to *ε*-ring derivatives was 0.77 in wild-type M37W, 6.73 in TM1 (*Zmpsy1+PacrtI*), 5.85 in TM2 (*Zmpsy1+PacrtI+Gllycb*), 7.83 in TM3 (*Zmpsy1+PacrtI+Gllycb+Pacrt*W) and 6.39 in TM4 (*Zmpsy1+PacrtI+Gllycb+Pacrt*W+*Glbch*) at 30 DAP. As observed in transgenic canola [14] and rice [26], the *β*, *β*-branch of the pathway appears to be favored, perhaps implying the existence of a rate-limiting step in the *β*, *ε*-branch. Relative quantification through real time RT-PCR demonstrated higher accumulation levels of *Zmlycb* mRNA in wild-type M37W and TM2 while in TM1, TM3 and TM4 they were lower. In addition, it was observed that *Zmlyce* was induced in the transgenic plants.

Several hydroxycarotenoids were detected in the transgenic lines, including *β*-cryptoxanthin, *α*-cryptoxanthin, lutein and zeaxanthin. The latter being always the most abundant pigment. The high levels of hydroxylated products and lower levels of *β*-carotene in TM1, TM2 and TM3 could indicate the efficient hydroxylation of *α*- and *β*-carotenes in these three transgenic lines. Hydroxylases convert pro-vitamin A carotenes to non-vitamin A xanthophylls, which typically have a hydroxyl group at C3 of the ionone ring [23]. Hydroxylation of the *β*- and *ε*-rings is carried out by *β*-hydroxylases and *ε*-hydroxylase, respectively [20]. Following gene duplication and divergence, many plants have multiple *β*-carotene hydroxylases, including *Arabidopsis* [27], tomato [28], saffron [29] and corn. Hydroxylase levels play a key role in the regulation of pro-vitamin A carotenes in corn endosperm. Accumulation levels of *Zmbch1* mRNA were similar in all lines, whereas accumulation levels of *Zmbch2* mRNA were higher in the TM1 and TM4, especially in TM1 and lower in TM2 and TM3. The highest accumulation levels of *ZmCYP97A* mRNA were observed in wild-type M37W, TM2 and TM4 while the lowest levels were observed in TM1 and TM3. Wild-type M37W showed the highest levels of *ZmCYP97B*, followed by TM2 and TM4. TM1 and TM3 exhibited similar levels of *ZmCYP97B* but in lower levels than wild-type M37W. The accumulation levels of *ZmCYP97C* mRNA were much lower in all the transgenic lines than in wild-type endosperm.

Antheraxanthin showed a similar behavior of accumulation in the four transgenic lines during all the time period studied. Nevertheless, the content of antheraxanthin in TM2 was clearly higher than in the other lines (Fig. 6.N). Zeaxanthin can be converted into antheraxanthin by the action of the enzyme zeaxanthin epoxidase (ZEP). We found the highest *ZmZep2* transcript levels in TM2, which is consistent with the higher accumulation of this compound in this line.

The synthesis of adonixanthin, echinenone (4-keto-*β*-carotene) and 3-hydroxyechinenone in TM4, and these three carotenoids plus astaxanthin (3,3'-dihydroxy-4,4'-diketo-*β*-carotene) in TM3 can be explained because the biosynthetic pathway has been extended to include ketocarotenoids such as astaxanthin by expressing *Paracrt*W. This transgene was expressed together with *Zmpsy1, Pacrt*I and *Gllycb* in TM3 and TM4, the latter also expressing *Glbch*. Astaxanthin is formed from *β*-carotene by the addition of keto groups at the 4 and 4' positions and hydroxyl groups at the 3 and 3' positions of

the *β*-ionone rings. These reactions are catalyzed by *β*-carotene ketolase and *β*-carotene hydroxylase, respectively. In the first step, each enzyme can carry out its reaction independently, but further events depend critically on which reaction occurs first [30]. *Paracoccus β*-carotene ketolase has a strong preference for carotenoids with at least one non-hydroxylated *β*-ionone ring, e.g. *β*-carotene, *β*-cryptoxanthin, echinenone and 3-hydroxyechinenone. In contrast, 3-hydroxylated *β*-ionone rings like zeaxanthin, 3'-hydroxyechinenone and adonixanthin are poor substrates for this enzyme [31].

The product of the *Paracrt*W transgene utilizes the same substrate as *β*-carotene hydroxylase, an unsubstituted *β*-ionone ring. The hydroxylase and ketolase thus compete at four stages for different substrates in the extended carotenoid pathway: for *β*-carotene, the unsubstituted side of *β*-cryptoxanthin, echinenone and 3-hydroxyechinenone (Fig. 2).

Because the 3-hydroxylated *β*-ionone ring is poorly ketolated [31], the ketolase has to overcome the hydroxylase twice – first during the ketolation of *β*-carotene, then during the ketolation of either echinenone or 3-hydroxyechinenone – or astaxanthin is not formed. Therefore, the accumulation of astaxanthin is determined by the abundance of the ketolase relative to the hydroxylase. Only plants expressing *Paracrt*W produce enough ketolase to ensure the formation of astaxanthin. Otherwise, adonixanthin is the final keto-hydroxy product of the pathway, as appears to be the case in TM4, where total concentrations of ketolated carotenoids are much lower than in TM3, and the pathway stops without the second ketolation at the level of adonixanthin. TM4, expressing *Glbch* and *Paracrt*W, did not accumulate astaxanthin due to the competition between these two enzymes. TM3 had the highest ketocarotenoid levels and was the only line to synthesize astaxanthin, probably reflecting the relatively low hydroxylase levels (no GlBCH activity) and high ketolase levels (high ParaCRTW activity). For many plants transformed with a ketolase gene such as *Paracrt*W, the conversion of adonixanthin to astaxanthin appears to be an important limiting step in astaxanthin biosynthesis. These data indicate that avoiding adonixanthin accumulation was crucial for astaxanthin production in transgenic corn endosperm.

3.6 CONCLUSIONS

The accumulation profiles of individual carotenoids indicate that although carotenoid synthesis begins at the earliest stages of endosperm development, their accumulation depends on feedback regulations. For example, accumulation of zeaxanthin is already observed at 15 DAP in all four transgenic lines whereas the accumulation of *β*-carotene (its precursor) is detected at 15 DAP in TM1, after 15 DAP in TM3 and TM4 and after 20 DAP in TM2. The accumulation of *β*-carotene could not be detected earlier than zeaxanthin because it was consumed to make the end product. This behavior was observed for several carotenoid precursors and end products.

Combinatorial nuclear transformation permitted the increase (up to 100.2-fold) of the carotenoid content in maize endosperm and the generation of transgenic lines with high levels of carotenoids, including *β*-carotene, hydroxycarotenoids and ketocarotenoids. Thus, it demonstrated that it was a

versatile approach that could be used to modify any metabolic pathway and pathways controlling other biochemical, physiological, or developmental processes.

Although many of the regulatory mechanisms affecting carotenoid biosynthesis in corn endosperm are still unclear, a comparative investigation in the different transgenic lines recovered focusing on targeted carotenoid transcript and metabolite analysis allowed the identification and complement rate-limiting steps in the pathway and to demonstrate competition between *β*-carotene hydroxylase and *β*-carotene ketolase for substrates in 4 sequential steps of the extended pathway. The comparative analysis of these lines provided confirmation that PSY1 is a key enzyme-limiting carotenoid biosynthesis in maize endosperm. Another rate-limiting steps identified is the conversion of phytoene to lycopene, catalyzed by endogenous desaturases and isomerases.

3.7 REFERENCES

[1] Yuan D, Bassie L, Sabalza M, Miralpeix B, Dashevskaya S, Farre G, Rivera S, Banakar R, Bai C, Sanahuja G, Arjó G, Avilla E, Zorrilla-López U, Ugidos-Damboriena N, López A, Almacellas D, Zhu C, Capell T, Hahne G, Twyman RM, Christou P (2011) The potential impact of plant biotechnology on the Millennium Development Goals. Plant Cell Reports.30:249-65.

[2] Misawa N, Yamano S, Linden H, De Felipe MR, Lucas M, Ikenaga H, Sandmann G (1993) Functional expression of the Erwinia uredovora carotenoid biosynthesis gene crtl in transgenic plants showing an increase of *β*-carotene biosynthesis activity and resistance to the bleaching herbicide norflurazon. Plant Journal.4:833-40.

[3] Chen Y, Li F, Wurtzel ET (2010). Isolation and characterization of the Z-ISO gene encoding a missing component of carotenoid biosynthesis in plants. Plant Physiology.153:66-79.

[4] Zhu C, Bai C, Sanahuja G, Yuan D, Farré G, Naqvi S, Capell T, Christou P (2010) The regulation of carotenoid pigmentation in flowers. Archives of Biochemistry and Biophysics.504:132-41.

[5] Bai C, Twyman RM, Farré G, Sanahuja G, Christou P, Capell T, Zhu C (2011) A golden era-pro-vitamin A enhancement in diverse crops. In Vitro Cellular and Developmental Biology - Plant.47:205-21.

[6] Kim M, Kim SC, Song KJ, Kim HB, Kim IJ, Song EY, Chun SJ (2010) Transformation of carotenoid biosynthetic genes using a micro-cross section method in kiwifruit (*Actinidia deliciosa* cv. Hayward). Plant Cell Reports.29:1339-49.

[7] Wong JC, Lambert RJ, Wurtzel ET, Rocheford TR (2004). QTL and candidate genes phytoene synthase and *ζ*-carotene desaturase associated with the accumulation of carotenoids in maize. Theoretical and Applied Genetics.108:349-59.

[8] Li F, Vallabhaneni R, Yu J, Rocheford T, Wurtzel ET (2008) The maize phytoene synthase gene family: Overlapping roles for carotenogenesis in endosperm, photomorphogenesis, and thermal stress tolerance. Plant Physiology.147:1334-46.

[9] Shewmaker CK, Sheehy JA, Daley M, Colburn S, Ke DY (1999) Seed-specific overexpression of phytoene synthase: Increase in carotenoids and other metabolic effects. Plant Journal.20:401-12.

[10] Cong L, Wang C, Chen L, Liu H, Yang G, He G (2009) Expression of phytoene synthase1 and carotene desaturase crt/ genes result in an increase in the total carotenoids content in transgenic elite wheat (*Triticum aestivum L.*). Journal of Agricultural and Food Chemistry.57:8652-60.

[11] Zhu C, Naqvi S, Breitenbach J, Sandmann G, Christou P, Capell T (2008) Combinatorial genetic transformation generates a library of metabolic phenotypes for the carotenoid pathway in maize. Proceedings of the National Academy of Sciences of the United States of America.105:18232-7.

[12] Rosati C, Aquilani R, Dharmapuri S, Pallara P, Marusic C, Tavazza R, Bouvier F, Camara B, Giuliano G (2000) Metabolic engineering of beta-carotene and lycopene content in tomato fruit. Plant Journal.24:413-9.

[13] D'Ambrosio C, Giorio G, Marino I, Merendino A, Petrozza A, Salfi L, Stigliani AL, Cellini F (2004) Virtually complete conversion of lycopene into *β*-carotene in fruits of tomato plants transformed with the tomato lycopene β-cyclase (tlcy-b) cDNA. Plant Science.166:207-14.

[14] Ravanello MP, Ke D, Alvarez J, Huang B, Shewmaker CK (2003) Coordinate expression of multiple bacterial carotenoid genes in canola leading to altered carotenoid production. Metabolic Engineering.5:255-63.

[15] Naqvi S, Zhu C, Farre G, Sandmann G, Capell T, Christou P (2011) Synergistic metabolism in hybrid corn indicates bottlenecks in the carotenoid pathway and leads to the accumulation of extraordinary levels of the nutritionally important carotenoid zeaxanthin. Plant Biotechnology Journal.9:384-93.

[16] Farré G, Bai C, Twyman RM, Capell T, Christou P, Zhu C (2011). Nutritious crops producing multiple carotenoids - a metabolic balancing act. Trends in Plant Science.16:532-40.

[17] Britton G, Liaaen-Jensen S, Pfander H (2004) Carotenoids handbook: 1st ed; Birkhäuser: Basel, Switzerland. pp. 3-404.

[18] Rivera S, Vilaró F, Canela R (2011) Determination of carotenoids by liquid chromatography/mass spectrometry: Effect of several dopants. Analytical and Bioanalytical Chemistry.400:1339-46.

[19] Farré G (2012) Towars vitamin biofortification in staple cereal crops in a socio-political and food security contex. Doctoral thesis, University of Lleida, Lleida, Spain.

[20] Hirschberg J (2001) Carotenoid biosynthesis in flowering plants. Current Opinion in Plant Biology.4:210-8.

[21] Calucci L, Capocchi A, Galleschi L, Ghiringhelli S, Pinzino C, Saviozzi F, Zandomeneghi M (2004) Antioxidants, free radicals, storage proteins, puroindolines, and proteolytic activities in bread wheat (*Triticum aestivum*) seeds during accelerated aging. Journal of Agricultural and Food Chemistry.52:4274-81.

[22] Buckner B, Miguel PS, Janick-Buckner D, Bennetzen JL (1996) The y1 gene of maize codes for phytoene synthase. Genetics.143:479-88.

[23] Howitt CA, Pogson BJ (2006) Carotenoid accumulation and function in seeds and non-green tissues. Plant, Cell and Environment.29:435-45.

[24] Li F, Tzfadia O, Wurtzel ET (2009) The phytoene synthase gene family in the Grasses: Subfunctionalization provides tissue-specific control of carotenogenesis. Plant Signaling and Behavior.4:208-11.

[25] Cunningham Jr FX, Pogson B, Sun Z, McDonald KA, DellaPenna D, Gantt E (1996) Functional Analysis of the [beta] and [epsilon] Lycopene Cyclase Enzymes of Arabidopsis Reveals a Mechanism for Control of Cyclic Carotenoid Formation. The Plant Cell Online.8:1613-26.

[26] Ye X, Al-Babili S, Klöti A, Zhang J, Lucca P, Beyer P, Potrykus I (2000) Engineering the provitamin A (*β*-carotene) biosynthetic pathway into (carotenoid-free) rice endosperm. Science.287:303-5.

[27] Rissler HM, Pogson BJ (2001) Antisense inhibition of the beta-carotene hydroxylase enzyme in Arabidopsis and the implications for carotenoid accumulation, photoprotection and antenna assembly. Photosynthesis Research.67:127-37.

[28] Liu YS, Gur A, Ronen G, Causse M, Damidaux R, Buret M, Hirschberg J, Zamir D (2003) There is more to tomato fruit colour than candidate carotenoid genes. Plant Biotechnology Journal.1:195-207.

[29] Castillo R, Fernández JA, Gómez-Gómez L (2005) Implications of carotenoid biosynthetic genes in apocarotenoid formation during the stigma development of Crocus sativus and its closer relatives. Plant Physiology.139:674-89.

[30] Fraser PD, Miura Y, Misawa N (1997) In vitro characterization of astaxanthin biosynthetic enzymes. Journal of Biological Chemistry.272:6128-35.

[31] Fraser PD, Shimada H, Misawa N (1998) Enzymic confirmation of reactions involved in routes to astaxanthin formation, elucidated using a direct substrate in vitro assay. European Journal of Biochemistry.252:229-36.

Chapter 4

Engineering ketocarotenoid biosynthesis in maize endosperm

4.1 ABSTRACT

Ketocarotenoids such as astaxanthin have attracted great interest because they have remarkable singlet oxygen-quenching activity and have been associated with a range of health benefits [1]. Therefore, the group of Applied Plant Biotechnology of the UdL investigated the impact of expressing sCrBkt on the accumulation of astaxanthin in maize endosperm by using the combinatorial nuclear transformation method. Several transgenic maize lines were recovered expressing this gene. I analyzed these lines and described the carotenoid accumulation in the target tissue. In addition, I was involved in exploring relationships between gene expression and the accumulation of metabolites in the different transgenic lines. Finally, I performed preliminary assays to identify the new pigments found in the transgenic lines expressing sCrBk.

4.2 INTRODUCTION

Astaxanthin is a red pigment abundant in marine animals including salmon, trout, shrimp and lobster [2]. It is also present in birds such as flamingos and quails. These animals cannot synthesize this pigment but they accumulate significant amounts through their diet. Ketocarotenoids are rarely found in flower petals of higher plants, but many microorganisms such as the marine bacteria *Agrobacterium aurantiacum* (reclassified as *Paracoccus* sp. N81106) and *Alcaligenes* sp. PC-1 (reclassified as *Paracoccus* sp. PC-1), fresh water algae such as *Haematococcus pluvialis*, and the yeast *Xanthophyllomyces dendrorhous* (former *Phaffia rhodozyma*) synthesize ketocarotenoid pigments [1]. The presence of hydroxyl and keto functional groups in ketocarotenoids makes them excellent antioxidants compared to the other carotenoids. Astaxanthin is a strong antioxidant [3, 4] and contributes to general eye and skin health [1, 5]. It has anti-inflammatory properties and inhibits oxidation of low-density lipoprotein in humans [6]. It is also implicated in the prevention of diabetic nephropathy in diabetic db/db mice [7], exhibits anticancer activity [8, 9], and enhances immune responses [10, 11].

Currently, a large proportion of ketocarotenoids including astaxanthin and canthaxanthin are produced through chemical synthesis. However, synthetic astaxanthin contains the stereoisomer by-products 3*S*,3*R*' and 3*R*,3*R*' in addition to the naturally occurring 3*S*,3*S*' stereoisomer [12]. The presence of the by-products may have an inhibitory effect on the biological activity of astaxanthin [1, 12]. Additionally, chemically-synthesized astaxanthin may be contaminated with other reaction by-products or intermediates. Thus, its commercial use is restricted mostly to feed supplementation particularly in aquaculture [13]. Astaxanthin can also be produced biologically since several microorganisms are able to accumulate the compound at relatively high levels. For example, the alga *H. pluvialis*, which produces astaxanthin at levels representing 4–5% of its dry weight, is used for the commercial production of this pigment as a functional food supplement for human consumption. However, this organism requires high light-intensities that increase production costs and its slow growth rate in culture increases the risks of contamination, which hinder its broader utility [5, 14]. The yeast *X. dendrohous* is another microorganism which can accumulate astaxanthin up to 0.5% of its dry weight. However, the pigment produced by this microorganism has the 3*R*,3*R*' configuration [15]. Metabolic engineering in higher plants using cloned heterologous genes is potentially one of the most powerful tools to produce astaxanthin, since plants have the ability to accumulate carotenoids in the thylakoid membranes and in the lipid globules within the plastid at very high concentrations [16].

In both prokaryotes and eukaryotes, *β*-carotene is converted into astaxanthin by the addition of keto groups at the 4 and 4' position and hydroxyl groups at the 3 and 3' positions of the *β*-ionone rings via several ketocarotenoid intermediates (Fig. 1). These reactions are catalyzed by *β*-carotene ketolase (4,4'-oxygenase; CRTW, BKT or CRTO) and *β*-carotene hydroxylase (3,3'-oxygenase; BCH or CRTZ), respectively [1]. Several ketolase and hydroxylase encoding carotenogenic genes have been

identified in microorganisms and higher plants. The hydroxylation reaction is widespread in higher plants, but ketolation is restricted to a few bacteria, fungi, and some unicellular green algae [17]. Even though higher plants synthesize different hydroxylated carotenoids, they are not able to form ketocarotenoids, other than very few species such as *Adonis* [18], which accumulates ketocarotenoids in flowers.

There exist three highly homologous functional *bkt* genes in *H. pluvialis* [19] encoding putative amino acid sequences ranging from 86.1% to 99.4%. These are *bkt1* from *H. pluvialis* 34/7 and *bkt2* and *bkt3* from *H. pluvialis* Flotow NIES-144 [19-21]. It has also been demonstrated that *bkt1* and *bkt2* coexist in a single strain of *H. pluvialis* while *bkt3* is a third ketolase identified that share 95% identity with *bkt2* [19]. The overexpression of *H. pluvilis bkt* under the control of the chromoplast-associated tomato *pds* promoter resulted in the accumulation of high levels of astaxanthin and other ketocarotenoids in the nectary, a flower tissue rich in xanthophyll-containing chromoplasts [16]. This finding demonstrated that ketocarotenoid accumulation in higher plants can be genetically engineered by overexpression of a *β*-carotene ketolase gene. Genetic modification for enhanced ketocarotenoid accumulation has been accomplished in bacteria [22], yeast [23], and with mixed success in model plants and several crops including tomato [24], potato [25], carrot [26], rapeseed and maize [27].

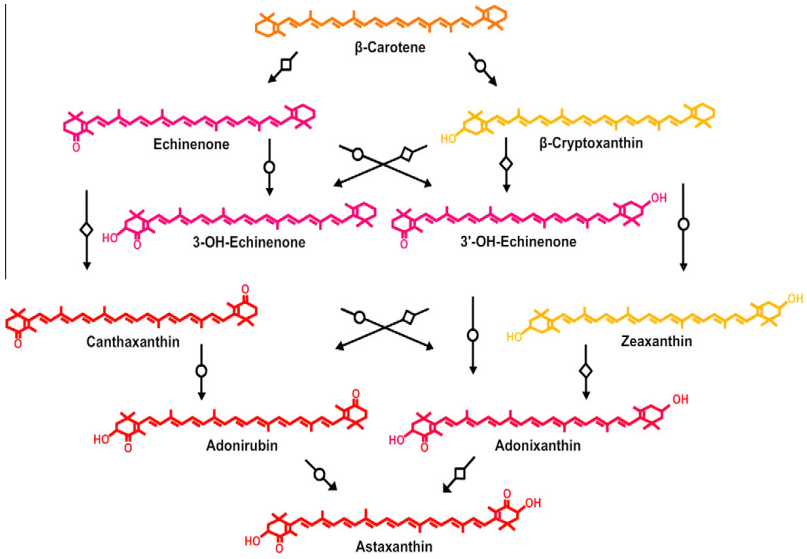

Figure 4-1. Astaxanthin biosynthesis pathway from *β*-carotene. Arrow with inset square represents *β*-carotene ketolase – BKT, CRTW or CRTO. Arrow with inset circle represents *β*-carotene hydroxylase (HYDB) – BCH, CYP97A, CYP97B or CRTZ [28].

4.3 OBJECTIVES

- To describe the carotenoid profile of several transgenic maize lines expressing *sCrBkt* for the production of ketocarotenoids.
- To use the metabolite profile of carotenoids to investigate the specific contribution(s) of carotenogenic genes in the carotenoid pathway considering the mRNA levels.
- To carry out preliminary assays to identify the new pigments found in the transgenic lines expressing the *sCrBkt* gene.

4.4 MATERIALS AND METHODS

4.4.1 Chemicals

β-Carotene, lycopene, lutein, *β*-cryptoxanthin, astaxanthin, were purchased from Sigma-Aldrich Fine Chemicals (St. Louis, MO, USA). Canthaxanthin and zeaxanthin were acquired from Fluka (Buchs SG, Switzerland). Phytoene, violaxanthin, and antheraxanthin were purchased from Carotenature (Lupsingen, Switzerland). MeOH, ethyl acetate, ethyl eter, TBME, ACN and acetone (HPLC grade purity) were acquired from J.T. Baker (Deventer, The Netherlands). Water was prepared using a Milli-Q reagent water system.

4.4.2 Plant material

The transgenic maize was generated by combinatorial nuclear transformation, as reported in Zhu et al. [27]. The TM analyzed were: TM5, expressed *Zmpsy*1*,* biochemically synthesized *sCrBkt* from *Chlamydomonas reinhardtii* and biochemically synthesized *sBrcrtZ* from *Brevundimonas* sp. Strain SD212; TM6 and TM7 corresponded to the cross of TM5 with two wild-type maize plants, NSL26 and NSL76 respectively. Therefore, they expressed *Zmpsy*1, *sCrBkt,* and *sBrcrtZ.* TM8 corresponded to the cross of TM1 (expressing *Zmpsy1* and *Pacrt*I; described in chapter 3) with TM5. Therefore, it expressed *Zmpsy*1, *CrBkt,* and possibly *PacrtI* and *sBrcrtZ*. The NSL26 and NSL76 wild-types were used since they have a high fat content. The difference between these two wild-types is that NSL76 synthesizes carotenoids in the endosperm while the NSL26 does not. Table 1 summarizes the genes expressed in the different transgenic lines.

Table 4-1. Transgenic lines recovered.

Line	Genes
TM5	*Zmpsy*1, *sCrBkt*, *sBrcrtZ*
TM6	Cross of TM5 with wild-type NSL26: *Zmpsy*1, *sCrBkt, sBrcrtZ*
TM7	Cross of TM5 with wild-type NSL76: *Zmpsy*1*, sCrBkt, sBrcrtZ*
TM8	Cross of TM5 with TM1: *Zmpsy*1, *PacrtI, sCrBkt, sBrcrtZ*

4.4.3 Extraction of carotenoids

To protect carotenoids from degradation and oxidation, the extraction was conducted under limited light. Samples were freeze-dried and ground into a fine powder using a mortar and pestle. 50 or 100[5] mg of sample was extracted with 15 mL of MeOH: ethyl acetate (6:4, v/v) at 60 °C for 20 min and this mixture was continuously shaken. It was then put on ice until it reached room temperature and the liquid phase was filtered into a separatory funnel (if the residue exhibited color after extraction, then it was re-extracted with 5 mL of MeOH: ethyl acetate (6:4, v/v) at 60 °C for 5 min and the second extract was combined with the first one). 15 mL of hexane: diethyl ether (9:1, v/v) was added to the organic extract and the mixture was shaken vigorously. Then, 20 mL of saturated sodium chloride solution was added and again the mixture was shaken. The aqueous phase was removed and the organic phase was washed with water once again. The organic phase was dried under N_2 at 37 ºC. When the sample was completely dry, Ar was flushed into the vial and carotenoids were stored at -80 ºC until LC analysis. Each extraction was carried out in triplicate.

4.4.4 Chromatographic analysis

Chromatographic systems used to analyze the transgenic lines were the same employed in chapter 2, section 2.4.6.

4.4.4.1 UHPLC-PDA-MS analysis

UHPLC analysis was carried out using an ACQUITY Ultra Performance LC™ system linked to a PDA 2996 detector (Waters, Milford, MA, USA). Mass detection was carried out using an Acquity™ TQD tandem-quadrupole MS equipped with a Z-spray electrospray interface (Manchester, UK). MassLynx™ software version 4.1 (Waters, Milford, MA, USA) was used to control the instruments and also for data acquisition and processing.

UHPLC chromatographic separations were performed on reversed-phase column ACQUITY UPLC® C18 BEH 130Å, 1.7 μm, 2.1×100 mm (Waters, Milford, MA). Mobile phase consisted of solvent A: ACN: MeOH 7:3, v/v and solvent B: water 100%. The gradient program used is shown in Table 2. The column and sample temperatures were set at 32 °C and 25 °C respectively. Injection volume was 5 μL.

Each sample extract for LC analysis was dissolved in 300 μL and 600 μL (for light and dark color extract respectively) of the injection solvent [ACN: MeOH 7:3, v/v]: acetone 6.7:3.3, v/v. Before use, all solutions were filtered through Millex 0.2 μm nylon membrane syringe filters (Millipore, Bedford, MA, USA).

[5] For pale color maize samples, extract 100 mg of sample. For darker color maize samples, it is sufficient to extract 50 mg of sample.

Table 4-2. Gradient profile used in the separation of carotenoids by UHPLC. Linear gradient.

Time[a] (min)	Flow rate (mL/min)	A (%, v/v)	B (%, v/v)
Initial	0.4	80	20
2.0	0.4	80	20
3.0	0.4	100	0
7.0	0.4	100	0
8.0	0.6	100	0
11.6	0.6	100	0
12.6	0.4	80	20

[a] After this time, the system was left 2 min more to reach its re-equilibration before injecting a new sample.

4.4.4.2 MS conditions

Optimized MS conditions are listed in Table 3.

Table 4-3. MS conditions.

MS conditions	APCI
Polarity	Positive
Corona (kV)	4.0
Cone (V)	30
Extractor (V)	3
RF (V)	0.1
Source Temperature (°C)	150
Probe Temperature (°C)	450
Cone Gas Flow (L/h)	10
Desolvation Gas Flow (L/h)	150
Collision Gas Flow (mL/min)	0.15

4.4.4.3 HPLC-PDA analysis

HPLC analysis separations was carried out using a Waters Alliance 2695 separation module linked to a PDA 2998 detector (Waters, Milford, MA, USA). Empower software version 2 (Waters, Milford, MA, USA) was used to control the instruments and also for data acquisition and processing.

HPLC chromatographic separations were performed on a YMC C30 carotenoid 3 μm, 2.0×100 mm column (Waters, Milford, MA). Mobile phase consisted of solvent A: MeOH: water 8:2, v/v and solvent B: TBME 100%. The gradient program used is shown in Table 4. Both, the column and the sample temperatures were set at 25 °C. Injection volume was 10 μL.

Table 4-4. Gradient profile used in the separation of carotenoids by HPLC. Linear gradient.

Time[a] (min)	Flow rate (mL/min)	A (%, v/v)	B (%, v/v)
Initial	0.25	97	3
6.0	0.25	97	3
7.0	0.25	62	38
15.0	0.25	62	38
16.0	0.25	32	68
18.0	0.25	32	68
19.0	0.25	0	100
25.0	0.25	0	100
26.0	0.25	32	68
27.0	0.25	50	50
28.0	0.25	70	30
29.0[b]	0.25	97	3

[a] After this time, the system was left 6 min more to reach its re-equilibration before injecting a new sample.

4.4.5 Carotenoid identification and quantification

Identification of carotenoids was carried out by analysis and comparison of the following parameters: chromatographic retention time, UV-vis spectra, %III/II [29] and *m/z* fragments according literature data [30] and that of the authentic standards. Those standards were also used for quantitation.

5.5 RESULTS AND DISCUSSION

4.5.1 Metabolic engineering of ketocarotenoid biosynthesis in maize endosperm

In order to produce useful ketocarotenoids such as astaxanthin efficiently, it is considered to be necessary to introduce many key-gene candidates for carotenoid biosynthesis into plants and evaluate which genes play important roles in the production of the ketocarotenoids. Therefore, the group of Applied Plant Biotechnology of UdL genetically engineered maize with *Zmpsy*1, *sCrBkt*, *sBrcrtZ* and *PacrtI* in order to elucidate the biosynthetic step(s) that lead to the kecarotenoid accumulation in maize endosperm.

Individual lines expressing the same combination of genes were analyzed. For TM5, TM6, TM7 and TM8, one, four, three and two lines were recovered, respectively, and each line was analyzed in triplicate. To identify individual lines expressing the same combination of genes obtained from the same crossing, the use of letters of the alphabet was employed in their names. Thus, for TM6, where four individual lines were recovered, the nomenclature TM6A, TM6B, TM6C and TM6D was used.

4.5.1.1 Carotenoid profile of transgenic lines expressing sCrBkt

Figs. 2 and 3 show the chromatograms obtained for TM5, TM6, TM7 and TM8. In the wild-type NSL26, used to make the crossing with TM5 in order to obtain the TM6, carotenoids were not detected, whereas the wild-type NSL76, used to make the crossing with TM5 in order to obtain the TM7, exhibited a total carotenoid concentration of 15.47 μg/g DW (Table 5) comprising lutein and

zeaxanthin (10.92 and 4.55 μg/g respectively). A higher total carotenoid content was obtained for TM5, TM6, TM7 and TM8 in comparison with the wild-type NSL76 (Table 5 and 6). The highest total carotenoid content was observed in the TM8 and it ranged from 55.62 to 70.12 μg/g DW (Table 6). TM6 showed a lower total carotenoid content than TM7. The total carotenoid content ranged from 20.97 to 35.16 μg/g DW and from 38.02 to 48.63 μg/g DW for TM6 and TM7 respectively. TM5, expressing *Zmpsy*1, *sCrBkt* and *sBrcrtZ* had a total carotenoid content equal to 32.97 μg/g DW.

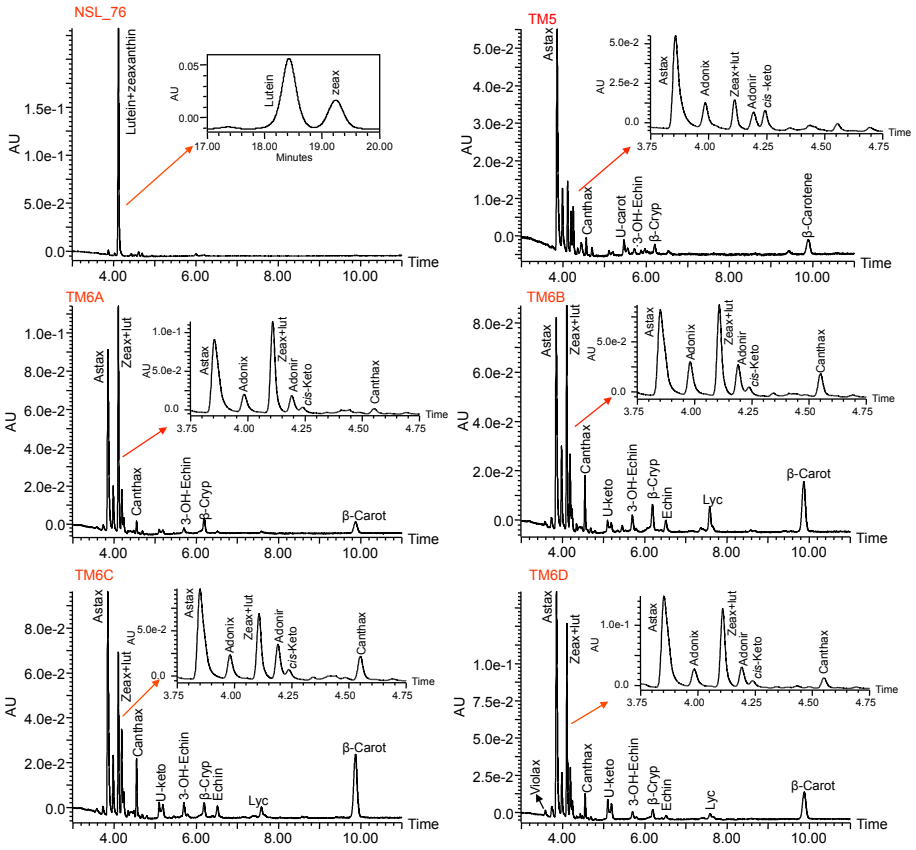

Figure 4-2. Carotenoid profile in wild-type NSL76, TM5 (expressing *Zmpsy*1, *sCrBkt* and *sBrcrtZ*) and TM6 (cross between TM5 and NSL26, therefore, expressing *Zmpsy*1, *sCrBkt* and *sBrcrtZ*). Abbreviations: Violax, violaxanthin; Astax, astaxanthin; Zeax, zeaxanthin; Lut, lutein; Adonix, adonixanthin; Adonir, adonirubin; *cis*-Keto, *cis*-unknown ketocarotenoid; U-keto, unknown ketocarotenoids; Canthax, canthaxanthin; U-cart, unknown carotenoid; 3-OH-Echinen, 3-OH-echinenone; Echin, echinenone; β-Cryp, β-cryptoxanthin; Lyc, lycopene; β-Carot, β-carotene.

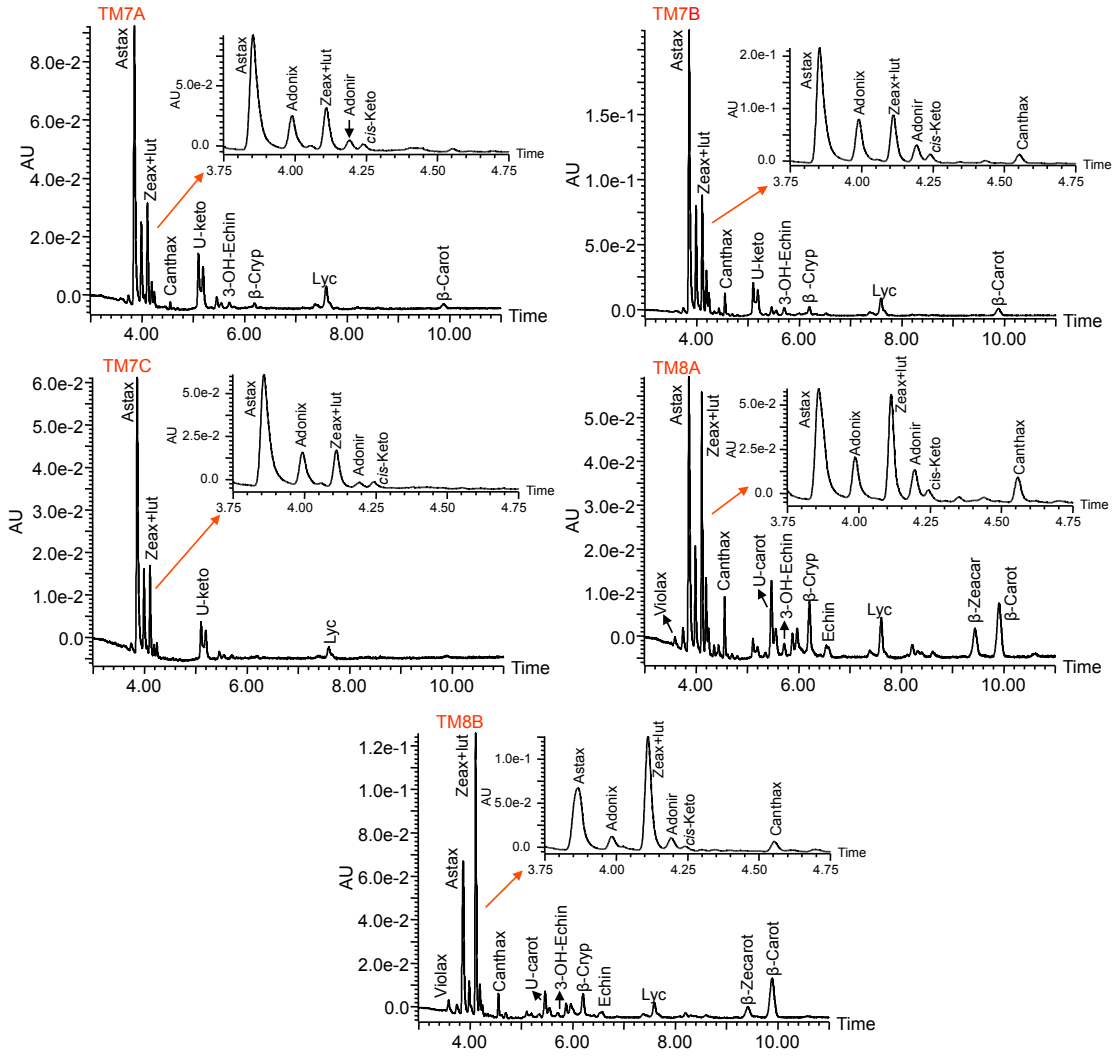

Figure 4-3. Carotenoid profile in TM7 (cross between TM5 and NSL76, therefore, expressing *Zmpsy*1, *sCrBkt* and *sBrcrtZ*) and TM8 (cross between TM1 and TM5, therefore, expressing *Zmpsy*1, *sCrBkt* and possibly *PacrtI* and *sBrcrtZ)*. Abbreviations: Violax, violaxanthin; Astax, astaxanthin; Zeax, zeaxanthin; Lut, lutein; Adonix, adonixanthin; Adonir, adonirubin; *cis*-Keto, *cis*-unknown ketocarotenoid; U-keto, unknown ketocarotenoids; Canthax, canthaxanthin; U-cart, unknown carotenoid; 3-OH-Echinen, 3-OH-echinenone; Echin, echinenone; *β*-Cryp, *β*-cryptoxanthin; Lyc, lycopene; *β*-Zeacarot, *β*-zeacarotene, *β*-Carot, *β*-carotene.

Table 4-5. Carotenoid content and composition in wild type NSL76 and transgenic maize TM5 and TM6.

Carotenoid	NSL76 μg/g DW	TM5 μg/g DW	TM6A μg/g DW	TM6B μg/g DW	TM6C μg/g DW	TM6D μg/g DW
Zeaxanthin	4.55±0.45	2.30±0,23	4.30±0.17	3.07±0.10	3.01±0.11	3.56±0.15
Lutein	10.92±0.63	0.78±0.11	0.36±0.10	0.45±0.01	0.26±0.05	0.65±0.08
Violaxanthin	-	-	-	-	-	0.19±0.02
Astaxanthin	-	13.03±0.18	8.58±0.55	7.07±0.15	9.52±0.16	10.61±0.25
Adonixanthin	-	2.86±0.03	1.49±0.09	1.93±0.02	1.76±0.04	1.52±0.07
Adonirubin	-	2.03±0.02	1.48±0.14	1.78±0.08	2.75±0.08	1.75±0.05
cis-Keto	-	2.07±0.05	0.59±0.13	0.58±0.04	0.92±0.07	0.65±0.07
U-keto	-	-	-	0.82±0.07	1.55±0.08	2.00±0.19
U-carot	-	1.24±0.03	-	-	-	-
Canthaxanthin	-	0.78±0.00	0.54±0.29	1.37±0.05	1.96±0.09	0.80±0.02
3-OH-Echin	-	0.35±0.03	0.28±0.03	0.57±0.03	0.66±0.05	0.37±0.02
β-Cryp	-	0.83±0.04	1.14±0.17	1.30±0.08	1.05±0.07	0.74±0.05
Echinenone	-	-	-	0.55±0.01	0.67±0.03	0.25±0.03
Lycopene	-	-	-	2.41±0.16	1.44±0.14	1.26±0.13
β-Zeacarotene	-	-	-	-	-	-
β-Carotene	-	3.78±0.02	2.22±0.22	5.40±0.31	8.86±0.55	4.54±0.23
Phytoene	-	2.91±0.01	-	0.73±0.01	0.77±0.03	-
Total Conc.	15.47±1.08	32.97±0.15	20.97±1.39	28.02±0.81	35.16±1.04	28.88±0.71
% Ketocarot.	-	64.06	61.77	52.34	56.23	62.14

Wild-type, NSL76; TM5, expressing *Zmpsy*1, *sCrBkt* and *sBrcrtZ* and TM6, which is the cross between TM5 and NSL26, therefore, expressing *Zmpsy*1, *sCrBkt* and *sBrcrtZ*. Abbreviations: *cis*-Keto, unknown *cis*-ketocarotenoid; U-keto, unknown ketocarotenoids; U-carot, unknown carotenoid; 3-OH-Echinen, 3-OH-echinenone; β-Cryp, β-cryptoxanthin; Total Conc., total carotenoid concentration; % Ketocarot, % Ketocarotenoids.

Table 4-6. Carotenoid content and composition in transgenic maize TM7 and TM8.

Carotenoid	TM7A μg/g DW	TM7B μg/g DW	TM7C μg/g DW	TM8A μg/g DW	TM8B μg/g DW
Zeaxanthin	2.41±0.04	3.26±0.22	3.05±0.45	3.93±0.26	8.37±0.88
Lutein	1.06±0.13	1.28±0.10	0.67±0.12	0.50±0.01	2.86±0.41
Violaxanthin	-	-	-	0.24±0.02	0.83±0.09
Astaxanthin	15.47±0.33	18.83±0.57	18.96±0.72	10.87±0.51	14.59±1.00
Adonixanthin	4.22±0.07	6.28±0.33	4.91±0.12	3.11±0.58	2.36±0.51
Adonirubin	1.06±0.02	2.33±0.21	0.78±0.08	2.23±0.08	2.12±0.15
cis-Keto	0.74±0.03	1.12±0.02	0.85±0.02	0.83±0.02	0.79±0.08
U-keto	7.11±0.25	5.48±0.01	5.53±0.23	-	-
U-carot	-	-	-	3.23±0.26	2.73±0.21
Canthaxanthin	0.27±0.01	1.15±0.04	-	1.69±0.05	1.51±0.12
3-OH-Echin	0.38±0.01	0.64±0.01	-	0.51±0.00	0.38±0.05
β-Cryp	0.41±0.03	0.86±0.07	-	2.95±0.10	2.57±0.30
Echinenone	-	-	-	0.88±0.08	0.49±0.04
Lycopene	4.21±0.57	4.51±0.26	3.27±0.47	4.13±0.62	4.93±0.75
β-Zeacarotene	-	-	-	3.69±0.18	3.30±0.26
β-Carotene	1.20±0.11	2.02±0.14	-	6.80±0.61	11.89±1.42
Phytoene	0.41±0.02	0.89±0.04	-	10.02±0.21	10.38±0.67
Total Conc.	38.95±0.21	48.63±1.19	38.02±1.93	55.62±3.57	70.12±6.46
% Ketocarot.	75.12	73.66	81.63	36.20	31.73

TM7, which is the cross between TM5 and NSL76, therefore, expressing *Zmpsy*1*, sCrBkt* and *sBrcrtZ* and TM8, which is the cross between TM1 and TM5, therefore, expressing *Zmpsy*1, *sCrBkt* and possibly *PacrtI* and *sBrcrtZ*. Abbreviations: *cis*-Keto, unknown *cis*-ketocarotenoid; U-keto, unknown ketocarotenoids; U-carot, unknown carotenoid; 3-OH-Echinen, 3-OH-echinenone; β-Cryp, β-cryptoxanthin; Total Conc., total carotenoid concentration; % Ketocarot, % Ketocarotenoids.

Astaxanthin showed the highest accumulation among the different carotenoids detected in the different transgenic lines: 13.03, up to 10.61, up to 18.96 and up to 14.59 μg/g in TM5, TM6, TM7 and TM8, respectively (Tables 5 and 6). Other ketocarotenoids including adonixanthin, adonirubin, canthaxanthin and 3-hydroxyechinenone were also found in these lines, reaching levels up to 6.28, 2.75, 1.96 and 0.66 μg/g, respectively (Tables 5 and 6). Echinenone was only found in TM6 and TM8 and reached levels up to 0.88 μg/g (Tables 5 and 6). The percentage of ketocarotenoids in TM5, TM6 and TM7 ranged from 52 to 82% while in TM8 it ranged from 32 to 36% (Tables 5 and 6). These results demonstrated that the expression of the transgene *sCrBkt* along other genes (Table 1) allowed the production of ketocarotenoids, especially the target pigment astaxanthin in the maize seeds.

Other carotenoids found in these transgenic lines were lutein, zeaxanthin, β-cryptoxanthin, lycopene, β-carotene and phytoene reaching levels up to 2.86, 8.37, 2.95, 4.93, 11.89 and 10.38 μg/g, respectively (Tables 5 and 6), while the following carotenoids were only detected in certain lines: β-

zeacarotene (up to 3.69 μg/g) detected in the TM8; violaxanthin (up to 0.83 μg/g) detected in TM6D and TM8, unknown ketocarotenoids with RT between 5.0 and 5.25 min detected in TM6 and TM7 and another unknown carotenoid with RT at 5.47 min detected in TM5 and TM8.

4.5.1.2 Correlation between gene expression and carotenoid profiles

Only accumulation of *Zmpsy*1, *sCrBkt* and *sBrcrtZ* mRNA has been determined in certain lines. Thus, the correlation between gene expression and carotenoid profiles in maize endosperm constitutes simply an overview of the first set of experiments. At present, the group of Applied Plant Biotechnology is determining the transgene integration and expression characteristics of these lines, work that is being undertaken by Gemma Farré.

The combination of *Zmpsy*1, *sCrBkt* and *sBrcrtZ* in TM5, TM6 and TM7 generated orange–red phenotypes whereas the combination of *PacrtI* in addition to *Zmpsy*1, *sCrBkt,* and *sBrcrtZ* in TM8 produced a distinct orange–yellow color. Wild-types NSL26 and NSL76 exhibited white and yellow colors respectively (Fig. 4).

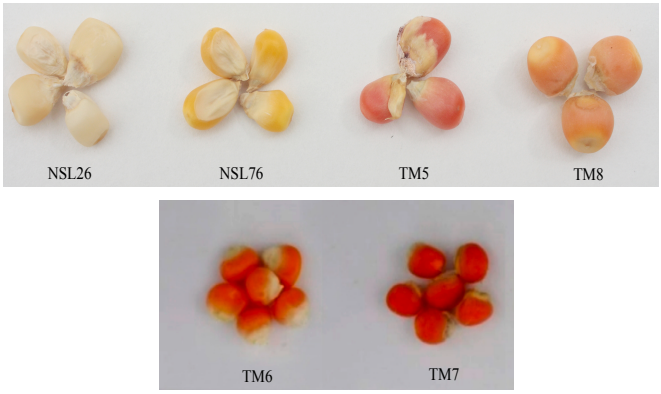

Figure 4-4. Endosperm colors of wild-types NSL26 and NSL76 and four different transgenic maize lines. TM5, expressing *Zmpsy*1, *sCrBkt* and *sBrcrtZ*; TM6 and TM7, is the cross of TM5 with two wild-type maize plants, NSL26 and NSL76 respectively, therefore, in both cases expressing *Zmpsy*1, *sCrBkt,* and *sBrcrtZ* and TM8, which is the cross of TM1 (expressing *Zmpsy1* and *Pacrt*I) with TM5, therefore, expressing *Zmpsy*1, *sCrBkt* and possibly *PacrtI* and *sBrcrtZ*.

All the transgenic lines showed a high variety of β-branch carotenoids (Tables 5 and 6) while lutein was the only ε-ring derivative detected. In addition, the lutein content of TM7 was reduced compared with its control, the wild-type NSL76. For example, lutein content in wild-type NSL76 was 10.92 μg/g whereas in TM7A, TM7B and TM7C it was 1.06, 1.28 and 0.67 μg/g, respectively. Thus, these results suggested diversion of lycopene towards β-branch carotenoid synthesis.

These transgenic lines were able to synthesize various ketocarotenoids, e.g., adonixanthin, adonirubin, canthaxanthin, echinenone and 3-hydroxyechinenone as well as astaxanthin. Total ketocarotenoid content in TM6A, TM6B, TM6C and TM6D was 12.95, 14.66, 19.77 and 17.95 μg/g corresponding to 61.77, 52.34, 56.23 and 62.14% of the total, respectively (Tables 5 and 6). In TM7A, TM7B and TM7C, total ketocarotenoid content was 29.26, 35.82 and 31.03 μg/g corresponding to 75.12, 73.66,

81.63% of the total, respectively (Tables 5 and 6). In TM8A and TM8B, total ketocarotenoid content was 20.13 and 22.25 μg/g corresponding to 36.20 and 31.73% of the total, respectively (Tables 5 and 6). Because several ketocarotenoid intermediates involved in the formation of astaxanthin were detected, these data demonstrated the activities of both β-carotene ketolase and hydroxylase. Therefore, it is thought that astaxanthin in maize endosperm might have been derived from both adonirubin and adonixanthin (Fig. 1). Similarly to our results, Jayaraj et al. 2008 [26] detected astaxanthin and several ketocarotenoid intermediates involved in the formation of astaxanthin including adonirubin, canthaxanthin, echinenone and adonixanthin by expressing an *H. pluvialis bkt* gene in carrot tissues. In addition, they demonstrated that heterologous expression of β-carotene hydroxylase was not required for ketocarotenoid synthesis due to the up-regulation of endogenous hydroxylases in transgenic leaves and roots.

Gene expression of *sBrcrtZ* was only determined in wild-type NSL26, TM6 and TM7 through mRNA blot analysis. The results demonstrated absence of *sBrcrtZ* transcript in wild-type NSL26 whereas in TM6 and TM7 the expression of *sBrcrtZ* (Fig. 5) was observed. Although the expression of this gene was not determined in TM5, its expression was assumed in this line due the fact that it is the parental of TM6 and TM7, which expressed this transgene.

No *sCrBkt* transcript was detected in wild-types NSL26 and NSL76 whereas in TM6, TM7 and TM8 the expression of this gene was observed. However, TM7 showed higher accumulation levels of *sCrBkt* mRNA than TM8 (Fig. 5). Although the expression of *sCrBkt* was not determined in TM5, its expression was assumed in this line due to the fact that it is the parental of TM6 and TM7. In addition, mRNA blot analysis revealed the absence of *Zmpsy*1 transcript in wild-type NSL26 while TM6, TM7 and TM8 showed high expression levels (Fig. 5).

In the first attempt to accumulate astaxanthin in maize endosperm [27]; the group of Applied Plant Biotechnology of UdL used as β-carotene ketolase the bacterial gene *Paracrt*W. However, despite the carotenoid pathway being extended, astaxanthin was not the main ketocarotenoid accumulated in the maize endosperm and only one transgenic plant (Ph-6) showed astaxanthin accumulation (4.46 μg/g DW) [27]. In addition, fewer ketocarotenoid intermediates were observed in the transgenic plants expressing the *Paracrt*W gene. Thus, as a result of using a different β-carotene ketolase –*sCrBkt*- and co-expressing it with a new combination of genes (e.g. *Zmpsy*1 and *sBrcrtZ*), the second attempt to accumulate astaxanthin in maize endosperm, which is discussed in this chapter, appeared to be more successful since astaxanthin was the main carotenoid accumulated in the TM5, TM6 and TM7 (up to 19 μg/g DW).

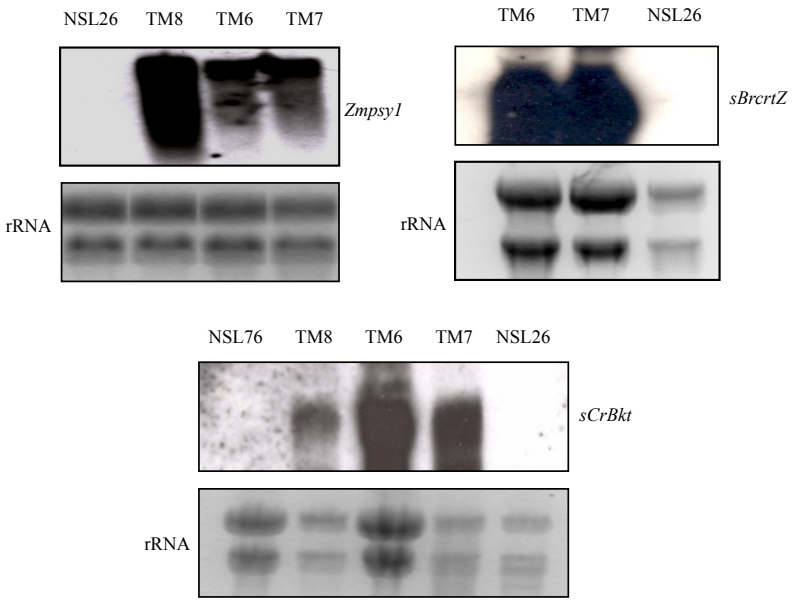

Figure 4-5. mRNA blot analysis to monitor transgene expression in wild-types NSL26 and NSL76 and transgenic maize TM6, TM7 and TM8 at 30 DAP.

4.5.2 Preliminary tests to identify carotenoids present in the transgenic maize lines

Although most of the carotenoids present in the different transgenic lines were identified, there were some pigments for which it was not possible to establish their identity. For example, in the TM6 and TM7, three carotenoids with RT between 5.0 and 5.25 min were not identified (Figs. 2 and 3). In order to find information that allowed the identification of these compounds, I determined their UV-vis and mass spectra. Fig. 6.A shows that these three pigments were not properly separated under the UHPLC chromatographic conditions (section 4.4.4.1), hence, I carried out modifications on this LC system (e.g. change gradient elution, flow, column temperature, etc.) in order to improve their resolution. Fig. 6.B shows the best separation obtained for these compounds and their UV-vis spectra. The carotenoid with RT at 2.81 min exhibited a λmax at 468 nm and a symmetrical spectrum shape. Therefore, these spectral characteristics indicated that this compound should be a ketocarotenoid (Chapter 1, section 1.2.3). Similarly, the spectral characteristics determined for the two unknown pigments coeluting at 3.01 min (Fig. 6.B) suggested that one or both of these pigments might be a ketocarotenoid.

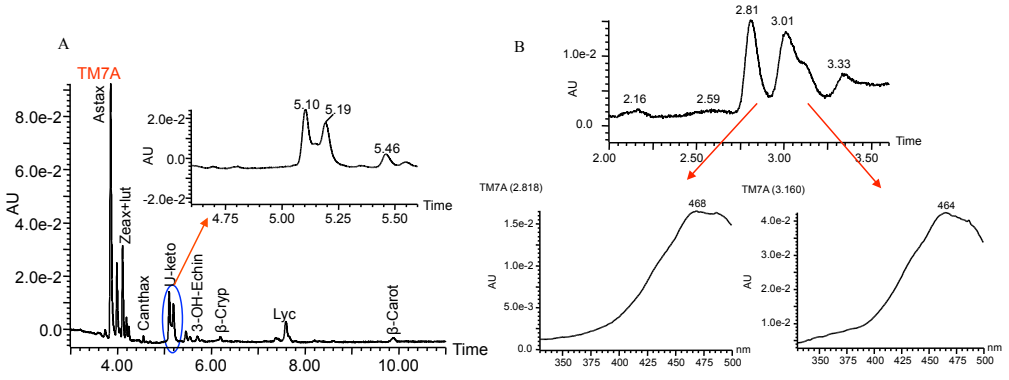

Figure 4-6. (A) Separation of the carotenoids present in the TM7A (cross between TM5 and NSL76, therefore, expressing *Zmpsy*1*, sCrBkt, sBrcrtZ*); (B) UV-vis spectra of the unknown carotenoids found in the TM7A. Right side, separation of the carotenoids achieved using an ACQUITY UPLC® C18 BEH 130Å, 1.7 μm, 2.1×100 mm (Waters, Milford, MA), mobile phase consisted of solvent A: MeOH 100% and solvent B: water 100%. Isocratic elution: 85% A and 15% B, flow: 0.35 mL/min and column temperature: 25 ºC.

In the positive ion APCI mass spectra determined for these molecules (see Supplementary data) ions at *m/z* 567-568 and 549 were observed. These fragment ions have already been observed for 3-hydroxyechinenone (chapter 2, section 2.5.2.1) and corresponded to its $[M+H]^+$ and $[M+H-H_2O]^+$, respectively. Thus, based on these preliminary results and the analysis of the metabolic pathway of the carotenoids, it was suggested that one of these compounds might be the 3'-hydroxyechinenone, which only differs from the 3-hydroxyechinenone in the position of one hydroxyl group. Fig. 7 illustrates the molecular structure of these carotenoids.

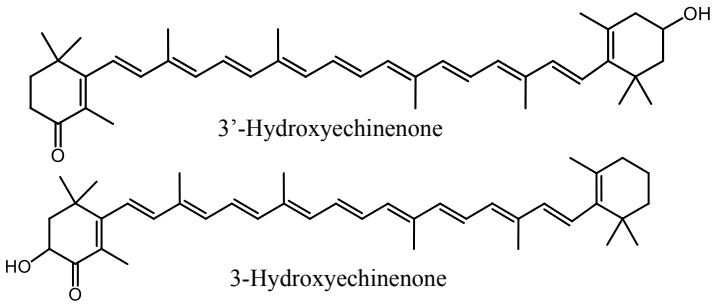

Figure 4-7. Molecular structures of 3- and 3'-hydroxyechinenone.

Finally, in the TM5 and TM8 another compound with RT at 5.46 min was not identified. This compound can be spotted in the chromatograms as "U-carot" (Figs. 2 and 3). Although its UV-vis and mass spectra were determined (Fig. 8), I was not able to suggest a possible candidate for this molecule since little information could be concluded from its mass spectrum. However, because its absorption appears between 400 and 500 nm, this unknown compound may be a carotenoid.

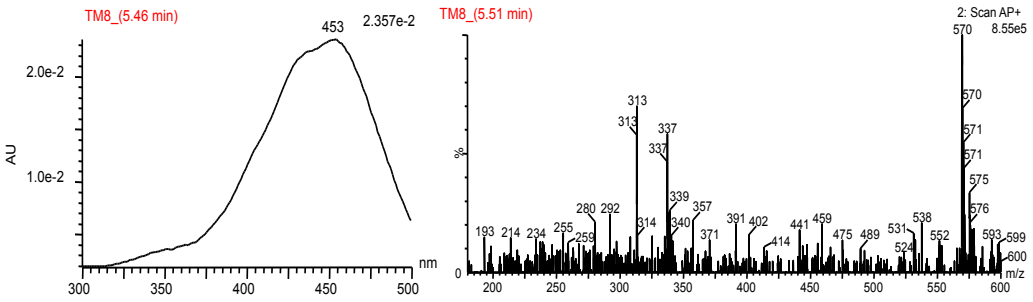

Figure 4-8. UV-vis and mass spectra of the unknown compound found in the TM8.

The results shown here are only preliminary tests and, therefore, the identity of these unknown pigments cannot be concluded with a high degree of confidence. To continue investigating into their identity, other tests need to be conducted, such as chemical reactions used to identify carotenoids [31], high resolution mass spectrometry or determination of their NMR spectra.

4.6 CONCLUSIONS

Astaxanthin showed the highest accumulation among the different carotenoids detected in the different transgenic lines (up to 19 μg/g DW). Thus, the production of the target pigment astaxanthin in the maize seeds was achieved by expressing *sCrBkt* in addition to *Zmpsy*1 and *sBrcrtZ* in TM5, TM6, TM7 and in addition to *Zmpsy*1 in TM8. Furthermore, the β, β-branch of the pathway showed to be favored since a high variety of β-branch carotenoids was detected.

New carotenoids have been found in the transgenic lines, the structure of one of them has been assigned to 3'-hydroxyechinenone. However, given that the UV–vis spectrum of many carotenoids is similar and a number of structurally related molecules coelute, it is important to complement the identification of carotenoids carrying out either chemical reactions on the analyte of interest to confirm the presence or absence of a given functional group or using other detection methods such as NMR spectroscopy or high resolution mass spectrometry.

4.7 REFERENCES

[1] Zhu C, Naqvi S, Capell T, Christou P (2009) Metabolic engineering of ketocarotenoid biosynthesis in higher plants. Archives of Biochemistry and Biophysics.483:182-90.

[2] Dhankhar J, Kadian SS, Sharma A (2012) ASTAXANTHIN: A POTENTIAL CAROTENOID. International Journal of Pharmaceutical Sciences and Research.3:1246-1259.

[3] Miki W (1991) Biological functions and activities of animal carotenoids. Pure Appl Chem.63:141-6.

[4] Zhong YJ, Huang JC, Liu J, Li Y, Jiang Y, Xu ZF, Sandmann G, Chen F (2011) Functional characterization of various algal carotenoid ketolases reveals that ketolating zeaxanthin efficiently is essential for high production of astaxanthin in transgenic Arabidopsis. Journal of Experimental Botany.62:3659-69.

[5] Guerin M, Huntley ME, Olaizola M (2003) Haematococcus astaxanthin: Applications for human health and nutrition. Trends in Biotechnology.21:210-6.

[6] Iwamoto T, Hosoda K, Hirano R, Kurata H, Matsumoto A, Miki W, Kamiyama M, Itakura H, Yamamoto S, Kondo K (2000) Inhibition of low-density lipoprotein oxidation by astaxanthin. Journal of atherosclerosis and thrombosis.7:216-22.

[7] Naito Y, Uchiyama K, Aoi W, Hasegawa G, Nakamura N, Yoshida N, Maoka T, Takahashi J, Yoshikawa T (2004) Prevention of diabetic nephropathy by treatment with astaxanthin in diabetic db/db mice. BioFactors.20:49-59.

[8] Tanaka T, Morishita Y, Suzui M, Kojima T, Okumura A, Mori H (1994) Chemoprevention of mouse urinary bladder carcinogenesis by the naturally occurring carotenoid astaxanthin. Carcinogenesis.15:15-9.

[9] Chew B, Park J, Wong M, Wong T (1999) A comparison of the anticancer activities of dietary beta-carotene, canthaxanthin and astaxanthin in mice in vivo. Anticancer research.19:1849.

[10] Chew BP, Park JS (2004) Carotenoid action on the immune response. The Journal of nutrition.134:257S-61S.

[11] Ahn MJ, Noh SA, Ha SH, Back K, Lee SW, Bae JM (2012) Production of ketocarotenoids in transgenic carrot plants with an enhanced level of β-carotene. Plant Biotechnology Reports.6:133-40.

[12] Hasunuma T, Miyazawa SI, Yoshimura S, Shinzaki Y, Tomizawa KI, Shindo K, Choi SK, Misawa N, Miyake C (2008) Biosynthesis of astaxanthin in tobacco leaves by transplastomic engineering. Plant Journal.55:857-68.

[13] Grewe C, Griehl C (2008) Time-and media-dependent secondary carotenoid accumulation in Haematococcus pluvialis. Biotechnology journal.3:1232-44.

[14] Margalith P (1999) Production of ketocarotenoids by microalgae. Applied Microbiology and Biotechnology.51:431-8.

[15] Johnson EA, An GH (1991) Astaxanthin from microbial sources. Critical Reviews in Biotechnology.11:297-326.

[16] Mann V, Harker M, Pecker I, Hirschberg J (2000) Metabolic engineering of astaxanthin production in tobacco flowers. Nature Biotechnology.18:888-92.

[17] Gerjets T, Sandmann G (2006) Ketocarotenoid formation in transgenic potato. Journal of Experimental Botany.57:3639-45.

[18] Cunningham Jr FX, Gantt E (2011) Elucidation of the pathway to astaxanthin in the flowers of Adonis aestivalis. Plant Cell.23:3055-69.

[19] Huang JC, Chen F, Sandmann G (2006) Stress-related differential expression of multiple β-carotene ketolase genes in the unicellular green alga *Haematococcus pluvialis*. Journal of Biotechnology.122:176-85.

[20] Lotan T, Hirschberg J (1995) Cloning and expression in *Escherichia coli* of the gene encoding [beta]-C-4-oxygenase, that converts [beta]-carotene to the ketocarotenoid canthaxanthin in *Haematococcus pluvialis*. FEBS Letters.364:125-8.

[21] Kajiwara S, Kakizono T, Saito T, Kondo K, Ohtani T, Nishio N, Nagal S, Misawa N (1995) Isolation and functional identification of a novel cDNA for astaxanthin biosynthesis from *Haematococcus pluvialis*, and astaxanthin synthesis in Escherichia coli. Plant Molecular Biology.29:343-52.

[22] Misawa N, Shimada H (1998) Metabolic engineering for the production of carotenoids in non-carotenogenic bacteria and yeasts. Journal of Biotechnology.59:169-81.

[23] Visser H, Ooyen AJJ, Verdoes JC (2003) Metabolic engineering of the astaxanthin-biosynthetic pathway of Xanthophyllomyces dendrorhous. FEMS yeast research.4:221-31.

[24] Ralley L, Enfissi EMA, Misawa N, Schuch W, Bramley PM, Fraser PD (2004) Metabolic engineering of ketocarotenoid formation in higher plants. Plant Journal.39:477-86.

[25] Morris WL, Ducreux LJM, Fraser PD, Millam S, Taylor MA (2006) Engineering ketocarotenoid biosynthesis in potato tubers. Metabolic Engineering.8:253-63.

[26] Jayaraj J, Devlin R, Punja Z (2008) Metabolic engineering of novel ketocarotenoid production in carrot plants. Transgenic research.17:489-501.

[27] Zhu C, Naqvi S, Breitenbach J, Sandmann G, Christou P, Capell T (2008) Combinatorial genetic transformation generates a library of metabolic phenotypes for the carotenoid pathway in maize. Proceedings of the National Academy of Sciences of the United States of America.105:18232-7.

[28] Zhu C, Bai C, Sanahuja G, Yuan D, Farré G, Naqvi S, Shi L, Capell T, Christou P (2010) The regulation of carotenoid pigmentation in flowers. Archives of Biochemistry and Biophysics.504:132-41.

[29] Britton G, Liaaen-Jensen S, Pfander H (2004) Carotenoids handbook: 1st ed; Birkhäuser: Basel, Switzerland. pp. 3-404.

[30] Rivera S, Vilaró F, Canela R (2011) Determination of carotenoids by liquid chromatography/mass spectrometry: Effect of several dopants. Analytical and Bioanalytical Chemistry.400:1339-46.

[31] Rivera SM, Canela-Garayoa R (2012) Analytical tools for the analysis of carotenoids in diverse materials. Journal of Chromatography A.1224:1-10.

Chapter 5

Exploring relationships between gene expression and carotenoid accumulation in rice callus

5.1 ABSTRACT

In order to produce nutritionally relevant carotenoids such as β-carotene, it is necessary to introduce many candidate genes for carotenoid biosynthesis into plants and evaluate which genes play important roles in the production of target carotenoids. However, plant genetic transformation is very time consuming and labor. Use of callus derived from rice endosperm may be a feasible approach to reduce the time and effort required for analyzing gene function. Thus callus cells might serve as a tool to analyze the relationship between the metabolism of a number of phytochemicals and the expression of the corresponding genes encoding the necessary enzymes for their biosynthesis. In order to investigate carotenoid accumulation mechanisms and enhance the carotenoid content of rice endosperm, the group of Applied Plant Biotechnology of the UdL genetically engineered rice with multiple carotenogenic genes and a particular developmental gene affecting carotenoid accumulation in planta using combinatorial nuclear transformation. A diverse population of transgenic rice calli was recovered which expressed combinations of different input transgenes. I pursued the identification of the accumulated carotenoids and I participated in efforts to explore relationships between gene expression and the accumulation of metabolites in the different transgenic rice cell lines. I also performed preliminary experiments to identify a new carotenoid found in the transgenic rice callus.

5.2 INTRODUCTION

Carotenoids play fundamental roles in human nutrition, functioning as antioxidants and vitamin A precursors. The mechanisms that control carotenoid accumulation in plants are complex and only partly understood. Carotenoid levels in plant tissues and organs do not appear to depend solely on carotenogenic enzyme activities. The amount of β-carotene (pro-vitamin A) produced by plants can be enhanced by increasing the availability of carotenoid precursors, by expressing enzymes in the common part of the pathway (between GGPP and lycopene), by biasing the pathway towards the β-branch through the expression of LYCB at the expense of LYCE, or by increasing the storage capacity for carotenoids [1].

The first approach has been successful in producing plants that synthesize high levels of GGPP, but because this is used in several pathways not all of the flux is directed towards carotenoid synthesis. For example, the overexpression of DXP synthase in tomato and potato increased the total carotenoid content by up to 1.6-fold compared to wild type, but the levels of tocopherols and plastoquinones were also affected [2].

In plants, carotenoids are synthesized in the plastids via the methylerythritol-4-phosphate (MEP) pathway, also known as the non-MVA pathway. Initially, pyruvate and D-glyceraldehyde-3-phosphate are converted into 1-deoxy-D-xylulose-5-phosphate (DXP) by DXP synthase (DXS), and DXP is then converted into the isomeric C5 precursors isopentenyl diphosphate (IPP) and dimethylallyl pyrophosphate (DMAPP) [4]. Three molecules of IPP condense with one molecule of DMAPP to form the C20 precursor geranylgeranyl diphosphate (GGPP), which is used for the synthesis of carotenoids, tocopherols, chlorophylls, plastoquinones and gibberellins [5]. The first committed reaction in carotenoid biosynthesis is the conversion of GGPP to phytoene by phytoene synthase (PSY) (Fig.1). A complete and detailed description of the synthesis of carotenoids from phytoene can be found in chapter 3, section 3.2.

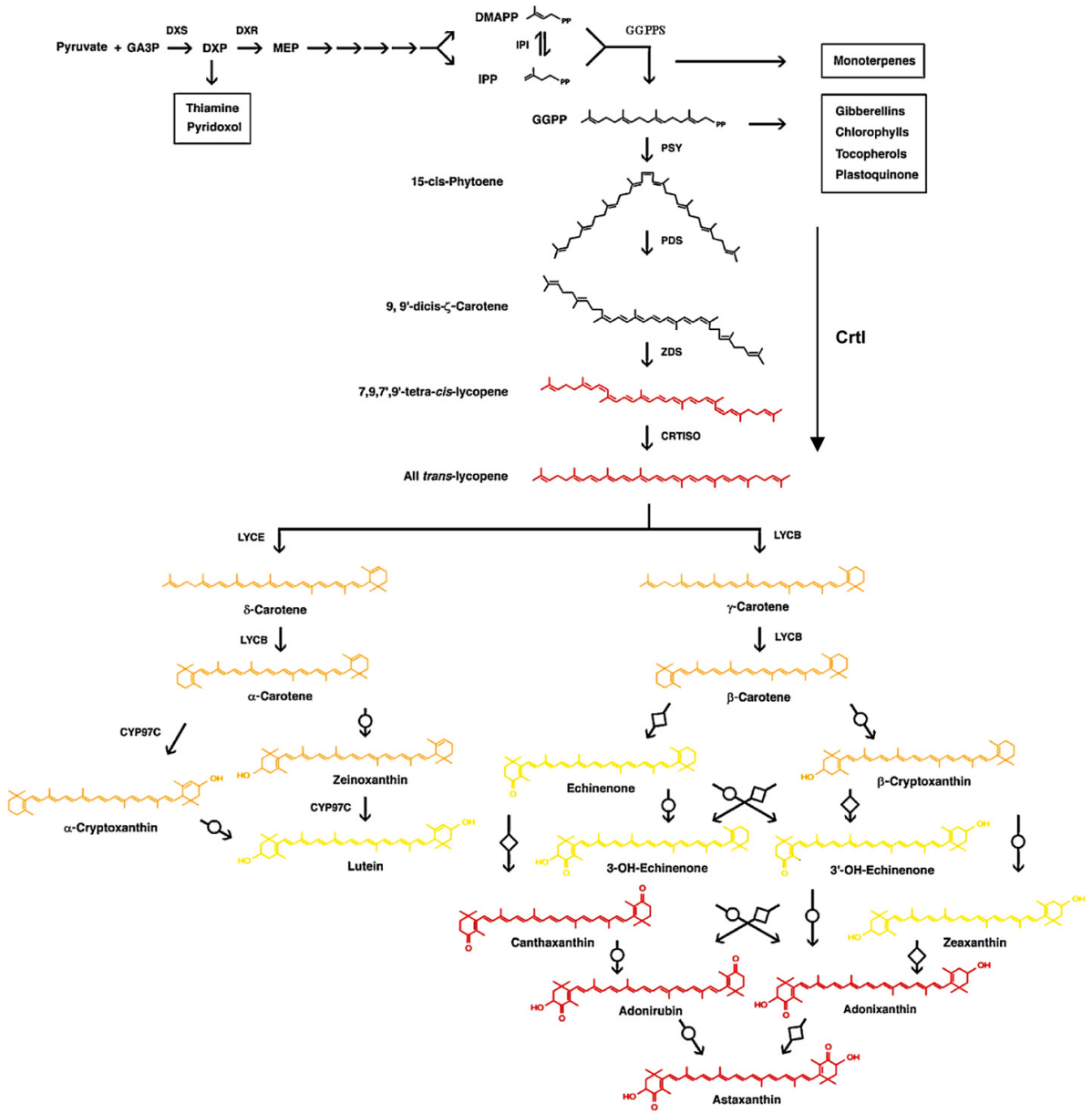

Figure 5-1. The extended carotenoid biosynthetic pathway in plants. The precursor for the first committed step in the pathway is GGPP (geranylgeranyl pyrophosphate), which is converted into phytoene by phytoene synthase (PSY). GGPP is formed by the condensation of IPP (isopentenyl pyrophosphate) and DMAPP (dimethylallyl pyrophosphate) which are derived predominantly from the plastidial MEP (methylerythritol 4-phosphate) pathway as depicted in the upper part of the figure. The pathway is linear until between phytoene and lycopene, and there are three steps that are catalyzed by separate enzymes in plants but by the single, multifunctional enzyme *CrtI* in bacteria. Lycopene is the branch point for the α- and β-carotene pathways, which usually end at lutein and zeaxanthin, respectively, through the expression of β-carotene hydroxylases (arrows with circles). An elaborated ketocarotenoid pathway can be introduced by expressing β-carotene ketolases (arrows with diamonds) since these compete for substrates with β-carotene hydroxylases and generate diverse products. Other abbreviations: GA3P, glyceraldehyde 3-phosphate; DXP, 1-deoxy-D-xylulose 5-phosphate; DXS, DXP synthase; DXR, DXP reductoisomerase; IPI, IPP isomerase; GGPS, GGPP synthase; PDS, phytoene desaturase; ZDS, ζ-carotene desaturase; CRTISO, carotenoid isomerase; CrtI, phytoene desaturase; LYCB, lycopene β-cyclase; LYCE, lycopene ε-cyclase; HydE, carotene ε-hydroxylase [3].

The expression of enzymes in the committed part of carotenoid pathway is a more targeted approach, and is particularly necessary in cereal grains where the pathway is blocked at the first committed step. In rice endosperm, for example, the carotenoid pathway terminates at GGPP because there is very limited PSY activity. The 'Golden Rice' project was the first significant application of carotenoid engineering and was envisaged as a humanitarian mission to alleviate vitamin A deficiency, which results in millions of cases of preventable blindness every year in developing countries [3, 6]. Large numbers of people subsist on monotonous diets of milled rice grains which contain little vitamin A, so a research project was conceived to introduce a partial carotenoid biosynthesis pathway into rice endosperm allowing the grains to accumulate *β*-carotene. Genetic engineering was the only way that Golden Rice (GR) could be produced because no carotenoid-producing rice germplasm is known to exist [7]. GR contains heterologous phytoene synthase (*psy*) and phytoene desaturase (*crtI*) genes and has an endosperm carotenoid content of 1.6 μg/g DW, showing that these two genes alone provide significant enhancement [7]. GR was originally produced by transformation of the Japonica variety Taipei 309 [7], and the technology was subsequently shown to be functional in different cultivars of rice that are relevant in Asia [8, 9]. All these lines contained the same transgenes as the original GR (daffodil *psy* and bacterial *crt*I) and the carotenoid levels were similar [7, 8, 10, 11]. The product of the two carotenoid biosynthesis transgenes used in GR is lycopene (Fig. 1), which is red in color. However, the endosperm of GR is yellow due to the accumulation of *β*-carotene and xanthophylls. The absence of lycopene in GR demonstrated that the pathway continued beyond the transgenic end point and thus the endogenous pathway downstream of lycopene must be present in rice endosperm. By using qRT-PCR, Schaub et al. 2005 [12] showed in wild type rice endosperm the mRNA expression of the relevant carotenoid biosynthetic enzymes encoding PDS, ZDS, CRTISO, LYCB and BCH; only *psy* mRNA was virtually absent. Syngenta scientists focused on optimizing the expression of *psy* [13]. Through systematic testing of PSY enzymes from different plants such as daffodil (used in all previous versions of GR), carrot, tomato, rice and maize, *psy* from maize was found to give the best results in a maize callus model. The endosperm of Golden Rice 2 (GR2) accumulated up to 37 μg/g carotenoids (a 23-fold increase compared to GR) with *β*-carotene representing ~84% of the total [13]. In these experiments, no phytoene was detected in the transgenic plants indicating that *crtI* was able to complete the desaturation of all phytoene produced. These results indicated that the source of the *psy* transgene is essential in the generation of high levels of *β*-carotene content. *crtI* was also regarded as a rate limiting enzyme in GR because it was barely detectable in the endosperm [14]. The low protein levels may reflect weak transcription from the CaMV35S promoter or suboptimal codon usage. The amount of CRTI protein was increased by expressing a synthetic *crt*I gene, codon optimized to match rice storage proteins. The gene was expressed under the control of the endosperm-specific glutelin B1 promoter. Transgenic plants expressing the unmodified *crtI* gene using the endosperm-specific glutelin B1 promoter were also generated. The endosperm-specific promoter made a significant difference to *crtI* levels in T1 rice endosperm even in the absence of codon

optimization, but this did not lead to a significant increase in the carotenoid content. The conclusion was that *crtI* is not rate limiting in rice endosperm after all, even at very low levels [14].

An alternative strategy to achieve *β*-carotene accumulation in plants is to modify the storage capacity of chromoplasts, where *β*-carotene accumulates in specialized lipoprotein-sequestering structures. A spontaneous mutation in the cauliflower *Orange* (*Or*) gene resulted in deep orange cauliflower heads associated with the hyperaccumulation of carotenoids in chromoplasts [15, 16] and the mutant allele has been cloned and expressed in potato tubers, where it increased the level of *β*-carotene 10-fold and turned the tuber flesh orange [17].

5.3 OBJECTIVES

- To describe the carotenoid profile of transgenic rice callus expressing different carotenogenic gene combinations and exhibiting distinct metabolic phenotypes.
- To use the metabolite profile of carotenoids to investigate the specific contribution(s) of carotenogenic genes in the carotenoid pathway considering mRNA levels.
- To perform preliminary experiments to identify a new carotenoid found in the transgenic rice callus.

5.4 MATERIALS AND METHODS

5.4.1 Chemicals

β-Carotene, lutein, astaxanthin, were purchased from Sigma-Aldrich Fine Chemicals (St. Louis, MO, USA). Canthaxanthin and zeaxanthin were acquired from Fluka (Buchs SG, Switzerland). Phytoene, violaxanthin, and antheraxanthin were purchased from Carotenature (Lupsingen, Switzerland). MeOH, ethyl acetate, ethyl eter, TBME, ACN and acetone (HPLC grade purity) were acquired from J.T. Baker (Deventer, The Netherlands). Water was prepared using a Milli-Q reagent water system.

5.4.2 Plant material

The transgenic rice callus were generated by combinatorial nuclear transformation as reported in Zhu et al. [18]. The following TC were used for this study: a TC1, expressing *Zea mays* phytoene synthase 1 (*Zmpsy1)* and *Pantoea ananatis* phytoene desaturase (*PacrtI*); TC2, expressing *Zmpsy*1, *Pacrtl* and Orange gene from *Arabidopsis thaliana* (*AtOr*); TC3, expressing *Zmpsy*1, *Pacrtl* and 1-deoxy-D-xylulosa 5-phosphate synthase from *Arabidopsis thaliana* (*Atdxs*); TC4, expressing *Zmpsy*1, *Pacrtl* and *β*-carotene ketolase from *Brevundimonas* sp. Strain SD212 chemically synthesized (s*BrcrtW*) and TC5, expressing *Zmpsy*1, *Pacrtl* and biochemically synthesized *sCrBkt* from *Chlamydomonas reinhardtii.* Table 1 summarizes the genes expressed in the different transgenic rice callus.

Table 5-1. Transgenic lines used for this study.

Line	Expressed genes
TC1	*Zmpsy1*, *Pacrt*I
TC2	*Zmpsy1, Pacrt*I, *AtOr*
TC3	*Zmpsy1, Pacrt*I, *Atdxs*
TC4A	*Zmpsy1, Pacrt*I, s*BrcrtW*
TC4B	*Zmpsy1, Pacrt*I, s*BrcrtW*
TC5	*Zmpsy1, Pacrt*I, *sCrBkt*

5.4.3 Extraction of carotenoids

To protect carotenoids from degradation and oxidation, the extraction was conducted under limited light. Samples were freeze-dried and ground into a fine powder using a mortar and pestle. 10 or 20[6] mg of sample was extracted with 15 mL of MeOH: ethyl acetate (6:4, v/v) at 60 °C for 20 min and this mixture was continuously shaken. It was then put on ice until it reached room temperature and the liquid phase was filtered into a separatory funnel (if the residue exhibited color after extraction, then it was re-extracted with 5 mL of MeOH: ethyl acetate (6:4, v/v) at 60 °C for 5 min and the second extract was combined with the first one). 15 mL of hexane: diethyl ether (9:1, v/v) was added to the organic extract and the mixture was shaken vigorously. Then, 20 mL of saturated sodium chloride solution was added and again the mixture was shaken. The aqueous phase was removed and the organic phase was washed with water once again. The organic phase was dried under N_2 at 37 ºC. When the sample was completely dry, Ar was flushed into the vial and carotenoids were stored at -80 ºC until LC analysis. Each extraction was carried out in duplicate.

5.4.4 Chromatographic analysis

Chromatographic systems used to analyze the transgenic lines were the same employed in chapter 2, section 2.4.6.

5.4.4.1 UHPLC-PDA-MS analysis

UHPLC analysis was carried out using an ACQUITY Ultra Performance LC™ system linked to a PDA 2996 detector (Waters, Milford, MA, USA). Mass detection was carried out using an Acquity™ TQD tandem-quadrupole MS equipped with a Z-spray electrospray interface (Manchester, UK). MassLynx™ software version 4.1 (Waters, Milford, MA, USA) was used to control the instruments, and also for data acquisition and processing.

UHPLC chromatographic separations were performed on reversed-phase column ACQUITY UPLC® C18 BEH 130Å, 1.7 μm, 2.1×100 mm (Waters, Milford, MA). Mobile phase consisted of solvent A: ACN: MeOH 7:3, v/v and solvent B: water 100%. The gradient program used is shown in Table 2.

[6] For pale color maize samples, extract 20 mg of sample. For darker color maize samples, it is sufficient to extract 10 mg of sample.

The column and sample temperatures were set at 32 °C and 25 °C respectively. Injection volume was 5 μL. Each sample extract for LC analysis was dissolved in 300 μL and 600 μL (for light and dark color extracts respectively) of the injection solvent [ACN: MeOH 7:3, v/v]: acetone 6.7:3.3, v/v. Before use, all solutions were filtered through Millex 0.2 μm nylon membrane syringe filters (Millipore, Bedford, MA, USA).

Table 5-2. Gradient profile used in the separation of carotenoids by UHPLC. Linear gradient.

Time[a] (min)	Flow rate (mL/min)	A (%, v/v)	B (%, v/v)
Initial	0.4	80	20
2.0	0.4	80	20
3.0	0.4	100	0
7.0	0.4	100	0
8.0	0.6	100	0
11.6	0.6	100	0
12.6	0.4	80	20

[a] After this time, the system was left 2 min more to reach its re-equilibration before injecting a new sample.

5.4.4.2 MS conditions

Optimized MS conditions are listed in Table 3.

Table 5-3. MS conditions

MS conditions	APCI
Polarity	Positive
Corona (kV)	4.0
Cone (V)	30
Extractor (V)	3
RF (V)	0.1
Source Temperature (°C)	150
Probe Temperature (°C)	450
Cone Gas Flow (L/h)	10
Desolvation Gas Flow (L/h)	150
Collision Gas Flow (mL/min)	0.15

5.4.4.3 HPLC-PDA analysis

HPLC analysis separations was carried out using a Waters Alliance 2695 separation module linked to a PDA 2998 detector (Waters, Milford, MA, USA). Empower software (Waters, Milford, MA, USA) was used to control the instruments, and also for data acquisition and processing.

HPLC chromatographic separations were performed on a YMC C30 carotenoid 3 μm, 2.0×100 mm column (Waters, Milford, MA). Mobile phase consisted of solvent A: MeOH: water 8:2, v/v and solvent B: TBME 100%. The gradient program used is shown in Table 4. Both, the column and the sample temperatures were set at 25 °C. Injection volume was 10 μL.

Table 5-4. Gradient profile used in the separation of carotenoids by HPLC. Linear gradient.

Time[a] (min)	Flow rate (mL/min)	A (%, v/v)	B (%, v/v)
Initial	0.25	97	3
6.0	0.25	97	3
7.0	0.25	62	38
15.0	0.25	62	38
16.0	0.25	32	68
18.0	0.25	32	68
19.0	0.25	0	100
25.0	0.25	0	100
26.0	0.25	32	68
27.0	0.25	50	50
28.0	0.25	70	30
29.0	0.25	97	3

[a] After this time, the system was left 6 min more to reach its re-equilibration before injecting a new sample.

5.4.4.4 Carotenoid identification and quantification

Identification of carotenoids was carried out by analysis and comparison of the following parameters: chromatographic retention time, UV-vis spectra, %III/II [19] and mass fragments with literature data [20] and with that of the authentic standards. Those standards were also used for quantitation.

5.5 RESULTS AND DISCUSSION

5.5.1 Exploring the mechanism of carotenoid accumulation in rice callus through multi-gene engineering

The following data presented in the study constitutes simply an overview of the correlation between gene expression and carotenoid profiles in rice callus. A more detailed study about this correlation is being undertaken by Chao Bai.

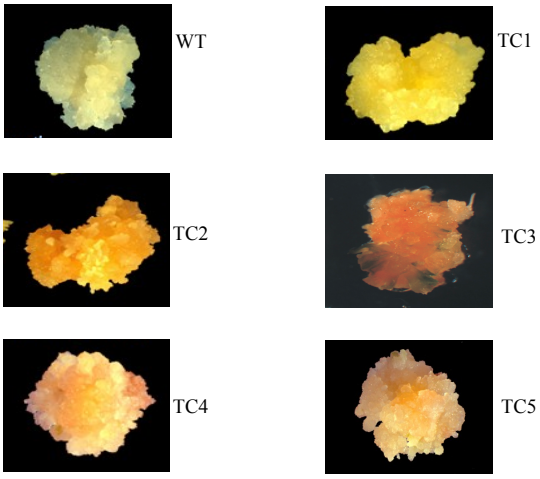

Figure 5-2. Colors of 6 different transgenic rice calli. WT, wild-type; TC1, expressing *Zmpsy1*, *Pacrt*I; TC2, expressing *Zmpsy1, Pacrt*I, *AtOr*; TC3, expressing *Zmpsy1, Pacrt*I, *Atdxs;* TC4, expressing *Zmpsy1, Pacrt*I, *BdcrtW* and TC5, expressing *Zmpsy1, Pacrt*I, *sCrBkt*.

5.5.1.1 Overexpression of Zmpsy1, PacrtI and Arabidopsis dxs in rice endosperm

The combination of *Zmpsy*1 and *Pacrt*I in TC1 generated a yellow phenotype, whereas the combination of *Zmpsy1, Pacrt*I, *Atdxs* in TC3 produced an orange phenotype. Wild-type callus exhibited a pale yellow color (Fig. 2). Figs. 4 and 5 show the chromatograms obtained for the wild-type callus, TC1 and TC3. Wild-type callus showed a low total carotenoid content (8.87 μg/g DW) comprising violaxanthin (3.89 μg/g), antheraxanthin (1.00 μg/g), lutein (3.46 μg/g) and zeaxanthin (0.52 μg/g) (Table 5). On the other hand, TC1 and TC3 showed a higher total carotenoid content (72.38 and 489.37 μg/g DW, respectively). TC1 contained violaxanthin (4.54 μg/g), antheraxanthin (1.38 μg/g), zeaxanthin (1.46 μg/g), lutein (4.46 μg/g), α-carotene (13.98 μg/g), β-Carotene (40.62 μg/g) and phytoene (5.94 μg/g), while TC3 contained violaxanthin (17.51 μg/g), lutein (13.13 μg/g), α-carotene (72.94 μg/g), β-Carotene (354.59 μg/g) and phytoene (31.21 μg/g) (Table 5).

mRNA blot analysis revealed the absence of *Zmpsy*1 and *PacrtI* transcripts in wild-type callus while TC1 and TC3 showed expression levels (Fig. 3). The *Zmpsy*1 mRNAs were similar in TC1 and TC3 while the *PacrtI* mRNAs were most abundant in TC3. Only TC3 demonstrated a presence of *Atdxs* transcript.

In wild-type rice, immature endosperm synthesizes geranylgeranly diphosphate (GGPP), the immediate precursor for carotenoid biosynthesis [21]. The ability of PSY expression alone to produce phytoene but not desaturated products [21] indicates that at least PDS activity is missing. Similarly, the expression of bacterial *crtI* (which can replace plant PDS, ZISO, ZDS and CRTISO) alone did not produce rice with colored endosperm due to the lack of PSY activity [12]. Therefore, carotenoid accumulation in GR and GR2 required both *psy* and *crt*I transgenes [7, 13]. The bacterial *crtI* is not rate-limiting in rice endosperm [13, 14]. Paine et al. 2005 [13] proposed that the daffodil *psy* gene used in GR was therefore the limiting step in carotenoid accumulation. The maize PSY was identified to be the best replacement after comparing the maize, pepper, tomato, rice and daffodil enzymes [13]. The maize *psy* gene was therefore used to develop GR2.

It has been shown that carotenoid levels in plant tissues and organs do not depend solely on carotenogenic enzyme activities, as pathways leading to the upstream precursors IPP and GGPP may also play a role [2]. No phytoene was detected in GR or GR2 [7, 13] so here it is proposed that the supply of GGPP could be another rate-limiting step in GR2. Therefore, to test the effects of Arabidopsis *dxs* overexpression on carotenoid accumulation in rice endosperm, the group of Applied Plant Biotechnology of the UdL genetically engineered rice with *Zmpsy*1, *Pacrt*I and Arabidopsis *dxs* genes.

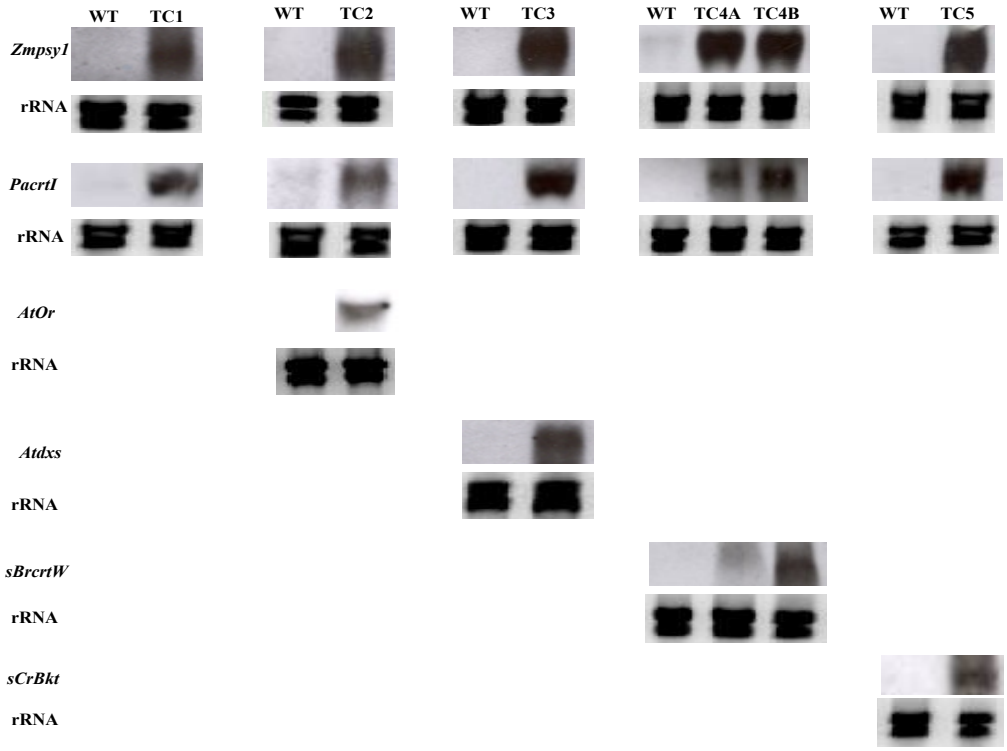

Figure 5-3. mRNA blot analysis to monitor transgene expression in wild-type callus, TC1, expressing *Zmpsy1*, *Pacrt*I; TC2, expressing *Zmpsy1, Pacrt*I, *AtOr*; TC3, expressing *Zmpsy1, Pacrt*I, *Atdxs;* TC4, expressing *Zmpsy1, Pacrt*I, s*BrcrtW* and TC5, expressing *Zmpsy1, Pacrt*I, *sCrBkt*.

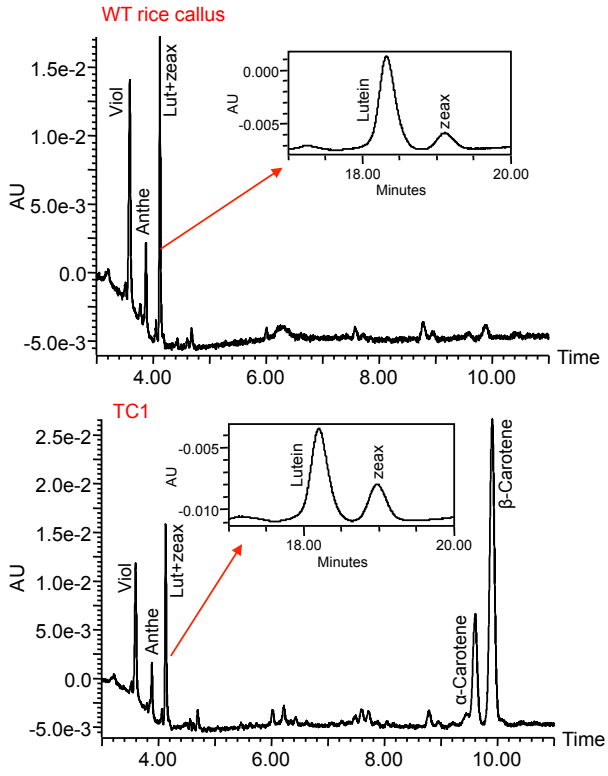

Figure 5-4. Carotenoid profile in wild-type callus and TC1 (expressing *Zmpsy1* and *Pacrt*I). Abbreviations: Viol, violaxanthin; Anthe, antheraxanthin; Zeax, zeaxanthin and Lut, lutein.

5.5.1.2 Overexpression of Zmpsy1 and PacrtI and Arabidopsis Or in rice endosperm

The orange callus TC2 (Fig. 2) contained 331.49 μg total carotenoids per gram DW comprising 242.42 μg/g of β-carotene, 16.27 μg/g of phytoene, 57.06 μg/g of α-carotene, 7.10 μg/g of lutein, 2.09 μg/g of zeaxanthin and 6.56 μg/g of violaxanthin (Table. 5). mRNA blot analysis confirmed that the TC2 expressed all three transgenes *Atdxs*, *Zmpsy1* and *AtOr* (Fig.3).

All tissues that accumulate high levels of carotenoids have a mechanism for carotenoid sequestration such as crystallization, oil deposition, membrane proliferation or protein-lipid sequestration [22]. The recent identification and characterization of a novel gene mutation in cauliflower (*Or*), which induces the differentiation of proplastids and/or non-colored plastids into chromoplasts that actively accumulate carotenoids revealed that the creation of a metabolic sink to sequester carotenoids could be used to enhance their accumulation in plants [23]. The non-carotenogenic starchy rice endosperm has a very low lipid content and apparently lacks any such means for carotenoid deposition. This may limit carotenoid accumulation in GR and GR2 regardless of increased flux provided by metabolic transgenes [13, 24]. Consequently, in order to investigate the effects of *AtOr* on carotenoid accumulation in rice endosperm, the group of Applied Plant Biotechnology of the UdL genetically engineered rice with *Zmpsy*1, *Pacrt*I and *AtOr* genes.

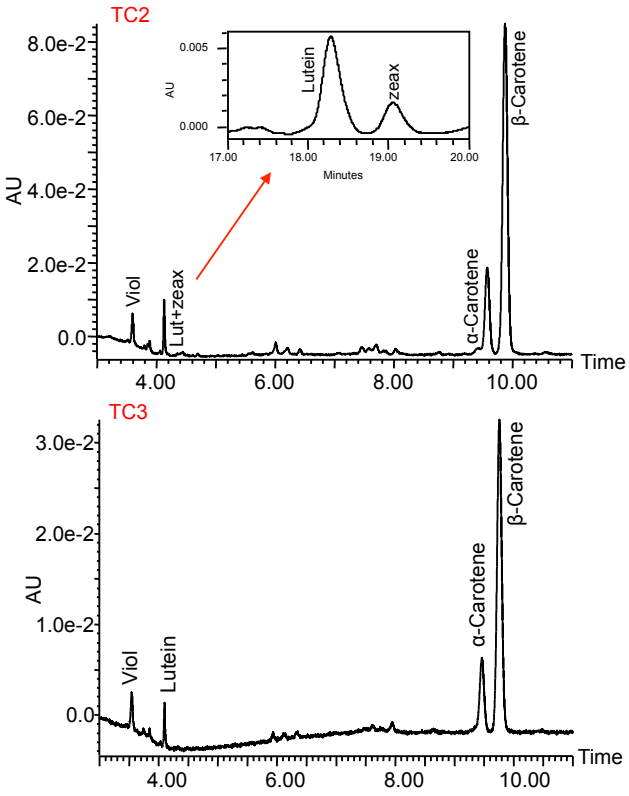

Figure 5-5. Carotenoid profile in TC2 (expressing *Zmpsy1*, *Pacrt*I and *AtOr*) and TC3 (expressing *Zmpsy1*, *Pacrt*I and *Atdxs*). Abbreviations: Viol, violaxanthin; Anthe, antheraxanthin; Zeax, zeaxanthin and Lut, lutein.

5.5.1.3 Understanding β-carotene accumulation by comparing different combinations of genes through the rice callus system

The amount and the percentage of *β*-carotene obtained in TC1 (40.62 *μ*g/g and 56%, respectively), TC2 (242.42 *μ*g/g and 73%, respectively) and TC3 (354.59 *μ*g/g and 72%, respectively) demonstrated that the combination of *Zmpsy1* and *Pacrt*I alone (TC1) or in combination with either *AtOr* (TC2) or *Atdxs* (TC3) led mainly to the accumulation of *β*-carotene. In addition, these results indicated that a higher *β*-carotene accumulation can be achieved by increasing the availability of carotenoid precursors or by increasing the storage capacity for carotenoids. Thus, when expressing *AtOr* in order to increase the storage capacity for carotenoids in TC2, *β*-carotene levels increased 6-fold compared with TC1 (expressing only *Zmpsy1* and *Pacrt*I). Similarly, when carotenoid precursors were increased by expressing *Atdxs* in TC3 (in addition to the carotenogenic genes *Zmpsy1* and *Pacrt*I), *β*-carotene increased 8.7-fold compared with TC1.

Because no accumulation of lycopene was observed in these transgenic rice callus, these results indicated that both *Zmpsy1* and *Pacrt*I were able to complete the biosynthesis of *β*-carotene as well as the formation of further downstream xanthophylls without the need to introduce *lcyb*. At present, the group of Applied Plant Biotechnology of the UdL is determining the endogenous gene expression of the transgenic rice callus described in this study in order to complement the elucidation of the key biosynthetic steps in the carotenoid pathway.

The ratio of *β*- to *ε*-ring derivatives was 1.56 in wild-type callus, 2.6 in TC1 (*Zmpsy1+PacrtI*), 3.91 in TC2 (*Zmpsy1+PacrtI+AtOr*), and 4.32 in TC3 (*Zmpsy1+PacrtI+Atdxs*). Thus, the *β*, *β*-branch of the pathway appears to be favored, perhaps implying the existence of a rate-limiting step in the *β*, *ε*-branch.

5.5.1.4 Transgenic rice callus producing ketocarotenoids

Ketocarotenoids such as astaxanthin have attracted great interest because they have remarkable singlet oxygen-quenching activity and have been associated with a range of health benefits [1]. Therefore, the group of Applied Plant Biotechnology of the UdL investigated the impact of expressing *sCrBkt* and s*Brcrt*W on the accumulation of astaxanthin. Three lines: TC4A, TC4B and TC5 showed *β*-carotene ketolase gene expression (Fig. 3). Because TC4A and 4B exhibited the same combination of genes but in a different level (Fig. 3), they were distinguished by the use of letters of the alphabet in their names.

The highest total carotenoid content was obtained in TC5 followed by TC4B and TC4A (346.69, 109.54 and 30.75±2.12 *μ*g/g DW, respectively). The amount and percentage of ketocarotenoids obtained in TC4A, TC4B and TC5 was 17.54 *μ*g/g and 57.03%, 76.1 *μ*g/g and 69.47% and 16.09 *μ*g/g and 4.64%, respectively. Ketocarotenoids such as astaxanthin, adonixanthin, adonirubin and canthaxanthin were detected (Table 5) in these lines, reaching levels up to 22.01, 9.14, 16.41 and 19.04 *μ*g/g, respectively. In addition, 3-hydroxyechinenone (4.58 *μ*g/g) and echinenone (4.92 *μ*g/g)

were detected in TC4B (Table 5). It should be noted that the main ketocarotenoid accumulated in these lines was astaxanthin whose concentration was 6.64, 22.01 and 6.15 μg/g in TC4A, TC4B and TC5, respectively.

Violaxanthin, α-carotene, β-carotene and phytoene were also detected in these transgenic rice calli (Table 5). However, the presence or absence of lutein and zeaxanthin could not be determined due to the fact that they were coeluting with an unknown compound, possibly a ketocarotenoid (Fig. 6) whose UV-vis spectrum always predominated. Neither UHPLC nor HPLC systems allowed the separation of these pigments. Table 5 shows the individual and total carotenoid content obtained for each transgenic line.

Astaxanthin is synthesized from β-carotene by the introduction of keto and hydroxyl moieties at the 4,4' and 3,3' positions of the β-ionone ring. These reactions are catalyzed by β-carotene ketolase (4,4'-oxygenase; CRTW, BKT or CRTO) and β-carotene hydroxylase (3,3'-oxygenase; BCH or CRTZ), respectively [1, 25] (Fig. 1). mRNA blot analysis revealed the absence of s*Brcrt*W and *sCrBkt* transcript in wild-type callus while TC4 and TC5 showed expression levels of s*Brcrt*W and *sCrBkt*, respectively (Fig. 3). The accumulation level of s*BrcrtW* mRNA was more abundant in TC4B than TC4A, which was correlated with the higher ketocarotenoids content found in TC4B than in TC4A (Table 5). In addition, mRNA blot analysis confirmed that the TC4 and TC5 co-expressed the transgenes *Zmpsy1* and *Pacrt*I (Fig.3). These lines appeared pink in comparison to the wild-type callus (Fig. 2). As discussed in section 5.4.1.3, the combination of *Zmpsy1* and *Pacrt*I led to the accumulation mainly of β-carotene. However, when β-carotene ketolase genes were co-expressed with these genes, β-carotene was not accumulated in all the cases in a higher proportion than the other carotenoids. Table 5 shows the percentages of β-carotene and ketocarotenoids obtained in these lines. Therefore, the synthesis of ketocarotenoid affects β-carotene accumulation. Based on these results, higher accumulation of ketocarotenoids was observed when accumulation of β-carotene was lower (Table 5). Morris et al. 2009 [26] have also described the relationship between ketocarotenoid and β-carotene contents. *Solanum tuberosum* cultivar Desiree, a low carotenoid-accumulating cultivar, was engineered with the *crtB* and Haematococcus *bkt* genes. The ketocarotenoid levels in tubers of *S. tuberosum* Desiree co-expressing *crtB*, encoding phytoene synthase, and *bkt*, were not enhanced in contrast to lines expressing *bkt* alone [26]. As some *bkt*/*crtB* transgenic tubers accumulated β-carotene, this substrate was not utilized efficiently by the ketolase enzyme in the transgenic tuber. The authors postulated that β-carotene was stored in a form inaccessible to the ketolase or that the ketolase does not readily use β-carotene as a substrate in tubers [26].

Table 5-1. Carotenoid content and composition in wild-type and transgenic rice callus.

Carotenoid	WT callus μg/g DW	TC1 μg/g DW	TC2 μg/g DW	TC3 μg/g DW	TC4A μg/g DW	TC4B μg/g DW	TC5 μg/g DW
Violaxanthin	3.89±0.08	4.54±0.31	6.56±0.40	17.51	2.41±0.31	2.38±0.39	5.41±0.02
Antheraxanthin	1.00±0.06	1.38±0.08	-	-	-	-	-
Astaxanthin	-	-	-	-	6.64±0.91	22.01±0.61	6.15±0.46
Adonixanthin	-	-	-	-	4.66±0.41	9.14±0.16	3.03±0.11
Lutein	3.46±0.07	4.46±0.32	7.10±0.43	13.13	-	-	-
Zeaxanthin	0.52±0.06	1.46±0.10	2.09±0.01	-	-	-	-
Adonirubin	-	-	-	-	2.84±0.21	16.41±0.01	3.88±0.13
Canthaxanthin	-	-	-	-	3.40±0.06	19.04±0.22	3.02±0.18
3-OH-Echinenone	-	-	-	-	-	4.58±0.06	-
Unknown carotenoid	-	-	-	-	-	6.42±0.09	-
Echinenone	-	-	-	-	-	4.92±0.19	-
α-Carotene	-	13.98±0.35	57.06±2.99	72.94	-	5.34±0.51	64.17±2.43
β-Carotene	-	40.62±2.44	242.42±0.14	354.59	6.85±1.45	11.27±0.30	222.67±0.49
Phytoene	-	5.94±0.54	16.27±0.66	31.21	3.96±0.79	8.04±0.11	38.36±1.54
TOTAL	8.87±0.12	72.38±1.11	331.49±1.34	489.37	30.75±2.12	109.54±0.76	346.69±0.68
β/ε ratio	1.56	2.6	3.91	4.32	*	16.82	3.8
% β-Carotene	-	56.12	73.13	72.46	22.28	10.29	64.23
% Ketocarot.	-	-	-	-	57.03	69.47	4.64

WT, wild-type; TC1, expressing *Zmpsy1*, *Pacrt*I; TC2, expressing *Zmpsy1, Pacrt*I, *AtOr*; TC3, expressing *Zmpsy1, Pacrt*I, *Atdxs;* TC4, expressing *Zmpsy1, Pacrt*I, s*BrcrtW*; TC5, expressing *Zmpsy1, Pacrt*I, *sCrBkt*. Abbreviations: β/ε ratio: the ratio of β-ring to ε-ring derivatives; % Ketocarot, % Ketocarotenoids. Mean value ± SD of 2 individual samples, except for TC3 where only one sample was analyzed.

* Absence of ε-ring derivatives.

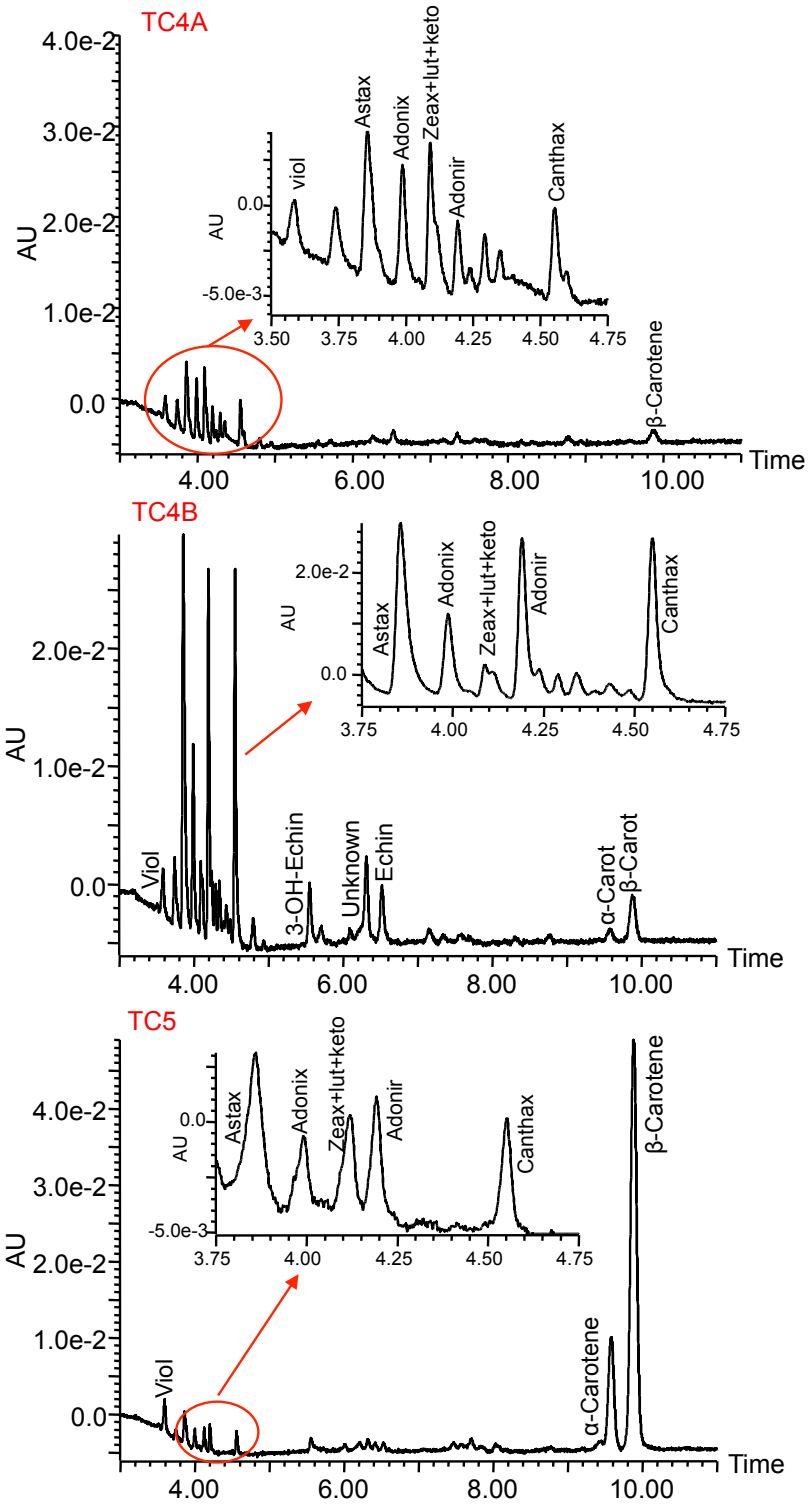

Figure 5-6. Carotenoid profile in TC4A and TC4B (expressing *Zmpsy1*, *Pacrt*I and s*BrcrtI* (expressing *Zmpsy1*, *Pacrt*I and *sCrBkt*). Abbreviations: Viol, violaxanthin; Anthe, anth Astax, astaxanthin; Zeax, zeaxanthin; Lut, lutein; Adonix, adonixanthin; Adonir, adonirubi canthaxanthin; 3-OH-Echinen, 3-hydroxyechinenone; Echin, echinenone; Unknown, unknowr *α*-Carot, *α*-carotene; *β*-Carot, *β*-carotene.

5.5.2 Identification of carotenoids in transgenic rice callus

Although most of the carotenoids present in the different transgenic rice callus were identified, there were some pigments for which it was not possible to establish their identity. For example, in the TC4B one carotenoid with RT 6.35 min was not identified (Fig. 6). In order to find information that allowed the identification of this compound, I determined its UV-vis and mass spectra.

Initially, I determined the positive ion APCI mass spectra of this pigment in order to try to identify the $[M+H]^+$, which is the one that tends to form in APCI (chapter 2, section 2.5.1). Fig. 7 shows that in its mass spectra, the ion at *m/z* 552 (peak base) predominated. Because the molecular weight of the carotenoids detected in the transgenic samples ranged from 536 to 600 g/mol, it was suggested that this ion might be the protonated molecular ion of the unknown pigment. Therefore, its molecular weight should be around 551 g/mol. Reviewing the literature, it was found that echinenone exhibited a molecular weight of 550.86 g/mol [20].

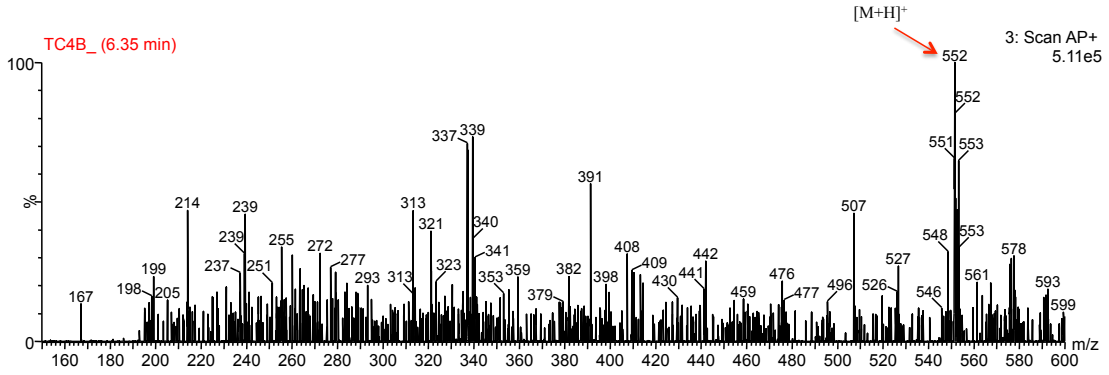

Figure 5-7. Positive ion APCI mass spectra of the unknown carotenoid found in the TC4B, with RT at 6.35 min.

Further experiments were carried out with the mass detector. For example, I used the $[M+H]^+$ obtained for this molecule to build transitions with the ions that can be related with functional groups present in the carotenoid structures (chapter 2, section 2.5.2.1). Although different transitions were tested, Fig. 7 only illustrates those that gave an important signal for this analyte.

The characteristic transitions used to identify echinenone (551.6>69, 551.6>93 and 551.6>203.1) were given by the unknown carotenoid (Fig. 8). Therefore, this finding suggested that the unknown pigment might have a similar structure to the echinenone. In addition, transitions built with the precursor ion at *m/z* 551.6 and the daughter ion at *m/z* 203.1 revealed that the unknown compound bears a keto group conjugated to the polyene chain [27]. Furthermore, the transition 551.6>123.1, being one of the most intense transitions given by this compound (Fig. 8), hinted that a ε-ring might be present in its structure.

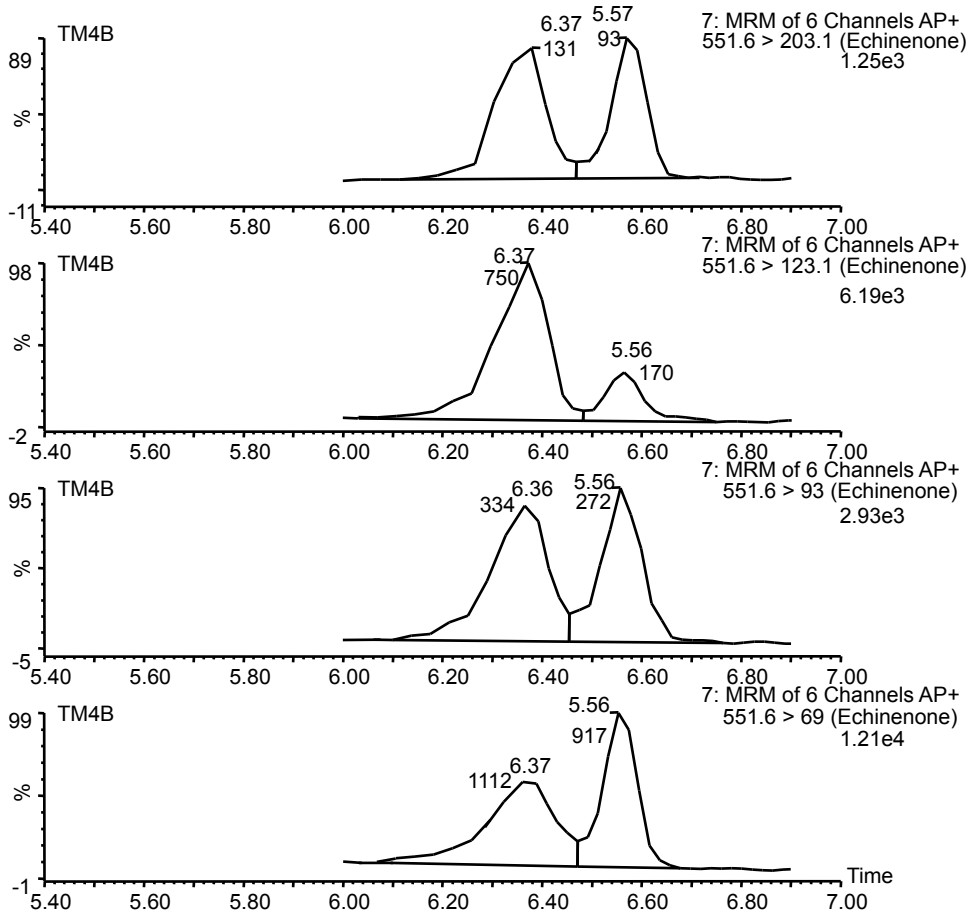

Figure 5-8. Transitions given by the unknown carotenoid.

Based on these results I proposed the structure indicated in Fig. 9 for this unknown pigment. Its structure is very similar to the echinenone, only differing in the position of one endocyclic double bond (Fig. 9).

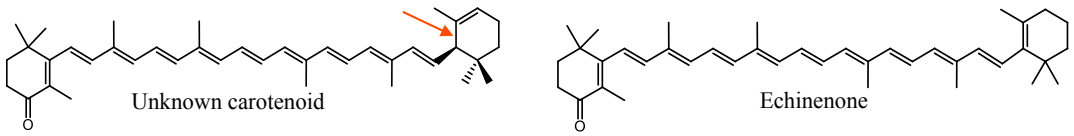

Figure 5-9. Left side, structure proposed for the unknown carotenoid; right side, structure of the echinenone.

In order to find more information that allowed me to support the structure proposed, I analyzed its UV-vis spectrum and RT. Under the chromatographic conditions used to analyze the TC4B (section 4.4.4.1), the maximum absorption (λmax) of echinenone was observed at 461 nm (chapter 1, section 1.7). Therefore, it was expected that the λmax of this unknown pigment would display a lower wavelength than echinenone since the possible presence of a ε-ring in its structure would cause the breaking of the conjugation sooner than in the structure of the echinenone. The red arrow in the Fig. 9 indicates where the breaking of the conjugation in its

structure would occur. Although, the UV-vis spectrum of the unknown pigment (Fig. 10) exhibited a lower λmax than that observed for echinenone, it did not show a symmetrical spectrum as is usually observed for many ketocarotenoids (chapter 1, section 1.2.3).

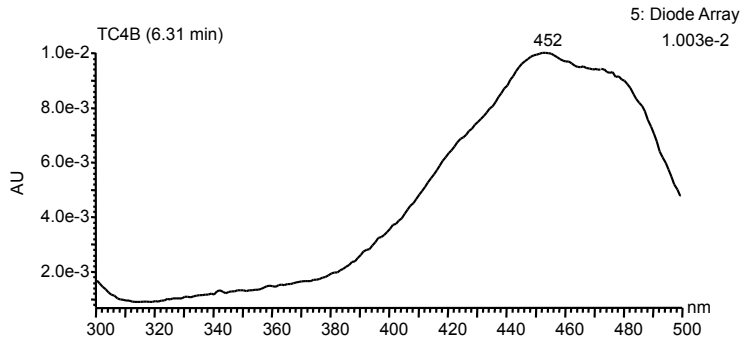

Figure 5-10. UV-vis spectrum of the unknown carotenoid.

Finally, under the UHPLC chromatographic conditions used to separate the carotenoids, it has been observed that carotenoids, which differ by the position of a double bond in one of the terminal rings, can exhibit different RT. For example, α-carotene with β,ε-rings elutes before its isomer β-carotene, with β,β-rings. Based on this behavior it should be expected that the "proposed pigment" eluted before its isomer echinenone since they only differ in the position of a double bond in one of the terminal rings.

The results shown here are only preliminary tests and, therefore, the identity of this unknown compound cannot be concluded with a high degree of confidence. To continue investigating into its identity, other tests need to be conducted, such as chemical reactions used to identify carotenoids [28] or determination of its NMR spectra.

5.6 CONCLUSIONS

Carotenoid content could be enhanced by increasing the availability of carotenoid precursors as demonstrated with the TC3 (expressing *Atdxs*, in addition to the carotenogenic genes *Zmpsy1* and *Pacrt*I) and by increasing the storage capacity for carotenoids as demonstrated with the TC2 (expressing *AtOr*, in addition to the carotenogenic genes *Zmpsy1* and *Pacrt*I). In addition, these combinations of genes mainly allowed the accumulation of β-carotene, whose percentage was higher than 50% of the total carotenoid content in TC1, TC2 and TC3. The expression of s*Brcrt*W and *sCrBkt* in rice endosperm allowed the production of ketocarotenoids such as astaxanthin, adonixanthin, canthaxanthin and adonirubin. In addition, it was observed that a higher synthesis of ketocarotenoids in transgenic rice callus is accompanied by a decrease in β-carotene level.

A new carotenoid has been found in the TC4B whose structure is thought might be similar to that of echinenone. However, given that the UV–vis spectrum of many carotenoids is similar and a number of structurally related molecules coelute, it is important to complement the identification of this carotenoid carrying out either chemical reactions to confirm the presence or absence of a given functional group or using other detection methods such as NMR spectroscopy.

5.7 REFERENCES

[1] Zhu C, Naqvi S, Capell T, Christou P (2009) Metabolic engineering of ketocarotenoid biosynthesis in higher plants. Archives of Biochemistry and Biophysics.483:182-90.

[2] Enfissi E, Fraser PD, Lois LM, Boronat A, Schuch W, Bramley PM (2005) Metabolic engineering of the mevalonate and non-mevalonate isopentenyl diphosphate-forming pathways for the production of health-promoting isoprenoids in tomato. Plant Biotechnology Journal.3:17-27.

[3] Farré G, Sanahuja G, Naqvi S, Bai C, Capell T, Zhu C, Christou P (2010) Travel advice on the road to carotenoids in plants. Plant Science.179:28-48.

[4] Cazzonelli CI (2011) Carotenoids in nature: Insights from plants and beyond. Functional Plant Biology.38:833-47.

[5] Eisenreich W, Schwarz M, Cartayrade A, Arigoni D, Zenk MH, Bacher A (1998) The deoxyxylulose phosphate pathway of terpenoid biosynthesis in plants and microorganisms. Chemistry & biology.5:R221-R33.

[6] Yuan D, Bassie L, Sabalza M, Miralpeix B, Dashevskaya S, Farre G, Rivera S, Banakar R, Bai C, Sanahuja G, Arjó G, Avilla E, Zorrilla-López U, Ugidos-Damboriena N, López A, Almacellas D, Zhu C, Capell T, Hahne G, Twyman RM, Christou P (2011) The potential impact of plant biotechnology on the Millennium Development Goals. Plant Cell Reports.30:249-65.

[7] Ye X, Beyer P (2000) Engineering the provitamin A (*β*-carotene) biosynthetic pathway into (carotenoid-free) rice endosperm. Science.287:303-5.

[8] Datta K, Baisakh N, Oliva N, Torrizo L, Abrigo E, Tan J, Rai M, Rehana S, Al-Babili S, Beyer P (2003) Bioengineered 'golden'indica rice cultivars with β-carotene metabolism in the endosperm with hygromycin and mannose selection systems. Plant Biotechnology Journal.1:81-90.

[9] Hoa TTC, Al-Babili S, Schaub P, Potrykus I, Beyer P (2003) Golden Indica and Japonica rice lines amenable to deregulation. Plant Physiology.133:161-9.

[10] Parkhi V, Rai M, Tan J, Oliva N, Rehana S, Bandyopadhyay A, Torrizo L, Ghole V, Datta SK (2005) Molecular characterization of marker-free transgenic lines of indica rice that accumulate carotenoids in seed endosperm. Molecular Genetics and Genomics.274:325-36.

[11] Baisakh N, Rehana S, Rai M, Oliva N, Tan J, Mackill DJ, Khush GS, Datta K, Datta SK (2006) Marker-free transgenic (MFT) near-isogenic introgression lines (NIILs) of 'golden'indica rice (cv. IR64) with accumulation of provitamin A in the endosperm tissue. Plant Biotechnology Journal.4:467-75.

[12] Schaub P, Al-Babili S, Drake R, Beyer P (2005) Why is Golden Rice golden (yellow) instead of red? Plant Physiology.138:441-50.

[13] Paine JA, Shipton CA, Chaggar S, Howells RM, Kennedy MJ, Vernon G, Wright SY, Hinchliffe E, Adams JL, Silverstone AL (2005) Improving the nutritional value of Golden Rice through increased pro-vitamin A content. Nature Biotechnology.23:482-7.

[14] Al-Babili S, Hoa TTC, Schaub P (2006) Exploring the potential of the bacterial carotene desaturase Crtl to increase the *β*-carotene content in Golden Rice. Journal of Experimental Botany.57:1007-14.

[15] Li L, Paolillo DJ, Parthasarathy MV, DiMuzio EM, Garvin DF (2001) A novel gene mutation that confers abnormal patterns of β-carotene accumulation in cauliflower (*Brassica oleracea* var. *botrytis*). The Plant Journal.26:59-67.

[16] Lu S, Van Eck J, Zhou X, Lopez AB, O'Halloran DM, Cosman KM, Conlin BJ, Paolillo DJ, Garvin DF, Vrebalov J, Kochian LV, Küpper H, Earle ED, Cao J, Li L (2006) The cauliflower Or gene encodes a DnaJ cysteine-rich domain-containing protein that mediates high levels of β-carotene accumulation. Plant Cell.18:3594-605.

[17] Lopez AB, Van Eck J, Conlin BJ, Paolillo DJ, O'Neill J, Li L (2008) Effect of the cauliflower or transgene on carotenoid accumulation and chromoplast formation in transgenic potato tubers. Journal of Experimental Botany.59:213-23.

[18] Zhu C, Naqvi S, Breitenbach J, Sandmann G, Christou P, Capell T (2008) Combinatorial genetic transformation generates a library of metabolic phenotypes for the carotenoid pathway in maize. Proceedings of the National Academy of Sciences of the United States of America.105:18232-7.

[19] Britton G, Liaaen-Jensen S, Pfander H (2004) Carotenoids handbook: 1st ed; Birkhäuser: Basel, Switzerland. pp. 3-404.

[20] Rivera S, Vilaró F, Canela R (2011) Determination of carotenoids by liquid chromatography/mass spectrometry: Effect of several dopants. Analytical and Bioanalytical Chemistry.400:1339-46.

[21] Burkhardt PK, Beyer P, Wünn J, Klöti A, Armstrong GA, Schledz M, Von Lintig L, Potrykus I (1997) Transgenic rice (*Oryza sativa*) endosperm expressing daffodil (*Narcissus pseudonarcissus*) phytoene synthase accumulates phytoene, a key intermediate of provitamin A biosynthesis. Plant Journal.11:1071-8.

[22] Camara B, Hugueney P, Bouvier F, Kuntz M, Moneger R (1995) Biochemistry and molecular biology of chromoplast development. International Review of Cytology.163:175-247.

[23] Li L, Van Eck J (2007) Metabolic engineering of carotenoid accumulation by creating a metabolic sink. Transgenic research.16:581-5.

[24] Rabbani S, Beyer P, Lintig JV, Hugueney P, Kleinig H (1998) Induced β-Carotene Synthesis Driven by Triacylglycerol Deposition in the Unicellular Alga Dunaliella bardawil. Plant Physiology.116:1239-48.

[25] Zhu C, Bai C, Sanahuja G, Yuan D, Farré G, Naqvi S, et al (2010) The regulation of carotenoid pigmentation in flowers. Archives of Biochemistry and Biophysics.504:132-41.

[26] Morris WL, Ducreux LJM, Fraser PD, Millam S, Taylor MA (2006) Engineering ketocarotenoid biosynthesis in potato tubers. Metabolic Engineering.8:253-63.

[27] Van Breemen RB, Dong L, Pajkovic ND (2012) Atmospheric pressure chemical ionization tandem mass spectrometry of carotenoids. International Journal of Mass Spectrometry.312:163-72.

[28] Rivera SM, Canela-Garayoa R (2012) Analytical tools for the analysis of carotenoids in diverse materials. Journal of Chromatography A.1224:1-10.

GENERAL CONCLUSIONS

1. Several factors such as the polarity of particular carotenoids present in plant tissues, sample preparation prior to extraction, and the chemical form of carotenoids in a given sample matrix (free form or bound to other compounds) need to be considered in order to develop the most optimal extraction method(s) from different matrices.

2. The ACQUITY UPLC® BEH C18 column was demonstrated to be an optimal stationary phase to separate several carotenoids simultaneously. The UHPLC system developed allowed for a reduction of the time of the analysis compared to conventional HPLC systems.

3. The polarity range of carotenoids and their concentrations in the samples make it necessary for chromatographic systems to be adapted to suit the particular carotenoid profile being analyzed. Thus, injection volume, injection solvent and composition of the mobile phase should be optimized for optimal resolution and to increase sensitivity, better selectivity and more reliable quantitation.

4. APCI was demonstrated to be a more appropriate method to ionize carotenoids than ESI or APPI. Using APCI in positive ion mode, characteristic fragments were obtained for carotenoids, which could be related with functional groups and consequently help to identify and elucidate the structure(s) of these pigments.

5. Using APPI in positive ion mode, the signal strength of the carotenoids was improved using acetone, toluene, anisole and chlorobenzene as dopants. However, the highest enhancement of the signal strength was observed with carotenes.

6. Analytical method validation demonstrated that the method was suitable for the determination of carotenoids in maize seeds. A satisfactory level of accuracy (%Er below 18%) and intra-day precision (%RSD below 13.15%) was observed for most of the carotenoids with the concentration level studied. In addition, most of the carotenoids studied exhibited excellent relative recoveries (ranging from 82 to 108%) and the calibration curves exhibited good linearity (ranging from 0.02 to 35 μg/mL and R^2>0.9952).

7. The accumulation profiles of individual carotenoids in transgenic maize lines TM1, TM2, TM3 and TM4 indicated that although carotenoid synthesis begins at the earliest stages of endosperm development, their accumulation depends on feedback regulations.

8. Combinatorial nuclear transformation resulted in up to 100-fold increase in the carotenoid content in maize endosperm and the generation of transgenic lines accumulating high levels of carotenoids, including *β*-carotene, hydroxycarotenoids and ketocarotenoids.

9. PSY1 is the key enzyme limiting carotenoid biosynthesis in maize endosperm and the conversion of phytoene into lycopene, catalyzed by endogenous desaturases and isomerases, is another rate-limiting step in the pathway.

10. High levels of astaxanthin were obtained in transgenic maize lines TM5, TM6, TM7 and TM8 by expressing *sCrBkt* in addition to *Zmpsy*1 and *sBrcrtZ*. Furthermore, the results suggested diversion of lycopene towards *β*-branch carotenoid synthesis since several carotenoids with *β*,*β*-rings were detected in these lines (e.g. *β*-carotene, *β*-cryptoxanthin, zeaxanthin, canthaxanthin, among others).

11. New carotenoids were detected in transgenic maize lines TM5, TM6, TM7 and TM8. The structure of one of such carotenoid was determined as 3'-hydroxyechinenone. However, given that the UV–vis spectrum of many carotenoids is similar and a number of structurally related molecules coelute, it is important to complement the identification of carotenoids through further analyses using NMR spectroscopy or high resolution mass spectrometry.

12. Carotenoid content could be enhanced by increasing the availability of carotenoid precursors as demonstrated in transgenic callus TC3 (expressing *Atdxs*, in addition to the carotenogenic genes *Zmpsy1* and *Pacrt*I) or by creating a metabolic sink for carotenoids as demonstrated in transgenic callus TC2 (expressing *AtOr*, in addition to the carotenogenic genes *Zmpsy1* and *Pacrt*I). In addition, these combinations of genes mainly allowed the accumulation of *β*-carotene, whose percentage was higher than 50% of the total carotenoid content in transgenic rice callus TC1, TC2 and TC3.

13. The expression of s*Brcrt*W and *sCrBkt* in rice endosperm allowed the production of ketocarotenoids such as astaxanthin, adonixanthin, canthaxanthin and adonirubin. In addition, it was observed that a higher accumulation of ketocarotenoids in transgenic rice callus is accompanied by a decrease in *β*-carotene levels.

OUTPUTS

Publications related to carotenoid analysis:

Sol Rivera and Ramon Canela (2012) Influence of Sample Processing on the Analysis of Carotenoids in Maize. Molecules. *17*: 11255-11268 **(See Supplementary data)**.

Rivera SM, Canela-Garayoa R (2012) Analytical tools for the analysis of carotenoids in diverse materials. Journal of Chromatography A.1224:1-10 **(See Supplementary data)**.

Rivera S, Vilaró F, Canela R (2011) Determination of carotenoids by liquid chromatography/mass spectrometry: Effect of several dopants. Analytical and Bioanalytical Chemistry.400:1339-46 **(See Supplementary data)**.

Other publications:

Eduard Pérez-Massot, Raviraj Banakar, Sonia Gómez-Galera, Uxue Zorrilla-López, Georgina Sanahuja, Gemma Arjó, Bruna Miralpeix, Evangelia Vamvaka, Gemma Farré **Sol Maiam Rivera**, Svetlana Dashevskay, Judit Berman, Maite Sabalza, Dawei Yuan, Chao Bai, Ludovic Bassie, Richard M. Twyman, Teresa Capell, Paul Christou, Changfu Zhu (2012) The contribution of transgenic plants to better health through improved nutrition: opportunities and constraints. Genes Nutr. DOI: 10.1007/s12263-012-0315-5.

Farre G, Naqvi S, Sanahuja G, Bai C, Zorrilla-Lopez U, **Rivera SM**, Canela R, Sandman G, **Twyman RM**, Capell T, Zhu C, Christou P (2012) Combinatorial genetic transformation of cereals and the creation of metabolic libraries for the carotenoid pathway. In: Dunwell JM, Wetten AC (eds) *Transgenic Plants: Methods and Protocols.* Methods in Molecular Biology volume 847. Humana Press Inc., NJ.

Yuan D, Bassie L, Sabalza M, Miralpeix B, Dashevskaya S, Farre G, **Rivera SM**, Banakar R, Bai C, Sanahuja G, Arjo G, Avilla E, Zorrilla-Lopez U, Ugidos –Damboriena N, Lopez A, Almacellas D, Zhu C, Capell T, Hahne G, Twyman R, Christou P (2011). The potential impact of plant biotechnology on the Millennium Development Goals. Plant Cell Rep. DOI: 10.1007/s00299-010-0987-5.

Christou P, T Capell, L Bassié, C Zhu, S Naqvi, A Peremartí, K Ramessar, S Gómez, S Dashevskaya, D Yuan, M Sabalza, G Farré, **SM Rivera**, B Miralpeix (2011) Canviar els gens per millorar el món . Pagés Editors. ISBN: 9788499751436.

K Ramessar, S Naqvi, S Dashevskaya, A Peremartí, D Yuan, S Góme, **SM Rivera**, G Farré, M Sabalza, B Miralpeix, R Twyman, C Zhu, L Bassié, T Capell and Paul Christou (2009) The Contribution of Plant Biotechnology to Food Security in the 21st Century. Nova Science Publishers. Hauppage, NY 11788 pp. 453-455 ISBN 978-1-60692-977-3 (www.novapublishers.com).

Participation in conferences:

Christou P, Farre G, Bai C, **Rivera SM**, Sanahuja G, Capell T and Zhu C (2011) Multi-gene Constructs Invited Presentation. Meeting of the Society for In Vitro Biology Junes 4-8 Raileigh, North Carolina, USA.

Gemma Farre, **Sol M Rivera**, Ramon Canela, Gerhard Sandmann, Changfu Zhu, Teresa Capell and Paul Christou (2011). TERPNET. Transgenic corn plants engineered with the Arabidopsis homologue of the Orange (Or) gene. 10th International Meeting: Biosynthesis and function of isoprenoids in plants, microorganisms and parasites. May 22-May 26, 2011, Kalmar, Sweden.

Bai C, **Rivera SM**, Medina V, Sandmann G, Canela R, Zhu C, Capell T and Christou P (2011) An effective in vitro functional expression assay for carotenogenic genes in rice. TERPNET 2011, 10th International Meeting: Biosynthesis and function of isoprenoids in plants, microorganisms and parasites. May 22-May 26, 2011, Kalmar, Sweden. pp.141.

C. Bai, **SM Rivera**, V. Medina, R. Canela, G. Sandmann, T. Capell, P. Christou, and C. Zhu (2010) Exploring the mechanism of carotenoid accumulation in rice (Oryza sativa) endosperm through multi-gene engineering. First Global Conference in Biofortification Washingtown DC USA, 8-11 November.

Rivera SM, Vilaró F, Canela R. (2010) Effect of several dopants on the determination of carotenoids by liquid chromatography / atmospheric – pressure photoionization / mass spectrometry. 28th International Symposium on Chromatography (ISC), Valencia, Spain, September 12-16.

Rivera SM, Vilaró F, Canela R. (2010) A novel UHPLC system for carotenoid profiling in transgenic maize. 35th International Symposium on High Performance Liquid Phase Separations and Related Techniques, Boston, United States, June 19-24.

Bai C, **Rivera SM**, Medina V, Canela R, Sandmann G, Capell T, Christou P, Zhu C (2010) metabolic engineering of carotenoid accumulation in rice endosperm through combinatorial genetic transformation. In the 12th World Congress of the International Association for Plant Biotechnology (12th IAPB) and the 2010 In Vitro Biology Meeting of the Society for In Vitro Biology (SIVB) held in St. Louis, MO, USA, June 6-11.

Bai C, **Rivera SM**, Medina V, Canela R, Sandmann G, Capell T, Christou P, Zhu C (2010) Carotenoid biofortification of rice endosperm through multiplex gene transformation. Gordon Research Conference in Carotenoids January 17-22 Ventura Beach Marriot, Ventura CA, USA.

SUPPLEMENTARY DATA

Chapter 1. Development and optimization of analytical methods to analyze carotenoids in cereals

- Supplemental UV-vis spectra of carotenoids from section *1.5.3 chromatographic and spectral characteristics of carotenoids*.

Chapter 2. Factors influencing carotenoid analysis

- Supplemental data from section *2.5.1 Effect of the ESI, APCI, and APPI systems on carotenoid ionization*.
- Supplemental data of carotenoid structures from section *2.5.2 Improvements in the detection of carotenoids using mass detector*.
- Supplemental fragmentation of the carotenoids from section *2.5.2.1 APCI-MS/MS*.
- Supplemental data of the stability of carotenoid ions from section *2.5.2.2 Distinguishing carotenoids through comparison of the intensities of their fragments*.

Chapter 4. Engineering ketocarotenoid biosynthesis in maize endosperm

- Supplemental data from section *4.5.2 Preliminary tests to identify carotenoids present in the* transgenic maize lines.

Chapter 1. Development and optimization of analytical methods to analyze carotenoids in cereals

Supplemental UV-vis spectra of carotenoids from section ***1.5.3 chromatographic and spectral characteristics of carotenoids***. Unless it is mentioned, the UV-vis spectra correspond to the *trans* form of the carotenoid. The UV-vis spectra are shown following the same elution orders that in the UHPLC system.

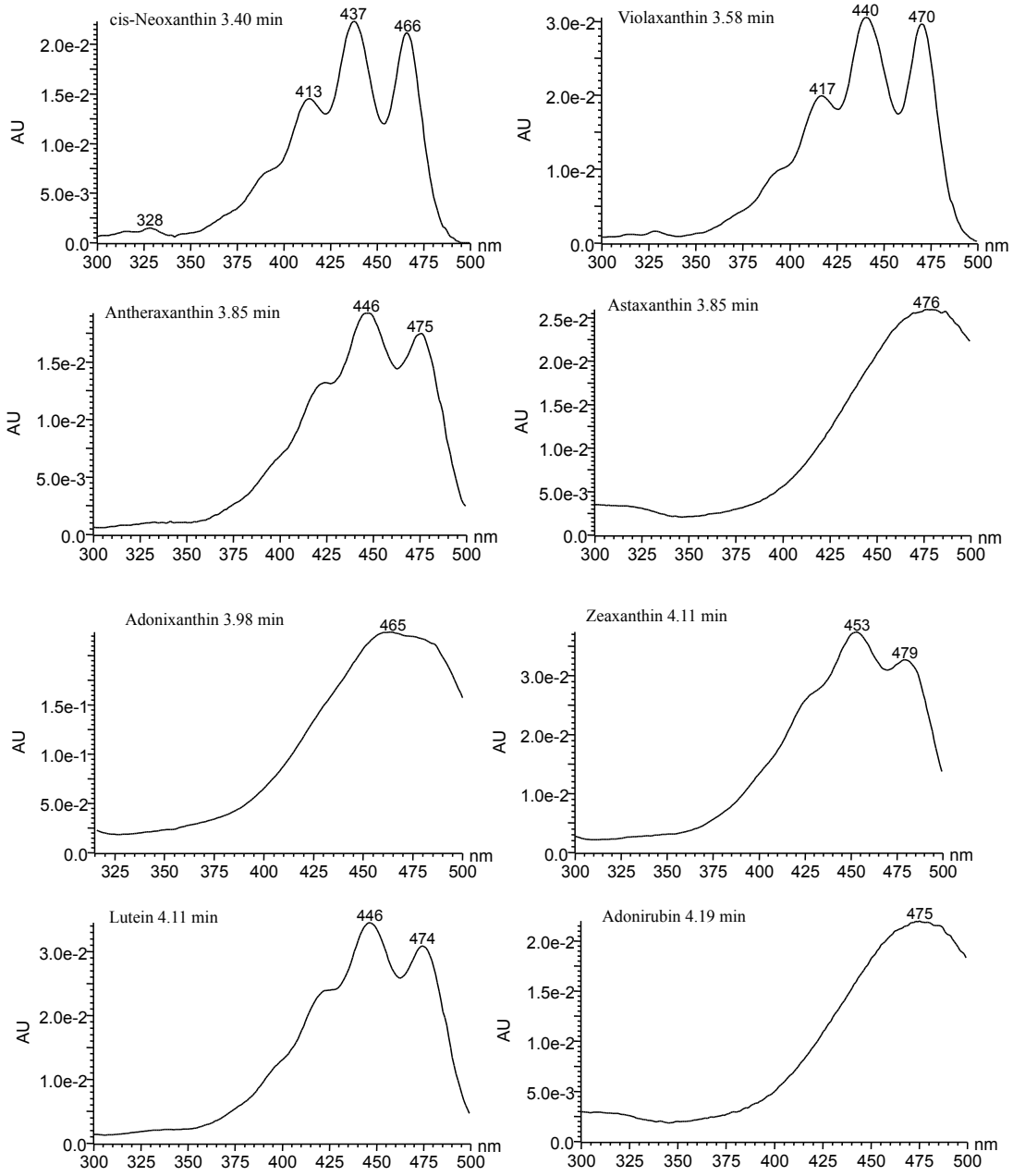

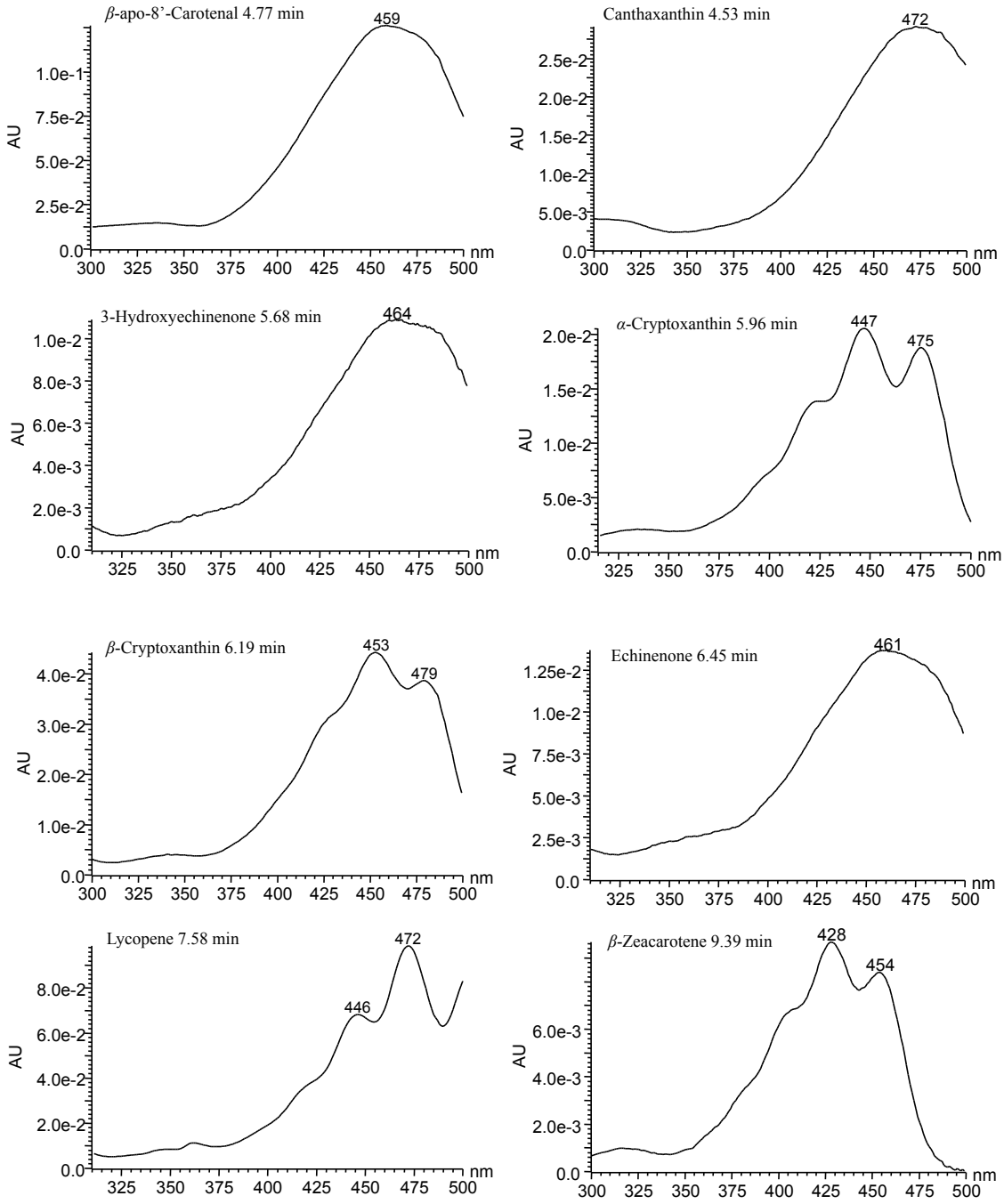
β-apo-8'-Carotenal 4.77 min
459
Canthaxanthin 4.53 min
472
3-Hydroxyechinenone 5.68 min
464
α-Cryptoxanthin 5.96 min
447
475
β-Cryptoxanthin 6.19 min
453
479
Echinenone 6.45 min
461
Lycopene 7.58 min
472
446
β-Zeacarotene 9.39 min
428
454
AU
nm

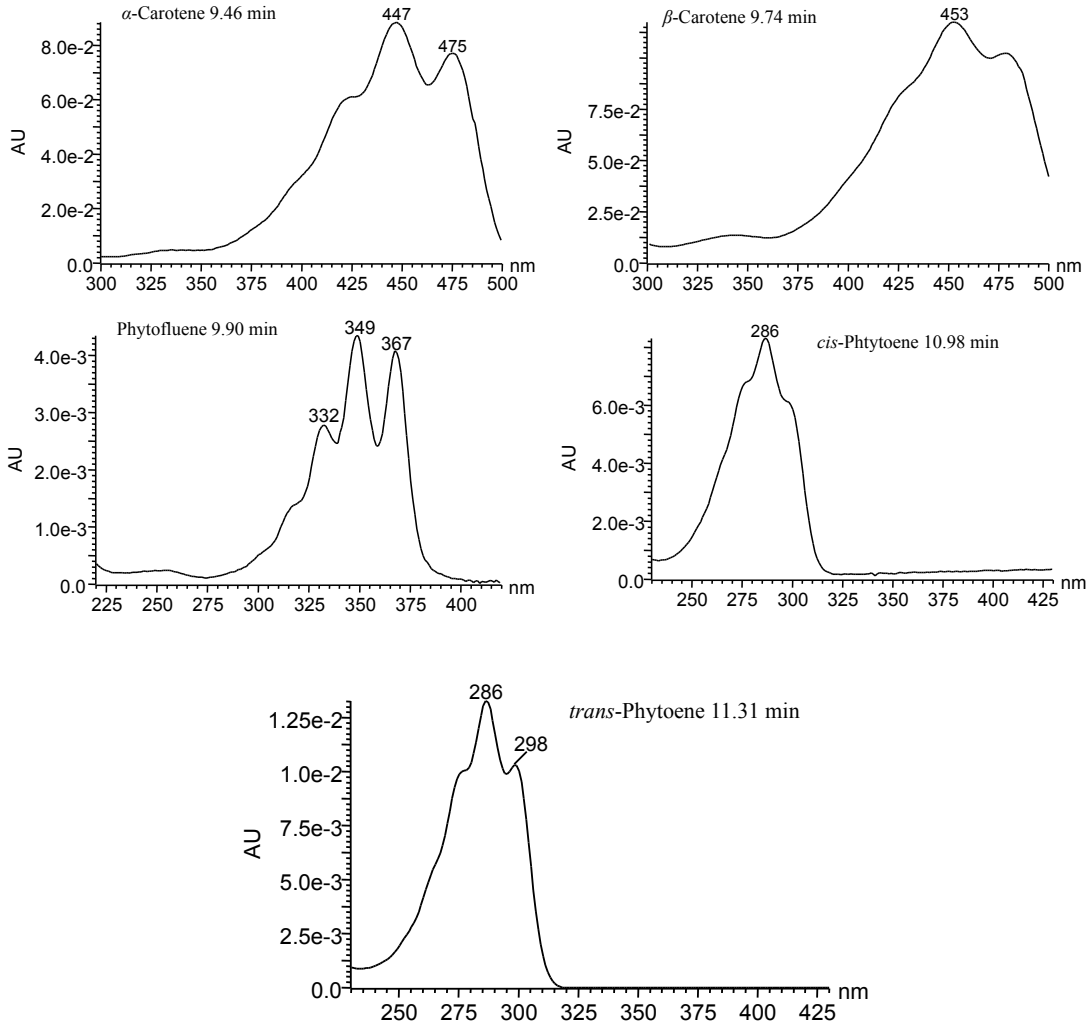
α-Carotene 9.46 min
447
475
AU
nm
β-Carotene 9.74 min
453
Phytofluene 9.90 min
349
367
332
cis-Phytoene 10.98 min
286
trans-Phytoene 11.31 min
286
298

Chapter 2. Factors influencing carotenoid analysis

Supplemental data of the carotenoids from section ***2.5.1 Effect of the ESI, APCI, and APPI systems on carotenoid ionization*.** Neither antheraxanthin nor astaxanthin showed signals when the transitions of its counterpart species were monitored.

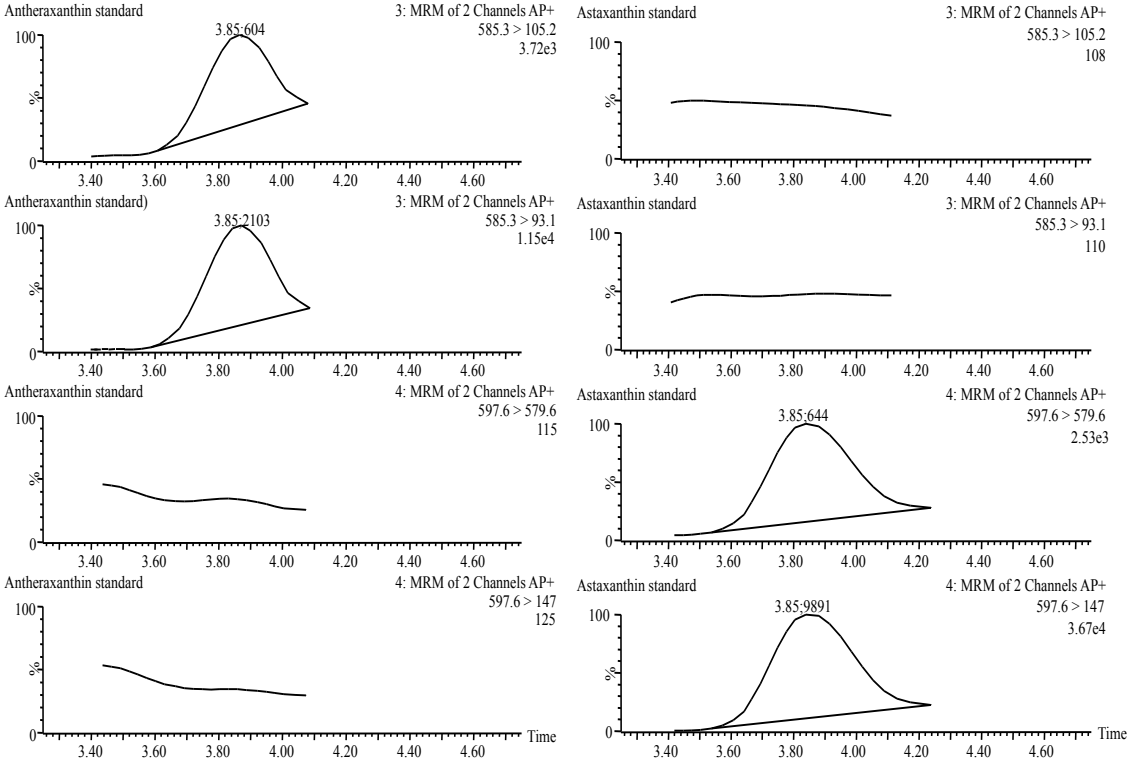

Supplemental data of carotenoid structures from section ***2.5.2 Improvements in the detection of carotenoids using mass detector*.**

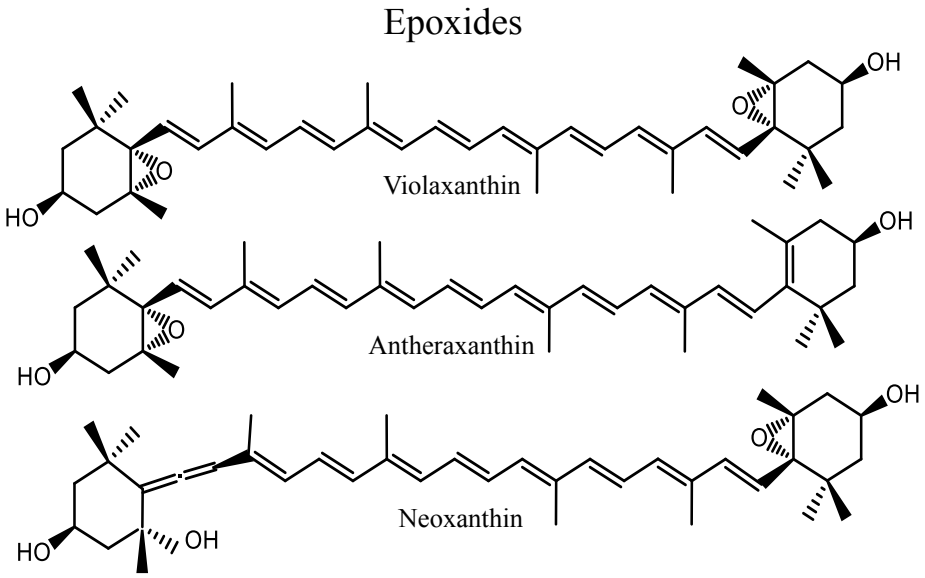

Carotenes

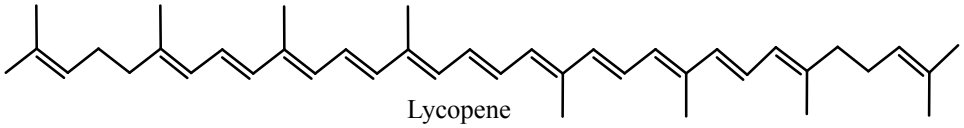

Lycopene

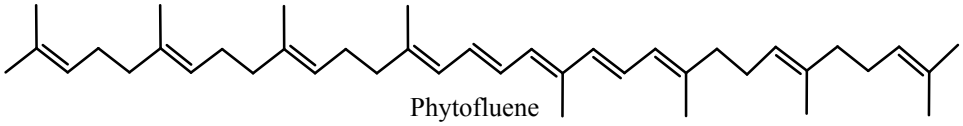

Phytofluene

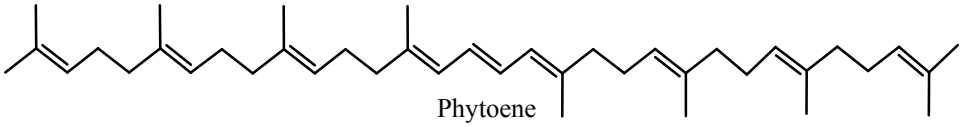

Phytoene

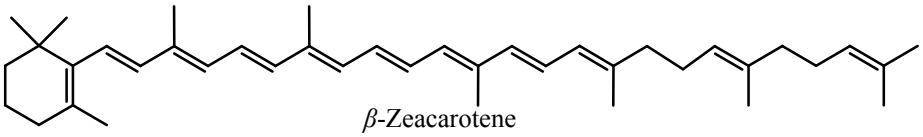

β-Zeacarotene

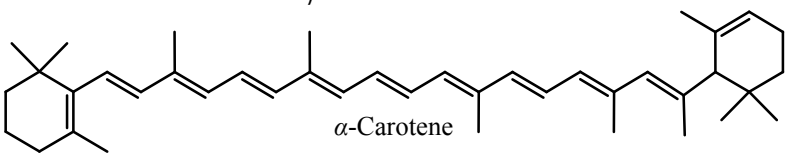

α-Carotene

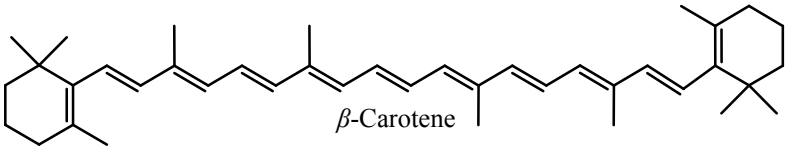

β-Carotene

Hydroxycarotenoids

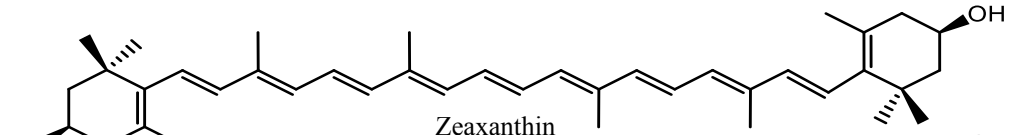

Zeaxanthin

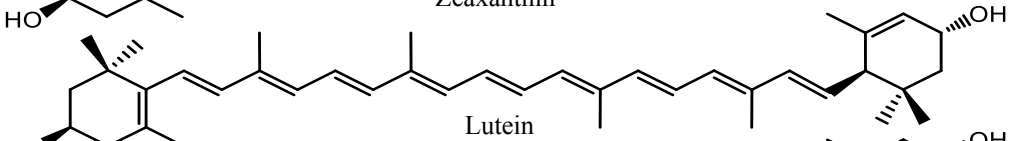

Lutein

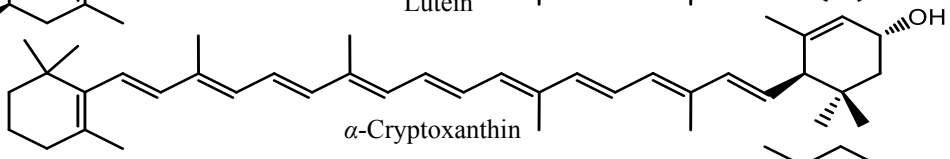

α-Cryptoxanthin

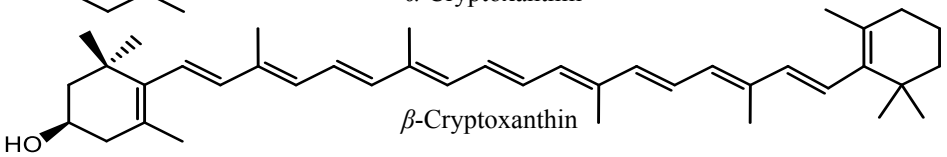

β-Cryptoxanthin

Ketocarotenoids

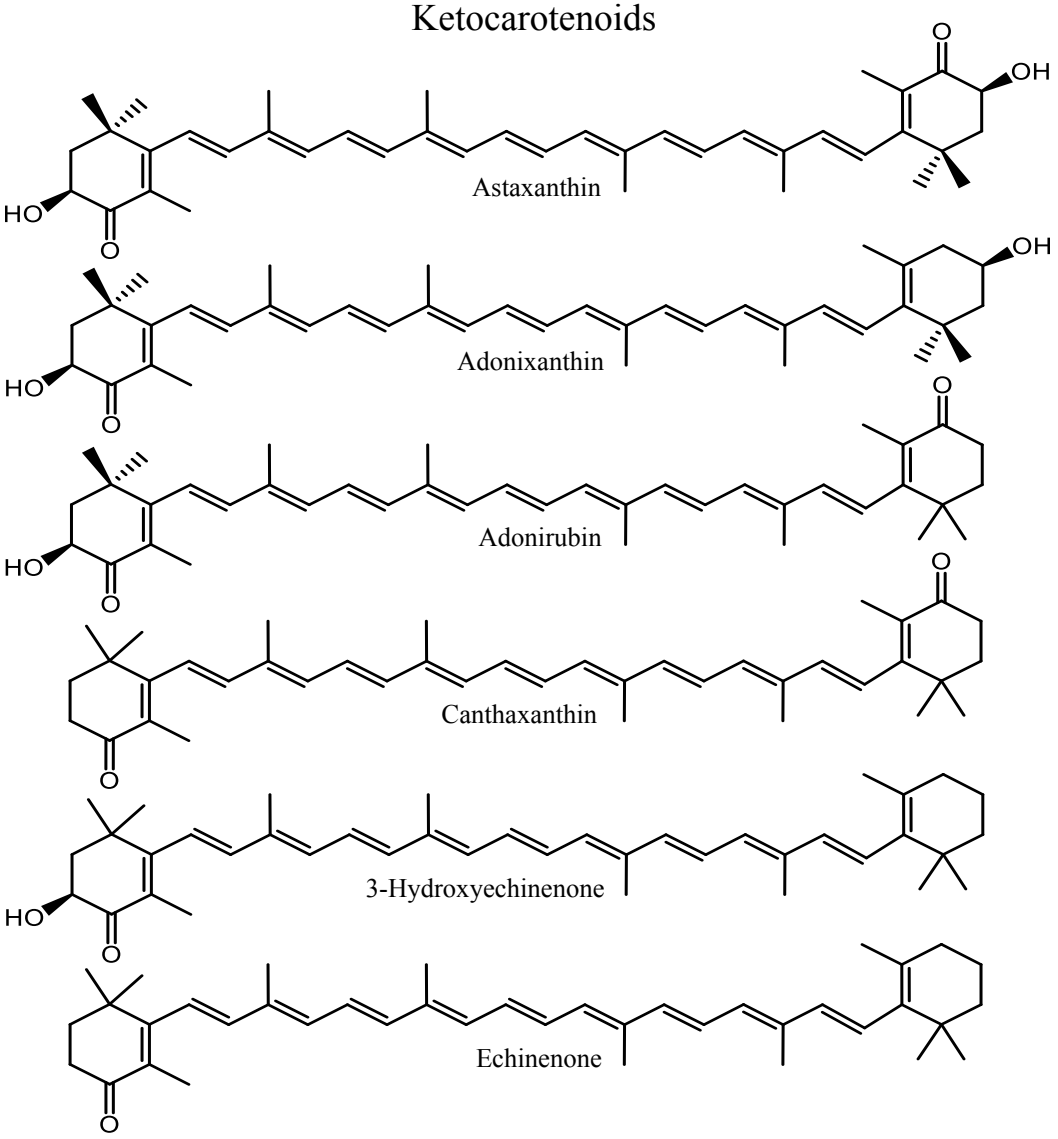

Supplemental fragmentation of the carotenoids from section ***2.5.2.1 APCI-MS/MS.*** Characteristic fragment ions that may be related with functional groups present in the carotenoid structures.

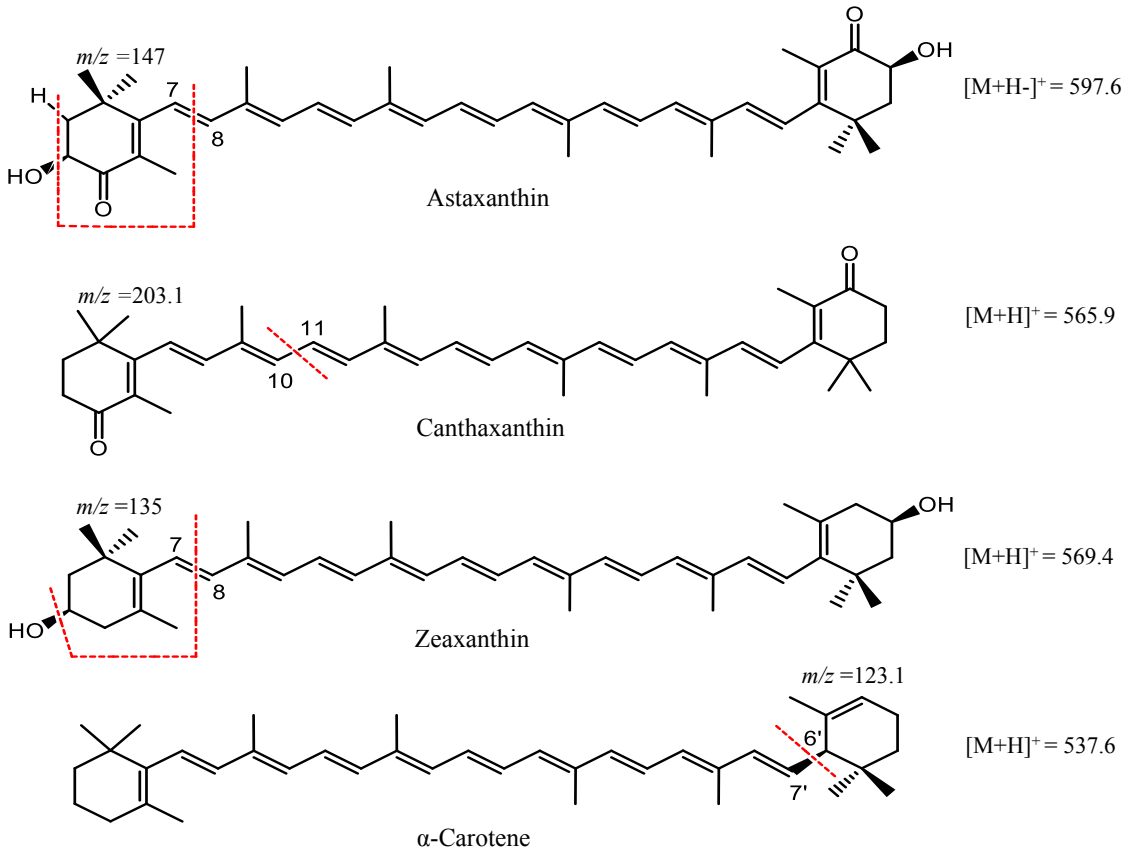

Supplemental data of the stability of carotenoid ions from section ***2.5.2.2 Distinguishing carotenoids through comparison of the intensities of their fragments.*** The loss of water due to the presence of the hydroxyl group in an allylic position (a hydroxyl group located in ε-ring) produces the $[M-18]^+$ ion, which is stabilized by mesomeric effects.

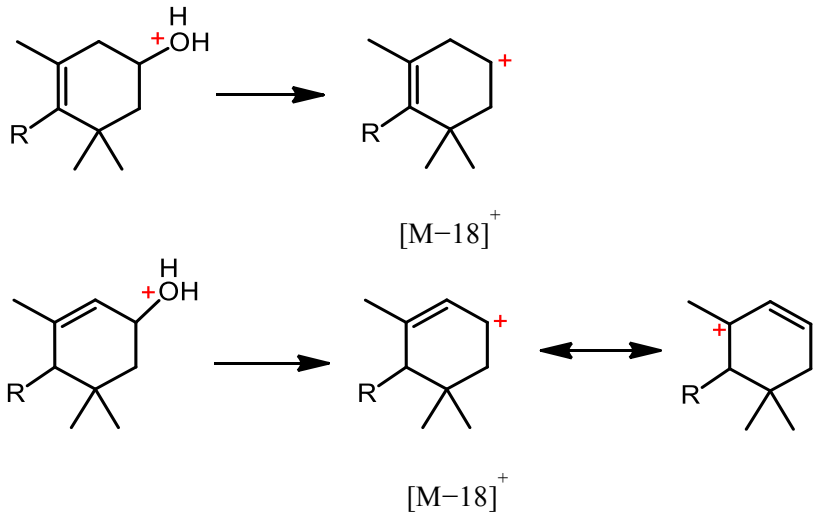

Formation of the ion at *m/z* 123.1 was facilitated by the position of the double bond in the terminal ring, which helped stabilize the resulting carbocation.

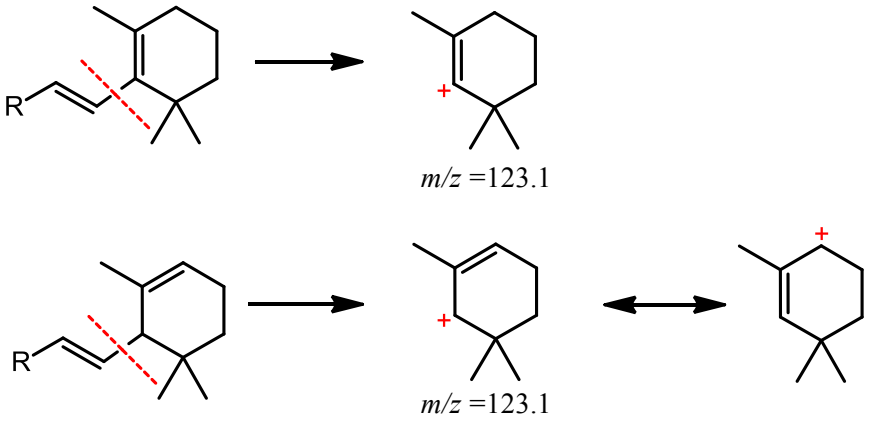

Chapter 4. Engineering ketocarotenoid biosynthesis in maize endosperm

Supplemental data from section ***4.5.2 Preliminary tests to identify carotenoids present in the transgenic maize lines.*** Mass spectra of the unknown pigments found in TM7. Left mass spectra corresponds to the carotenoid with RT at 2.81 min. Right mass spectra corresponds to the carotenoids with RT at 3.01 min.

In the positive ion APCI mass spectra determined for these unknown molecules were observed ions at *m/z* 567-568 and 549. These fragment ions have already been observed for 3-hydroxyechinenone and corresponded to its protonated molecular ion and loss of water respectively.